



# **Elucidating structural and functional aspects of prokaryotic membrane microdomains**

**Aufklärung struktureller und funktioneller Aspekte von prokaryotischen  
Membranmikrodomänen**

Doctoral thesis for a doctoral degree at the Graduate School of Life Sciences,  
Julius-Maximilians-Universität Würzburg,  
Section: Infection & Immunity

Submitted by  
**Benjamin Mielich-Süß**

from  
Ellwangen (Jagst)

Würzburg, July 2017

Submitted on: .....

Office stamp

### Members of the thesis committee:

Chairperson: Prof. Dr. Thomas Dandekar

Primary Supervisor: Dr. Daniel López

Supervisor (Second): Prof. Dr. Thomas Rudel

Supervisor (Third): Prof. Dr. Marc Bramkamp

Date of Public Defence: .....

Date of Receipt of Certificates: .....

## SUMMARY

Bacterial functional membrane microdomains (FMMs) are membrane platforms that resemble lipid rafts of eukaryotic cells in certain functional and structural aspects. Lipid rafts are nanometer-sized, dynamic clusters of proteins and lipids in eukaryotic cell membranes that serve as signaling hubs and assembling platforms. Yet, studying these structures can often be hampered by the complexity of a eukaryotic cell. Thus, the analogous structures of prokaryotes are an attractive model to study molecular traits of this type of membrane organization.

Similar to eukaryotic lipid rafts, the bacterial FMMs are comprised of polyisoprenoid lipids, scaffold proteins and a distinct set of membrane proteins, involved in signaling or secretion. Investigating bacterial FMMs not only contributes to the understanding of the physiological importance of FMMs in bacteria, but also helps to elucidate general principles of rafts beyond prokaryotes.

In this work, a bacterial model organism was used to investigate effects of synthetic overproduction of the raft scaffolding proteins on bacterial physiology. This overexpression causes an unusual stabilization of the FMM-harbored protease FtsH and therefore the proteolytic targets of FtsH are not correctly regulated. Developmental defects and aberrances in shape are the consequence, which in turn negatively affects cell physiology. These findings may be adapted to better understand lipid raft processes in humans, where flotillin upregulation is detected along with development of neurological diseases.

Moreover, it was aimed at understanding the FMM-proteome of the human pathogen *Staphylococcus aureus*. An in-depth quantitative mass-spectrometry analysis reveals adaption of the protein cargo during different conditions, while maintaining a distinct set of core FMM proteins. As a case study, the assembly of the type VII secretion system was shown to be dependent on FMM integrity and more specifically on the activity of the FMM-scaffold flotillin. This secretion system is important for the virulence of this pathogen and its secretion efficiency can be targeted by small molecules that inhibit flotillin activity. This opens new venues for non-conventional antimicrobial compounds to treat staphylococcal infections.

## ZUSAMMENFASSUNG

Funktionelle Membranmikrodomänen (FMMs) in Bakterien sind Membranplattformen, die in strukturellen und funktionellen Aspekten mit Lipid Rafts eukaryotischer Zellen vergleichbar sind. Diese Nanometer-großen, dynamischen Protein-/Lipid-Cluster in der eukaryotischen Zellmembran dienen als Signalzentrum und Assemblierungsplattformen. Allerdings ist die Arbeit an diesen Strukturen durch die Komplexität der eukaryotischen Zellen oft eingeschränkt. Daher sind prokaryotische Zellen attraktive Modellsysteme, um molekulare Eigenschaften dieser Art von Membranorganisation zu untersuchen.

Ähnlich wie eukaryotische Lipid Rafts, bestehen FMMs aus polyisoprenoiden Lipiden, Scaffold-Proteinen und bestimmten Membranproteinen, die z.B. an Signalweiterleitung und Sekretion beteiligt sind. Die Untersuchung bakterieller FMMs trägt nicht nur dazu bei, die physiologische Relevanz der FMMs in Bakterien selbst zu verstehen, sondern auch um generelle Membranorganisationsprinzipien aufzuklären, die über Bakterien hinausgehen.

In dieser Arbeit wurde daher ein bakterieller Modellorganismus benutzt, um Effekte von synthetischer Überproduktion von Raft-assoziierten Scaffold-Proteinen zu untersuchen. Diese Überexpression führt zu einer unüblichen Stabilisierung der Protease FtsH, die in den FMMs zu finden ist, was eine fehlerhafte Regulierung der Zielproteine von FtsH zur Folge hat. Demzufolge sind Entwicklungsdefekte und Anomalien in der Zellform die Konsequenzen, die im Umkehrschluss die Zellphysiologie negativ beeinträchtigen. Diese Ergebnisse können dazu dienen, Lipid-Raft Prozesse in Menschen besser zu verstehen, wo die Hochregulierung von Flotillin im Zusammenhang mit neurologischen Krankheiten steht.

Darüber hinaus zielt diese Arbeit darauf ab, das FMM-Proteom des humanen Pathogenes *Staphylococcus aureus* besser zu verstehen. Eine detaillierte, quantitative Massenspektrometrieanalyse hat ergeben, dass das Proteincargo der FMMs sich zwar verschiedenen Bedingungen anpasst, aber auch ein bestimmtes Kernproteom in allen getesteten Bedingungen beibehält. Als Fallstudie wurde gezeigt, dass die Assemblierung des Typ VII Sekretionssystems von den FMMs, und im Detail von der Aktivität des Scaffoldproteins Flotillin, abhängig ist. Dieses Sekretionssystem ist wichtig für die

Virulenzausbildung dieses Pathogenes und die Sekretionseffizienz kann durch kleine Moleküle verringert werden, die die Aktivität von Flotillin inhibieren. Diese Strategie eröffnet neue Möglichkeiten für die Anwendung unkonventioneller, antimikrobieller Substanzen, um Staphylokokken-Infektionen zu behandeln.

# TABLE OF CONTENTS

<b>Summary</b> .....	<b>i</b>
<b>Zusammenfassung</b> .....	<b>ii</b>
<b>Table of contents</b> .....	<b>iv</b>
<b>I Introduction</b> .....	<b>1</b>
I.1 Membrane heterogeneity and the lipid raft model.....	1
I.2 Proteins in lipid rafts and associated processes.....	4
I.3 Eukaryotic flotillins .....	6
I.4 Lipid raft analogues in bacteria: Functional membrane microdomains (FMMs) .	8
I.5 FMMs in the model organism <i>B. subtilis</i> .....	11
I.6 Bacterial processes regulated by FMMs.....	14
I.6.1 Developmental processes .....	14
I.6.2 Kinase signaling.....	16
I.6.3 Cell shape and division.....	16
I.6.4 Secretion .....	18
I.7 Bacterial model systems to study FMMs .....	24
I.8 Aims of this work.....	26
<b>II Overexpression of flotillins in <i>B. subtilis</i></b> .....	<b>28</b>
<b>III Global DRM proteome analysis</b> .....	<b>49</b>
III.1 Preface.....	49
III.2 Identification and label-free quantification (LFQ) of <i>S. aureus</i> DRMs.....	50
<b>IV The scaffolding activity of FloA is important for the assembly of the T7SS protein complex</b> .....	<b>56</b>
IV.1 Preface.....	56
IV.2 T7SS proteins are part of the DRM.....	56
IV.3 Flotillin transiently interacts with EssB in <i>S. aureus</i> cells.....	59
IV.4 T7SS secretion is reduced in <i>S. aureus</i> cells lacking flotillin .....	61
IV.5 Flotillin mediates T7SS inter-molecular interactions.....	62
IV.6 Flotillin mediated T7SS defect impairs infectivity .....	67
IV.7 Small anti-FMM molecules reduce T7SS activity.....	68
<b>V Discussion</b> .....	<b>73</b>
V.1 The lipid raft controversy .....	73
V.2 Bacterial models to study molecular traits of lipid rafts .....	76
V.3 The <i>S. aureus</i> DRM proteome and T7SS assembly as a case study .....	78
<b>VI Material &amp; Methods</b> .....	<b>85</b>
VI.1 Chemicals and materials .....	85

VI.1.1	Common chemicals and consumables.....	85
VI.1.2	Proteins, enzymes and specialized chemicals.....	85
VI.1.3	Laboratory equipment.....	86
VI.1.4	Software.....	87
VI.1.5	Buffers formulations.....	87
VI.2	Microbiology.....	91
VI.2.1	Microorganisms.....	91
VI.2.2	Glycerol stocks.....	91
VI.2.3	Sterilization.....	91
VI.2.4	Standard growth conditions.....	91
VI.2.5	Growth media.....	91
VI.2.6	Media formulations.....	92
VI.2.7	Antibiotics and media supplements.....	93
VI.3	Microbiology techniques.....	94
VI.3.1	Bacterial two-/three-hybrid.....	94
VI.3.2	Crosslinking.....	95
VI.3.2.1	<i>In vivo</i> crosslinking with DSP.....	95
VI.3.2.2	Paraformaldehyde crosslinking.....	95
VI.3.3	Biofilms and Pellicles.....	96
VI.4	Molecular biology techniques.....	96
VI.4.1	Polymerase chain reaction.....	96
VI.4.1.1	Polymerase chain reaction PCR (Phu/Taq).....	96
VI.4.1.2	Colony PCR.....	97
VI.4.1.3	Joining PCR.....	97
VI.4.2	DNA quantification with Nanodrop.....	98
VI.4.3	DNA Isolation.....	99
VI.4.3.1	Plasmid DNA isolation.....	99
VI.4.3.2	Isolation of genomic DNA.....	99
VI.4.3.3	DNA purification from gel / PCR.....	99
VI.4.4	Restriction.....	100
VI.4.5	Gel electrophoresis and gel documentation.....	100
VI.4.6	Ligation.....	100
VI.4.7	<i>E. coli</i> transformation.....	101
VI.4.7.1	Preparation of frozen aliquots of electro-competent cells.....	101
VI.4.7.2	Transformation by electroporation.....	101
VI.4.8	Sanger Sequencing.....	101
VI.5	Generation of genetically modified strains.....	102
VI.5.1	<i>Bacillus subtilis</i> .....	102
VI.5.1.1	Competent cells.....	102
VI.5.1.2	Deletions with resistance gene marker cassettes.....	102
VI.5.1.3	Marker-less gene deletion with pMAD.....	102
VI.5.1.4	Phage transduction.....	103
VI.5.1.5	Cloning vectors.....	104
VI.5.2	<i>Staphylococcus aureus</i> .....	105
VI.5.2.1	Competent Cells + Transformation.....	105
VI.5.2.2	Deletions pMAD and labeling with pMAD derivatives.....	105
VI.5.2.3	Phage transduction.....	106
VI.6	Biochemistry.....	107
VI.6.1	Sample preparation.....	107
VI.6.1.1	Preparation of cell extracts.....	107

---

VI.6.1.2	Isolation of cytosolic fraction and crude membrane fraction .....	107
VI.6.1.3	Isolation of DRM/DSM.....	107
VI.6.1.4	Culture supernatants .....	108
VI.6.1.5	Biofilm Matrix .....	108
VI.6.1.6	BN-PAGE samples.....	108
VI.6.2	Precipitation of proteins.....	109
VI.6.2.1	TCA precipitation.....	109
VI.6.2.2	Aceton precipitation.....	109
VI.6.3	Quantifying Proteins with Nanodrop .....	109
VI.6.4	Pulldowns.....	109
VI.6.5	Gel-electrophoresis .....	110
VI.6.5.1	SDS-PAGE.....	110
VI.6.5.2	BN-PAGE .....	110
VI.6.6	Western blotting.....	111
VI.6.6.1	Semi-dry/wet blotting.....	111
VI.6.6.2	Fixing proteins and blocking PVDF membrane .....	111
VI.6.6.3	Antibody incubation.....	112
VI.6.6.4	Development .....	112
VI.6.7	Coomassie staining.....	112
VI.6.8	Recombinant protein expression .....	113
VI.6.8.1	EsxA-D, YtnP .....	113
VI.6.8.2	EsaAEssABC + FloA and size exclusion chromatography .....	113
VI.7	Microscopy .....	114
VI.7.1	Sample preparation for microscopy .....	114
VI.7.2	Fluorescence microscopy.....	114
VI.7.3	Structured illumination microscopy.....	115
VI.7.4	Stereoscope .....	115
VI.8	Flow cytometry .....	115
VI.9	Animal experiments & ELISA .....	115
<b>VII</b>	<b>References .....</b>	<b>117</b>
<b>VIII</b>	<b>Abbreviations.....</b>	<b>139</b>
<b>IX</b>	<b>Appendix 1 .....</b>	<b>141</b>
IX.1	List of strains .....	141
IX.2	List of primers .....	144
IX.3	List of figures .....	147
IX.4	List of tables .....	148
<b>X</b>	<b>Appendix 2 .....</b>	<b>149</b>
X.1	Statement of individual author contribution .....	149
X.2	Affidavit .....	150
X.3	Publications.....	151
X.4	Acknowledgments .....	153
X.5	Curriculum Vitae .....	154



# I INTRODUCTION

## I.1 Membrane heterogeneity and the lipid raft model

One of the most important features of every living cell is the plasma membrane. Composed of amphipathic lipids, it serves as a physical barrier that encases the cytosol and essential organelles to preserve genetic information and defines a cell as a functional unit. Membranes are mainly constituted of phospholipids that have a lipophilic tail and a hydrophilic head group resulting in the formation of an energy-favorable lipid bilayer with an inner and an outer leaflet. The hydrophilic head groups of the lipid molecules face the outer sides of the bilayer and protecting the hydrophobic tail from aqueous moieties [1]. Besides the family of phospholipids, there is a great variety of lipids with distinct physicochemical properties found in cellular membranes [2]. Besides lipids, the cell membrane also harbors a vast amount of membrane proteins that can account 20 – 30 % of the entire proteome of a cell [3] and decorate up to 20 % of the cells surface area [4].

The first model describing the organization of lipids and proteins in the cell membrane was suggested by Singer and Nicholson [5]. In their landmark paper from 1972, they proposed the fluid mosaic model. They postulated that all membrane proteins and lipids are diffusely arranged in the bilayer in a mosaic-like pattern. However, subsequent reports called this theory into question by proposing that there is heterogeneity in the distribution of lipids *in vitro* and that certain lipid species have the ability to cluster into domains due to their physicochemical properties [6]. Those early reports on membrane lipid heterogeneity suggested ‘quasicrystalline’ lipid regions that are more rigid and surrounded by freely dispersed lipid molecules, which in turn are more fluid [7]. This lipid organization principle gradually evolved and in 1982 a concept of lipid domains was proposed, where lipids were suggested to cluster into a so-called ‘more ordered state’, in which cholesterol was attributed a critical role in formation of those lipid domains [8,9]. These observations in model membranes suggested the coexistence of liquid-disordered and liquid-ordered membrane regions, with the latter being characterized by lower diffusivity and higher molecular packing [10-14].

*In vivo* evidences for membrane heterogeneity emerged from studying phenotypical traits of polarized epithelial cells, where the apical and basolateral membrane are marked by substantial differences in both protein and lipid composition [15]. It was suggested that a lipid sorting mechanism specifically delivers sphingolipids from the Golgi apparatus to the apical side of the cell and their diffusion is restricted via tight junctions [16-18]. The sorting of specialized lipids to the apical side allows to specifically recruit GPI-anchored proteins to this site [19]. Thereupon, by taking into consideration that not only lipids, but also proteins are heterogeneously organized in the membrane, Simons and Ikonen introduced the lipid raft model. This model implies that there is a lateral segregation of proteins and lipids into domains that are held together by lipid-lipid-, lipid-protein- and protein-protein interactions and float in the cell membrane like rafts [20].

The original lipid raft model proposed that the charged sphingolipid head groups in the outer leaflet of the bilayer tend to associate with each other by weak interactions. Due to the size of the polar head group, the carbon tails cannot align as closely as for other lipids and the resulting gaps are filled by cholesterol molecules, which leads to very tight packaging of these domains [20]. The selective incorporation of membrane transport and signaling proteins into those cholesterol/sphingolipid membrane regions, functionally assigns lipid rafts as membrane platforms, where cellular processes are condensed to increase specificity and spatial confinement [20].

The lipid raft theory is based on experimental observations that lipid rafts are resistant to detergent treatment, caused by the tight association of sphingolipids with intercalated cholesterols [19]. Thus, lipid rafts can be extracted from cell membranes using cold Triton X-100, a non-ionic detergent that disrupts the fluid, liquid-disordered, non-raft containing-membrane fractions, while sphingolipid-cholesterol rafts remain intact. Subsequently, this detergent resistant membrane (DRM) can be separated from detergent-sensitive membrane (DSM) as a buoyant fraction in low-density regions on a sucrose gradient [19]. This molecular propensity got established as a gold-standard to isolate lipid rafts, including both raft lipids and raft-associated proteins [21].

Furthermore, membrane fractions containing lipid rafts are not only resistant to detergent treatment, but they are also resistant to disruption by elevated pH and addition of carbonate that disperses liquid-disordered regions. Likewise, separation of

pH/carbonate resistant membrane fractions on a sucrose density gradient allows to enrich lipid rafts [22]. In the following years, more studies were conducted using a multitude of lipid raft extraction procedures. For instance, different detergents were used (e.g. Lubrol WX, Lubrol PX, Brij 58, Brij 96, Brij 98, Nonidet P40, CHAPS, and octylglucoside) [23-28] or membranes were extracted with an isotonic buffer and fractions were separated on Percoll gradients [29]. Also, some authors reported isolation of lipid rafts with detergent-free protocols after mechanical cell lysis [30].

Yet, it must be emphasized that detergent- or carbonate-resistant membranes cannot be equalized with lipid rafts. In several cases, discrepancies between the extraction procedures were reported [31,32]. For instance, DRM-preparations were proposed to co-isolate raft-associated organelles [33]. Also, it was suggested that extraction of membrane fractions with detergents induces unspecific clustering into liquid-ordered membrane phases and thus might leading to falsified results [34,35]. Differences between lipid raft-enrichment protocols became evident when proteomic profiles of lipid rafts isolation with different procedures were compared in detail: Although a core set of authentic raft-associated proteins can be identified with all tested protocols, the authors found subtle differences in the lipid raft proteome depending on the raft-enrichment protocol [30,36]. Thus, the lipid raft enrichment procedures should be selected empirically and findings must be confirmed with morphological assays, such as fluorescence (superresolution) microscopy or protein-protein interaction studies [37,38].

Applying these techniques allows to isolate two morphologically different types of lipid rafts: Firstly, flask-shaped rafts, which are also known as Caveolae [39,40]. These structures were initially identified by electron microscopy as flask-shaped membrane-invasions [41,42]. They are characterized by the presence of the scaffold protein caveolin and their co-purification in the DRM or other raft-enrichment procedures, categorizes caveolae as a specialized raft [43]. On the other hand, planar rafts are also co-isolated in DRM preparations, which are morphologically indistinguishable from the remainder of the cell membrane and are typically devoid of Caveolin. Instead, planar rafts harbor a functionally analogous scaffold protein named reggie/flotillin and are thus often referred to as reggie- or flotillin-microdomains [44-46].

Both types of lipid rafts have been assigned a variety of distinct membrane related functions in the cell, including the regulation of signal transduction [39,47,48], interaction with the cytoskeleton [38], intracellular trafficking [21], and the contribution to endo- and exocytosis events [21,49]. Despite the plethora of associated functions, both types of rafts rely on the presence of sphingolipids and cholesterol, are enriched with GPI-anchored proteins and typically harbor scaffold proteins. Lipid rafts provide an environment for a spatial and temporal concentration of membrane proteins to promote their interaction guided by the action of scaffold proteins. Thus, in a keystone symposium leading lipid raft researchers integrated all facets and current findings to define lipid rafts as:

*“...small (10 – 200 nm), heterogeneous, highly dynamic, sterol- and sphingolipid-enriched domains that compartmentalize cellular processes. Small rafts can sometimes be stabilized to form larger platforms through protein-protein and protein-lipid interactions.” [50]*

Besides being referred to as lipid rafts, another definition of those membrane microdomains is membrane rafts, yet this term did not prevail in the literature. The intention to call these domains membrane rafts instead of lipid rafts was to deflect the notion that their formation is solely depending on lipids, rather than both lipids and proteins [50]. In the course of this work however, the term lipid rafts will be used. The concept of lipid rafts is a simplistic description of an important principle that can be found in many biological systems, which is the compartmentalization of processes into limited areas. This facilitates efficiency of physiological processes mediated by the close proximity of involved molecules [47].

## **I.2 Proteins in lipid rafts and associated processes**

Since the discovery of lipid domains and the postulation of the lipid raft concept, the first raft proteins that led to the support of this theory were identified by co-purification with the DRM fraction. Amongst those were GPI-anchored proteins that are sequestered to the apical site of epithelial cells in a sphingolipid/cholesterol depending manner [51-53]. In the following years, more proteins were described to be part of lipid rafts, as they fulfill several criteria to be licensed as a lipid-raft protein: This includes co-purification with DRMs, co-localization and -purification with raft-marker molecules (e.g. the glycosphingolipid GM1 or the scaffold protein flotillin), focal distribution and functional

and spatial dependence on raft lipids, such as cholesterol. This led to the identification of entire signaling pathways that are regulated by the action of lipid rafts [47].

A well-studied process that depends on the integrity of lipid rafts is the signaling cascade of the T-cell receptor during antigen presentation. The T-cell receptor is a multi-subunit receptor complex that requires several events of maturation to eventually form a micrometer-sized immunological synapse [54]. During this process, the T-cell receptor is crosslinked by binding to the antigen, which in turn increases its affinity to the lipid raft membrane phase [55]. This lateral reorganization into rafts provides a distinct microenvironment for the receptor complex to get in close proximity of raft-harbored tyrosine kinases (e.g. Lck, Fyn or LAT). Those reside in lipid rafts and are critical for maturation of the T-cell receptor complex [56-58]. The association of rafts with the cytoskeleton further promotes the clustering of the raft-nanodomains into macrodomains [59]. This results in formation of a micrometer-sized immunological synapse – synonymous with a raft-macrodomain – on the site of antigen binding to polarize the T-cell. This whole process is depending on the presence of raft-lipids (e.g. cholesterol) and is guided by scaffold proteins to spatially and temporally organize this signaling cascade [60].

Similar activation and macrodomain formation has been studied in detail for the activation of the B-cell receptor [61], the IgE/FC $\epsilon$ RI signaling complex [62] and seemingly more complexes might follow similar mechanisms [47]. Conceptually, rafts provide a distinct microenvironment for signaling receptor complexes by shielding their assembly and activation from unwanted signaling inputs, e.g. kinases reside in rafts, whereas cognate phosphatases are often excluded [47].

Furthermore, planar rafts can serve as entry or budding sites for infectious agents such as Ebola virus, human immunodeficiency virus (HIV) or the malaria causing parasite *Plasmodium falciparum* [63]. For instance, HIV and *P. falciparum* attach to host cells via interaction with the raft-harboring chemokine receptor CD4. Host cell attachment of these pathogens leads to a local raft-depending clustering of the CD4 receptor and subsequent fusion of the virus with the host cell or the formation of a parasite containing vacuole [64,65]. Therefore, lipid rafts may also fulfill important roles during entry of those microorganisms and their pathogenesis [43].

Since the abovementioned signaling and membrane transport processes are critical for any cell type, the involvement of lipid rafts have been suggested for a vast variety of physiological processes, including cell migration, adherence, polarization, signaling and mechanotransduction [21,38,39,47-49]. Nonetheless, there are still ongoing debates, whether lipid rafts are an artefact due to isolation or labeling procedures [34,66]. For instance, labeling of proteins and lipids can interfere with their behavior and thus, a direct visualization of lipid rafts *in vivo* has been elusive. It is currently under debate at which time scale raft exist and how big they are. Previous reports showing that rafts exist only for several nanoseconds [67] and have a size only a few nanometers [68]. However, this is not in agreement with typical turnover times of kinases, neither can a 20-nm sized rafts carry more than 15-20 lipid molecules and 3-5 membrane proteins [69]. Thus, it remains to be clarified if rafts exist only transiently as nanoscale assemblies, which can form bigger raft platforms to initiate signaling [70].

### **I.3 Eukaryotic flotillins**

The coordinated interaction of protein partners within rafts and the assembly of large raft platforms is typically guided by scaffold proteins. Scaffold proteins are non-catalytic chaperones that spatially organize binding partners and thus facilitate their interaction and oligomerization, for instance in multi-enzymatic reactions [71-73]. One important class of lipid-raft harbored scaffold proteins is found in planar rafts: These proteins are called flotillins due to their ability to float in low-density fractions of a sucrose gradient after Triton X-100 extraction [74]. Simultaneously, flotillins were discovered during axon regeneration in neuron cells as one of the most upregulated genes and are thus often referred to as 'reggies', indicating their importance during this regeneration process [75,76]. Flotillins are consistently detected in raft-isolation procedure and were among the first non-GPI-anchored proteins associated with lipid rafts. Therefore, flotillins are considered *bona fide* raft proteins and often used as lipid raft markers [43].

Most eukaryotic genomes typically encode for two flotillin proteins, called flotillin-1 and flotillin-2. The corresponding descriptions are reggie-2 and reggie-1, respectively. In this work however they will be exclusively referred to as flotillins. Flotillins are conserved between fly and man with a homology of 64 % [77,78]. They associate with the inner leaflet of the membrane and both N- and C-terminus face the cytoplasm. They are decorated with post-translational modifications, such as myristylation or palmitoylation

that were suggested to target them to the lipid rafts [79,80]. Close to the N-terminus, flotillins harbor a SPFH domain (stomatin, prohibitin, flotillin, HflK/C domain) [81,82], synonymous with PHB domain (prohibitin homology domain) [83]. The function of this domain is not entirely clear, but it is suggested that it might bind lipid moieties for raft targeting and might also contribute to oligomerization [82]. The C-terminus has a region with several coiled-coil motifs, that is often referred to as flotillin domain. The flotillin domain is involved in homo- and hetero-oligomerization of flotillin-1 and flotillin-2, which is important for their function and localization [82,84].

In addition to its high degree of conservation, eukaryotic flotillins are widely expressed in several tissues and cell lines, suggesting important roles in cellular processes [43,85]. Although a detailed molecular mechanism on how flotillin works is still elusive, it is widely accepted that flotillins act as raft-associated scaffolding proteins. They facilitate the interaction of raft components and are therefore important for structural and functional integrity of lipid rafts. Consistent with this, a variety of processes was found to be directly associated with the action of flotillins [48,85]. The initial co-purification and co-localization in light and electron microscopy with GPI-anchored proteins (e.g. Thy-1 [86], F3/contactin [87]) or Prp<sup>c</sup> [88]) and Src-family kinases [87,89,90] led to the assumption that the scaffolding activity of flotillins is important for raft-mediated signaling processes [43]. Indeed, the scaffolding activity of flotillins is crucial for priming T-cell receptor (TCR)-mediated signaling cascades by promoting the coalescence of proteins residing in lipid raft nanodomains, like LAT or Lyn kinases, into macrodomains to eventually form the immunological synapse and initiate signaling [60]. Another physiological process flotillins are connected to, is the involvement in axon regeneration [75,76]. In order to contribute to this process, flotillins re-organize the actin cytoskeleton. It was shown that flotillin overexpression leads to membrane ruffling via interaction with several cytoskeleton modifiers [80]. Likewise, flotillins interact and co-localize with proteins involved in axon regeneration, endocytosis, cholesterol uptake, insulin signaling or cell proliferation [43,85].

The involvement in such a variety of physiological processes also suggests a connection of flotillins to the development of several diseases. For instance, flotillin is involved in disease progression of Alzheimer's and Parkinson's disease [43,85]. Alzheimer's disease is characterized by aberrant production, secretion and accumulation of amyloid proteins in the neuronal cortex, leading to formation of senile plaques and thus impairment in

neurological signal transmission [91]. The proteases that balance the regular production of those amyloid proteins are part of the lipid rafts [92]. In damaged tissue, flotillins are significantly upregulated and accumulate at the sites of plaque production [93]. Similarly, in Parkinson's disease flotillin expression is significantly increased in affected brain regions that show the typical loss of neuron cells [94]. Yet, it is unclear if this upregulation of flotillins is causative of this disease, an accompanying effect or an effort of cells to counteract disease progression. In prions diseases (such as bovine spongiform encephalopathy, Creutzfeldt-Jacob or scrapie), flotillins co-localize and can be co-purified with the Prion-protein PrP, a GPI-anchored protein with unknown function. Upon unknown stimuli PrP cooperatively misfolds from from harmless, cellular PrP<sup>c</sup> into PrP<sup>sc</sup> aggregates, which eventually causes disease [88]. However, in this disease the role of flotillins and their involvement to disease progression is not understood. Moreover, Hazarika et al. reported that flotillins are upregulated in metastatic melanomas, suggesting that flotillins are also involved in cancer metastasis and invasion [95].

Thus, flotillins are nowadays accepted as important raft-associated protein chaperones, that scaffold the signaling processes in rafts to mediate protein-protein interactions. Their connection to a variety of proteins and accompanying processes seems to be a general mechanism for scaffolding in lipid rafts and their presence and functionality is crucial for the integrity of rafts. However, as pointed out above, the molecular mechanisms how flotillins mediate protein-protein interactions and if and how they interact with lipids is still elusive.

#### **I.4 Lipid raft analogues in bacteria: Functional membrane microdomains (FMMs)**

Although major work on membrane organization has been done in eukaryotic models, the concept of heterogeneity in membrane organization is not unique to this domain of life. Surprisingly, bacteria also show a remarkably high degree of complexity in terms of membrane organization. For instance, many bacterial membrane proteins have been shown to have a non-homogenous membrane distribution and localize in foci or are enriched at poles or the division septum [96,97].

With the use of fluorescent dyes that specifically stain distinct lipids species, it became evident that not only proteins, but also lipids are not uniformly distributed in bacteria. This heterogeneous distribution of lipids in bacterial membranes was proposed after



discovering an accumulation of cardiolipin in poles and division septa of *Bacillus subtilis* and *Escherichia coli* membranes by using the fluorescent dye Nonyl-Acridin Orange [98-100]. More recently, the existence of membrane regions with increased fluidity was proposed that consist of more fluid, probably poly-unsaturated lipid species. These regions particularly attract proteins like MreB, PlsX or MurG and both lipids and proteins disperse upon membrane depolarization, which in turn leads to malfunction of associated processes [101,102].

All these findings add up to the fact that bacterial membranes are not homogeneous in their lipid and protein composition, which argues against the fluid mosaic models and reinforces the idea of a more intricate membrane organization. The concept of bacterial lipid raft analogues is a rather novel concept in microbiology, since most bacterial membranes are devoid of cholesterol and sphingolipids, which are the major component of laterally-driven microdomain formation in eukaryotic cells. Typically, bacterial membranes are primarily composed of phosphatidylglycerol (PG), cardiolipin (CL) and phosphatidylethanolamine (PE) and their ratios vary depending on the species. For instance, in *E. coli* the PE:PG:CL ratio is 7:2:1, whereas in *B. subtilis* cardiolipin is more abundant and makes up to 25 % of the entire membrane [103,104]. Unlike eukaryotic lipid rafts, where cholesterol and sphingolipids represent the major components of membrane microdomains, bacteria are unable to produce either of those lipids themselves and only a few selective species can be found to incorporate host-produced cholesterol in their own membranes, like *Borrelia burgdorferii*, *Ehrlichia chaffeensis*, *Anaplasma phagocytophilum* or *Mycoplasma spp.* [105-107].

Instead, several bacterial species produce hopanoids that have physicochemical properties similar to sterol compounds. Therefore, hopanoids might provide the basis to form membrane microdomains similar to eukaryotic cholesterol and sphingolipids [108]. For example, hopanoids can replace the exogenously acquired cholesterol in membranes of mycoplasma [109], they can modify the rigidity of membranes *in vivo* and they can form discrete membrane domains [110,111]. Similar to cholesterol, hopanoids are classified as terpenoids or isoprenoids that have highly diverged lipid synthesis pathways. Their synthesis is based on isoprene-based precursors (e.g. farnesyl pyrophosphate) that can be converted into cyclic or non-cyclic terpenoids (Fig. I.1). Cholesterol for instance is based on head-to-head condensation of isoprenoid precursors to acyclic squalene, which is then further cyclized to its final form. Although the pathway

to convert squalene precursors to cholesterol is absent in prokaryotes, bacteria can cyclize squalene precursors into hopanoids (e.g. sporulenes) [112,113]. Distinct hopanoids can provide similar physicochemical properties to bacterial membranes as cholesterol and might serve as sterol surrogates in bacteria [110,111]. Another type of isoprenoid-based lipids are carotenoids, which are acyclic terpenoids produced from the same precursor as hopanoids (namely farnesyl diphosphate). Carotenoids are ubiquitously present in bacterial species and their biological functions are very versatile, including contribution to virulence [114], the pigmentation and coloration of bacterial cells, or scavenging oxygen radicals to combat oxidative stress [115]. Interestingly, carotenoids have been described to decrease fluidity of the bilayer similar to sterol compounds and hence may also be involved in lipid domain formation [116].

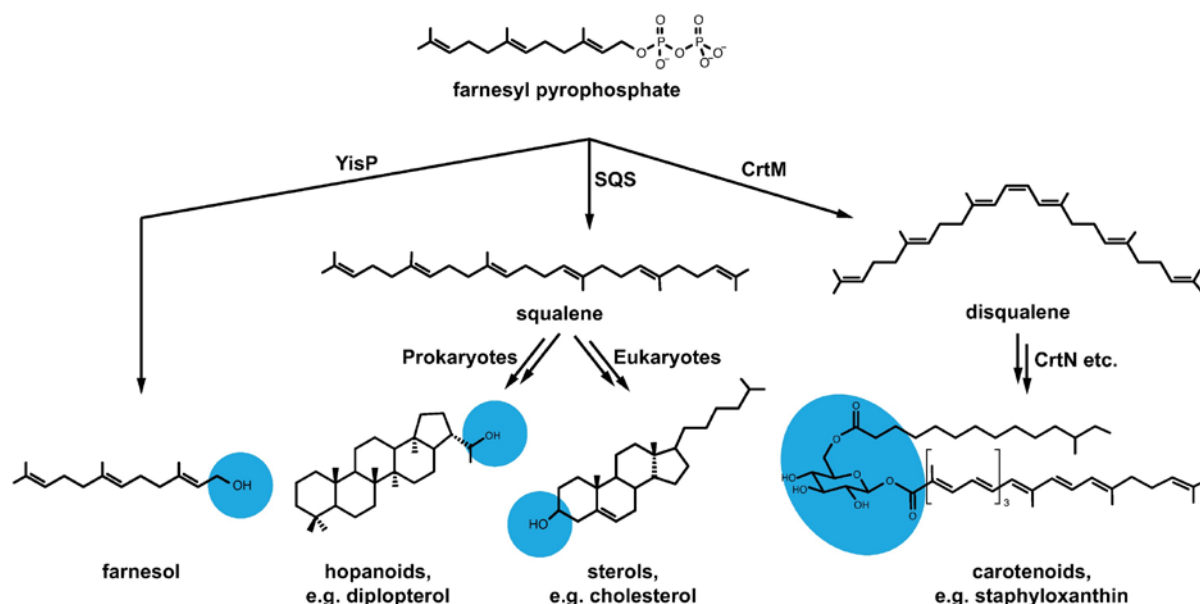


**Fig. 1.1: Biosynthetic pathway to produce terpenoids**

Farnesyl pyrophosphate (FPP) is a terpenoid precursor molecule that is a substrate of the squalene synthetase homologues YisP (found only in *B. subtilis*), SQS (e.g. *Homo sapiens*) and CrtM (e.g. *S. aureus*). Although these enzymes are structurally similar, they catalyze different reactions. YisP dephosphorylates FPP to farnesol. Squalene synthetases (SQS) use FPP to produce squalene, the precursor of hopanoids in prokaryotes and sterols in eukaryotes. CrtM of *S. aureus* catalyzes the reaction of FPP to disqualene to eventually produce staphyloxanthin. All exemplarily chosen molecules are predominantly hydrophobic, except for hydrophilic residues (highlighted in blue), which allows them to unidirectionally organize in the inner or outer leaflet of a lipid bilayer.

The concept of bacterial lipid rafts analogues emerged with the discovery of a functional dependence of physiological processes on both flotillin and on production of carotenoid-like lipid species in bacteria [117]. The correct sub-cellular localization and functionality of DRM-associated proteins in *B. subtilis*, depends on the catalytic activity of the enzyme

YisP that catalyzes the dephosphorylation of farnesyl diphosphate to farnesol (see also Fig. I.1) [117,118]. Interestingly, farnesol itself displays cholesterol-like properties: It recovers the physiological defects of a YisP deletion mutant and may thus represent a potential cholesterol-surrogate of bacteria [118]. Along with the discovery of potential domain forming lipids in bacteria, it was appreciated that bacteria harbor flotillin-like proteins in their genomes, which are highly conserved [81,119,120]. Similar to eukaryotic flotillins, bacterial flotillin-like proteins might represent an important architectural feature and physiological processes in these microdomains. This resembles the typical hallmarks defined for eukaryotic lipid rafts and thus, the bacterial lipid-raft analogues were named functional membrane microdomains (FMMs).

### **I.5 FMMs in the model organism *B. subtilis***

The first definition of bacterial lipid raft-analogues, along with the appreciation that the raft-scaffold protein flotillin is conserved in bacterial species, is indicative that FMM-mediated membrane organization is a conserved principle in prokaryotes. Before the first functional description of FMMs in bacteria was proposed, the association of flotillin-homologues with the DRM was already described in *Bacillus halodurans* [121]. However, a functional role of flotillin-proteins was not assigned and a connection to bacterial membrane organization remained elusive. The first functional description of bacterial flotillins and its possible connection to lipid raft-like structures was made in the soil-dwelling bacterium *Bacillus subtilis*. The bacterial flotillin homologue FloT was found to organize in punctate patterns in the membrane and to be part of the DRM, since it was readily floating on a Triton-X100 sucrose gradient, a key hallmark of proteins of eukaryotic lipid rafts [122]. This study described the first molecular function of flotillins in bacteria, suggesting FloT is in a complex with FtsH, a FMM-harbored protease that indirectly affects Spo0A-regulated pathways [122-126]. In *E. coli*, a functional connection of FtsH with flotillin homologues (HflK/HflC) was already discovered, but a role of flotillins as FMM scaffolding proteins in bacteria was not proposed. Similar to *B. subtilis*, the flotillin-homologues HflK and HflC of *E. coli* form a tight complex with FtsH, which is essential for the functionality of FtsH [127-130]. Further investigation of the *B. subtilis* FtsH-flotillin interaction found that both flotillin homologues of *B. subtilis*, FloA and FloT, physically interact with FtsH and the simultaneous depletion of both flotillins leads to delocalization and malfunction of FtsH. A consequence of this is an

accumulation of FtsH substrates, which eventually disturbs FtsH-regulated processes, like biofilm formation or sporulation efficiency [122,126].

The *B. subtilis* flotillin homologue FloT (previously YuaG) is a 55.9 kDa protein that is membrane-associated and both C- and N-terminus face the cytosol, similar to eukaryotic flotillins [122,131]. Moreover, FloT also forms oligomeric complexes with variable sizes ranging from 110 kDa (Dimer) to approximately 2 MDa (36-mer), which was independently demonstrated for recombinant FloT, as well as FloT from *B. subtilis* membrane extracts [131,132]. FloT foci can be observed in the membrane as ~60 nm foci that are highly dynamic, yet the size might differ depending on the strain background [133]. Due to differential activity of the promoter controlling the operon containing the FloT gene, only 1-3 FloT foci are present during exponential growth phase. Cells of stationary growth phase have increased promoter activity and thus form of up to 6-7 foci per cell [122,132]. The difference in protein abundance could be explained with the proteins that interact with FloT and require its scaffolding activity, because most of the FloT-regulated proteins fulfill functions in secondary metabolism and are important for adaption to the stationary growth phase [132].

The flotillin protein FloA of *B. subtilis* (previously YqfA) is a 35.6 kDa protein and the N-terminus is highly similar to FloT, likewise both termini face the cytosol. The soluble part on the C-terminus is shorter than FloT, but also oligomerizes into multimers bigger than 600 kDa [133]. FloA is ubiquitously expressed during exponential and stationary growth phase and forms between 10 and 20 membrane foci [117,126,132]. Similar to FloT, the foci of FloA are highly dynamic and have been independently reported to be ~45 nm in size [132,133].

Both *B. subtilis* flotillins, FloA and FloT, have a conserved SPFH domain (synonymous with PHB domain), which is potentially involved in lipid binding [82,119]. It was reported that a recombinant SPFH/PHB domain of FloT readily forms oligomers, suggesting that this domain also contributes to flotillin oligomer formation *in vitro* [131]. The soluble part on the C-terminal end of FloA and FloT shows differences in length and interestingly, this portion defines the shape and size of the membrane foci: A genetic exchange of the C-terminus of FloA and FloT switches shape, size and number of the membrane foci [132]. This region contains four repeats of glutamate (E) and alanine (A), so-called EA-repeats, that encode coiled-coil motifs. In the SPFH protein family,

these motifs are unique to flotillins and thus this region is often referred to as flotillin domain [82,84]. As discussed in the previous section, EA-repeats in eukaryotic flotillins were reported to mediate oligomerization [134]. Indeed, site-directed mutagenesis of EA-repeats of FloA and FloT in *B. subtilis* results in flotillin delocalization and disperses the membrane foci, suggesting that the EA-repeats are critical to form the oligomers *in vivo* [132]. It remains elusive if and how EA-repeats mediate the differences in foci formation and also if EA-repeats are involved in binding to other FMM proteins to sequester them to FMMs.

Apart from a few exceptions, in most bacterial species flotillins are co-transcribed as the second gene of an operon containing two and sometimes three genes in total [81,120,135]. The proteins encoded upstream of flotillin belongs to the class of NfeD proteins. In *B. subtilis*, NfeD and flotillin proteins co-localize and can be co-purified in the DRM suggesting that NfeD proteins also fulfill a critical role in the FMMs of bacteria [132,136,137]. Although molecular details on potential functional connections to FMMs remains elusive, a deletion of both flotillin and NfeD proteins exerts strong pleiotropic defects on the cell suggesting that presence of both proteins is essential for their functionality [136]. The protein encoded downstream of flotillin is not conserved in all flotillin harboring operons. YuaI, the cognate partner of FloT, is part of the family of GCN5-related acetyl transferases, yet the function of this protein is still unknown [119].

As discussed in the previous chapter, in *B. subtilis* the putative squalene synthase YisP plays a critical role in FMM-associated processes such as biofilm formation [117]. Although it shows high sequence homology to other squalene synthases (such as the human SQS or CrtM of *S. aureus*), this enzyme is not a squalene synthase, but a phosphatase that removes a phosphate groups from farnesyl diphosphate to generate farnesol [118]. The inhibition of this enzyme with small molecules or a genetic depletion of YisP cause malfunctioning of FMM-associated processes, e.g. biofilm formation [117]. These defects can be recovered by exogenously adding farnesol to the cells, although it is not known if farnesol itself is a constituent lipid of the FMM or if it is part of a pathway to generate other lipid species [118]. Moreover, it is unknown if this is the only lipid species constituting FMMs in *B. subtilis* or if other lipid species contribute to FMM formation.

## I.6 Bacterial processes regulated by FMMs

Since the discovery of bacterial FMMs, several physiological processes have been functionally linked to bacterial raft analogues and FMM-integrity seems to depend on both flotillins and the constituent FMM-lipids. FMM-associated proteins in bacteria were identified in several studies by co-immunoprecipitation assays with tagged flotillin [137], by isolation of protein complexes associated with flotillin [132] or by identification of DRM proteins with mass-spectrometry [117,126,138]. Although many of the identified proteins have been proven to be functionally linked to FMMs, there is still an ongoing debate if the entity of FMM proteins form stable microdomains clusters. Super resolution microscopy data showed that only a small fractions of flotillin-interaction proteins indeed colocalize with flotillin in the same clusters [133]. This raises the questions if flotillin forms stable microdomains with all DRM proteins or if there are distinct clusters and flotillin only transiently interacts with other FMM proteins. Further studies will be required to clarify the precise molecular function of flotillin and its role in FMM integrity. The next paragraphs sum up the current knowledge about physiological processes in bacteria regulated by FMMs.

### I.6.1 Developmental processes

The first physiological processes connected to bacterial FMMs were developmental programs in *B. subtilis* [117,122]. Bacteria are able to develop complex multicellular communities with a heterogeneous population of cells. Although genetically identical, different phenotypic subpopulation coexist that share explicit tasks to specialize for certain needs. One well-characterized example of microbial development, is the elaboration of surface-attached microbial communities in *B. subtilis* [139-141]. These so-called biofilms consist of cells encased in a self-produced, extracellular matrix composed of proteins and polysaccharides [142]. The proteins TasA and BslA are two major proteinaceous components providing structure to the biofilm matrix [143-145]. Additionally, polysaccharides produced by enzymes of the *eps*-operon contribute to the structural integrity of the biofilm [142,146,147]. In *B. subtilis* biofilm formation is regulated by a complex network with Spo0A as a master regulator. Spo0A was initially found as a main transcription factor to initiate endospore formation [148]. However, intermediate levels of Spo0A phosphorylation were found to activate the above mentioned *eps* and *tasA* operons leading to the differentiation of a subpopulation of cells that produces the extracellular biofilm matrix [149].

To initiate Spo0A-mediated differentiation programs, the cells must sense environmental signals and incorporate the status of nutrient availability to effectively coordinate development of subpopulations [150]. The activation of the Spo0A-signaling cascade is mediated by five histidine kinases (KinA-E) that sense diverse environmental stimuli, for instance (micro-)nutrients (glycerol, manganese, L-malic acid by KinD) [151], oxygen (by KinA and KinB) [152] and intercellular or interspecies signaling molecules (e.g. nystatin or surfactin by KinC) [153]. Upon sensing the corresponding stimulus, the kinases feed into a phosphorelay system consisting of Spo0B and Spo0F that successively pass the phosphate group to Spo0A (See Fig. I.2)[154]. An additional level of complexity in regulating these differentiation programs is added by the action of Rap phosphatases. While stimuli and regulation of those phosphatases are largely unknown, it was described that they dephosphorylate Spo0B and Spo0F of the phosphorelay and thus negatively contribute to Spo0A phosphorylation [155,156].

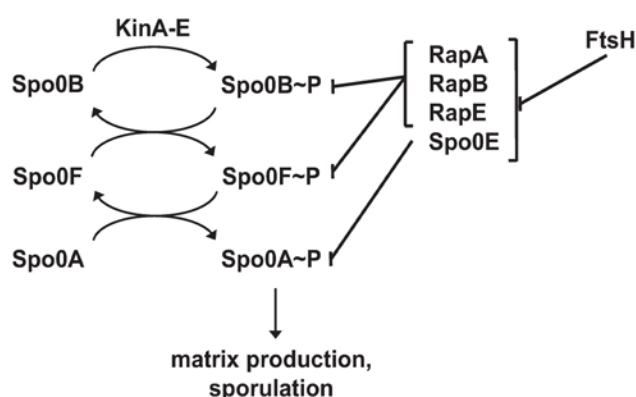


**Fig. I.2: Signaling cascade that regulates subpopulations of matrix producers and spores**

The five kinases KinA – KinE sense diverse environmental stimuli and feed into a phosphorelay system by phosphorylating Spo0B. The phosphate group is passed to Spo0F and eventually to Spo0A. Spo0A regulates different cascades of genes depending on the level of its own phosphorylation (either matrix producers or spore formation). The proteins of the phosphorelay can be dephosphorylated by the phosphatases RapA, RapB, RapE and Spo0E, which are proteolytic targets of FtsH.

FMMs are involved in Spo0A-mediated differentiation by organizing membrane-related regulatory processes by two different mechanisms: First, the kinase KinC is part of the DRM and has been shown to delocalize in absence of intact FMMs, for instance by depletion of the FMM-scaffold flotillin or by diminishing production of FMM lipids via YisP deletion or inhibition [117]. Additionally, the activity of the FMM-harbored protease FtsH depends on the integrity of the FMMs. FtsH proteolytically degrades Rap-phosphatases, which in turn dephosphorylate proteins of the Spo0A-phosphorelay [125]. Malfunctioning of FtsH (e.g. by flotillin depletion) leads to a constitutive

dephosphorylation of the phosphorelay proteins and thus cause defects in coordinated differentiation [122,124,126,157]. Thus, FMMs are crucial for organizing signaling processes that lead to the environmentally-driven formation of multicellular communities.

### **I.6.2 Kinase signaling**

The integration of extracellular information and adaption in gene expression is mediated by membrane-bound histidine kinases that sense distinct environmental stimuli like presence of (micro-)nutrients, oxygen availability or cell wall integrity [158]. As a platform to concentrate signaling processes, the localization in FMM restricts the interaction of interaction partners to a defined area. An important role of the flotillin scaffold activity on kinase dimerization was proposed for the *B. subtilis* histidine kinases KinC, PhoR and ResE [159].

It has been reported that KinC colocalizes with FloT and that KinC activity depends on FMMs [117]. Moreover, it was demonstrated that FloT physically interacts with KinC and the scaffold activity of FloT influences KinC dimerization [160]. Two recent studies, where different genetic approaches were used [161], challenged these findings and argue that KinC activity is independent of flotillins [162] and that KinC colocalization with flotillins is only transient [133]. Thus, further experimental evidence is required to elucidate the functional relationship of KinC, flotillin and FMMs [163].

A similar scaffolding activity of flotillins has been reported for the *B. subtilis* sensor kinases PhoR and ResE, whose correct function depends on FloA and FloT, respectively. Individual defects in the PhoR- and ResE-regulon were reported, when the cognate flotillin protein was deleted [132]. For instance, ResE regulates genes involved in adaption to oxygen limiting conditions (e.g. nitrate respiration) [164]. In turn, depletion of FloT and malfunctioning of the ResE (probably by insufficient dimerization) reduces the capability of *B. subtilis* to grow in nitrate respiration conditions when atmospheric oxygen is reduced [132].

### **I.6.3 Cell shape and division**

In eukaryotic cells lipid rafts are inevitably linked to the cytoskeleton. As discussed in chapter I.3, the association of rafts with the cytoskeleton is important for a variety of physiological processes. In bacteria, the cytoskeletal elements FtsZ and MreB are crucial



for division and maintaining cell shape [165-167]. The actin-homologue MreB fulfills a critical role in shape maintenance of rod-shaped bacteria, since it is in a complex with proteins of the cell-wall polymerization machinery. Malfunctioning of this machinery often leads to shape defects and although pleiotropic shape defects of a double mutant of FloT and dynamin-protein DynA were reported, there are no evidences supporting a connection of FMMs or flotillin with the tubulin homologue MreB [168]. In contrast, it has been demonstrated recently, that MreB organizes regions of increased fluidity, which are – in contrast to FMMs – characterized by decreased rigidity and thus higher fluidity [101,102].

Besides MreB, bacteria possess another cytoskeletal element namely the tubulin-homologue FtsZ. During cell division, this protein forms a cytokinetic ring (Z-ring) at midcell [169-171]. The Z-ring serves as a scaffold to recruit a plethora of proteins in a spatiotemporally controlled manner to form the divisome protein complex [172,173], that eventually drives membrane and cell wall invagination by a treadmilling mechanisms [174-176]. In a highly coordinated fashion, the cell elongates, separates the two nucleoids and finally the Z-ring constricts. Along with this constriction the newly synthesized cell wall separates the two daughter cells and the accurate timing of cell division in respect to cell elongation defines cell length [165]. The positioning of the Z-ring at midcell involves several systems that restrict the spontaneous polymerization of FtsZ subunits to this site of the cell. Firstly, the nucleoid occlusion system prevents formation of the Z-ring to sites where DNA is absent [177,178]. The second system that directs Z-ring formation to midcell is the Min-system, which inhibits FtsZ polymerization at the cell poles [179,180]. Various proteins have been described as regulators for FtsZ polymerization that can affect this process in a positive or negative manner [181].

A controversial role in Z-ring assembly is attributed to the protein EzrA (extra Z-rings A). Initially, EzrA was described as a negative regulator for Z-ring assembly due to deletion studies demonstrating that a loss of EzrA results in generation of additional Z-rings in polar sites [182]. This observation was strengthened by *in vitro* polymerization studies of FtsZ indicating that EzrA indeed has negative effects on FtsZ polymerization by directly interfering with the GTPase activity of FtsZ [183]. Contradictory, EzrA co-localizes with Z-ring at midcell [173,182], which is unexpected for a negative regulator of FtsZ-assembly. Moreover, EzrA deletion strains have an increased cell length, albeit they are capable of generate multiple Z-rings [182,184].

studies in *B. subtilis* FMMs suggested that EzrA might be part of the protein cargo [126]. Although no molecular mechanisms are known how FMMs and cell division are connected, EzrA might fulfill an important role during this process.

#### **I.6.4 Secretion**

In order to export proteins from the cytosol to the extracellular space, the hydrophobic membrane barrier must be overcome and thus bacteria have evolved highly specialized secretion systems to pass peptidic macromolecules over their cell membrane. Bacterial translocation systems are typically composed of several protein subunits and can form multimeric complexes with a size up to several megadalton that often require complex assembling procedures [185]. As membrane signaling and assembling platforms, it can be speculated that FMMs are involved in the assembly or functionality of these membrane spanning protein complexes.

For example, the general secretory pathway, the Sec-system, requires FMMs for its function in *B. subtilis* [137]. Translocation of unfolded substrates via the Sec-system is considered the 'standard' secretion pathway and is conserved within bacteria and even in mitochondria [186-188]. The Sec-system consists of several proteins that bind, unfold and deliver substrates to a membrane-spanning secretion channel. This channel consists of SecY, SecE and SecG, through which unfolded substrates are translocated into the extracellular space and refold [189]. Interestingly, the channel component SecY was found as a direct interaction partner of FloT in *B. subtilis* [137]. Moreover, FloT and SecY foci co-localize and gene deletions that perturb FMM architecture, like single or double depletion of *B. subtilis* flotillins as well as depletion of the FMM-lipid producing enzyme YisP, decreased of the extracellular protein content [137]. This suggests an important role of FMMs during secretion and although molecular details are still elusive, one might suggest that FMMs serve as a platform to assemble the Sec translocon, maybe by delivering or stabilizing SecY to effectively assemble the SecYEG secretion channel. Interestingly, it was already described that SecY preferentially associates with negatively charged lipids, similar to FloT, which associates with the negatively charged lipid cardiolipin [122,190].

Besides the Sec-secretion system, bacteria can encode specialized secretion systems that fulfil a variety of functions, such as the delivery of proteins in the extracellular space, specifically into host cells or other bacteria, but there are also secretion system variants

that mediate pilus assembly or micronutrient uptake. So far, nine different secretion systems (Type I – Type IX) had been described experimentally [185,191-197]. Since most of them consist of several protein subunits to form a macromolecular complex on the membrane, it is tempting to speculate that FMMs and its flotillins scaffold serve as assembling platforms for at least some of those secretion systems, similar to the SecYEG translocon [137]. Indeed, the *Campylobacter jejuni* flotillin homologue Cj0268c was reported to be essential for T3SS (type III secretion system)-mediated virulence [198,199]. Likewise, depletion of the flotillin homologue HP0248 of *Helicobacter pylori* leads to reduced virulence, probably by a malfunctioning T4SS (type IV secretion system) [200].

The nomenclature of Type-secretion systems in bacteria is somewhat misleading, because some authors suggest to use the type I - VIII secretion systems exclusively for Gram-negative secretion systems. Other secretion systems, that are present in both Gram-positive and Gram-negative or exclusively in Gram-positives, should be listed according to their function, like Tat, Sec, WSS (WXG100 secretion system), FEA (flagellar export apparatus), FPE (Fimbillin-protein exporter)[193]. For this work however, another nomenclature was used, as proposed by Abdallah et al. [191] and Abby et al. [195]. These authors argue that type VII and VIII secretion systems of Gram-negative species – as proposed by Desvaux and co-workers [193] – are no secretion systems *per se*, because they only translocate Sec-secreted proteins from the periplasm to the extracellular space over the outer membrane. Thus, type VII secretion system should be used exclusively for secretion systems that secrete substrates with WXG100 motifs, that are typically present only in Gram-positive species [191,195,201].

Important in this work is the association of *S. aureus* FMMs with the type VII secretion system (T7SS). The T7SS was first discovered in mycobacteria and is also called Esx- or ESAT-6 secretion system, referring to the name of the cognate substrate ESAT-6 (Early secretory antigen target with a size of 6 kDa), which is synonymous to EsxA [202]. Another less frequently used description is WSS (WXG secretion system), highlighting the presence of a crucial WXG (tryptophan – X – glycine) motif found in several substrates, such as EsxA; the role of this motif is discussed below. In mycobacteria, this system is an important virulence factor and is involved in development of tuberculosis [191,203]. Initially, the importance of T7SS-mediated virulence was discovered by elucidating the avirulent phenotype of the tuberculosis vaccine strain BCG that lacks a

large portion of its genome including the operon encoding the T7SS [204]. Mycobacterial species harbor several variants of the T7SS (often referred to as ESX1 through ESX5) that are specialized in translocating substrates out of the cells [201], but have also been suggested to be involved in iron homeostasis [205-207] or DNA uptake [208,209].

The central and conserved players in the operon organization of all T7SSs harboring species are an ATPase that potentially forms a hexameric ring upon substrate binding and thus representing a central part of the translocon, and at least one substrate with an WXG100 motif (depending on the nomenclature typically called EsxA or EsxB) [210-212]. Besides mycobacteria, only Gram-positive species are found to contain homologues of T7SSs in their genome and particularly mycobacteria harbor more than a single T7SS copy in their genome [191,201]. T7SSs have been functionally described in *B. subtilis* [213,214], *Streptomyces scabies* [215], *Bacillus anthracis* [216], *Listeria monocytogenes* [217] and *Staphylococcus aureus* [218,219], where at least one substrate is translocated under the investigated conditions. While the biological role of the T7SS in *Bacillus* species is unknown, the T7SS in *S. scabies* is dispensable for plant-pathogenicity, yet important for spore development [215]. Likewise, in *L. monocytogenes* the T7SS is not only dispensable for virulence, but rather detrimental [217]; a biological role of T7SSs in many Gram-positive bacteria remains thus to be elucidated.

The best-studied example in Gram-positive bacteria is the T7SS of *S. aureus*, where it is involved in modulating the immune response to establish persistent infections [220], abscesses [218,221], nasal colonization [219], modulation of cytokine responses [222], host-cell apoptosis [223] and competition with other bacteria [224]. An overview of the *S. aureus* T7SS operon organization and distribution of the proteins in the cell is presented in Fig. I.3.

The T7SS of *S. aureus* consists of essential, accessory and secreted proteins, which is reflected in their original gene description as Esa- (ESAT-6 secretion accessory), Ess- (ESAT-6 secretion essential) and Esx-proteins (ESAT-6 secretion extracellular). Like all T7SSs, central to the *S. aureus* version is EssC, a FtsK/SpoIIIE-homologue ATPase, that has an N-terminal FHA domain, potentially to interact with other components of the T7SS [225], followed by two transmembrane segments and two ATPase domains, that might power the translocation [212,226]. Structural studies of EssC homologues suggest a model of EssC multimerization upon substrate binding and thereby creating a

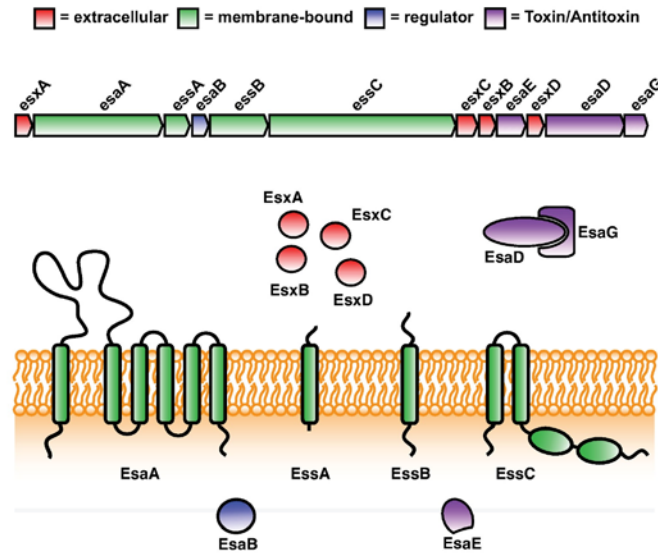


**Fig. I.3 Organization of the type VII secretion system (T7SS) of *S. aureus***

The upper panel shows the organization of the T7SS operon of *S. aureus*, the lower panel shows the organization of the T7SS proteins within a cell. Membrane proteins that build a putative secretion complex are colored in green, the genetic regulator of T7SS expression in blue, the extracellular proteins are colored in red and proteins that encode a toxin-/antitoxin system are colored in purple.

potential secretion channel with a 30 angstrom pore [210,212]. Besides EssC, three other membrane components are essential for secretion in *S. aureus*: (I.) EssA is a small transmembrane protein with no homology to any known protein or domain and its deletion abolishes secretion of T7SS substrates [218-220]. Similarly, EssA homologues of *L. monocytogenes* or *Bacillus* species are essential for secretion and likewise the function of EssA during secretion is unknown [213,214,217]. (II.) EsaA has six transmembrane domains and a large extracellular domain. Initially, EsaA was not considered essential for secretion of substrates in *S. aureus*, when using a mariner based transposon mutant [218]. However, the transposon was inserted on the far C-terminus and probably still rendered functional protein [218,219]. In turn, secretion is indeed diminished in a clean deletion of EsaA, which leads to the misleading description as a non-essential accessory protein of the T7SS (EsaA = ESAT-6 secretion accessory A). The extracellular domain of the *B. subtilis* homologue of EsaA forms oligomeric fibers that can be hijacked by bacteriophages [227-229], suggesting that EsaA-homologues might span peptidoglycan meshwork. (III.) EssB is a single-pass transmembrane protein with a 25 kDa N-terminus facing the cytosol and an equally sized C-terminus on the outside of the cell. *In vitro* studies with recombinant EssB variants suggested that both extracellular and intracellular domains tend to form conditional dimers [230,231]. Transmission electron microscopy demonstrated that full-length EssB forms rod-shaped oligomers [232]. Moreover, these structural analyses suggested a pseudokinase-fold

reminiscent of serine-threonine kinases that might serve as a hub for potential interactions with other proteins of the complex, for instance with the FHA domain of EssC [212]. Surprisingly, EssB was only detected as monomer *in vivo* without any notable interaction to any other membrane component of the T7SS [233]. Thus, it remains elusive if proteins of the T7SS of *S. aureus* act in a cooperative manner as a 'sequential secretion system' or the membrane bound components indeed form a multiprotein secretion complex as its homologues in mycobacteria [234,235], which is very sensitive to purification and extraction from the cell membrane.

Besides these essential membrane bound-proteins, the T7SS operon of *S. aureus* encodes several secreted proteins and the presence of EssA, EssB, EssC and EsaA is essential for their secretion. Initially, EsxA and EsxB were described as the main secreted effectors of the T7SS [218]. They are considered prototypical T7SS substrates due to the presence of a conserved WXG motif that forms a flexible loop consisting Trp-X-Gly and this loop connects two anti-parallel alpha helices [236]. The family of WXG100 proteins – small proteins with 100 amino acids and the WXG motif – are besides the FtsK/SpoIIIE ATPase the only conserved component in all T7SSs [191,211].

In mycobacteria, the WXG100-family proteins ESAT-6 (=EsxA) and CFP-10 (=EsxB) are the main virulence factors to establish the pathogenic outcome tuberculosis [203]. They form heterodimers and the extended C-terminus of EsxB carries a Met-X-Phe recognition motif that is crucial for its secretion [237]. Moreover, the binding of EsxB homologues from *Thermomonospora curvata* to the ATPase promotes ATPase multimerization and potentially initiates secretion. Interestingly, EsxA counteracts this mechanism by cooperatively binding to EssC and suggestively regulates secretion [210]. Also, WXG100 proteins in mycobacterial T7SSs seem to be interdependent [238] and are essential for secretion of non-WXG substrates via T7SS [201].

In *S. aureus*, deletion of EsxA and EsxB leads to reduced formation of renal and kidney abscesses in a mouse model, proposing an important role of these substrates in infective scenarios [218]. Initially, it was proposed that EsxA of *S. aureus* might act as a transporter or adaptors for other T7SS-secreted virulence factors [236]. However, it has been shown that transfection of epithelial cell lines with EsxA alone has a direct effect on the apoptosis pathway, which implies that EsxA itself might be a virulence factor [223].

Similar to mycobacteria that also secrete non-WXG proteins via T7SS, the T7SS operon of *S. aureus* encodes several secreted proteins without prototypical WXG motifs: EsxC, EsxD, EsaD and EsaG. EsxA through EsxD were all named after their location outside of the cell (ESAT-6 secretion extracellular) and similar to reports in mycobacteria, secreted factors (both WXG and non-WXG proteins) show interdependence for secretion [222,238,239]. Deletion of a single Esx-protein abolishes secretion of any other Esx proteins and in some cases even affects their stability [239]. Moreover, it is unknown, which of the secreted factors (apart from EsxA) interact with host cell targets to mediate virulence. Additionally, EsxC was shown to be immunogenic and generates an immune response, both in murine models and in patient sera, which suggests a role as a potential virulence factor itself [220]. Yet, it cannot be ruled out that only EsxA or other non-Esx proteins are the actual T7SS-virulence factors and EsxBCD only act as adaptor proteins, chaperons or co-substrates that are only involved in efficient secretion without being a toxin *per se*.

Apart from Esx proteins, the *S. aureus* T7SS specifically secretes proteins of a toxin-antitoxin system to compete with other staphylococci [224,240]. It has been shown that the T7SS of *S. aureus* is highly versatile and shows an unexpected genetic diversity amongst different clinical isolates [211]. While membrane bound components and EsxA are conserved in staphylococci, genes encoded downstream of EssC show high variability. This region also includes proteins of a toxin-antitoxin system comprised of EssD, EsaE and EsaG found in well-studied clinical isolates like Newman, COL or clones of the USA300 and USA700 lineage. In contrast, antitoxins are absent in strains of clonal complex 8, strains of the sequence type 398 (ST398), as well as laboratory strains such as RN4220 or RN6390 [211,224]. The first description of the nuclease toxin EsaD as an essential component of the secretion apparatus turned out to be a product of a nuclease-deactivating point mutation during cloning in *E. coli*, since this nuclease can only be cloned in the presence of the antitoxin EsaG [224,240,241]. This EsaDG protein complex is delivered to the membrane via EsaE and secreted, which leads to dissociation of toxin and antitoxin. The toxin can attack other bacteria, particularly other *S. aureus* isolates that do not encode the antitoxin [224]. Mechanistic insights into the action of this toxin as well as how it is delivered into susceptible *S. aureus* cells without the antitoxin is unknown.

## I.7 Bacterial model systems to study FMMs

Several studies showed the existence of FMMs and flotillin homologues in several bacterial species including *B. burgdorferii* [138,242,243], *B. anthracis* [244], *H. pylori* [200] or *S. aureus* [245], which highlights the importance of FMMs in bacterial physiology. Major work on FMMs has been done in the model organism *B. subtilis* [117,122,132,133]. Along with the discovery of fluorescent proteins and the establishment of fluorescent microscopy to visualize proteins within bacterial cells, *B. subtilis* also rapidly evolved as a model organism in bacterial cell biology. The size of about 2  $\mu\text{m}$  in length facilitates localization studies on a fluorescence microscope. Being a model organism for the study of spore formation, competence, biofilm formation and cell biology, a plethora of genetic tools are available to modify the genome of this bacterium. The presence of FMMs in *B. subtilis* was detected occasionally by studying factors involved in biofilm formation: The biofilm-triggering kinase KinC was shown to co-localizes with flotillins and KinC activity depends on lipid compounds produced by YisP [117]. Due to its genetic tractability, size and well-known molecular mechanisms, *B. subtilis* turned out to be ideal to study bacterial FMMs and functionally associated processes. Moreover, *B. subtilis* encodes two flotillin proteins with both redundant and specialized roles in cellular processes similar to eukaryotic systems [131,132,160]. Contrary, several other bacterial species have been described to harbor only a single flotillin operon in their genomes [120]. This raises the question as to why species evolved with more than one flotillin-containing operon and what are the specialized roles for those flotillin. On the other hand, how can bacteria with a single flotillin-containing operon coordinate a multitude of FMM-processes without being able to dedicate distinct FMMs for specialized needs? Thus, central to this work is the use of *S. aureus* as an organism with only a single flotillin operon in its genome.

*S. aureus* is a commensal resident of the human skin and nose and an opportunistic pathogen, that can cause a variety of infections ranging from harmless skin-lesions, hair-follicle traumas, or furuncles to life-threatening diseases like pneumonia, osteomyelitis, formation of abscesses or bacterial sepsis. The difficulty in the treatment of staphylococcal infections is due to the ability of *S. aureus* to form hard-to-disperse biofilms on medical implants and catheters. Additionally, *S. aureus* species harbor an arsenal of virulence factors, including hemolysins, clumping factors, adhesins and superantigens. *S. aureus* has a high recombination rate, leading to the emerge and



spread of antibiotic resistance. This is a problem in treatment of community and hospital associated *S. aureus* infections with mortality rates up to 20 % for the latter [246,247].

Concerning FMMs, *S. aureus* displays an interesting architecture. Firstly, it only bears a single homologue of flotillin in its genome (FloA, syn. SA1402, NWMN\_1472, USA300HOU\_1574) that has a 78 % sequence identity to FloA of *B. subtilis* (and only 34 % to FloT). The lack of a second flotillin (FloT homologue) raises the question how this bacterium can organize a variety of FMM-associated processes with a single flotillin scaffold (and thus only one type of membrane microdomain) and why other bacteria such as *B. subtilis* require two flotillins (and probably three types microdomains: FloA-, FloT- and FloAT-containing microdomains).

Another interesting feature of *S. aureus* FMMs are the constituent lipids. Although still nothing is known about the precise lipid molecules that compose FMMs, the homologue of the *B. subtilis* FMM-lipid producing enzyme YisP in *S. aureus* is called CrtM. In comparison to YisP, which is a phosphatase, CrtM is a dihydrosqualene synthetase [118]. This enzyme is part of an operon involved in the production of the carotenoid pigment staphyloxanthin. Staphyloxanthin is responsible for the typical golden coloration of *S. aureus* and fulfills important roles during infections. Its properties as an antioxidant can counteract attacks of the immune system with reactive oxygen species [248,249]. Structurally, staphyloxanthin belongs to the class of non-cyclic terpenoids and treatment with zaragozic acid leads to decoloration of *S. aureus* cells concomitantly with reduced protease secretion [117]. Thus, staphyloxanthin is an authentic candidate for FMM-constituting lipids and its chemical structure resembles eukaryotic raft lipids.

Both models can reveal important aspects of flotillins and lipids that contribute to FMM formation and elucidate both differences and redundancy of FMMs harboring only a single flotillin (FloA, FloT) or two (FloA and FloT). Moreover, preliminary evidences suggest that the major lipid species in the FMMs of *B. subtilis* and *S. aureus* both belong to the class of terpenoids, but due to differences in the involved enzymes, the lipid product produced in those pathway might be substantially different. Moreover, using bacterial models allows to ask more intricate questions about membrane organization by flotillins and FMMs. Although bacteria are considered less complex than eukaryotic cells, they follow the same principles for membrane organization and thus, their high

genetic tractability and simpler genetic architecture facilitates studies about lipid raft-/FMM-driven membrane organization.

## **I.8 Aims of this work**

The existence of bacterial lipid raft analogues emerged very recently and thus knowledge about raft-mediated membrane organization is just beginning to be elucidated. Established methods from eukaryotic raft research facilitated the investigation of bacterial FMMs, yet prokaryotes are genetically more tractable and might be an easier model to handle genetically. In turn, the simplicity and tractability of bacterial models will be used to study fundamental questions in membrane organization. In the first part of this study (chapter II), following question will be addressed: Can a bacterial model system be used to understand molecular principles of flotillin that are not only important for prokaryotes, but could be translated to eukaryotic, raft-mediated diseases? Interestingly, in severe neurological diseases, such as Alzheimer's or Parkinson's disease, the progression of diseases concomitantly occurs with an upregulation of flotillin [60,93]. Using the bacterial model organism *B. subtilis*, it will be investigated if flotillin overexpression has negative effects on FMM-associated physiological processes.

The conservation of FMMs in bacteria suggests important roles in bacterial physiology. However, only a handful of studies pointed towards the importance of FMMs and flotillins in bacterial pathogens, including *B. burgdorferii* [138,242,243], *B. anthracis* [244], *H. pylori* [200] or *S. aureus* [245]. Thus, in the second part of this work (chapter III and IV) an in depth DRM proteome analysis will be conducted in a bacterial pathogen. To this end, *S. aureus* will be used to determine quantitative changes in the DRM proteome via mass spectrometry in different growth conditions. This type of proteomic assay will not only reveal dynamics of the DRM content and thus potential changes in FMM proteome, but also reveal protein complexes that might be functionally associated with FMM and the corresponding scaffold FloA. A particular emphasis will be put on complexes involved in virulence determination of *S. aureus*. If a protein complex can be found that is functionally dependent on FMM, several small molecules can be used to disturb this FMM-associated processes and thus interfere with progression of *S. aureus* pathogenesis. These small molecules or anti-FMM molecules have known inhibitory activity on FMM-lipid producing enzymes or are suggested to replace cholesterol-like

compounds from the membrane [245]. Using these molecules in have been shown to interfere with FMM integrity [117,244]. Targeting FMMs and FloA scaffold activity with anti-FMM molecules might be a novel therapeutic approach to treat staphylococcal infections.

## II OVEREXPRESSION OF FLOTILLINS IN *B. SUBTILIS*

In the publication 'Overexpression of flotillin influences cell differentiation and shape in *Bacillus subtilis*' it was shown that a synthetic bacterial model can help understanding fundamental questions related to the functionality of lipid rafts. *Bacillus subtilis* served as a simple and tractable model organism to elucidate the physiological defects of simultaneous overexpression of the FMM-scaffolds FloA and FloT. Interestingly, in eukaryotic lipid rafts increased flotillin levels have been associated with neurological diseases, however it is not known whether increased flotillin levels are the cause or consequence of disease.

Likewise, overexpression of the two flotillin proteins FloA and FloT in *B. subtilis* has a detrimental effect on cellular differentiation and cell shape. This effect was shown to be mediated by an unusual hyper-stabilization of the FMM-associated protease FtsH. FtsH is a known regulator of Spo0A-regulated differentiation pathways and its correct subcellular localization and activity depends on both FloA and FloT. Artificial overexpression of FloA and FloT and the resulting FtsH hyper-stabilization increases phosphorylation of the Spo0A-phosphorelay proteins Spo0B and Spo0F. This eventually leads to increased levels of phosphorylated Spo0A and substantially enlarges the subpopulation of matrix-producers and produces a wrinkled biofilm, even in the domesticated *B. subtilis* strain PY79.

Moreover, it was shown that FtsH activity influences the abundance of EzrA in the cell. EzrA is part of the FMM proteome in *B. subtilis* and regulates the formation of the cytokinetic FtsZ ring. The stabilization of FtsH activity by flotillin overexpression decreases the abundance of EzrA and thus leads to a more efficient septation guided by FtsZ. As a result, cells show severe defects in cell shape.

The work of this chapter shows that it is important to maintain physiological levels of the FMM-scaffold proteins FloA and FloT. Increases in flotillin levels may indeed influence FMM-associated proteins and cause a malfunction of FMM-harbored processes. This is an important finding, which might be applied to eukaryotic raft research.

## RESEARCH ARTICLE

# Overproduction of Flotillin Influences Cell Differentiation and Shape in *Bacillus subtilis*

Benjamin Mielich-Süss, Johannes Schneider, Daniel Lopez

Research Center for Infectious Diseases ZINF, Würzburg University, Würzburg, Germany

**ABSTRACT** Bacteria organize many membrane-related signaling processes in functional microdomains that are structurally and functionally similar to the lipid rafts of eukaryotic cells. An important structural component of these microdomains is the protein flotillin, which seems to act as a chaperone in recruiting other proteins to lipid rafts to facilitate their interaction. In eukaryotic cells, the occurrence of severe diseases is often observed in combination with an overproduction of flotillin, but a functional link between these two phenomena is yet to be demonstrated. In this work, we used the bacterial model *Bacillus subtilis* as a tractable system to study the physiological alterations that occur in cells that overproduce flotillin. We discovered that an excess of flotillin altered specific signal transduction pathways that are associated with the membrane microdomains of bacteria. As a consequence of this, we detected significant defects in cell division and cell differentiation. These physiological alterations were in part caused by an unusual stabilization of the raft-associated protease FtsH. This report opens the possibility of using bacteria as a working model to better understand fundamental questions related to the functionality of lipid rafts.

**IMPORTANCE** The identification of signaling platforms in the membrane of bacteria that are functionally and structurally equivalent to eukaryotic lipid rafts reveals a level of sophistication in signal transduction and membrane organization unexpected in bacteria. It opens new and promising venues to address intricate questions related to the functionality of lipid rafts by using bacteria as a more tractable system. This is the first report that uses bacteria as a working model to investigate a fundamental question that was previously raised while studying the role of eukaryotic lipid rafts. It also provides evidence of the critical role of these signaling platforms in orchestrating diverse physiological processes in prokaryotic cells.

Received 29 August 2013 Accepted 17 October 2013 Published 12 November 2013

Citation Mielich-Süss B, Schneider J, Lopez D. 2013. Overproduction of flotillin influences cell differentiation and shape in *Bacillus subtilis*. mBio 4(6):e00719-13. doi:10.1128/mBio.00719-13.

Editor Michael Gilmore, Harvard Medical School

Copyright © 2013 Mielich-Süss et al. This is an open-access article distributed under the terms of the [Creative Commons Attribution-Noncommercial-ShareAlike 3.0 Unported license](https://creativecommons.org/licenses/by-nc-sa/4.0/), which permits unrestricted noncommercial use, distribution, and reproduction in any medium, provided the original author and source are credited.

Address correspondence to Daniel Lopez, Daniel.Lopez@uni-wuerzburg.de.

Bacterial membranes are composed of different types of lipids, which tend to aggregate according to their physicochemical properties and accumulate into lipid domains that are immiscible with the surrounding lipids (1). The heterogeneous organization of membrane lipids leads to a lateral segregation of the embedded membrane proteins, which seems important for their functionality (2). One of the most interesting examples of the heterogeneous segregation of lipids and proteins is the formation of functional microdomains in the membrane of bacteria that are structurally and functionally equivalent to the lipid rafts of eukaryotic cells (3–5). Bacterial microdomains are membrane platforms that organize a group of proteins related to signal transduction and protein secretion (6). The integrity of these signaling platforms is essential for the correct functionality of the harbored proteins. Consequently, any alteration in their architecture severely inhibits the physiological processes related to the harbored proteins, such as biofilm formation, motility, competence, or protease secretion (6, 7).

The integrity of bacterial lipid rafts relies on the biosynthesis and aggregation of polyisoprenoid lipids and the presence of flotillin proteins (6, 8). Flotillins are membrane-bound proteins that localize exclusively in the lipid rafts and are usually considered a bona fide marker for the localization of lipid rafts. The function of

flotillins in lipid rafts is not entirely understood, yet it is believed that they may act as chaperone proteins to recruit protein cargo to lipid rafts and facilitate interactions and oligomerization (9–12). Hence, the presence of flotillin in lipid rafts is necessary for the correct functionality of the associated signaling processes. In eukaryotic cells, alterations in the functionality of flotillins often occur in association with severe physiological dysfunctions in cells (13). For instance, the development of Alzheimer's disease or Parkinson's disease is usually observed in cells that concomitantly overproduce flotillin proteins (14, 15), as well as in neuronal cells with severe lesions (16, 17). Despite this interesting correlation, it is still unclear whether the overproduction of flotillin contributes to the physiological alterations or is actually a consequence of the disease. The number of technical challenges associated with the manipulation of eukaryotic cells has complicated the study of the role of flotillins (18). This motivated us to use the bacterium *Bacillus subtilis* as a working model to evaluate whether the overproduction of flotillins causes any alteration in the cellular physiology of the bacterium and whether this effect could possibly result in cellular dysfunction.

The functional membrane microdomains of the bacterial model organism *Bacillus subtilis* contain two structurally similar flotillin-like proteins, which are referred to as FloA (formerly

YqfA) (6, 19) and FloT (formerly YuaG) (6, 8). Cells lacking FloA and FloT are defective in a number of signal transduction pathways that are associated with the protein cargo of the functional membrane microdomains (e.g., biofilm formation, sporulation, motility, or competence) (6, 8, 20, 21). Thus, it is believed that FloA and FloT facilitate the interaction and oligomerization of the protein cargo in the functional microdomains of *B. subtilis* in a fashion similar to that described for eukaryotic lipid rafts. Supporting this hypothesis, a direct interaction of FloA and FloT with the protein cargo protease FtsH (22) has been reported that is important for the protease activity of FtsH. Furthermore, an additional number of FloT-interacting proteins have been identified recently, including a number of proteins related to signal transduction and protein secretion (20). Accordingly, protein secretion was reduced in cells lacking flotillin, which suggests that the associated protein secretion machinery loses its functionality in the absence of flotillin (20).

The first signal transduction pathway described in association with the flotillins of *B. subtilis* leads cells to specialize in the production of extracellular matrix to ultimately form biofilms (6). The induction of this signaling pathway is driven by the activation of the master regulator Spo0A via phosphorylation (Spo0A~P) (23, 24). The membrane-bound sensor kinase KinC, responsible for phosphorylating Spo0A~P, is part of the protein cargo, and its activity depends on the functionality of FloA and FloT (6) in a similar manner to the protease FtsH (22). FtsH is responsible for degrading the phosphatase enzymes that ultimately inactivate Spo0A~P by dephosphorylation (25) and actively contributes to the differentiation of matrix-producing cells (22). Therefore, published data suggest that the signal transduction pathway that is involved in biofilm formation is controlled by regulatory proteins, which localize in the functional membrane microdomains.

Further evidence was presented that exponentially growing *B. subtilis* cells accumulate FloA and FloT in the septum of dividing cells (22), suggesting that flotillins interact with septum-localized proteins, with FtsH as one example of this kind. This suggests a possible involvement of flotillins in processes related to cell division or cell shape. Related to this observation, other laboratories have determined that *B. subtilis* cells lacking flotillins underwent an aberrant cell division process (7). Thus, these two physiological features involving cell division and biofilm formation seemed affected by FloA and FloT in *B. subtilis* cells and could be studied to monitor the functionality of flotillins in *B. subtilis* cells.

In this report, we show that a 5-fold induction in the production of FloA and FloT significantly increased the amount of flotillin harbored in the microdomains, and this severely affected biofilm formation and cell division in *B. subtilis*. The subpopulation of cells specialized to produce extracellular matrix increased due to an implementation of FtsH activity. Cells overproducing FloA and FloT showed a more efficient septation process, which resulted in shortened cells, minicells, and cells with aberrant septa. As a consequence of the FloA and FloT overproduction, an implementation of the FtsH protease activity occurs, which negatively affects the stability of the protein EzrA (Extra Z-rings assembly), an inhibitor of septum formation (26–28). Altogether, overproduction of flotillins severely affected important cellular processes that directly impacted the physiology of the cells and could potentially contribute to the development of severe diseases in other living organisms.

## RESULTS AND DISCUSSION

**The overproduction of FloT and FloA reached saturation in *B. subtilis*.** The bacterial model *B. subtilis* was used to overexpress the *floA* and *floT* genes under the control of an isopropyl- $\beta$ -D-thiogalactopyranoside (IPTG)-inducible promoter, P<sub>hp</sub> (the Hyperspank promoter). To first compare the overexpression levels to the natural expression levels, we generated translational fusions of *floA* and *floT* to a green fluorescent protein (GFP) gene (*gfp*) anchored to the cytosolic C-terminal part of the protein. PY79 P<sub>floA</sub>FloA-GFP-, P<sub>floT</sub>FloT-GFP-, P<sub>hp</sub>FloA-GFP-, and P<sub>hp</sub>FloT-GFP-labeled strains were grown in liquid cultures of the chemically defined medium MSgg at 30°C until they reached the stationary phase (29). Cells were harvested, fixed with paraformaldehyde, and examined with a fluorescence microscope. Expression from the native promoter showed that the fluorescence signal attributable to FloA and FloT was organized as discrete foci across the cellular membrane and was occasionally positioned in the septum of dividing cells, as previously reported (Fig. 1A and B) (22). The strains expressing P<sub>hp</sub>FloA-GFP and P<sub>hp</sub>FloT-GFP constructs showed expression levels below the natural level of expression in the absence of IPTG (see Fig. S1 in the supplemental material). Indeed, the addition of IPTG to the cultures induced the expression of FloA and FloT. Fluorescence microscopy analysis showed that 0.1 mM IPTG resulted in expression levels comparable to those of the native promoters (see Fig. S1). Saturation of flotillin levels was achieved by adding 15 mM IPTG to the cell cultures. No significant changes in the expression of FloA or FloT were detected in cells that grew with IPTG concentrations above 15 mM. The presence of IPTG did not cause any significant growth alteration in cultures of the PY79 strain (see Fig. S2 in the supplemental material).

Next, we compared the increment in the relative fluorescence signal between native expression and IPTG-inducible full expression. On average, our results showed that full induction by IPTG caused an approximately 5-fold increase in the production of FloA and FloT fluorescence signals in comparison to the native expression level. Further examination at the single-cell level showed that the induction of FloA and FloT expression resulted in an increase of the fluorescence intensity of the membrane foci and, to a lesser extent, in the number of foci. Figure 1C and D show the analysis of the subcellular organization of the fluorescence signal in representative single cells expressing FloA-GFP and FloT-GFP at native and full induction levels, respectively.

**Saturation of FloT and FloA affects biofilm formation and cell differentiation.** Biofilm formation in *B. subtilis* requires the differentiation of numerous cell types. Among those, the matrix-producing cell type is responsible for the production and secretion of the extracellular matrix of the biofilm (24, 30, 31). The subpopulation of matrix producers simultaneously expresses the *epsA-O* operon (henceforth called the *eps* operon) and the *tapA-sipW-tasA* operon (henceforth called the *tasA* operon). The *eps* operon encodes the enzymes responsible for the production of the extracellular exopolysaccharide (32–34). The *tasA* operon is required for the production of extracellular amyloid fibers that structurally give consistency to the biofilm (35–39).

To investigate whether the overexpression of FloA and FloT affects biofilm formation, strains overproducing FloA and FloT were constructed and used to assay biofilm formation. The morphology of *B. subtilis* colonies grown on solid biofilm-inducing

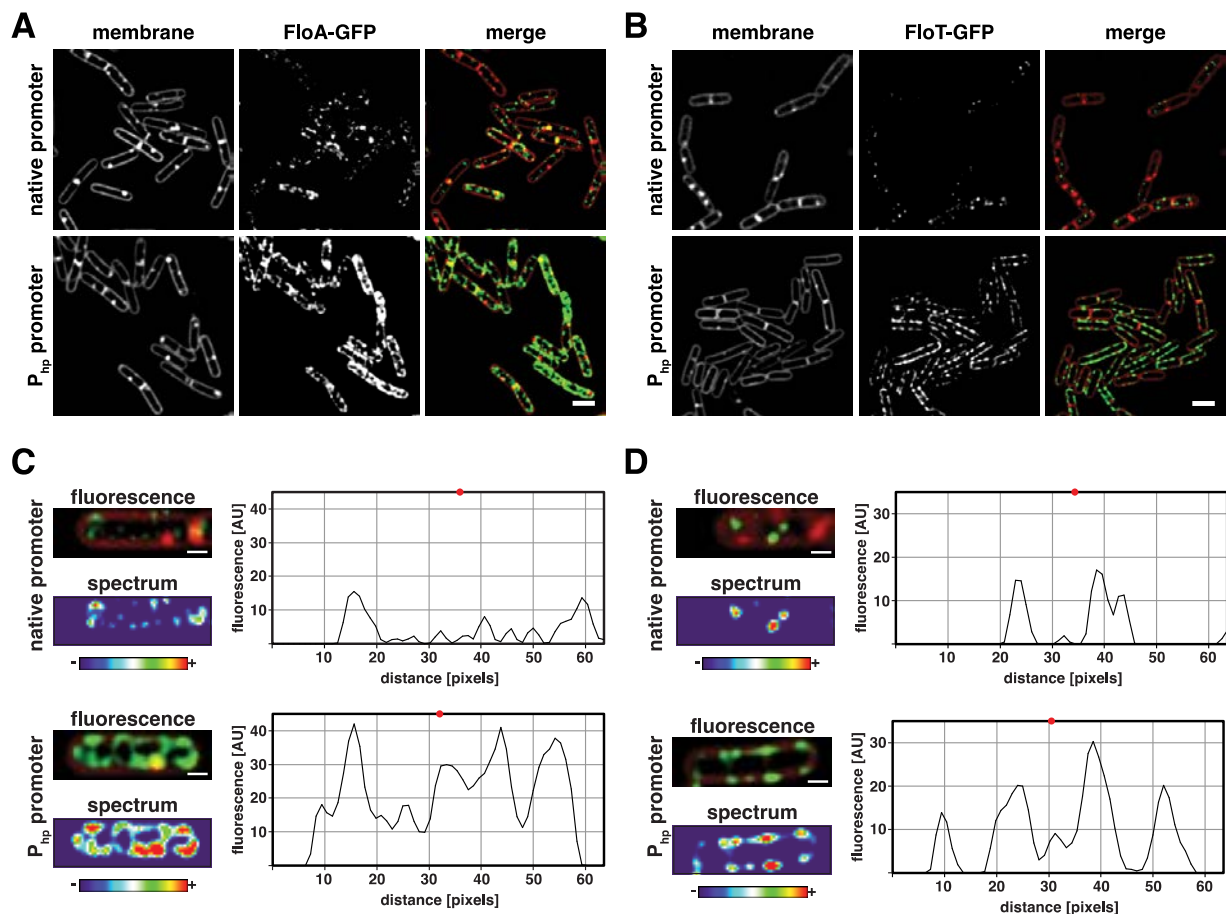
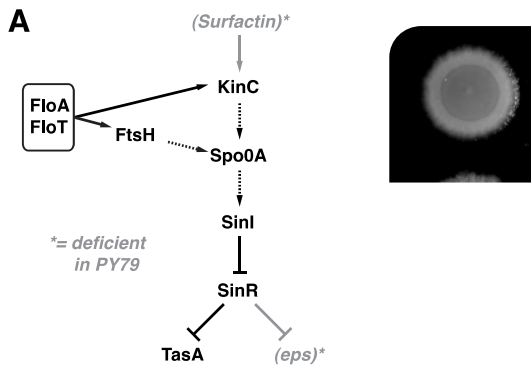


**FIG 1** Saturation of FloA and FloT in functional membrane microdomains of *B. subtilis*. Shown are levels of expression in cells expressing FloA-GFP (A) or FloT-GFP (B) under the control of an IPTG-inducible promoter ( $P_{hp}$ ) (bottom row) compared to natural expression levels obtained with their native promoters (upper row). Cells were grown in MSgg medium until they reached the stationary phase. IPTG was added to a final concentration of 15 mM. Membrane staining (left column) was performed with FM4-64 membrane dye. The center column shows the fluorescence signal emitted by the GFP. The right column shows the merged signals. The FM4-64 signal is false colored in red, and GFP is false colored in green. Scale bars are 2  $\mu\text{m}$ . (C and D) Quantification of the fluorescence signal in single cells expressing FloA-GFP and FloT-GFP. The upper row shows the fluorescence signal obtained when expressed under the control of their native promoters. The bottom row shows the fluorescence signal obtained when expressed under the control of an IPTG-inducible promoter. The fluorescent micrographs show membrane staining false colored in red and the GFP fluorescence signal false colored in green. Additionally, the relative GFP fluorescence signal is quantified in relation to the background fluorescence, using a color spectrum logarithmic scale. (The spectrum scale is presented on the bottom.) The relative fluorescence intensity values of each micrograph are represented in a graph (on the left of each micrograph). The x axis represents the cell length (in pixels), and the y axis represents the value of relative fluorescence intensity detected (in arbitrary units [AU]). The midcell is marked with a red dot. The scale bar is 1  $\mu\text{m}$ .

MSgg agar medium was examined. To generate biofilms on agar, 3  $\mu\text{l}$  of an LB preculture was spotted on MSgg medium supplemented with 15 mM IPTG and allowed to grow at 30°C for 72 h. After incubation, the biofilms develop into integrated microbial communities with great complexity, manifested by the number of wrinkles present on the surface of the biofilm, which is representative of the robustness and the consistency of the extracellular matrix of the biofilm. Two different genetic backgrounds were used to perform this assay—the PY79 and NCIB3610 strains. Strain PY79 is a laboratory strain that is partially deficient in biofilm formation due to the acquisition of a point mutation in the *eps* operon (Fig. 2A) (40). While this strain still possesses an intact *tasA* operon, the lack of extracellular polysaccharide makes the PY79 microbial communities flat, and they lack any distinctive complex architecture (40). A deletion of the transcriptional re-

pressor SinR, which uncouples the regulation of the biofilm (33, 41), resulted in a slightly wrinkled colony even in the absence of a functional *eps* operon, suggesting that overexpression of the *TasA* strain partially restored biofilm formation when overproduced in the PY79 strain. Accordingly, the double mutant  $\Delta\text{sinR } \Delta\text{tasA}$  strain showed a biofilm-null phenotype, suggesting that biofilms generated by PY79 are mainly caused by expression of *TasA* (Fig. 2B). In contrast, the NCIB3610 strain (henceforth 3610) is the undomesticated *B. subtilis* strain and is considered the ancestor strain of PY79 (32). This strain possesses intact and functional *eps* and *tasA* operons and shows a great ability to form biofilms. Mutations in the *eps* or the *tasA* operons significantly reduce the ability of this strain to form biofilm, and a depletion of SinR results in a hyperwrinkled colony that overproduces extracellular matrix (see Fig. S3 in the supplemental material).

Mielich-Süss et al.



of the strains overexpressing FloA or FloT were morphologically indistinguishable from the wild-type strain, indicating that the overexpression of a single flotillin protein did not influence biofilm formation (Fig. 2C). However, the  $P_{hp}$ FloA  $P_{hp}$ FloT strain that simultaneously overexpressed FloA and FloT resulted in a more robust, biofilm-like colony morphology that was especially evident in the experiments that used the PY79 strain (Fig. 2C; see Fig. S3 in the supplemental material to compare it to other genetic backgrounds). Because PY79 harbors a non-functional *eps* operon, we reasoned that the biofilm formation phenotype observed in the PY79  $P_{hp}$ FloA  $P_{hp}$ FloT strain was attributable to the overexpression of TasA protein and the high production of amyloid fibers. A similar effect was observed in the experiments that used the 3610 strain, although this genetic background showed milder effects for reasons that are unknown to us. Hence, based on the robustness and the consistency of the biofilm formation phenotype observed in the PY79 strain, we used this genetic background to further explore the molecular effects in cell differentiation associated with the overproduction of FloA and FloT in *B. subtilis*.

Subsequently, we tested whether the overexpression of *tasA* was responsible for the acquisition of biofilm formation in the PY79  $P_{hp}$ FloA  $P_{hp}$ FloT strain. To do this, we first compared the subpopulation of *tasA*-expressing cells in the wild-type strain and the flotillin-overexpressing strains. All strains were labeled with the yellow fluorescent protein (YFP) transcriptional fusion  $P_{tapA}$ -*yfp* and grown in MSgg medium plus IPTG (15 mM) at 30°C for 72 h. After incubation, cells were harvested and fixed with 4% paraformaldehyde. The fluorescence signal of 50,000 cells was monitored by flow cytometry and plotted on the graph presented in Fig. 2D. An unlabeled strain served as negative control with the absence of fluorescence signal. The wild-type strain harboring the  $P_{tapA}$ -*yfp* reporter served as a positive control, where the subpopulation of matrix producers represented approximately 30% of the total cell count. Overproduction of FloA or FloT did not alter the size of this subpopulation. However, when we assayed the size of the subpopulation of matrix producers in the  $P_{hp}$ FloA  $P_{hp}$ FloT strain, we detected a 3-fold increase in the number of cells that highly expressed the  $P_{tapA}$ -*yfp* reporter, suggesting that the overproduction of FloA and FloT led the cells to excessively produce

ed.

Strains expressing  $P_{hp}$ FloA,  $P_{hp}$ FloT, and  $P_{hp}$ FloA  $P_{hp}$ FloT were constructed in different genetic backgrounds. The resultant strains were assayed for variations in their ability to form biofilm by allowing them to grow in agar MSgg medium supplemented with 15 mM IPTG at 30°C for 72 h. After incubation, the biofilms



TasA, which ultimately induced biofilm formation in the PY79 strain.

**Overproduction of flotillin stimulates FtsH activity.** The genetic cascade responsible for the differentiation of matrix producers is triggered by phosphorylation of Spo0A~P. The membrane kinase KinC induces Spo0A~P phosphorylation in response to the secretion of the signal surfactin (Fig. 2A) (42). Moreover, the activity of the membrane-bound protease FtsH is equally important for matrix production, because FtsH degrades the phosphatases that are responsible for the deactivation of Spo0A~P by dephosphorylation (25). Importantly, both KinC and FtsH proteins localize to the functional membrane microdomains in *B. subtilis*, and their functionality is dependent on the activity of FloA and FloT (6, 22). Figure 2A shows an overview of the regulatory cascade leading to biofilm formation.

We hypothesized that the molecular mechanism underlying the evident increase in the subpopulation of matrix producers could be related to the positive effects of FloA and FloT on the activity of KinC or FtsH. Importantly, the PY79 strain is not able to produce surfactin due to the acquisition of a point mutation in the *sfp* gene during laboratory domestication (Fig. 2A) (40). The Sfp protein is a phosphopantetheinyl transferase that posttranslationally modifies the surfactin biosynthesis machinery. This is an essential process for the correct functionality of the surfactin biosynthesis machinery (43, 44). Thus, the activation of KinC via surfactin is not possible in the PY79 strain. This fact led us to focus on the activity of the membrane-bound protease FtsH.

FtsH indirectly affects the levels of Spo0A~P by degrading four regulatory phosphatase proteins, RapA, RapB, RapE, and Spo0E, which feed into the Spo0A phosphorelay to ultimately decrease the levels of Spo0A~P. The absence of FloA and FloT negatively affects the FtsH protein (22), which prevents the degradation of the RapA, RapB, RapE, and Spo0E phosphatases (25). To explore whether the overproduction of FloA and FloT decreased the levels of Spo0A~P via FtsH, we deleted the *ftsH* gene in the wild-type and  $P_{hp}FloA P_{hp}FloT$  strains, and we monitored biofilm formation. The  $\Delta ftsH$  and  $\Delta ftsH P_{hp}FloA P_{hp}FloT$  strains were grown in MSgg agar medium supplemented with 15 mM IPTG and were incubated at 30°C for 72 h. After incubation, the microbial communities of the  $\Delta ftsH P_{hp}FloA P_{hp}FloT$  strain showed no particular biofilm architecture but a flat morphology comparable to that of the wild-type and  $\Delta ftsH$  strains (Fig. 2E). Next, these strains were labeled with the  $P_{tapA-yfp}$  transcriptional fusion to monitor possible variations in the subpopulation of matrix producers by using flow cytometry. Flow cytometry analysis showed that the overproduction of FloA and FloT did not differentiate the subpopulation of matrix producers in cells lacking FtsH (Fig. 2F). This suggests that FtsH mediated the differentiation of matrix producers when FloA and FloT were artificially overproduced.

These results are in agreement with published literature showing that the oligomerization of FtsH in *E. coli* requires the chaperone activity of HflC and HflK, two proteins that are structurally similar to FloA and FloT (45–48). *B. subtilis* lacks the HflC and HflK proteins, and thus, it is possible that FloA and FloT might play the role of HflC and HflK in stabilizing FtsH in *B. subtilis*. To test this hypothesis, whole-cell extracts of the  $P_{hp}FloA P_{hp}FloT$  strain were used to semiquantitatively detect FtsH by immunoblot analysis using polyclonal antibodies against FtsH. An increase in FtsH protein was detected in normalized cell extracts from the  $P_{hp}FloA P_{hp}FloT$  strain compared to the wild-type strain

(Fig. 3A). Next, we observed that these higher levels of FtsH coincided with higher levels of TasA. We performed an immunoblot analysis using polyclonal antibodies against TasA. The extracts of cells that overproduced FloA and FloT, which showed higher levels of FtsH, also showed higher levels of TasA. Importantly, when the *ftsH* gene was deleted, the detection of TasA was not possible in the strain that overproduced FloA and FloT (Fig. 3B).

Altogether, the data are consistent with the hypothesis that the functional link between FloA/FloT and FtsH mediated the increase of the subpopulation of matrix-producing cells in the PY79 strain that overproduced FloA and FloT. This, in turn, caused an increase in the production of TasA, which resulted in an overproduction of biofilm formation. In those lines, the interaction of FtsH-like proteins with flotillin-like proteins has been described in many systems and organelles (e.g., mitochondria, yeast, or plants), and it has been shown that the stability of FtsH-like proteins depends on the presence of flotillin-like proteins (49, 50). It is hypothesized that the chaperone activity of the flotillin-like proteins acts as a regulator to fine-tune the proteolytic activity of FtsH (49, 50). It also is suggested that flotillins serve as scaffolding proteins to limit the mobility of the FtsH protease across the membrane (49). Based on these current hypotheses, it is probably not surprising that the overproduction of FloA and FloT affected the activity of FtsH of *B. subtilis*.

**Flotillin overexpression results in decreased cell length.** FtsH principally localizes to the septum of dividing cells (51), where the interaction with FloA and FloT presumably occurs (22). Possibly, flotillins provide stability to protein septum-associated proteins. Accordingly, there is evidence of a significant number of septum-localized proteins among the interactome of FloT (20, 22). Furthermore, the absence of flotillins in *B. subtilis* has been associated with pleiotropic effects on cell shape (7), which led us to reason that septum-localized membrane microdomains could influence septum-associated processes, like septum formation or shape determination.

Septum formation and cell shape determination were analyzed at the single-cell level in cells that overproduced flotillins. To do this, the  $P_{hp}FloA$ ,  $P_{hp}FloT$ , and  $P_{hp}FloA P_{hp}FloT$  strains were grown in liquid MSgg medium plus IPTG (15 mM) at 37°C with vigorous agitation until the late exponential growth phase (optical density at 600 nm [OD<sub>600</sub>] of 0.8 to 1.0). After incubation, cells were stained with the membrane dye FM4-64 before examination under the fluorescence microscope. We observed that under these growth conditions, the simultaneous overexpression of FloA and FloT resulted in a dramatic reduction of cell length (Fig. 4A, column 4; see Fig. S4 in the supplemental material). We randomly selected 500 cells from each microscopic field and measured the cell length (Fig. 4B). On average, wild-type cells showed a cell length of  $2.41 \pm 0.52 \mu\text{m}$ . This result was comparable to the length of cells expressing FloA ( $2.47 \pm 0.60 \mu\text{m}$ ) or FloT ( $2.34 \pm 0.65 \mu\text{m}$ ). However, overproduction of FloA and FloT resulted in a cell length of  $1.11 \pm 0.52 \mu\text{m}$ . Probably as a consequence of the reduction of cell length,  $P_{hp}FloA P_{hp}FloT$  cells also showed a partial loss of the typical *B. subtilis* rod shape, and a subfraction of cells (approximately 19% of the total) became spherical. Among those, we detected a significant number of small, circular, anucleate minicells (approximately 28% of the total) (52–54), as well as small, spherical cells that contained DNA (72% of the total).

The effect on cell length associated by the overexpression of FloA and FloT pointed to an influence of flotillins on the efficiency

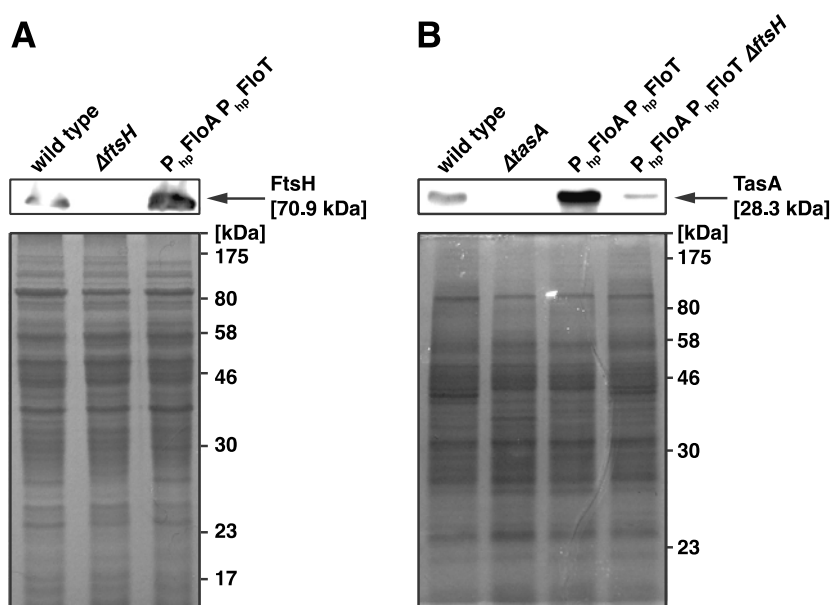


**FIG 3** Overproduction of FloA and FloT increase the levels of FtsH and TasA proteins. (A) Immunoblot analysis to detect FtsH in different mutants using polyclonal antibodies against FtsH. The wild-type strain is used as a positive control, while the  $\Delta ftsH$  mutant is used as a negative control. The immunoblot signal is presented in the upper panel, and the respective SDS-PAGE result is presented in the lower panel as a loading control. (B) Detection of TasA production in different mutants by immunoblot analysis using polyclonal antibodies against TasA. The wild-type strain (PY79) is used as a positive control, while the  $\Delta tasA$  mutant is used as a negative control. The immunoblot signal is presented in the upper panel, and the respective SDS-PAGE result is presented in the lower panel. Samples were obtained from the extracellular protein fraction of pellicles that were grown in liquid cultures for 24 h at 30°C. Protein levels were normalized relative to cell number.

of septum formation. To investigate the influence of FloA and FloT in the assembly of proteins with a relevant role in septum formation, we chose the FtsZ protein as a septum-related protein to monitor septum formation in *B. subtilis* cells. FtsZ forms a ring structure (Z-ring) to ultimately drive cell septation (55, 56), and mutants showing an increase in FtsZ assembly also showed additional division events per cell cycle, with the formation of extra septa that led to the occurrence of a minicell-like phenotype (55, 57). Thus, the phenotypic similarities between cells overexpressing FloA and FloT and cells with increases in FtsZ assembly led us to hypothesize a functional connection between these two genotypes. We first tested whether the overproduction of FloA and FloT affects the septation efficiency. To do this, cultures of the  $P_{hhp}FloA P_{hhp}FloT$  mutant were grown in liquid MSgg medium with vigorous agitation, and the cell length was measured at early stages of exponential growth ( $OD_{600}$  of 0.1). Our measurements of cell length showed that actively dividing cells were substantially shorter when overproducing FloA and FloT than wild-type cells (Fig. 5A). To elucidate if the reduction of cell length involved FtsZ, we constructed the  $P_{xy1}FtsZ$ -GFP and  $P_{hhp}FloA P_{hhp}FloT P_{xy1}FtsZ$ -GFP strains that expressed a labeled FtsZ under the control of a xylose-inducible promoter. In these strains, transcription of FtsZ-GFP is strictly dependent on the amount of xylose that was added to the cultures. This allowed us to correlate the variations in the FtsZ-GFP protein levels to the differences in protein processing or stability. We used these strains to determine that cell length per FtsZ ring (L/R ratio) (58) was significantly reduced in cells overexpressing FloA and FloT in comparison to that in the wild-type strain (Fig. 5B and C). Furthermore, cultures of cells that overproduced FloA and FloT showed a significant increase in the number

of Z-rings compared to that in the wild-type strain (Fig. 4D), suggesting an increase in the number of Z-rings in the shorter cells that overproduced FloA and FloT.

We revisited the pool of proteins associated with the functional membrane microdomains in *B. subtilis* to find those proteins whose activity affects the assembly of the Z-ring. To purify the protein fraction associated with the functional membrane microdomains, the membrane fraction was treated with nonionic detergents and separated by centrifugation in a sucrose gradient. This resulted in one fraction that was sensitive to detergents and another fraction that is composed of larger membrane fragments that were more resistant to detergent disruption (detergent-resistant membrane [DRM] fraction). It is known that the DRM fraction is enriched in proteins associated with lipid rafts (4, 59, 60) and is the fraction that contains the proteins of the functional membrane microdomains when assayed with *B. subtilis* membranes. We detected the protein EzrA in the DRM fraction of *B. subtilis*, with identification coverage of 53% (see Fig. S5 in the supplemental material) (22). EzrA is a negative regulator of the assembly of the Z-ring that localizes in the midcell in an FtsZ-dependent manner. Cells depleted of EzrA (Extra Z-rings assembly) show multiple Z-rings located at the polar and medial sites (27, 61). We hypothesized that overproduction of FloA and FloT could negatively affect the activity of EzrA to promote an accelerated assembly of FtsZ.

To address this question, we generated  $P_{xy1}EzrA$ -GFP and  $P_{hhp}FloA P_{hhp}FloT P_{xy1}EzrA$ -GFP strains to compare the levels of expression of EzrA in cells overexpressing FloA and FloT. Examination of cells under the fluorescence microscope did not render conclusive results. Instead, we performed a semiquantitative im-

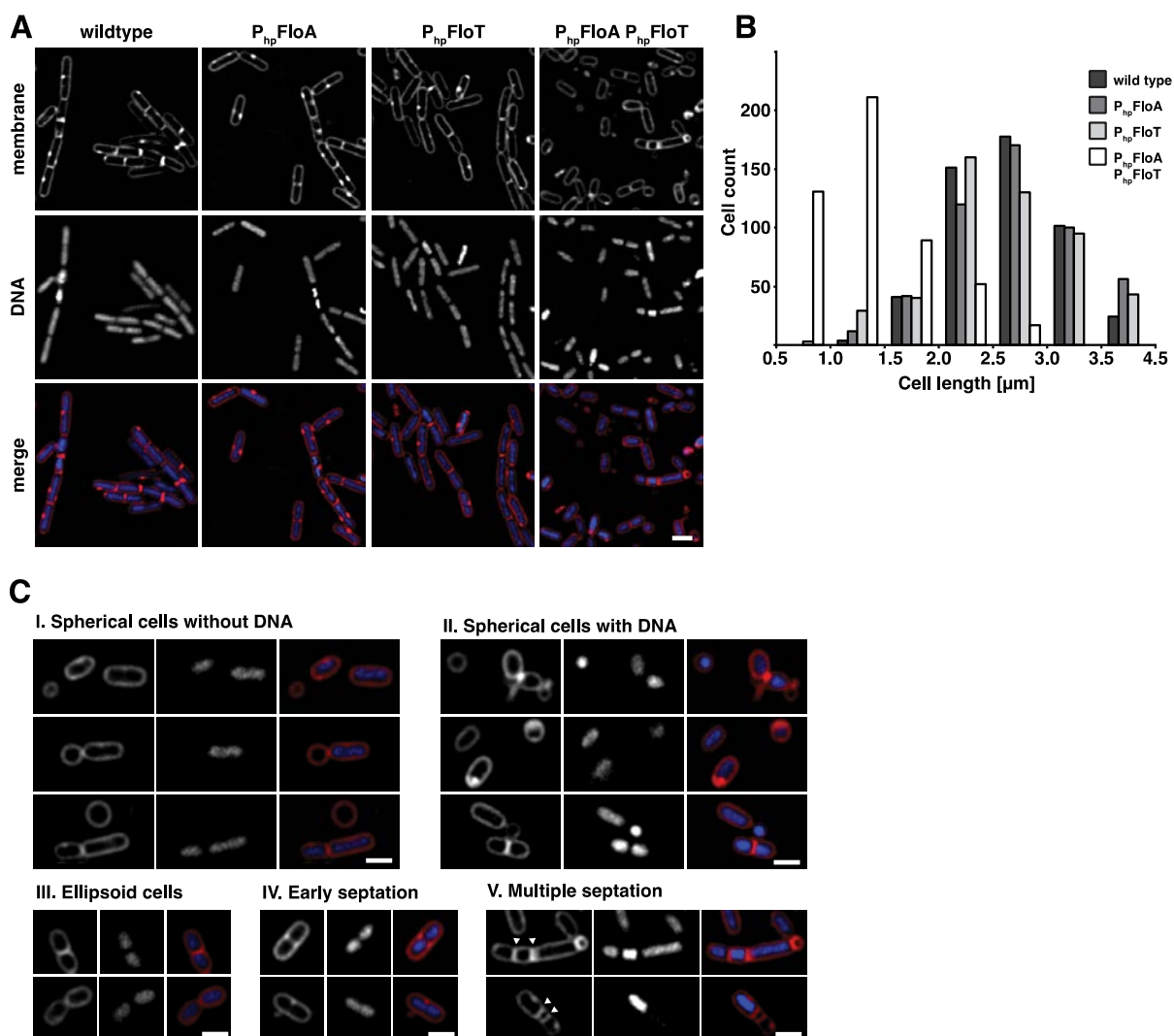


**FIG 4** Overexpression of FloA and FloT affects cell shape. (A) Fluorescence micrographs of strains overexpressing FloA, FloT, or both FloA and FloT compared to wild-type cells. The upper row presents membrane staining using FM4-64. The center row shows DNA staining using Hoechst 33342. The bottom row shows the merge of the previous images, with the membrane staining false colored in red and the DNA staining false colored in blue. Cells were grown in liquid MSgg medium at 37°C until they reached the late exponential growth phase. IPTG was added to a final concentration of 15 mM. The scale bar represents 2 μm. (B) Histogram representing the variation in cell length in the different mutants. The number of the cells considered for this analysis was 500. The cell count is represented in the y axis. Calculation of cell length was performed using Leica Application Suite Advance Fluorescence software. (C) Detailed view of cell shape aberrations in cells that simultaneously overexpressed FloA and FloT. Spherical cells are shown in panel I. Spherical anucleate cells are shown in panel II. Ellipsoid cells are shown in panel III, and cells with a failure in septation are shown in panels IV and V. The scale bars represent 2 μm.

munoblot assay using polyclonal antibodies against GFP. Using this assay, we observed a significant reduction of EzrA levels in the extracts of the  $P_{hp}FloA P_{hp}FloT P_{xyI}EzrA-GFP$  strains in comparison to the  $P_{xyI}EzrA-GFP$  strain (Fig. 6A). Although this result explained the higher efficiency to form Z-rings and septates in cells overproducing FloA and FloT, it was somewhat unexpected, as one might anticipate that an enhanced chaperone activity of flotillins should always affect the stability of the associated proteins in a positive fashion. One plausible hypothesis that could explain this result is that additional proteins that are stabilized by FloA and FloT negatively influence EzrA. Supporting this hypothesis, we found evidence in the literature that EzrA of *B. subtilis* is

degraded by an ATP-dependent protease that is structurally similar to FtsH (62), suggesting that FtsH could target EzrA in the strain that overexpressed FloA and FloT. This is consistent with the filamentous growth that is described in the mutant lacking FtsH, which is also observed in strains with defective cell septation (63). Consequently, we tested whether FtsH influenced the reduced levels of EzrA observed in cells overexpressing FloA and FloT. To do this, the levels of EzrA-GFP were tested in the presence or absence of FtsH by semiquantitative immunoblot assays, using whole-cell extracts of the  $P_{hp}FloA P_{hp}FloT P_{xyI}EzrA-GFP$  and  $\Delta ftsH P_{hp}FloA P_{hp}FloT P_{xyI}EzrA-GFP$  strains. Using this approach, we observed that cells lacking FtsH showed increased lev-

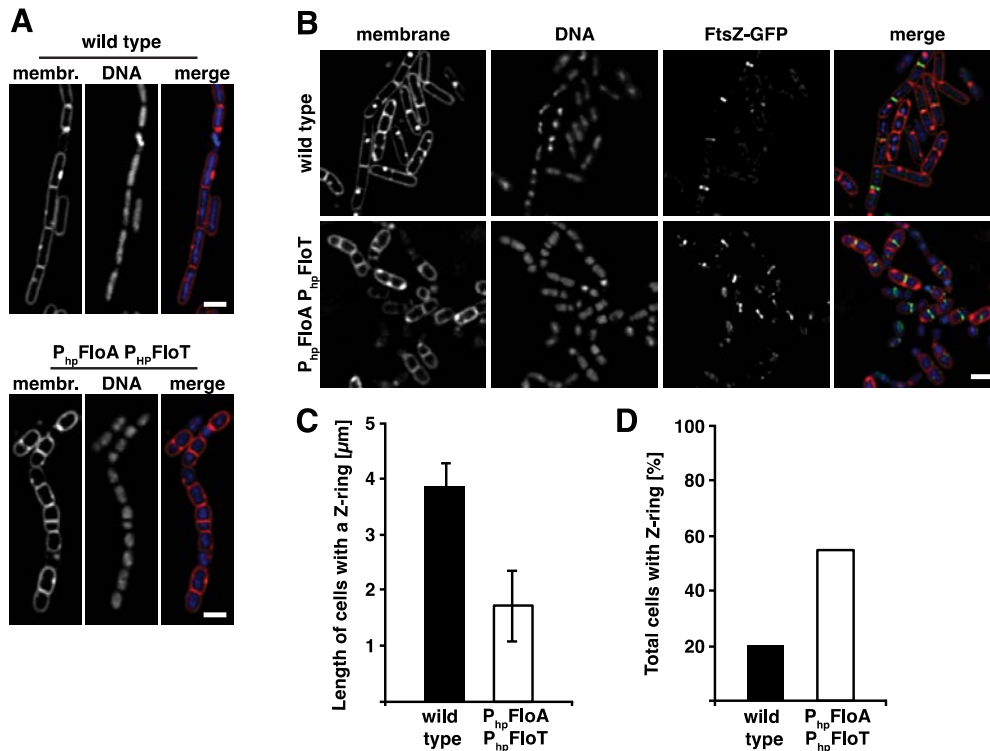


**FIG 5** Simultaneous overproduction of FloA and FloT affects formation of the division septum and formation of the Z-ring. (A) Comparison between wild-type cells and the P<sub>hp</sub>FloA P<sub>hp</sub>FloT strain during the early exponential growth phase. Cells were grown in liquid MSgg medium at 37°C until they reached an OD<sub>600</sub> of 0.1. For overexpression, the medium was supplemented with 15 mM IPTG. The membrane (membr.) was stained with FM4-64 (left panel), and the DNA was visualized with Hoechst 33342 (middle panel). The right panel shows merges of the two signals, with the membrane false colored in red and DNA false colored in blue. The scale bar represents 2 μm. (B) Visualization of Z-ring formation in a wild-type strain and the P<sub>hp</sub>FloA P<sub>hp</sub>FloT strain bearing an FtsZ-GFP fusion. The first column shows the membrane stained with FM4-64, the second column shows the DNA stained with Hoechst 33342, and the third column shows the FtsZ-GFP signal. In the fourth column, all signals were merged, with the membrane false colored in red, the DNA false colored in blue, and the GFP false colored with green. The cells were grown in liquid MSgg medium at 37°C and harvested in the exponential growth phase. IPTG was added to the growth medium at a final concentration of 15 mM, and basal induction of FtsZ-GFP was achieved with 1% (wt/vol) xylose. The scale bar is 2 μm. (C) Graphical illustration of the length of cells with a visible Z-ring. Approximately 500 cells were used for counting. (D) Graphical illustration of the percentage of cells with a Z-ring; approximately 500 cells were used for counting.

els of EzrA (Fig. 6B). Moreover, we generated the P<sub>hp</sub>FtsH P<sub>xyt</sub>EzrA-GFP strain, which overexpressed P<sub>hp</sub>FtsH, and whole-cell extracts of this strain were used to compare the abundance of EzrA before and after FtsH overproduction. Figure 6B shows that the overproduction of FtsH was associated with reduced EzrA levels. We detected an intriguing protein band in this strain that could be attributed to an alternative processed form of EzrA protein. More experiments should be performed in this direction to fully address whether a direct interaction exists between FtsH and EzrA. Experiments presented in this report are consistent with the idea that the overexpression of flotillins causes severe physiological changes in bacterial cells.

Overall, our study showed that overexpression of FloA and FloT in the functional membrane microdomains of *B. subtilis* resulted in severe defects in cell differentiation and cell shape. We provide evidence that physiological alterations were mediated by an unusual activity of the FtsH protease (22). We expect that other yet unknown molecular mechanisms may participate in this phenotype, since numerous signal transduction pathways are harbored in the functional membrane microdomains of *B. subtilis*.

Among those, we consider particularly interesting the dual role of the FtsH protease in regulating bacterial cell differentiation and cell shape, as illustrated in Fig. 7. It is probably not surprising that this important regulatory node localizes in the functional membrane microdomains, under the direct control of the two flotillin-like proteins FloA and FloT, in a manner similar to that found in other biological systems (49, 50). Yet, when focusing on *B. subtilis*, it is still unknown whether both FloA and FloT play redundant functions in the functional microdomains. Further experiments are necessary to clarify why the overexpression of two structurally different flotillin proteins is required to achieve the described effects. We tend to think that FloA and FloT are partially redundant and some physiological processes are functionally linked to both FloA and FloT, while other physiological processes are specifically linked to FloA or FloT.

## MATERIALS AND METHODS

**Strains, media, and culture conditions.** For general purposes, the *B. subtilis* strains PY79 and NCIB3610 were used in this study. *Escherichia coli* DH5α was used for cloning purposes. A detailed list of the genetically

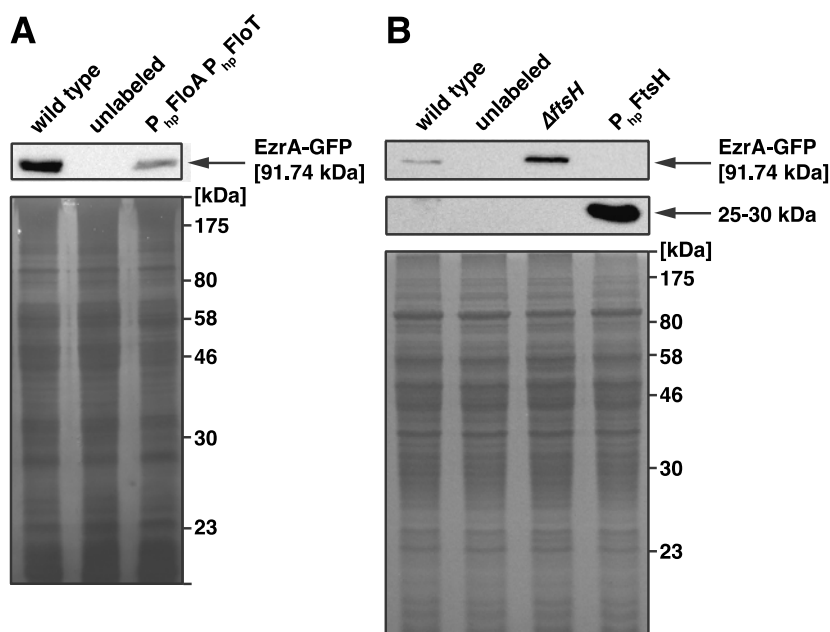


**FIG 6** Levels of EzrA are influenced by FtsH. (A and B) Western blot analysis of whole-cell extracts of different mutants to detect the level of EzrA-GFP using polyclonal antibodies against GFP. The extra protein band is shown at 25 to 30 kDa in panel B, which was only detected in the extract of cells that overproduced FtsH. SDS-PAGE results are shown as loading controls. The protein amount was normalized relative to cell number.

modified strains is shown in Table S1 in the supplemental material. For routine growth, cells were propagated on LB medium. Selective media were prepared in LB agar using the antibiotics (final concentrations in parentheses) ampicillin (100  $\mu\text{g/ml}$ ), kanamycin (50  $\mu\text{g/ml}$ ), chloramphenicol (5  $\mu\text{g/ml}$ ), tetracycline (5  $\mu\text{g/ml}$ ), spectinomycin (100  $\mu\text{g/ml}$ ), and erythromycin (2  $\mu\text{g/ml}$ ) plus lincomycin (25  $\mu\text{g/ml}$ ) for macrolide-lincosamide-streptogramin B (MLS) determination. Biofilm assays and growth of cells for microscopy or biochemical analysis were performed with MSgg medium (29). When required, MSgg culture medium was supplemented with 1% threonine. Unless otherwise stated, induced expression was achieved with 1 mM IPTG or 1% (wt/vol) xylose. To generate biofilms, 3  $\mu\text{l}$  of an LB overnight culture was spotted onto 1.5% agar MSgg plates and incubated for 72 h at 30°C. For liquid cultures, an overnight culture was diluted 1:20 in MSgg medium and grown at 30°C with agitation at 200 rpm until reaching the desired growth stage. If necessary, inducers were added to the culture as stated in the figure legends.

**Strain construction.** Genomic modifications in *B. subtilis* were performed according to standard protocols (64). Linearized plasmid DNA or PCR products were brought into cells by inducing natural competence, leading to incorporation of the foreign DNA into the genome by heterologous recombination (65). SPP1-mediated phage transduction was used to shuttle constructs among strains, in order to combine mutant alleles (66). For plasmid construction, genes were amplified from genomic DNA with primers carrying a 5' extension with desired restriction sites to clone the PCR product into the target plasmids. A list of all of the primers used in this study is presented in Table S2 in the supplemental material. For overexpression with the IPTG-inducible Hyperspank promoter, the genes were cloned into pDR111 (67, 68) or into the pBM001 plasmid, a chimera of pDR111 and pDR183 (kindly provided by David Rudner at the Harvard Medical School, Boston, MA). pBM001 has a pDR183 backbone to integrate the plasmid into the *lacA* locus combined with a fragment from pDR111 that carries the Hyperspank promoter, the multiple-cloning site, and the Lac repressor. The FtsZ-GFP strain was created with the plasmid pX (69), which integrates genes into the *amyE* locus and expresses them from a xylose-inducible promoter. FtsZ was joined with GFPmut1 by

long-flanking homology (LFH) PCR and inserted into pX. For the construction of EzrA-GFP, we made use of the pSG1154 plasmid (70), which allows in-frame fusions to GFPmut1 and further expression under the control of a xylose-inducible promoter. For the independent overexpression of both flotillins and a third xylose-inducible gene, we decided to construct a bicistronic mRNA of *floA* and *floT* via LFH-PCR, which was integrated into the *lacA* locus with pBM001. The strain showed similar overexpression of *floA* and *floT* in the presence of IPTG compared to expression of a single gene, as determined by reverse transcription (RT)-PCR (data not shown).

**Image analysis.** Biofilms were documented using a Nikon SMZ 1500 stereoscope equipped with a Leica DFC295 color camera and Zeiss Axio Vision software. Final processing of the images was done with Photoshop. For microscopy, an overnight culture was diluted 1:20 in MSgg medium and grown at 30°C with agitation at 200 rpm until reaching the desired growth stage. If necessary, inducers were added to the culture as stated in the figure legends. Prior to analysis, 1  $\mu\text{M}$  FM4-64 (Invitrogen, Carlsbad, CA) was added to stain the membrane, and Hoechst 33342 was added to a final concentration of 1  $\mu\text{g/ml}$  to stain the DNA. For static images, cells were fixed with 4% paraformaldehyde for 7 min and washed with phosphate-buffered saline (PBS) several times. Finally, cells were spotted on a microscopic slide covered with a 1% agarose pad made with PBS. Images were captured with a Leica DMI6000B microscope equipped with a Leica CRT6000 illumination system coupled with a Leica DFC630FX color camera. Deconvolution was performed with a software algorithm of the LAS AF software. Fluorescence quantification and generation of color spectra were performed with Fiji. Images were processed with Leica LAS AF software and Photoshop.

**Flow cytometry.** For flow cytometry analysis, 3-day-old biofilms were detached from the agar surface, resuspended in PBS, and mildly sonicated (power output of 0.7 and cycle of 50%) in order to separate cells from extracellular matrix material. Subsequently, cells were fixed with 4% paraformaldehyde for 7 min and washed several times. For analysis, cells were diluted 1:1,000 in PBS. Analysis was carried out with the benchtop MACSquant analyzer (Miltenyi Biotec, Germany). YFP signals were detected

varied according to the corresponding experiment. Cells were collected by centrifugation and subsequently lysed with 1 mg/ml lysozyme at 37°C for 30 min. After lysozyme treatment, samples were subjected to SDS-PAGE, and proteins were detected by Coomassie staining. The extracellular fraction was extracted as previously described (37, 71) with minor modifications. Briefly, cells were grown in liquid MSgg medium without agitation at 30°C. The floating biofilm, including the liquid medium, was recovered and mild sonication was applied to separate the extracellular fraction from the cells. After that, cells were pelleted and the supernatant was filter sterilized (0.2- $\mu$ m pore size). The extracellular proteins in the supernatant were precipitated with trichloroacetic acid with a final concentration of 10% (vol/vol). Precipitated proteins were harvested by centrifugation and taken up in 1 $\times$  SDS sample buffer. Immunoblot analysis was performed according to standard protocols. Antibodies were purchased from Invitrogen (anti-GFP) and Bio-Rad (anti-rabbit IgG, horseradish peroxidase [HRP] conjugate). The TasA antibody was kindly provided by Kürsad Turgay (Freie University of Berlin, Germany). The FtsH antibody was a kind gift from Thomas Wiegert (Hochschule Zittau/Görlitz, Germany).

#### SUPPLEMENTAL MATERIAL

Supplemental material for this article may be found at <http://mbio.asm.org/lookup/suppl/doi:10.1128/mBio.00719-13/-/DCSupplemental>.

Figure S1, EPS file, 1.9 MB.  
 Figure S2, EPS file, 1.2 MB.  
 Figure S3, EPS file, 20 MB.  
 Figure S4, EPS file, 8.9 MB.  
 Figure S5, EPS file, 1.2 MB.  
 Table S1, DOCX file, 0.1 MB.  
 Table S2, DOCX file, 0.1 MB.

#### ACKNOWLEDGMENTS

We thank all members of the Institute of Molecular Infection Biology (IMIB), especially Isa Westedt for technical assistance. We thank Thomas Wiegert (University of Bayreuth, Germany) and Kürsad Turgay (Freie University of Berlin, Germany) for kindly providing antibodies and the *ftsH::tet* mutant.

This work was funded by the Young Investigator Program of the Research Center of infectious diseases (ZINF) of the University of Würzburg (Germany) and grant LO 1804/2-1 from the German Research Foundation DFG. B.M.-S. was supported by the German Excellence Initiative to the Graduate School of Life Sciences of the University of Würzburg.

#### REFERENCES

1. Matsumoto K, Kusaka J, Nishibori A, Hara H. 2006. Lipid domains in bacterial membranes. *Mol. Microbiol.* 61:1110–1117.
2. Rudner DZ, Losick R. 2010. Protein subcellular localization in bacteria. *Cold Spring Harb. Perspect. Biol.* 2:a000307. doi:10.1101/cshperspect.a000307.
3. Simons K, Gerl MJ. 2010. Revitalizing membrane rafts: new tools and insights. *Nat. Rev. Mol. Cell Biol.* 11:688–699.
4. Simons K, Ikonen E. 1997. Functional rafts in cell membranes. *Nature* 387:569–572.
5. Simons K, Sampaio JL. 2011. Membrane organization and lipid rafts. *Cold Spring Harb. Perspect. Biol.* 3:a004697. doi:10.1101/cshperspect.a004697.
6. López D, Kolter R. 2010. Functional microdomains in bacterial membranes. *Genes Dev.* 24:1893–1902.
7. Dempwolff F, Moller HM, Graumann PL. 2012. Synthetic motility and cell shape defects for deletions of flotillin/reggie paralogs in *Bacillus subtilis* and interplay with NfeD proteins. *J. Bacteriol.* 194:4652–4661.
8. Donovan C, Bramkamp M. 2009. Characterization and subcellular localization of a bacterial flotillin homologue. *Microbiology* 155:1786–1799.
9. Zhao F, Zhang J, Liu YS, Li L, He YL. 2011. Research advances on flotillins. *Virol. J.* 8:479–484.
10. Stuermer CA. 2010. The reggie/flotillin connection to growth. *Trends Cell Biol.* 20:6–13.
11. Morrow IC, Parton RG. 2005. Flotillins and the PHB domain protein family: rafts, worms and anaesthetics. *Traffic* 6:725–740.



using a 488-nm laser with the corresponding 525/50-nm filter. The photomultiplier voltage was set at 462 V. For each sample, 50,000 nongated cells were measured. Data analysis was performed using the FlowJo v 9.5.1 software (Tree Star, Inc., Ashland, OR).

**Western blot analysis.** For extraction of whole-cell fractions, cells were grown in liquid MSgg medium at 30°C; the length of cultivation

12. Stuermer CA. 2011. Reggie/flotillin and the targeted delivery of cargo. *J. Neurochem.* 116:708–713.
13. Allen JA, Halverson-Tamboli RA, Rasenick MM. 2007. Lipid raft microdomains and neurotransmitter signalling. *Nat. Rev. Neurosci.* 8:128–140.
14. Kokubo H, Lemere CA, Yamaguchi H. 2000. Localization of flotillins in human brain and their accumulation with the progression of Alzheimer's disease pathology. *Neurosci. Lett.* 290:93–96.
15. Girardot N, Allinquant B, Langui D, Laquerrière A, Dubois B, Hauw JJ, Duyckaerts C. 2003. Accumulation of flotillin-1 in tangle-bearing neurones of Alzheimer's disease. *Neuropathol. Appl. Neurobiol.* 29:451–461.
16. Koch JC, Solis GP, Bodrikov V, Michel U, Haralampieva D, Shyptsyna A, Tönges L, Bähr M, Lingor P, Stuermer CA. 2013. Upregulation of reggie-1/flotillin-2 promotes axon regeneration in the rat optic nerve in vivo and neurite growth in vitro. *Neurobiol. Dis.* 51:168–176.
17. Schulte T, Paschke KA, Laessing U, Lottspeich F, Stuermer CA. 1997. Reggie-1 and reggie-2, two cell surface proteins expressed by retinal ganglion cells during axon regeneration. *Development* 124:577–587.
18. Munro S. 2003. Lipid rafts: elusive or illusive? *Cell* 115:377–388.
19. Butcher BG, Helmann JD. 2006. Identification of *Bacillus subtilis* sigma-dependent genes that provide intrinsic resistance to antimicrobial compounds produced by bacilli. *Mol. Microbiol.* 60:765–782.
20. Bach JN, Bramkamp M. 2013. Flotillins functionally organize the bacterial membrane. *Mol. Microbiol.* 88:1205–1217.
21. Dempwolff F, Möller HM, Graumann PL. 2012. Synthetic motility and cell shape defects associated with deletions of flotillin/reggie paralogs in *Bacillus subtilis* and interplay of these proteins with NfeD proteins. *J. Bacteriol.* 194:4652–4661.
22. Yepes A, Schneider J, Mielich B, Koch G, García-Betancur JC, Ramamurthi KS, Vlamakis H, López D. 2012. The biofilm formation defect of a *Bacillus subtilis* flotillin-defective mutant involves the protease FtsH. *Mol. Microbiol.* 86:457–471.
23. Hamon MA, Lazazzera BA. 2001. The sporulation transcription factor Spo0A is required for biofilm development in *Bacillus subtilis*. *Mol. Microbiol.* 42:1199–1209.
24. Lopez D, Vlamakis H, Kolter R. 2009. Generation of multiple cell types in *Bacillus subtilis*. *FEMS Microbiol. Rev.* 33:152–163.
25. Le AT, Schumann W. 2009. The Spo0E phosphatase of *Bacillus subtilis* is a substrate of the FtsH metalloprotease. *Microbiology* 155:1122–1132.
26. Haeusser DP, Garza AC, Buscher AZ, Levin PA. 2007. The division inhibitor EzrA contains a seven-residue patch required for maintaining the dynamic nature of the medial FtsZ ring. *J. Bacteriol.* 189:9001–9010.
27. Haeusser DP, Schwartz RL, Smith AM, Oates ME, Levin PA. 2004. EzrA prevents aberrant cell division by modulating assembly of the cytoskeletal protein FtsZ. *Mol. Microbiol.* 52:801–814.
28. Singh JK, Makde RD, Kumar V, Panda D. 2007. A membrane protein, EzrA, regulates assembly dynamics of FtsZ by interacting with the C-terminal tail of FtsZ. *Biochemistry* 46:11013–11022.
29. Branda SS, González-Pastor JE, Ben-Yehuda S, Losick R, Kolter R. 2001. Fruiting body formation by *Bacillus subtilis*. *Proc. Natl. Acad. Sci. U. S. A.* 98:11621–11626.
30. López D, Kolter R. 2010. Extracellular signals that define distinct and coexisting cell fates in *Bacillus subtilis*. *FEMS Microbiol. Rev.* 34:134–149.
31. Vlamakis H, Chai Y, Beauregard P, Losick R, Kolter R. 2013. Sticking together: building a biofilm the *Bacillus subtilis* way. *Nat. Rev. Microbiol.* 11:157–168.
32. Branda SS, González-Pastor JE, Dervyn E, Ehrlich SD, Losick R, Kolter R. 2004. Genes involved in formation of structured multicellular communities by *Bacillus subtilis*. *J. Bacteriol.* 186:3970–3979.
33. Kearns DB, Chu F, Branda SS, Kolter R, Losick R. 2005. A master regulator for biofilm formation by *Bacillus subtilis*. *Mol. Microbiol.* 55:739–749.
34. Chai L, Romero D, Kayatekin C, Akabayov B, Vlamakis H, Losick R, Kolter R. 2013. Isolation, characterization, and aggregation of a structured bacterial matrix precursor. *J. Biol. Chem.* 288:17559–17568.
35. Stöver AG, Driks A. 1999. Control of synthesis and secretion of the *Bacillus subtilis* protein YqxM. *J. Bacteriol.* 181:7065–7069.
36. Stöver AG, Driks A. 1999. Regulation of synthesis of the *Bacillus subtilis* transition-phase, spore-associated antibacterial protein TsaA. *J. Bacteriol.* 181:5476–5481.
37. Branda SS, Chu F, Kearns DB, Losick R, Kolter R. 2006. A major protein component of the *Bacillus subtilis* biofilm matrix. *Mol. Microbiol.* 59:1229–1238.
38. Romero D, Aguilar C, Losick R, Kolter R. 2010. Amyloid fibers provide structural integrity to *Bacillus subtilis* biofilms. *Proc. Natl. Acad. Sci. U. S. A.* 107:2230–2234.
39. Romero D, Vlamakis H, Losick R, Kolter R. 2011. An accessory protein required for anchoring and assembly of amyloid fibres in *B. subtilis* biofilms. *Mol. Microbiol.* 80:1155–1168.
40. McLoon AL, Guttenplan SB, Kearns DB, Kolter R, Losick R. 2011. Tracing the domestication of a biofilm-forming bacterium. *J. Bacteriol.* 193:2027–2034.
41. Chu F, Kearns DB, Branda SS, Kolter R, Losick R. 2006. Targets of the master regulator of biofilm formation in *Bacillus subtilis*. *Mol. Microbiol.* 59:1216–1228.
42. López D, Fischbach MA, Chu F, Losick R, Kolter R. 2009. Structurally diverse natural products that cause potassium leakage trigger multicellularity in *Bacillus subtilis*. *Proc. Natl. Acad. Sci. U. S. A.* 106:280–285.
43. Quadri LE, Weinreb PH, Lei M, Nakano MM, Zuber P, Walsh CT. 1998. Characterization of Sfp, a *Bacillus subtilis* phosphopantetheinyl transferase for peptidyl carrier protein domains in peptide synthetases. *Biochemistry* 37:1585–1595.
44. Reuter K, Mofid MR, Marahiel MA, Ficner R. 1999. Crystal structure of the surfactin synthetase-activating enzyme sfp: a prototype of the 4'-phosphopantetheinyl transferase superfamily. *EMBO J.* 18:6823–6831.
45. Schumann W. 1999. FtsH—a single-chain chaperonin? *FEMS Microbiol. Rev.* 23:1–11.
46. Ito K, Akiyama Y. 2005. Cellular functions, mechanism of action, and regulation of FtsH protease. *Annu. Rev. Microbiol.* 59:211–231.
47. Bieniossek C, Schalch T, Bumann M, Meister M, Meier R, Baumann U. 2006. The molecular architecture of the metalloprotease FtsH. *Proc. Natl. Acad. Sci. U. S. A.* 103:3066–3071.
48. Bieniossek C, Niederhauser B, Baumann UM. 2009. The crystal structure of apo-FtsH reveals domain movements necessary for substrate unfolding and translocation. *Proc. Natl. Acad. Sci. U. S. A.* 106:21579–21584.
49. Janska H, Kwasniak M, Szczepanowska J. 2013. Protein quality control in organelles—AAA/FtsH story. *Biochim. Biophys. Acta* 1833:381–387.
50. Tatsuta T, Langer T. 2009. AAA proteases in mitochondria: diverse functions of membrane-bound proteolytic machines. *Res. Microbiol.* 160:711–717.
51. Wehr L, Niederweis M, Schumann W. 2000. The FtsH protein accumulates at the septum of *Bacillus subtilis* during cell division and sporulation. *J. Bacteriol.* 182:3870–3873.
52. Barák I, Prepiak P, Schmeisser F. 1998. MinCD proteins control the septation process during sporulation of *Bacillus subtilis*. *J. Bacteriol.* 180:5327–5333.
53. Feucht A, Errington J. 2005. ftsZ mutations affecting cell division frequency, placement and morphology in *Bacillus subtilis*. *Microbiology* 151:2053–2064.
54. Reeve JN, Mendelson NH, Coyne SI, Hallock LL, Cole RM. 1973. Minicells of *Bacillus subtilis*. *J. Bacteriol.* 114:860–873.
55. Bi EF, Lutkenhaus J. 1991. FtsZ ring structure associated with division in *Escherichia coli*. *Nature* 354:161–164.
56. Errington J, Daniel RA, Scheffers DJ. 2003. Cytokinesis in bacteria. *Microbiol. Mol. Biol. Rev.* 67:52–65.
57. Bi E, Lutkenhaus J. 1993. Cell division inhibitors SulA and MinCD prevent formation of the FtsZ ring. *J. Bacteriol.* 175:1118–1125.
58. Weart RB, Lee AH, Chien AC, Haeusser DP, Hill NS, Levin PA. 2007. A metabolic sensor governing cell size in bacteria. *Cell* 130:335–347.
59. Brown DA. 2002. Isolation and use of rafts. *Curr. Protoc. Immunol.* Chapter 11:Unit 11.10. doi:10.1016/j.cell.2007.05.043.
60. Lingwood D, Simons K. 2007. Detergent resistance as a tool in membrane research. *Nat. Protoc.* 2:2159–2165.
61. Levin PA, Kurtser IG, Grossman AD. 1999. Identification and characterization of a negative regulator of FtsZ ring formation in *Bacillus subtilis*. *Proc. Natl. Acad. Sci. U. S. A.* 96:9642–9647.
62. Kang MS, Kim SR, Kwack P, Lim BK, Ahn SW, Rho YM, Seong IS, Park SC, Eom SH, Cheong GW, Chung CH. 2003. Molecular architecture of the ATP-dependent CodWX protease having an N-terminal serine active site. *EMBO J.* 22:2893–2902.
63. Zellmeier S, Zuber U, Schumann W, Wiegert T. 2003. The absence of FtsH metalloprotease activity causes overexpression of the sigmaW-controlled pbpE gene, resulting in filamentous growth of *Bacillus subtilis*. *J. Bacteriol.* 185:973–982.

Mielich-Süss et al.

64. Hardwood CR, Cutting SM. 1990. Molecular biological methods for *Bacillus*. Wiley, New York, NY.
65. Dubnau D. 1991. Genetic competence in *Bacillus subtilis*. Microbiol. Rev. 55:395–424.
66. Yasbin RE, Young FE. 1974. Transduction in *Bacillus subtilis* by bacteriophage SPP1. J. Virol. 14:1343–1348.
67. Britton RA, Eichenberger P, Gonzalez-Pastor JE, Fawcett P, Monson R, Losick R, Grossman AD. 2002. Genome-wide analysis of the stationary-phase sigma factor (sigma-H) regulon of *Bacillus subtilis*. J. Bacteriol. 184: 4881–4890.
68. Nakano S, Küster-Schöck E, Grossman AD, Zuber P. 2003. Spx-dependent global transcriptional control is induced by thiol-specific oxidative stress in *Bacillus subtilis*. Proc. Natl. Acad. Sci. U. S. A. 100: 13603–13608.
69. Kim L, Mogk A, Schumann W. 1996. A xylose-inducible *Bacillus subtilis* integration vector and its application. Gene 181:71–76.
70. Lewis PJ, Marston AL. 1999. GFP vectors for controlled expression and dual labelling of protein fusions in *Bacillus subtilis*. Gene 227:101–110.
71. Kobayashi K, Iwano M. 2012. BslA(YuaB) forms a hydrophobic layer on the surface of *Bacillus subtilis* biofilms. Mol. Microbiol. 85:51–66.



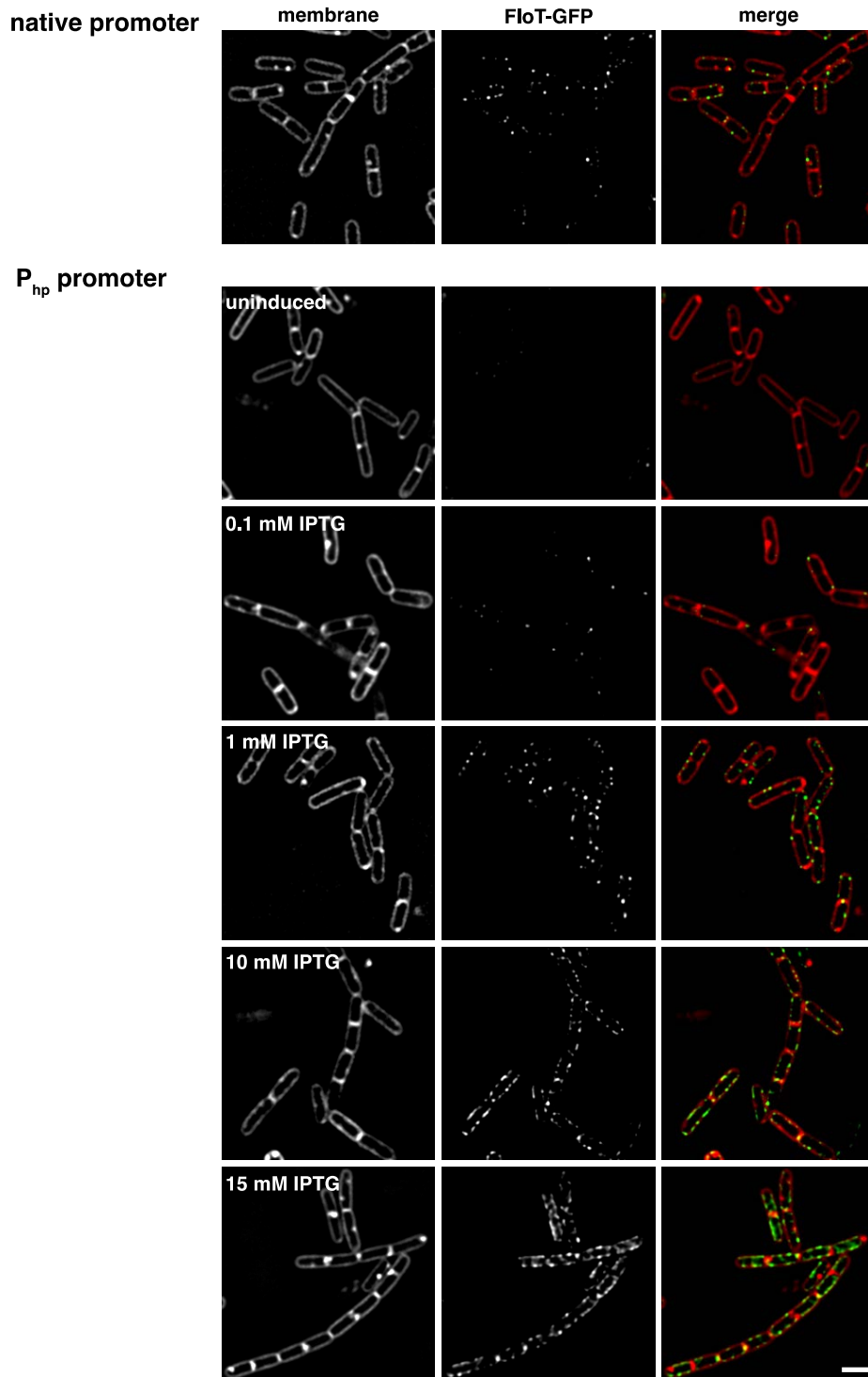
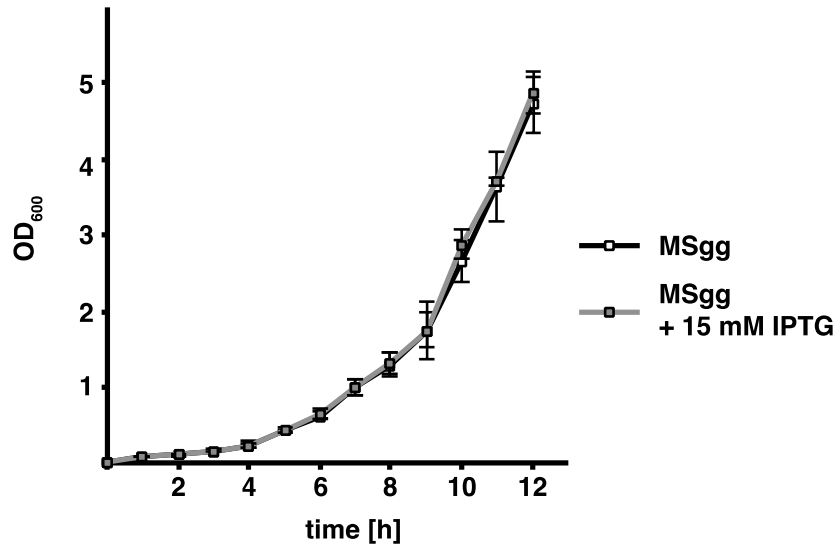
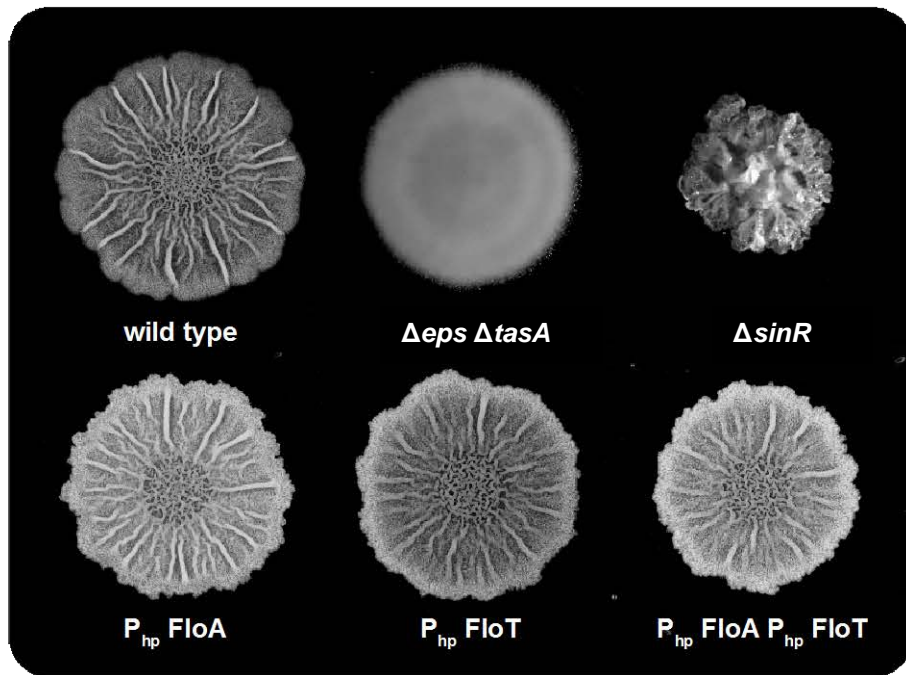


Figure S1



**Figure S2**



**Figure S3**

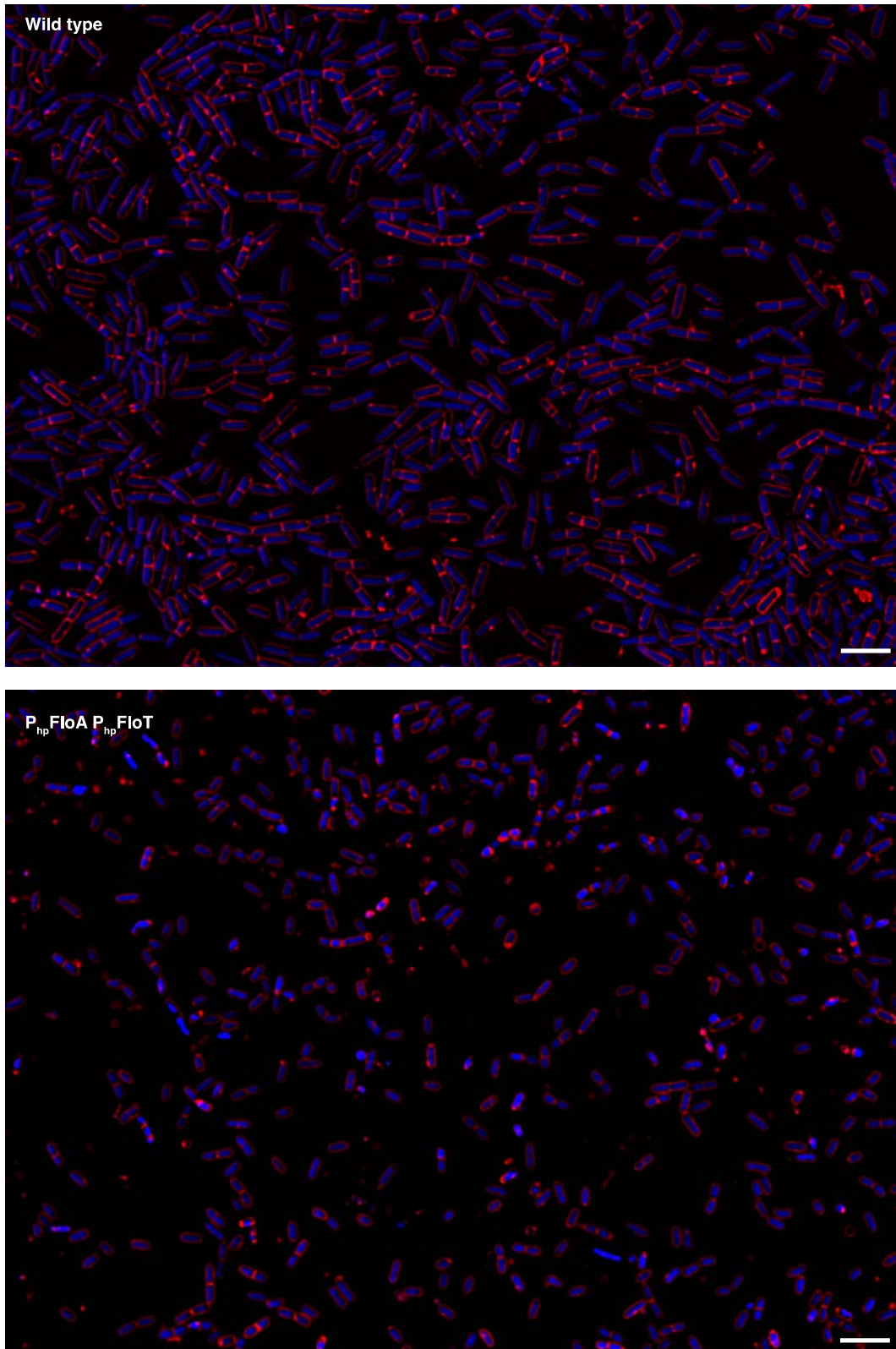


**Figure S4**

**EzrA (Coverage: 52.85%)**

MEFVIGLLIVLLALFAAGYFFRKKIYAEIDRLESWKIEILNRSIVEEMSKIKHLKMTG  
QTEEFFEKWREEWDEIVTAHMPKVEELLYDAEENADKYRFKKNQVLVHIDDLLTAAE  
SSIEKILREISDLVTSEEKSREEIEQVRERYSKSRKNLLAYSHLYGELYDSLEKDLDE  
IWSGIKQFEEETEGGNYITARKVLLQDRNLERLQSYIDDVPKLLADCKQTPVPGQIAK  
LKDGYGEMKEKGYKLEHIQLDKELNLSNQLKRAEHVLMTELDIDEASAILQLIDENI  
QSVYQQLEGEVEAGQSVLSKMPELIIAYDKLKEEKEHTKAETELVKESYRLTAGELGK  
QAFEKRLDEIGKLLSSVKDKLDAEHVAYSLLVEEVASIEKQIEEVKKEHAEYRENLO  
ALRKEELQARETSLNLKKTISE TARLLKTSNIPGIPSHIQEMLENAHHHIQETVNQLN  
ELPLNMEEAG AHLKQAEDIVNRASRESEELVEQVILIEKIIQFGNRRFRSQNHILSEQL  
KEAERRFYAFDYDDSYEIAAAAVEKAAPGAVEKIKADISA

**Table S1**

Strain	Genotype	Reference
<b><i>Bacillus subtilis</i> PY79</b>		
BM-18	Wild type PY79	Youngman et al. 1984
BM-224	<i>amyE::P<sub>yqeZ</sub> floA-gfp</i> (spc)	Yepes et al. 2012
BM-20	<i>amyE::P<sub>hp</sub> floA-gfp</i> (spc)	This study
BM-223	<i>amyE::P<sub>yuaF</sub> floT-gfp</i> (spc)	Yepes et al. 2012
BM-21	<i>amyE::P<sub>hp</sub> floT-gfp</i> (spc)	This study
BM-246	$\Delta$ <i>tasA::spc</i>	This study
BM-225	$\Delta$ <i>sinR::spc</i>	This study
BM-248	$\Delta$ <i>tasA::km</i> $\Delta$ <i>sinR::spc</i>	This study
BM-19	<i>amyE::P<sub>hp</sub> floA</i> (spc)	This study
BM-28	<i>amyE::P<sub>hp</sub> floT</i> (spc)	This study
BM-29	<i>amyE::P<sub>hp</sub> floT</i> (spc) <i>lacA::P<sub>hp</sub> floA</i> (mls)	This study
BM-247	<i>amyE::P<sub>hp</sub> floT</i> (spc) <i>lacA::P<sub>hp</sub> floA</i> (mls) $\Delta$ <i>tasA::km</i>	This study
BM-126	<i>thrC::P<sub>tapA</sub> yfp</i> (km)	This study
BM-243	<i>amyE::P<sub>hp</sub> floA</i> (spc) <i>thrC::P<sub>tapA</sub> yfp</i> (km)	This study
BM-244	<i>amyE::P<sub>hp</sub> floT</i> (spc) <i>thrC::P<sub>tapA</sub> yfp</i> (km)	This study
BM-242	<i>amyE::P<sub>hp</sub> floT</i> (spc) <i>lacA::P<sub>hp</sub> floA</i> (mls) <i>thrC::P<sub>tapA</sub> yfp</i> (km)	This study
BM-168	<i>amyE::P<sub>hp</sub> floT</i> (spc) <i>lacA::P<sub>hp</sub> floA</i> (mls) $\Delta$ <i>ftsH::km</i>	This study
BM-249	$\Delta$ <i>ftsH::tet</i>	This study
BM-250	$\Delta$ <i>ftsH::tet</i> <i>thrC::P<sub>tapA</sub> yfp</i> (km)	This study
BM-245	<i>amyE::P<sub>hp</sub> floT</i> (spc) <i>lacA::P<sub>hp</sub> floA</i> (mls) <i>thrC::P<sub>tapA</sub> yfp</i> (km) $\Delta$ <i>ftsH::tet</i>	This study
BM-222	<i>amyE::P<sub>xyI</sub> ftsZ-gfp</i> (cm)	This study
BM-226	<i>amyE::P<sub>xyI</sub> ftsZ-gfp</i> (cm) <i>lacA::P<sub>hp</sub> floT/floA</i> (mls)	This study
BM-144	<i>amyE::P<sub>xyI</sub> ezrA-gfp</i> (spc)	This study
BM-151	<i>amyE::P<sub>xyI</sub> ezrA-gfp</i> (spc) <i>lacA::P<sub>hp</sub> floT/floA</i> (mls)	This study
BM-198	<i>amyE::P<sub>xyI</sub> ezrA-gfp</i> (spc) <i>lacA::P<sub>hp</sub> floT/floA</i> (mls) $\Delta$ <i>ftsH::km</i>	This study
BM-197	<i>amyE::P<sub>xyI</sub> ezrA-gfp</i> (spc) $\Delta$ <i>ftsH::km</i>	This study

BM-207	<i>amyE::P<sub>xyl</sub> ezrA-gfp (spc)</i> <i>lacA::P<sub>hp</sub> ftsH (mls)</i>	This study
<b><i>Bacillus subtilis</i> NCIB3610</b>		
DL-1	Wild type NCIB3610	Branda et al. 2001
DL-7	$\Delta$ <i>tasA::spc</i> $\Delta$ <i>eps::tet</i>	Lopez et al. 2009
DL-5	$\Delta$ <i>sinR::spc</i>	Kearns et al. 2005
BM-40	<i>amyE::P<sub>hp</sub> floA (spc)</i>	This study
BM-37	<i>amyE::P<sub>hp</sub> floT (spc)</i>	This study
BM-59	<i>amyE::P<sub>hp</sub> floT (spc)</i> <i>lacA::P<sub>hp</sub> floA (mls)</i>	This study

## References

1. Youngman P, Perkins JB, Losick R. 1984. Construction of a cloning site near one end of Tn917 into which foreign DNA may be inserted without affecting transposition in *Bacillus subtilis* or expression of the transposon-borne erm gene. *Plasmid* 12:1–9.
2. Yepes A, Schneider J, Mielich B, Koch G, García-Betancur J-C, Ramamurthi KS, Vlamakis H, López D. 2012. The biofilm formation defect of a *Bacillus subtilis* flotillin-defective mutant involves the protease FtsH. *Mol Microbiol* 86(2):457-471.
3. Branda SS, González-Pastor JE, Ben-Yehuda S, Losick R, Kolter R. 2001. Fruiting body formation by *Bacillus subtilis*. *Proc. Natl. Acad. Sci. U.S.A.* 98:11621–11626.
4. Kearns DB, Chu F, Branda SS, Kolter R, Losick R. 2005. A master regulator for biofilm formation by *Bacillus subtilis*. *Mol Microbiol* 55:739–749.
5. López D, Vlamakis H, Losick R, Kolter R. 2009. Paracrine signaling in a bacterium. *Genes & Development* 23:1631–1638.

## Abbreviations

### Antibiotics

cm Encodes chloramphenicol resistance protein  
 km Encodes kanamycin resistance protein  
 mls Encodes erythromycin + lincomycin resistance protein  
 spc Encodes spectinomycin resistance protein  
 tet Encodes tetracycline resistance protein

### Protein tags

GFP Green fluorescent protein

### Promoters

P<sub>hp</sub> IPTG-inducible Hyperspank promoter  
 P<sub>xyl</sub> Xylose-inducible promoter  
 P<sub>yuaF</sub> Natural promoter that controls the expression of *yuaG*  
 P<sub>tapA</sub> Natural promoter that controls the expression of *tasA*

**Table S2**

<b>Purpose</b>	<b>Name</b>	<b>Sequence (5'-3')</b>
Overexpression of FloT	YuaGSallfw	AAAAGTCGACTAAGGAGGAACTACTATGACAATGCCGATTATAAT
	YuaGSphlrv	AAAAGCATGCTTACTCTGATTTTTGGATCG
Overexpression of FloA	YqfASallfw	AAAAGTCGACTAAGGAGGAACTACTATGGATCCGTCAACACTTA
	YqfASphlrv	AAAAGCATGCTTATGATTTGCGGTCTTCAT
Overexpression of FloA-GFP or FloT-YFP	GFPsphlrv	AAAAGCATGCTTATTTGTATAGTTCATCCATGC
Overexpression of bicistronic FloA+FloT	YuaGYqfAOp2	CAGTTACCATACGGTTCTG
	YuaGYqfAOp3	CAGAACCGTATGGTAACTGATGGATCCGTCAACACTTA
Overexpression of FtsH	FtsHSallfw	AAAAGTCGACTAAGGAGGAACTACTATGAATCGGGTCTTCCGT
	FtsHSphl	AAAAGCATGCAGAAAGCGAATTACTCTTTC
Translation fusion FtsZ-GFP	FtsZSpelfw	AAAAACTAGTTAAGGAGGAACTACTGCATGTTGGAGTTCGAAAC
	FtsZ-GFP 2	AGTTCTTCTCCTTTACTCATGCCGCGTTTATTACGGTT
	FtsZ-GFP 3	AACCGTAATAAACGCGGATGAGTAAAGGAGAAGAACT
	GFPBamHlrv	AAAAGGATCCATCTGAAGTCTGGACATTTA
Translational fusion EzrA-GFP	EzrAKpnlfw	AAAAGGTACCATGGAGTTTGTTCATTGGATT
	EzrAXholrv	AAAACTCGAGAGCGGATATGTTCAGCTTTG



## III GLOBAL DRM PROTEOME ANALYSIS

### III.1 Preface

Previous studies unraveling the proteome of prokaryotic FMMs were mostly limited to identifying selected proteins from the DRM [117,126], proteins of selected flotillin-associated complexes [132] or the FloT-interactome [137]. Only one study aimed at identifying the entity of all DRM-associated proteins during one specific condition [138].

Yet the proteome of bacterial cells is highly dynamic and specifically adapts to given environmental conditions. Abovementioned studies only provide a snapshot of a distinct condition at one specific time point. Particularly, pathogenic species like *S. aureus* are exposed to a plethora of microenvironments during an infection. Often, they reside as commensals on the skin or in biofilms attached to medical devices or implants. Occasionally they can enter the bloodstream, which is an extremely hostile environment with limited availability of nutrients and the presence of immune mechanisms that counteracts the invasion of the pathogen: For instance, innate immune mechanisms such as the reduction of the host's free iron, which is an essential micronutrient for microbial growth, limits the distribution of pathogens in the blood. Other innate and adaptive immune mechanisms, like the complement system or humoral immune responses aim at clearing the pathogenic.

During all stages of an infection, *S. aureus* adapts its proteome to efficiently thrive in the given niche. This involves not only the coordinated adaption of gene expression, but also the sensing of the environment via sensor kinases, the efficient transport of macromolecules (e.g. of nutrients) or secretion of niche-specific virulence factors. All these processes involve the bacterial membrane and many signaling and transport processes have been suggested to be associated with the integrity of FMMs [117,120].

To this end, it was aimed at quantifying the entire DRM protein content of *S. aureus* in various conditions. This will allow to elucidate dynamics of the DRM protein cargo during the lifespan of a bacterium and may contribute to understanding if the DRM protein content is static or dynamically adapts to individual conditions. Elucidating the DRM protein cargo may help to draw conclusion on FMMs in cell physiology and may

also provide insights how targeted FMM dispersion can decrease the infective potential of this pathogen.

### **III.2 Identification and label-free quantification (LFQ) of *S. aureus* DRMs**

To accurately identify and quantify the DRM proteome, mass-spectrometry (MS) based label-free quantification (LFQ) was employed [250-252]. This is a shot-gun MS approach that allows quantification of proteins without labeling. This is an advantage over other MS-based quantification techniques that required isotopic labeling of metabolites (SILAC) [253] or labeling methods based on chemical or enzymatic modification of proteins prior to identification [254-256]. Instead of comparing labeled versus unlabeled peptide spectra for quantification, label-free quantification is based on normalization of the measured protein abundance to the background protein signal, assuming a linear relation between input proteins and number of spectra or total ion intensity [257].

Thus, this technique allows to not only to assign proteins to either DRM or DSM, but also to show a quantitative enrichment in one phase or the other. This is an important advantage, because membrane proteins often cannot be assigned exclusively to either the raft- or to the non-raft phase [2]. Mostly they have a preference for a distinct phase or the other, which is not mutually exclusive. Moreover, lateral phase separation of proteins can be influenced by accompanying proteins in- or outside of the rafts or – at least in eukaryotic membranes – by posttranslational modifications that may modulate raft-affinity [2].

To understand if the FMM proteome is static or dynamic, membrane fractions were isolated of cells grown in four different conditions that resemble important stages during the infection and that are known to have substantial differences in the proteome. Firstly, stationary growth phase was chosen as a neutral stage and cells were harvested from an overnight culture. Secondly, it is known that during exponential growth the proteome is efficiently adapted towards the production of more cell material to drive the invagination into two daughter cells. As a third condition, iron-limiting conditions were chosen to mimic the limited access to iron during a bloodstream infection. To this end, cells were grown in the presence of the iron-chelating agent 2'2-dipyridyl. Finally, cells grown as multicellular aggregates, serve as the fourth condition. These multicellular

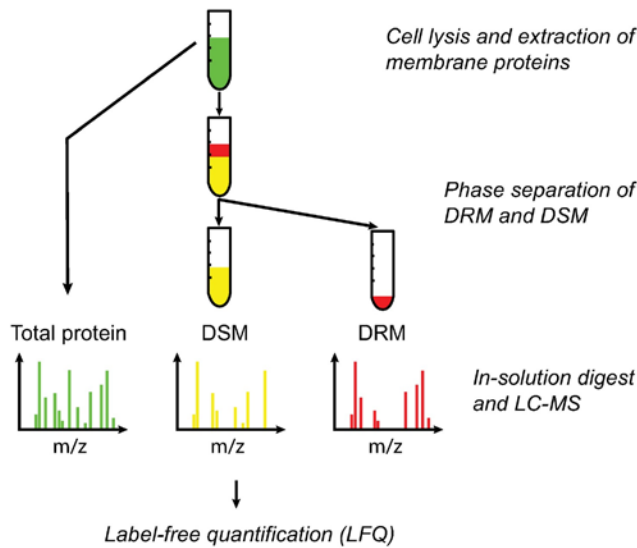


**Fig. III.1: Schematic overview of the LFQ workflow.**

Membrane proteins were isolated and separated into detergent resistant membrane (DRM) and detergent sensitive membrane fraction (DSM). Both DRM/DSM and total membrane protein digested in solution and consecutively measured using mass spectrometry. Measured spectra were then used to quantify proteins with the MaxQuant LFQ algorithm.

aggregates show the typical characteristics of a biofilm, like increased production of the *ica*-operon that constitutes *S. aureus* biofilms [258]. The membrane fraction of cells cultivated in the four abovementioned conditions were isolated and DSM and DRM fractions were separated. As shown in Fig. III.2, the membrane proteome of the abovementioned conditions is indeed versatile (lanes with TP = total protein). Moreover, equal volumes of DRM and DSM fraction were loaded on the gel after extraction. For each of tested conditions, it can be appreciated that proteins are enriched

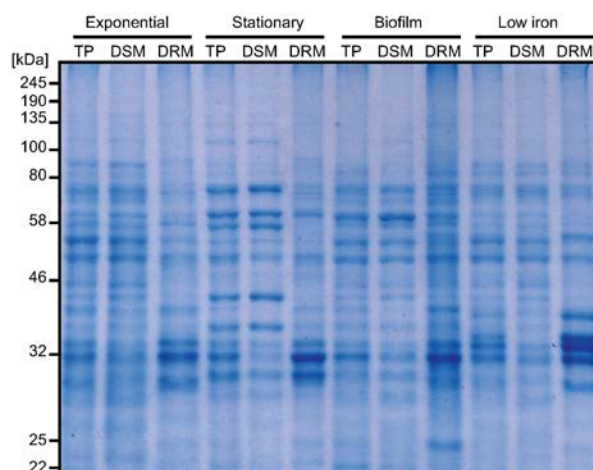


**Fig. III.2: SDS-PAGE analysis of proteins samples used for LFQ analysis.**

Equal amounts of total protein (TP), detergent sensitive membrane (DSM) and detergent resistant membrane (DRM) fractions from *S. aureus* grown in four experimental conditions were separated on a 10 % SDS-PAGE. The same samples were then used for MS-based LFQ.

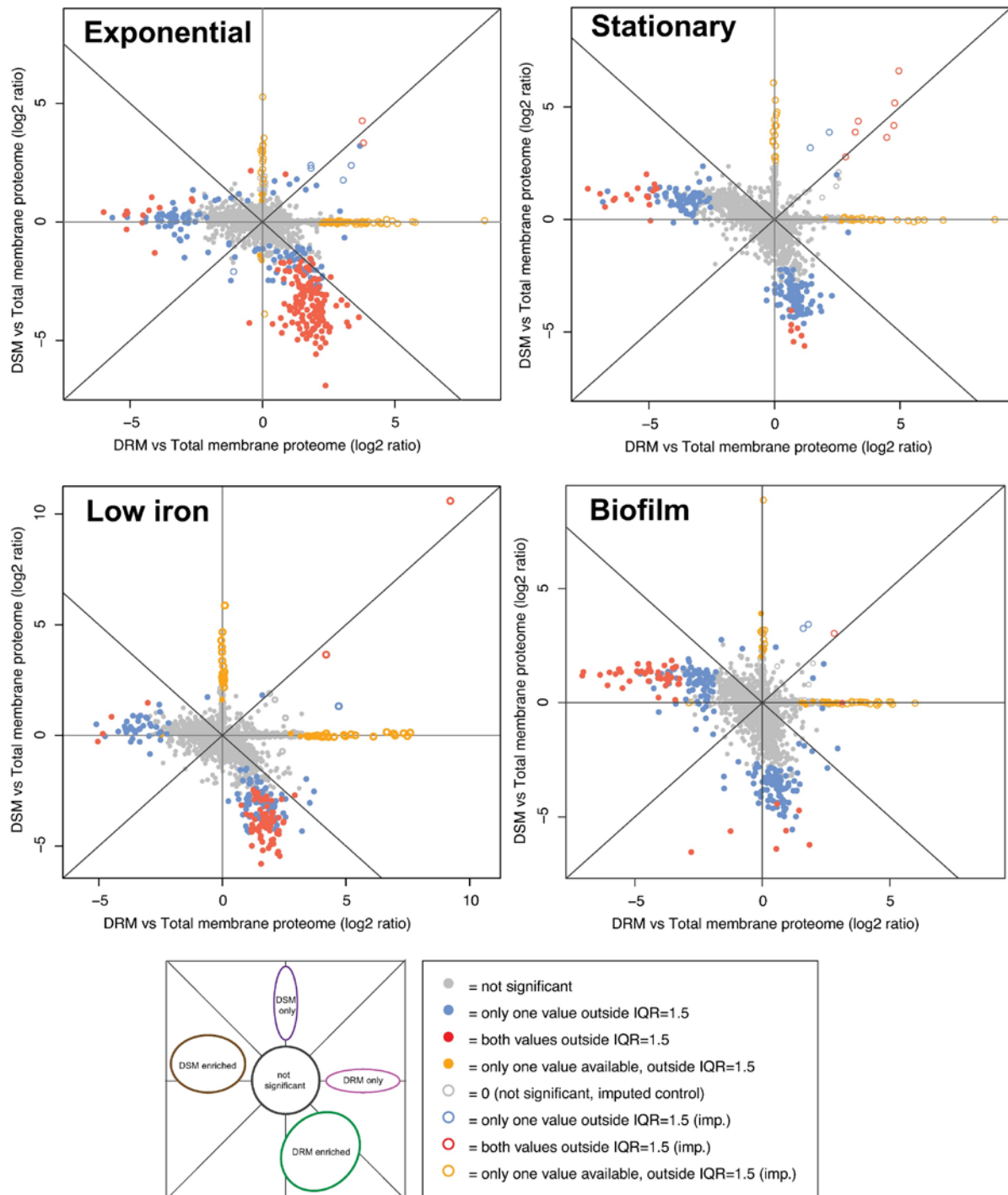


**Fig. III.3: Scatterplots of all identified proteins in LFQ analysis.**

Plots show normalized log<sub>2</sub> ratios of DRM (X-axis) and DSM (Y-axis) versus total membrane proteome of *S. aureus* grown in four different growth conditions. Colored dots are proteins that are outside of an interquartile range (IQR) of 1.5. Red dots represent proteins where both DRM and DSM measurements are outside of IQR = 1.5; blue dots are proteins with only one value outside of IQR = 1.5 and for yellow dots represent proteins where only one value was available. Grey dots are not significant. Unfilled circles are proteins of DRM or DSM measurement with imputed values for TP fraction. Scheme on the bottom shows different zones of the scatterplots representing proteins that are found exclusively or enriched in DSM and DRM, respectively. TP = Total protein, DSM = Detergent sensitive membrane, DRM = Detergent resistant membrane, IQR = interquartile range.

in either DRM or DSM, when comparing to the total membrane proteome. Also, some proteins were present in both DRM and DSM with similar or different abundance, which suggests that membrane proteins indeed cannot always be assigned to a single membrane fraction.

Next, samples were prepared for mass-spectrometry measurements and eventually calculate LFQ intensities with the MaxQuant algorithm [259]. To this end, DRM and DSM fractions, as well as the total proteome of all conditions were measured (Fig. III.1). The mass spectrometry proteomics data have been deposited to the ProteomeXchange Consortium via the PRIDE partner repository with the dataset identifier 'PXD006546'. Next, DRM and DSM intensities were normalized to the total protein content to obtain LFQ intensities and log<sub>2</sub>-ratios were calculated, which indicate an increase or decrease of protein in abundance in DRM or DSM compared to the total membrane proteome. Due to the bulk of proteins detected in the total proteome, some proteins were exclusively detected in DRM or DSM after extraction, but not in the total proteome. For the calculation of the log<sub>2</sub> ratio, in these cases an imputed value was set to 1.0. The DRM vs. total and DSM vs. total log<sub>2</sub> ratios of each of the four analyzed conditions are represented in Fig. III.3. Only values outside of the interquartile range (IQR) of IQR = 1.5 were considered significant. Color codes indicate proteins that were detected exclusively in DRM or DSM (yellow) or enriched in DRM or DSM (blue and red). Red colored dots indicate proteins that are enriched in DRM or DSM with both values outside of IQR = 1.5, for instance a significant enrichment in the DRM (positive DRM vs total log<sub>2</sub> ratio) concomitantly to a significant decrease in the DSM (negative DSM vs total log<sub>2</sub> ratio) or vice versa. Blue colored dots indicate that only one of the two log<sub>2</sub> ratios is statistically significant. For each condition, proteins can be assigned to be present exclusively in DSM, exclusively in DRM or enriched in either of the two fractions, validating the functionality of this technique to quantify membrane proteins in DRM or DSM membrane phases.

To compare the DRM proteins identified in this LFQ analysis of each condition, unsupervised hierarchical clustering analysis was performed. This analysis allows to cluster common proteins and shows diversification of proteins into clusters specific for one or more analyzed conditions. Figure Fig. III.4 shows the results of this analysis. Clearly, there are clusters identified that contain proteins, which are present in each condition that was analyzed (Cluster A and B, Fig. III.4). This set of proteins can be referred to as a 'core' set of proteins that might always locate in FMMS. Those values

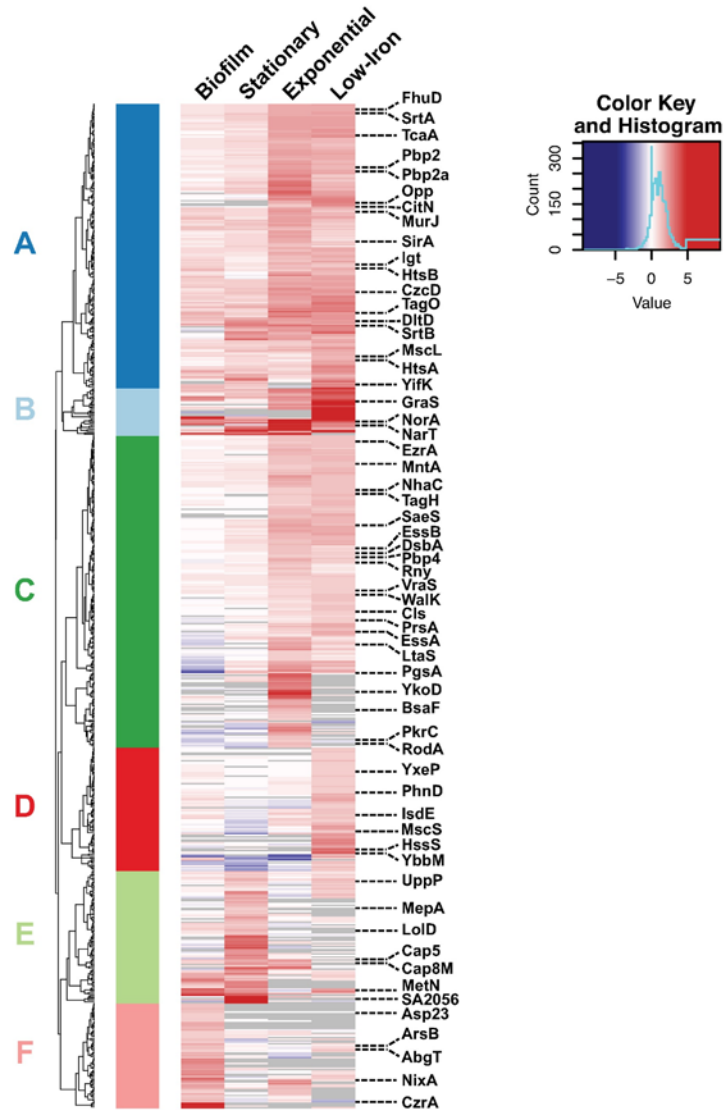


**Fig. III.4: Hierarchical clustering of DRM-membrane proteome during four different conditions:**

MS-based label-free quantification (LFQ) of the DRM-membrane proteome of four different conditions that represent important stages during an infection. Heatmap shows ratios of calculated protein abundance in DRM versus total membrane proteome by unsupervised hierarchical clustering. Red represents enrichment in DRM membrane fraction in respect to total membrane proteome, blue denotes a decrease. Grey boxes represent boxes with missing values. Heatmap only includes proteins that are significant in at least one of the four conditions.

have a positive DRM vs total log<sub>2</sub> ratio, whereby cluster B proteins are highly enriched in the DRM and cluster A represent proteins were both DRM and DSM measurements are enriched as well, but to a lesser extent. The core proteins include proteins important for the cell wall organization, like penicillin-binding proteins (PBP2, PBP2a), the sortases SrtA and SrtB or the DltD that is involved in the teichoic acid biosynthesis pathway.

Furthermore, the cluster analysis revealed that for each tested condition a defined set of proteins can be found in the DRM: Cluster C contains proteins that are highly DRM-

enriched in exponential growth phase and likewise cluster D for iron limiting conditions, cluster E for stationary growth phase and cluster F for biofilm. These proteins are often not detected in other conditions (grey boxes), which indicates that expression of these proteins is specific to the tested conditions, or they have a higher affinity to the DRM (represented by differences in the log<sub>2</sub> ratios). This suggests that during a distinct condition these proteins are undergoing a lateral reorganization, probably being actively sequestered to the FMM. Interestingly, the adaption of the DRM protein content that was unraveled by this LFQ-based cluster analysis, can be correlated to the adaption to the given condition. For instance, chelating iron from the medium with 2'2 dipyridyl leads to enrichment of heme sensing (HssS) and heme uptaking proteins (IsdE) in the DRM [260]. Likewise, proteins that are typically associated with septum establishment (EzrA, RodA) [261,262] or located in septal regions (Cls)[263] were associated with cluster C that show strong DRM-enrichment during exponential growth. Other examples are capsule production proteins (Cap5 or Cap8M) that are typically produced at early and late stationary phase and are found in cluster E [264].

Interestingly, the majority of proteins identified in this analysis were histidine-kinases, lipoproteins, transporters or components of protein complexes. For instance, 11 out of 13 known membrane-bound histidine kinases of *S. aureus* were detected enriched in the DRM in one or more of the analyzed conditions. Moreover, of all identified components of membrane transporters (ABC transporters; ion, nutrient and metabolite transporters), more than 90 % could be classified to the DRM-enriched clusters. These findings are consistent with the hypothesis that FMMs, which are highly concentrated in the DRM fractions, mainly contain proteins that require protein-protein interaction or are part of protein complexes.

## **IV THE SCAFFOLDING ACTIVITY OF FLOA IS IMPORTANT FOR THE ASSEMBLY OF THE T7SS PROTEIN COMPLEX**

### **IV.1 Preface**

The DRM proteome analysis of chapter III revealed a plethora of proteins and protein complexes as potential candidates that are regulated by the action of FMMs. As a clinically relevant pathogen, interference with virulent processes of *S. aureus* that depend on FMM-integrity might be an important strategy to ameliorate the infective potential of this pathogen. During data analysis, particular attention was paid to DRM proteins that are involved in virulence. Interestingly, proteins of the type 7 secretion system (T7SS) were consistently detected in the proteomic analysis, which suggests a functional dependence on FMMs and the scaffold activity of FloA. This recently discovered secretion system is involved in intermicrobial competition [224], as well as virulence processes, such as abscess formation [218,221], nasal colonization [219] or contribution to persistent infections [220].

Several small molecules are known that interfere with the activity of the FloA scaffold activity and the integrity of FMMs [245]. A functional dependence of T7SS activity on FMMs and the scaffold protein flotillin could thus be used as a novel therapeutic approach to treat staphylococcal infections that involve the action of the T7SS, such as formation of persistent kidney or liver abscesses [218,220].

### **IV.2 T7SS proteins are part of the DRM**

The membrane proteins EsaA, EssA, EssB were found to be enriched in the DRM, which suggests that the T7SS of *S. aureus* might be physically and functionally connected to FMMs.

Before assessing a functional connection of FMMs and the T7SS, several translational fusions were generated that were used in this chapter. EssA was fused to the codon-optimized RFP variant MARS [265] and EssB was N-terminally tagged with a GFP- or the FLAG-tag. These constructs will be used for different purposes in the course of this work. All constructs were generated using the pLac and pAmy plasmids [266,267] and integrated into mutants carrying the respective clean deletion of EssA or EssB. To



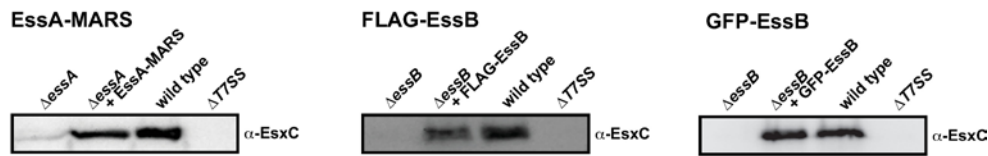


**Fig. IV.1. Synthetic strains render functional T7SS.**

Western blot analysis of culture supernatants of  $\Delta$ essA and  $\Delta$ essB and the corresponding complementation with EssA-MARS and FLAG-/GFP-EssB, respectively. Cells were grown until reaching early stationary growth phase, sterile-filtered supernatants were precipitated and an amount corresponding to 0.6 ml culture was used for immunoblotting and detected with  $\alpha$ -EsxC antibodies.

confirm the functionality of these translational fusions, it was checked if the secretion defect of a clean EssA or EssB deletion can be recovered by expressing the EssA-MARS, GFP-EssB or FLAG-EssB from a neutral locus. To this end, the mutants and the respective complemented strains were grown until early stationary growth phase, the supernatants were collected, filter-sterilized and concentrated by TCA precipitation. The samples were then subjected to SDS-PAGE and analyzed by western blotting using polyclonal antibodies against the secreted T7SS substrate EsxC [219]. Fig. IV.1 shows that the secretion defects of EssA or EssB deletions can be restored to wild type levels by expressing EssA-MARS or GFP-/FLAG-EssB from neutral loci.

To confirm the findings of the LFQ analysis presented in chapter III, DRM and DSM fractions were isolated to semi-quantitatively measure the presence of T7SS membrane proteins EsaA, EssA, EssB and EssC proteins by immunoblotting. EsaA, EssB and EssC were detected using polyclonal antibodies [219] and MARS-tagged EssA was detected using anti-mCherry antibodies. Western blot analyses showed an enrichment of EsaA, EssA and EssB in the DRM fraction. Signals attributable to EssB and EsaA were enriched in the DRM fraction (~10-fold and 2-fold, respectively). EssC was also present in both membrane phases, but enriched in the DSM. Immunodetection of EssA-MARS only showed a signal associated with the DRM fraction. These results are consistent with the findings of the LFQ mass spectrometry analysis in stationary phase (chapter III) and correlates the T7SS and FMM. Based on these results, it can be hypothesized that T7SS proteins might be associated with the FMMs of *S. aureus*.

Next, it was investigated whether T7SS-related membrane proteins detected in the DRM fractions are among the interacting proteins that are tethered by the *S. aureus* FMM

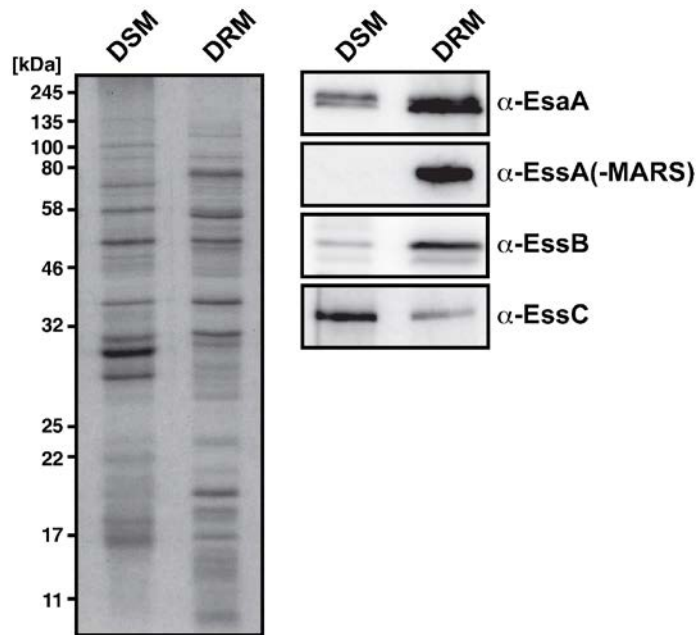


**Fig. IV.2: Proteins of the T7SS are confined to the FMM in *S. aureus*.**

Right panel shows immunoblot analysis of DRM and DSM using antibodies directed against EsaA, EssB, EssC and MARS-tagged EssA in DSM and DRM membrane fractions. The coomassie stained gel of DSM and DRM membrane fractions shown on the left was used as loading control.

scaffold protein flotillin (FloA). To answer this question, a bacterial-two hybrid assay in a heterologous *E. coli* system was performed, in which *S. aureus* flotillin (FloA) and T7SS membrane proteins were tagged with T25 or T18 fragments of an adenylate cyclase. Upon interaction of FloA with T7SS proteins, the enzyme is reconstituted, produces cAMP and triggers expression of a cAMP-inducible *lacZ* reporter that can be quantitatively measured [268]. Using this assay, a strong interaction between FloA and EssB was detected (> 2000 Miller Units; a 700 Miller Units threshold limit defines positive and negative interaction signals). Notably, this interaction was only observed when the adenylate cyclase fragment was fused to the N-terminus of EssB, indicating that also in this heterologous system EssB retains the predicted topology with the N-terminus facing the cytosol. An interaction of FloA with EsaA was also detected, but this interaction was inconsistently found in only one particular combination (T25-FloA + T18-EsaA). Since this interaction was not detected when reverting the fragments (T18-FloA + T25-EsaA), this interaction was considered as false positive. Furthermore, no interactions between FloA and EssA or EssC (Fig. IV.3) was detected. Thus, the protein-protein interaction analyses using a heterologous system suggest an interaction between FloA and the membrane-bound protein EssB from the T7SS of *S. aureus*.



FLAG-EssB detection was performed by immunoblotting using monoclonal anti-FLAG antibodies. A signal attributable to FLAG-EssB was detected in the eluted sample of the double-labeled strain, suggesting that EssB co-eluted with FloA. In contrast, no signal was detected in the elution fraction of FloA-His and FLAG-EssB single-labeled strains, which implies that EssB retention on the column was FloA-dependent (Fig. IV.4A).

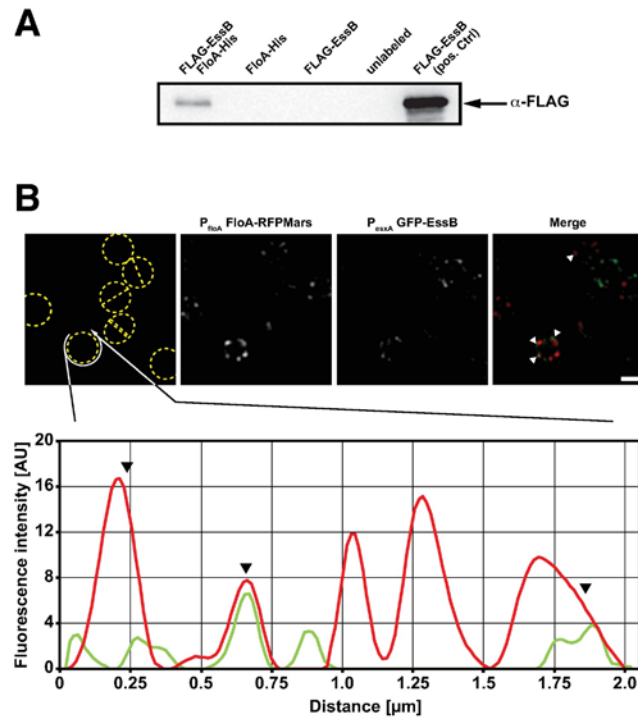


**Fig. IV.4: FloA interacts with the T7SS protein EssB.**

(A) Immunoblot analysis of pull-down assay to demonstrate the *in vivo* interaction of EssB and FloA in *S. aureus*. Lane 1 shows elution fraction of FLAG-EssB FloA-His from a Ni-NTA column. The negative controls in lane 2 and 3 are single labeled strains and lane 4 is an unlabeled strain. The positive control is the membrane fraction of FLAG-EssB FloA-His double-labeled strain. (B) Structured illumination microscopy (SIM) images of a FloA-MARS GFP-EssB double-labeled strain show individual foci of flotillin and EssB, which are occasionally co-localizing. The image on the left shows projected outline of the cells, image 2 and 3 represent signals from the red and green channel, respectively. The image on the right shows merge of red and green fluorescent signals, false colored in red and green, respectively. Arrowheads indicate regions of co-localization. The scale bar represents 0.5  $\mu\text{m}$ . The panel on the bottom shows the fluorescence intensity profile along a representative cell.

Furthermore, structured illumination microscopy was used to examine the colocalization of EssB and FloA signals in living cells. Structured illumination microscopy is a super-resolution technique that allows *in vivo* visualization of the subcellular localization of proteins using conventional fluorescent proteins [43,269]. A GFP-tagged variant of EssB (GFP-EssB) in a  $\Delta\text{essB}$  background was constructed. Its functionality was confirmed by complementing the secretion deficient phenotype of the  $\Delta\text{essB}$  mutant by using immunodetection of EsxC substrate in the culture supernatants (Fig. IV.1). Then, the GFP-EssB construct was used to generate a GFP-EssB FloA-MARS

double-labeled strain. The functionality of C-terminal fusion of fluorescent proteins to FloA was assessed recently and showed wild type behavior [245]. Using the double-labeled strain, FloA distributed in 1-6 fluorescent foci per cell, the GFP-tagged EssB formed 1-3 membrane foci. GFP-EssB foci showed regions of overlap with FloA foci (Pearson's Correlation Coefficient  $Rr=0.57$  in a region with approximately 150 cells), a representative image is shown in Fig. IV.4B. This experiment showed that not all EssB molecules detected in a cell are co-localizing with FloA. This suggests a transient interaction of FloA and EssB, whereby FloA might exerts its scaffolding activity to assemble interaction of EssB with itself or other proteins of the T7SS.

#### **IV.4 T7SS secretion is reduced in *S. aureus* cells lacking flotillin**

After having determined that EssB is associated with the FMMs and shows an interaction with FloA, the influence that FloA exerts on T7SS activity was investigated. This is an important aspect of *S. aureus* virulence since EssB is essential for secretion of T7SS effectors during infection [218,219,221,232]. To this end, the secretion levels of the prototypical T7SS substrates EsxA and EsxB, as well as EsxC in the presence and in the absence of FloA were determined. For this purpose, EsxA and EsxB were C-terminally labeled with a FLAG-tag and expressed under the control of a constitutive promoter. Supernatants from TSB cultures were collected, secreted proteins were concentrated by TCA precipitation and immunodetection of EsxA- and EsxB-FLAG proteins was performed using monoclonal anti-FLAG antibodies. EsxC was detected using specific polyclonal antibodies [219]. It is possible that the *S. aureus*  $\Delta floA$  mutant is affected in general secretory protein complexes, such as the Sec system, as this defect has been described in a flotillin-deficient strain in the closely related bacterium *Bacillus subtilis* [137]. Thus, normalizing to total extracellular protein content of wild type and  $\Delta floA$  mutant for immunoblotting may lead to inaccurate comparisons. Instead, it was normalized to cell culture optical density and an unrelated protein was added exogenously to the supernatants to a defined concentration. Thus, purified heat-inactivated and denatured YtnP lactonase from *B. subtilis* [270] was added to culture supernatants to a concentration of 25  $\mu\text{g/ml}$  before TCA precipitation. An anti-YtnP polyclonal antibody was used to track YtnP concentration during sample processing, to ensure that supernatants samples were concentrated to a comparable level. Using this approach, immunodetection of EsxA- and EsxB-FLAG showed a remarkable decrease in supernatants from  $\Delta floA$  mutant compared to wild type supernatants (Fig. IV.5A).

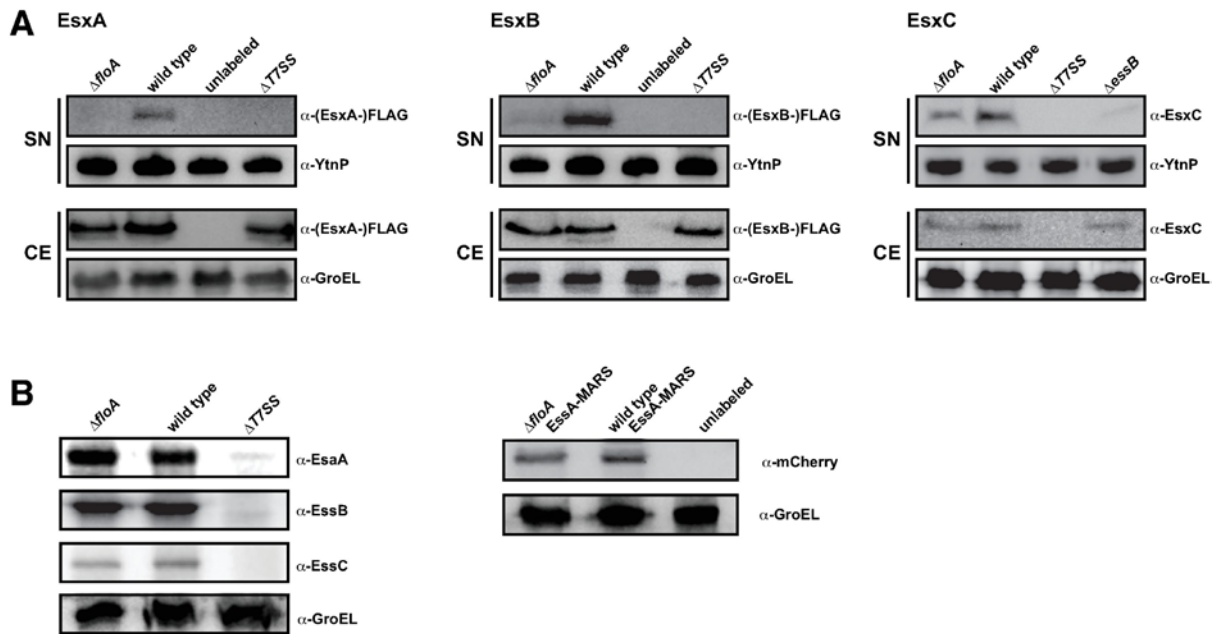


**Fig. IV.5: FloA deletion reduces secretion efficiency of T7SS substrates**

(A) Cells were grown to end of exponential growth phase. Filtered supernatants were supplemented with recombinant YtnP as a precipitation control. Supernatants (SN) were then immunoblotted and proteins were detected with antibodies directed against  $\alpha$ -FLAG,  $\alpha$ -YtnP and  $\alpha$ -EsxC. Cell extracts (CE) were probed against  $\alpha$ -FLAG and  $\alpha$ -EsxC. Detection of GroEL served as loading control. (B) Left panel: Wild type and mutants were grown over night. 20  $\mu$ l of cell extracts were used for immunoblot analysis and detected with antibodies directed against EsaA, EssB and EssC. Detection of GroEL served as loading control. Right panel: Wild type and  $\Delta floA$  mutant expressing complemented EssA-MARS construct were grown over night and 20  $\mu$ l of cell extracts were loaded on gel. Immunoblot analysis was performed using  $\alpha$ -mCherry antibody. An unlabeled wild type strain served as negative control and GroEL was detected as a loading control.

Likewise, a decrease in the presence of the EsxC substrate in  $\Delta floA$  culture supernatants was observed, suggesting an important role of flotillin for T7SS activity. These quantitative differences in T7SS substrates are likely due to reduced secretion efficiency of the T7SS rather than to reduced abundance of T7SS components, since immunodetection of EsaA, EssA, EssB and EssC membrane proteins in whole cell extracts showed similar protein levels in wild type and  $\Delta floA$  mutant (Fig. IV.5B).

#### IV.5 Flotillin mediates T7SS inter-molecular interactions

The most direct hypothesis of how flotillin influences T7SS activity is that the scaffold activity of flotillin promotes T7SS stability by tethering interacting partners [73]. In the absence of FloA, EssB might thus oligomerize less efficiently and negatively affect the correct organization of T7SS. To address this, it was analyzed whether the subcellular distribution of EssB is altered in cells that lacked FloA. Wild type and  $\Delta floA$  mutant were labeled with a GFP-EssB translational fusion and the subcellular distribution pattern of the fluorescence signal was analyzed using fluorescence microscopy. Compared to the

punctate pattern of GFP-EssB in a wild type background, the absence of flotillin in  $\Delta floA$  mutant showed remarkable differences. EssB-foci were not detectable, the signal attributable to GFP-EssB dispersed and was detectable over large portions along the membrane (Fig. IV.6), which suggests that the presence of flotillin is critical for the correct subcellular localization of EssB.

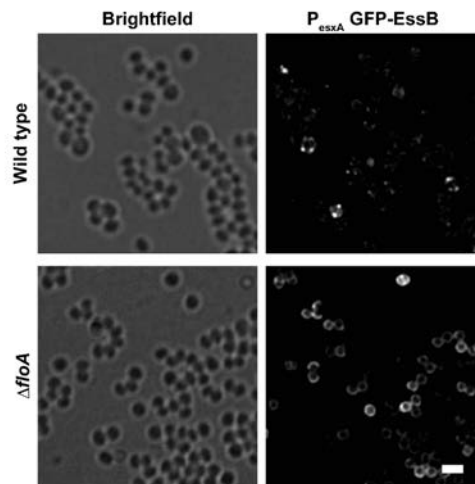


**Fig. IV.6: Absence of FloA affects subcellular localization of EssB**

Panel shows brightfield (left panel) and green fluorescence of GFP-EssB (right panel) controlled by its own promoter in a wild type (upper) and  $\Delta floA$  (lower) background. Scale bar represents 1.5  $\mu\text{m}$ .

Next, it was tested whether FloA scaffold activity affects EssB oligomerization directly, given that EssB is shown to oligomerize *in vitro* and forms conditional dimers [230-232] although homo- or hetero-oligomerization of this protein has not been detected *in vivo* [233]. To this end, the FLAG-tagged version of EssB was expressed in *S. aureus* and oligomerization of EssB was tested *in vivo* using Blue-Native PAGE (BN-PAGE). This technique allows the separation of membrane protein complexes in their natural oligomeric states [271-273]. *S. aureus* cells were grown to stationary growth phase, lysed, membrane fraction was collected and membrane proteins were extracted using 0.25 % DDM at 4°C to allow solubilization of all T7SS membrane proteins as well as FloA (Fig. IV.7A). BN-PAGE gels with a 3-12 % polyacrylamide gradient were used to resolve membrane-bound oligomers between 15 - 10,000 kDa. Identification of FLAG-EssB was determined by immunoblotting using monoclonal anti-FLAG antibodies. Using this approach, a signal attributable to EssB was detected at approximately 250 kDa, which is indicative that EssB is not a monomer *in vivo* (Fig. IV.7B, first lane). Moreover, when protein samples were stabilized using the amine-reactive crosslinker DSP (dithiobis(succinimidyl propionate)) prior to cell lysis, EssB-containing protein species

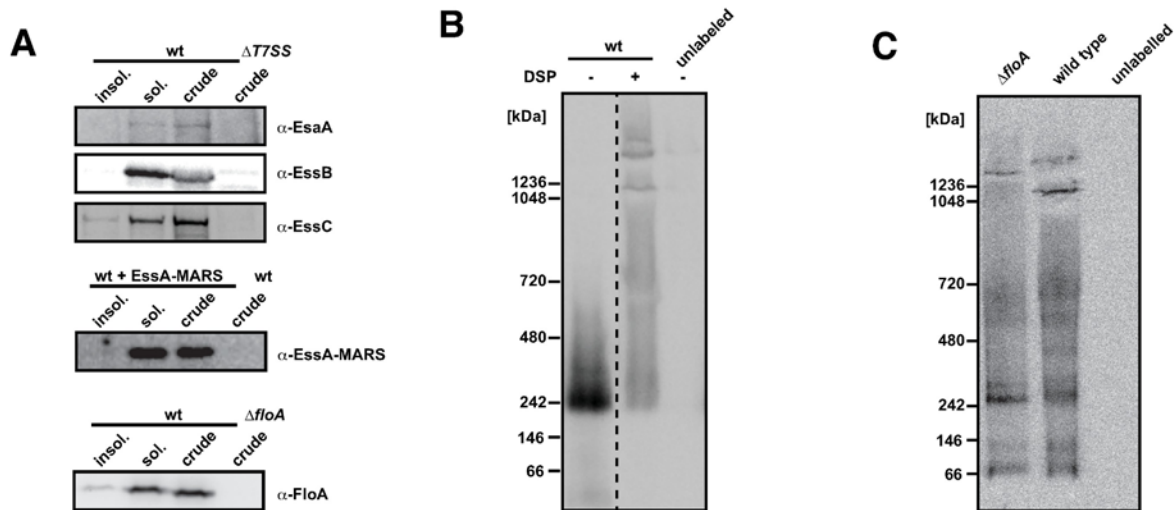


**Fig. IV.7: Absence of FloA affects oligomeric behavior of T7SS membrane proteins.**

(A) Western blot analysis to determine extraction of T7SS membrane proteins EssA, EssB, EssC and EsaA and FloA from *S. aureus* crude membranes using 0.25% DDM. Equal amounts of crude membranes and soluble (sol.) and insoluble (insol.) material were loaded on SDS-PAGE gel and detected with polyclonal antibodies directed against EsaA, EssB, EssC or FloA. EssA-MARS was detected using polyclonal antibodies against mCherry. (B) *In vivo* crosslinking with 1 mM DSP reveals oligomeric pattern of EssB. Stationary cells were treated with 1 mM DSP, lysed and isolated crude membrane fraction was solubilized with 0.25% DDM. Subsequently, solubilized proteins were mounted on a BN-PAGE gel and detected using polyclonal antibodies against EssB. (C) BN-PAGE analysis of DSP-crosslinked membrane fractions of *S. aureus* expressing complemented FLAG-EssB in a wild type or  $\Delta floA$  background.

of more than 1 MDa were detected (Fig. IV.7B, second lane), which pointed to the existence of large EssB-containing protein complexes in *S. aureus* cells. This experimental approach was used to compare the oligomerization efficiency of EssB in wild type and a  $\Delta floA$  mutant. To this end, the membrane fractions of FLAG-EssB labeled wild type and  $\Delta floA$  mutant were DSP-crosslinked, isolated and resolved by BN-PAGE. Immunodetection of the distinct EssB oligomeric states was performed using antibodies against FLAG epitope (Fig. IV.7C). In the wild type strain, two signals were observed corresponding to different EssB oligomeric states ( $> 1$  MDa). In the  $\Delta floA$  mutant, only one signal above 1 MDa was detected, which did not correspond to any of the two signals detected in the wild type sample, indicating a substantial difference in the EssB oligomeric species between wild type and a flotillin-deficient strain.

To ascertain whether these protein complexes are EssB homo-oligomers or in contrast, are constituted by other T7SS proteins, the strain expressing the FLAG-EssB construct was used to perform a pulldown analysis using FLAG-capture beads. For that the wild type and  $\Delta floA$  strains carrying the FLAG-EssB construct were used for membrane isolation and the solubilized membrane fraction was used to capture FLAG-labelled EssB as well as EssB-associated proteins. Proteins were separated from the beads by boiling



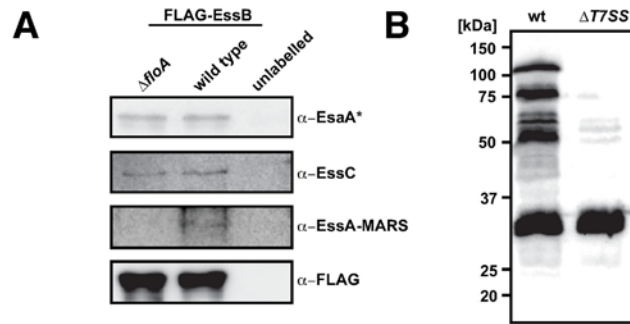


**Fig. IV.8: FloA is important for the interaction of EssB with EssA, but not EsaA or EssC**

(A) Pulldown analysis of FLAG-tagged EssB using FLAG-capture beads. The blots show the elution fractions of wild type, a FloA mutant and an unlabeled strain expressing FLAG-EssB. EsaA and EssC were detected using polyclonal antibodies, EssA-MARS was detected using a polyclonal antibody directed against the mCherry protein. The asterisk denotes that the signal detected for EsaA does not represent full-length protein, but a fragment of ~60 kDa. (B) Immunoblot analysis using crude membrane extracts of wild type and  $\Delta T7SS$  mutant strain to show fragmentation of EsaA using polyclonal antibodies against EsaA. Cells were grown until early stationary growth phase and 250  $\mu$ g total protein were loaded on each lane.

in Laemmli buffer and the eluted fractions were resolved by SDS-PAGE. Immunoblotting revealed the presence of EssA, EssC and an EsaA fragment in the elution fraction (Fig. IV.8A). Full-length EsaA protein was not detected during this pulldown analysis, but interestingly EsaA shows fragmentation pattern when membrane fractions were analyzed by immunoblotting using the polyclonal EsaA antibody. A similar fragmentation was also described for YueB, the EsaA homologue of *B. subtilis* [229]. This is indicative of either a functional importance or intrinsic instability of YueB/EsaA homologues. When comparing the eluted fractions of wild type and  $\Delta floA$  mutant, EssC and the EsaA fragment were detected in comparable amounts, but EssA was not detected in the eluted fraction of a  $\Delta floA$  mutant (Fig. IV.8A), suggesting that flotillin is involved in the interaction of EssB and EssA.

To gain more insight into the effect of flotillin on EssB-EssA interaction, a bacterial three-hybrid assay was performed [132,160] to quantitatively monitor EssB-EssA oligomerization efficiency in the presence or absence of FloA (Fig. IV.9). This assay is based on a classical bacterial two-hybrid assay, in which EssB and EssA were tagged with the T25 and T18 catalytic domains, respectively. The system was then complemented with a modular vector [274] that expressed *floA*. The assay showed no significant interaction between EssB and EssA in the absence of FloA. In the presence of FloA however, an increase in the EssB-EssA interaction signal was detected (Fig. IV.9). The presence of FloA did not affect the interaction of EssB to the other T7SS membrane proteins (EsaA or EssC), suggesting that the FloA scaffold activity is specific to the

interaction of EssB to EssA. This result showed the importance of FloA expression to protein-protein interaction of the T7SS and supports the hypothesis that flotillin acts as scaffold protein to promote EssB-EssA interaction.

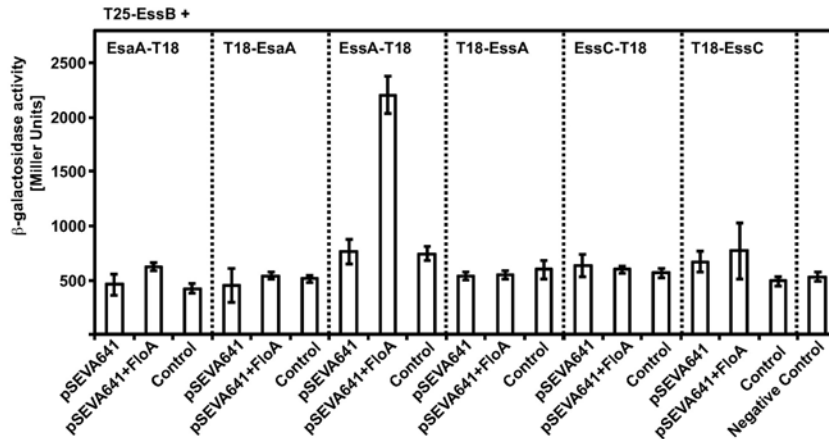


**Fig. IV.9: Bacterial three-hybrid analysis to probe interaction of EssB with other T7SS membrane proteins**  
T25-EssB fusion was tested for interaction against both C- and N-terminal fusions of T18 fragment. Interactions were assayed with empty plasmid (pSEVA641), plasmid carrying flotillin (pSEVA641-*floA*) or absence of the pSEVA plasmid. The negative control carries empty bacterial-two hybrid plasmids.

To determine whether this FloA activity is sufficient to promote T7SS protein oligomerization, an orthogonal T7SS system in *E. coli* was genetically engineered, in which oligomerization of the T7SS membrane proteins EsaA, EssA, EssB and EssC were isolated from their native complex oligomerization network, and thus free from interference by potential staphylococcal oligomerization inputs. In this orthogonal system, EsaA, EssA, EssB and EssC proteins were expressed in the presence (+FloA) and in the absence of FloA (-FloA). Membrane fractions were purified, proteins extracted and their oligomerization states were identified using size-exclusion chromatography. In the presence of flotillin, the elution profile showed peaks at 12, 18 and 20 ml (Fig. IV.10). In the absence of flotillin however, the elution profile showed quantitative and qualitative differences, in which the amount of 12 ml eluted oligomers were reduced and additional signals appeared at 15 ml retention volume, suggesting that the absence of flotillin compromises the oligomerization of T7SS proteins. In addition to this, 1 ml fractions of the retention volumes were analyzed to detect the presence of FloA, EsaA, EssB and EssC using western blot analyses (Fig. IV.10B). In the presence of flotillin, signals attributable to EsaA, EssB and EssC proteins were concentrated in fractions that eluted earlier from the column, in which high molecular weight protein complexes accumulated indicative of the formation of large protein complexes. In the absence of flotillin, the signal was equally detected fractions that eluted later and contained lower molecular weight

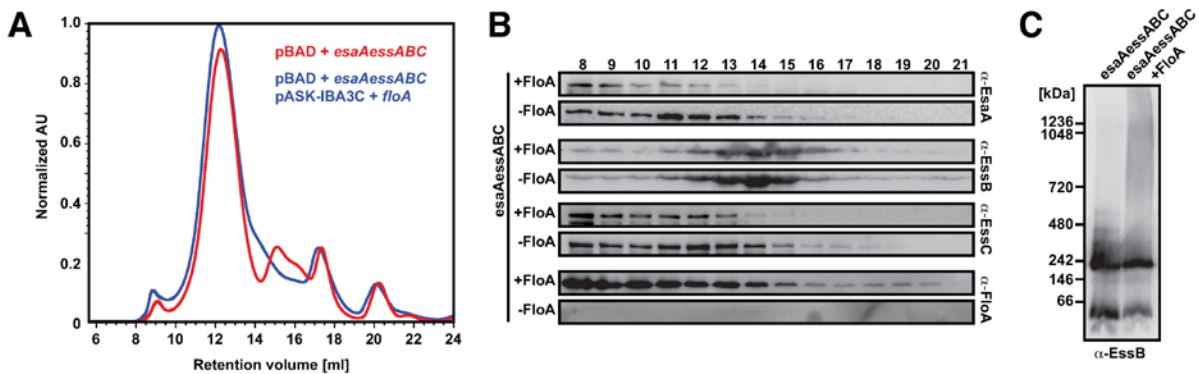


**Fig. IV.10: Impact of FloA on reconstituted T7SS in *E. coli***

(A) Size exclusion chromatography on a Superose 6 column with solubilized membrane fractions expressing structural T7SS proteins EsaA, EssA, EssB and EssC in the absence (red) or presence (blue) of FloA. (B) The fractions corresponding to the elution volumes of 8 - 21 ml were separated on SDS-PAGE and detected via immunoblotting with polyclonal antibodies against FloA, EsaA, EssB or EssC. (C) BN-PAGE and immunoblotting analysis of solubilized *E. coli* membranes expressing structural T7SS proteins EsaA, EssA, EssB and EssC in presence or absence of flotillin. EssB was detected using polyclonal antibodies.

protein complexes, indicative that a less efficiency protein oligomerization occurred (Fig. IV.10B). Additionally, the T7SS-proteins expressed in the heterologous expression system were used to perform BN-PAGE analysis. The membrane fractions of *E. coli* expressing EsaA, EssA, EssB and EssC in the presence or absence of flotillin were extracted and solubilized. The samples were subjected to a BN-PAGE gel and consecutive immunoblot analysis using an anti-EssB antibody. Similar to the gel filtration analysis a shift of EssB oligomeric species towards high molecular weight fractions was detected in the presence of FloA (Fig. IV.10C). These results using *E. coli* as expression system suggest that the presence of flotillin affects oligomerization of T7SS membrane proteins in a heterologous system and thus further highlights the importance of this scaffold protein to the T7SS of *S. aureus*.

#### IV.6 Flotillin mediated T7SS defect impairs infectivity

Targeting flotillin scaffold activity could be an appropriate strategy for fighting bacterial infection by simultaneously perturbing oligomerization of FMM-related protein complexes, including important virulence determinants such as the T7SS. In murine models, the Esx-substrates of the T7SS have been demonstrated to participate in the formation of persistent abscesses, likely due to the virulent activity of EsxA, EsxB, EsxC and EsxD secreted proteins [218,220,223,275]. In addition, it has been shown that EsxC is an immunogenic substrate and thus the establishment of kidney abscesses is detected along with the generation of antibodies against EsxC [220]. Hence, the connection between FloA inactivation and reduced *S. aureus* virulence mediated by reduced T7SS

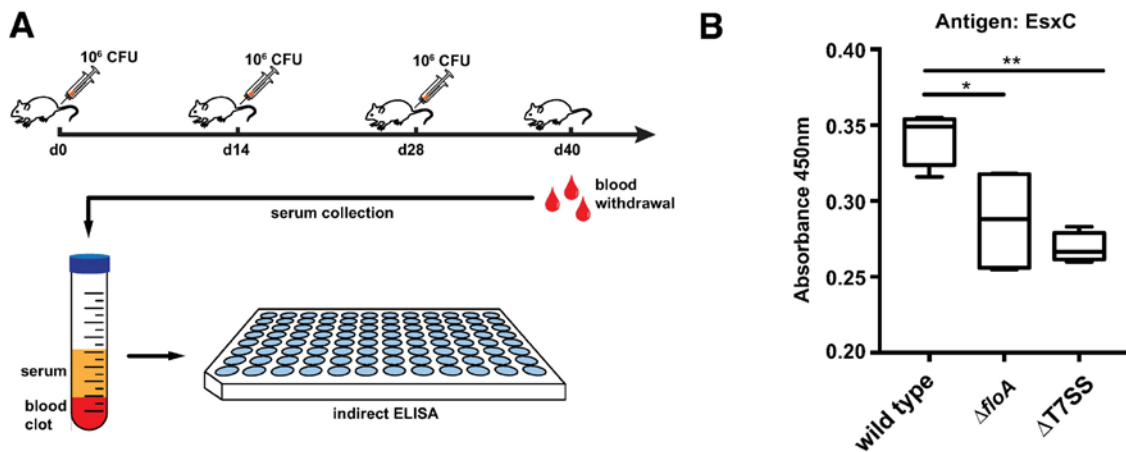


**Fig. IV.11: Absence of flotillin decreases antibody production in infected mice.**

(A) Schematic of workflow. Mice were challenged three times with sublethal doses of staphylococci ( $10^6$  CFU) on day 0, 14 and 28. After 40 d blood samples were collected, serum was isolated and used for indirect ELISA. (B) BALB/c mice were challenged according to scheme presented in (A). IgM antibody titers against EsxC were determined by indirect ELISA. Absorbance corresponds to 1:50 diluted sera. Statistical analysis was carried out using one-way ANOVA (\* $P < 0.05$ ; \*\* $P < 0.01$ ).

activity was evaluated using a murine infection model. An infection model was used similar to Burts et al. [220], in which immunoreaction for EsxC was measured after mice were infected with *S. aureus*. To this end, sub-lethal doses of staphylococcal wild type,  $\Delta floA$  mutant and  $\Delta T7SS$  mutant strains were intravenously injected to cohorts of 3-week old BALB/c mice. In order to boost the humoral immune response, the challenge with staphylococci was repeated on day 14 and day 28 as reported recently [276]. After 40 days, animals were sacrificed and the serum was collected to determine the immunoglobulin titers against EsxC in an indirect ELISA (an overview of the procedure is presented in Fig. IV.11A). By performing this assay a decrease in IgM antibody titers against EsxC in a  $\Delta floA$  mutant compared to wild type was detected, consistent with experiments presented in Fig. IV.5 that show a lowered secretion of EsxC in  $\Delta floA$  mutant *in vitro* (Fig. IV.11B). This points towards an important contribution of FMM integrity to T7SS-mediated virulence phenotypes in an *in vivo* infection.

#### IV.7 Small anti-FMM molecules reduce T7SS activity

To target the activity of flotillin exogenously in order to develop alternative strategies to fight staphylococcal infections, the activity of several small molecules was tested that are known to interfere with FMM organization in *S. aureus*. The small molecule zaragozic acid (ZA) is a potential inhibitor of flotillin activity [117], as it inhibits the *S. aureus* squalene synthase CrtM [277], necessary for the production of the polyisoprenoid lipids

(including staphyloxanthin) that stabilize flotillin in the FMM. When bacteria are exposed to nanomolar concentrations of ZA, flotillin organizes in a smaller number of membrane foci, concomitant with a reduction in its chaperone activity [117]. Similar to ZA, the cholesterol-lowering drug Simvastatin (SIM) – a commercially available drug to treat patients with hypercholesterolemia – inhibits the same biosynthetic pathways towards the production of polyisoprenoid lipids in *S. aureus*. This compound is a competitive inhibitor of the HMG-CoA reductase, an enzyme that is upstream of the squalene synthase on the constituent lipids biosynthesis pathway [278]. The small molecule 5-DSA (5-doxyyl stearic acid) was also included in this assay. This is a lipid probe that accumulates in biological membranes and is conventionally used to monitor membrane fluidity in studies of lipid raft organization in eukaryotic cells [279,280]. It is reported that 5-DSA can displace certain membrane lipids and alter the function of diverse membrane-associated proteins [281,282].

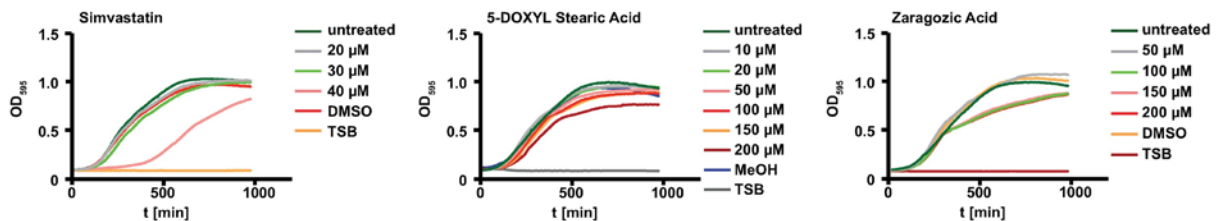


**Fig. IV.12 Growth of *S. aureus* in presence of different combinations of anti-FMM molecules**

Effect on growth of different concentrations of anti-FMM molecules Simvastatin (SIM), Zaragozic acid (ZA) or 5-doxyyl stearic acid (5-DSA) in TSB medium including solvent controls (DMSO and MeOH = Methanol).

First, wild type strains were grown in liquid TSB medium in the presence of different concentrations of Simvastatin, 5-DSA and ZA to determine the highest concentrations that did not affect *S. aureus* growth (20 μM Simvastatin, 150 μM 5-DSA and 50 μM ZA, Fig. IV.12). The activity of the anti-FMM molecules was monitored by evaluating the subcellular distribution of FloA using fluorescence microscopy. To this end the number of fluorescent foci of a FloA-MARS strain was quantified when grown in the presence of Simvastatin, 5-DSA acid or zaragozic acid. In untreated cells, most of the cells showed one, two or three fluorescent foci. Occasionally, cells without fluorescent foci or cells with four or more foci were detected. Treatment with 150 μM 5-DSA or 20 μM Simvastatin however reduced the fluorescent FloA-foci per cell and a majority of the cells did not show fluorescent foci at all or just a single FloA-focus per cell (Fig. IV.13A+B). The treatment with zaragozic acid of cells expressing FloA-MARS did not alter the number of foci, but rather caused a severe delocalization of FloA into

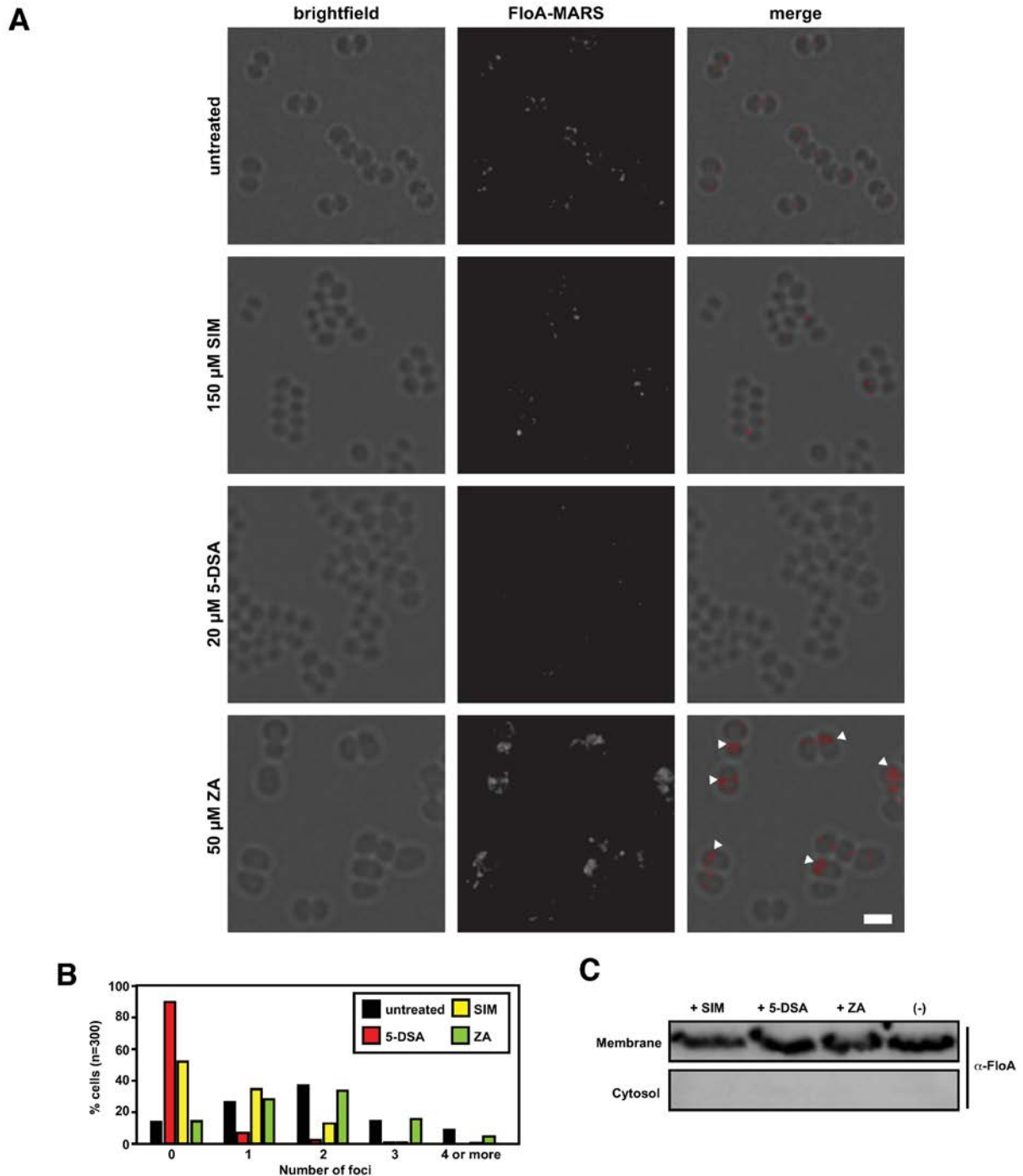


**Fig. IV.13: Anti-FMM affects focal membrane organization of FloA.**

(A) Fluorescence microscopy images of *S. aureus* cells expressing FloA-MARS were grown until late-exponential growth phase in the absence of anti-FMM molecules (upper row) and in the presence of 150  $\mu\text{M}$  5-Doxyl stearic acid (5-DSA), 20  $\mu\text{M}$  Simvastatin (SIM) or 50  $\mu\text{M}$  zaragozic acid (ZA). The left panel shows brightfield images and the middle panel shows deconvoluted red fluorescent signals of FloA-MARS. The panel of the right side shows a merge of those channels with the fluorescence signal false-colored in red. The arrowheads indicate regions of severe delocalization of the FloA-MARS signal after ZA treatment. The scale bar represents 2  $\mu\text{m}$ . (B) Counting fluorescent foci in FloA-MARS labeled cells after treatment with 20  $\mu\text{M}$  Simvastatin, 150  $\mu\text{M}$  5-DSA or 50  $\mu\text{M}$  ZA compared to untreated cells. (C) Immunoblot analysis of membrane and cytosol fractions of wild type cells treated with 20  $\mu\text{M}$  Simvastatin, 150  $\mu\text{M}$  5-DSA or 50  $\mu\text{M}$  zaragozic acid. Untreated cells served as control. FloA was detected using polyclonal anti-FloA antibody.

patches (Fig. IV.13A, indicated with arrowheads). Interestingly, the altered subcellular localization of FloA-MARS in the presence of anti-FMM molecules is not a result of decreased abundance of flotillin in the cell membrane or displacement of flotillin to the cytosol, as demonstrated by western blot analysis of fractionated cells after anti-FMM molecule treatment (Fig. IV.13C). The reduced number of fluorescent foci after Simvastatin or 5-DSA treatment is likely a result of foci dispersal throughout the whole membrane leading to a weaker foci fluorescence that is undetectable after image deconvolution. Thus, it is suggested that the presence of anti-FMM molecules severely affects FMM architecture and probably also affects associated processes.

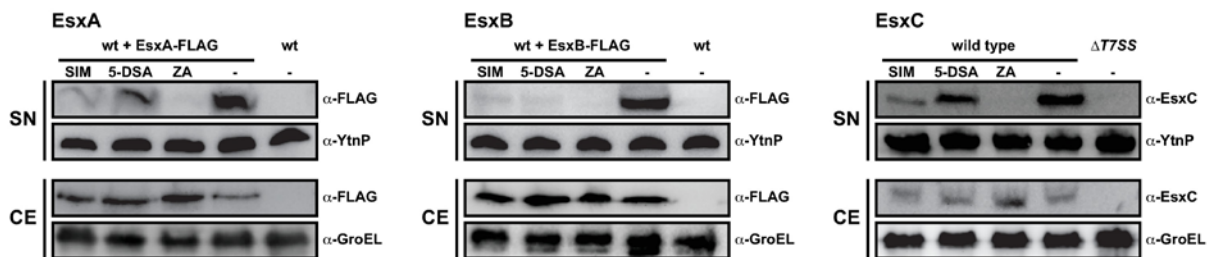


**Fig. IV.14: Anti-FMM molecules can inhibit secretion of T7SS substrates *in vitro*.**

Effect of anti-FMM molecules on secretion of T7SS substrates. Cells were grown to end of exponential growth phase in the presence of 20  $\mu$ M Simvastatin, 150  $\mu$ M 5-doxyyl stearic acid 5-DSA or 50  $\mu$ M zaragozic acid (ZA). Precipitated supernatant (SN) and cell extracts (CE) were loaded on a gel and probed in immunoblot against  $\alpha$ -FLAG or  $\alpha$ -EsxC antibodies, respectively.

Consequently, it was evaluated if treatment with Simvastatin, 5-DSA or ZA also has an inhibitory effect on T7SS activity *in vitro*. To this end, secretion of the T7SS-substrates EsxA, EsxB and EsxC was monitored in stationary phase cultures. Supernatants from untreated and Simvastatin-, 5-DSA- and ZA-treated cultures were collected, secreted proteins concentrated by TCA precipitation, subjected to SDS-PAGE and detected using western blot analyses. In the presence of anti-FMM molecules, a notable reduction of secreted EsxA, EsxB and EsxC in supernatants from treated cultures was observed (Fig. IV.14). It was particularly relevant in the case of ZA-treated cells, in which no EsxA, EsxB and EsxC signals were detectable in the supernatants. To determine the localization of EsxA, EsxB and EsxC, detection of western blot signal was also performed in cell extracts. In the cytoplasmic fraction of treated cultures, EsxA, EsxB and EsxC were detected, which indicates that Simvastatin, 5-DSA and ZA in *S. aureus* cultures compromises T7SS activity and thus reduced secretion of T7SS substrates. While treatment of *S. aureus* cultures likely affects the organization and assembly of T7SS, addition of Simvastatin, 5-DSA and ZA did not alter the concentration of EsxA, EsxB or EsxC in cell extracts (Fig. IV.15).

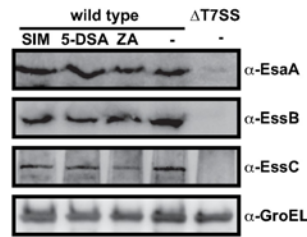


**Fig. IV.15: Anti-FMM molecules do not affect T7SS membrane protein abundance**

Immunoblot analysis to determine protein levels of EsaA, EssB and EssC in presence of 20  $\mu$ M Simvastatin (SIM), 150  $\mu$ M 5-doxyyl stearic acid (5-DSA) or 50  $\mu$ M zaragozic acid (ZA). Cells were grown overnight and whole cell extracts were loaded on a SDS-gel for immunoblot analysis using polyclonal antibodies directed against EsaA, EssB or EssC. A strain lacking the entire T7SS operon served as a negative control strain. Immunoblot against GroEL was used as a loading control.

The important inhibitory effect of ZA in T7SS activity via FMM-perturbation led us to test ZA-mediated T7SS inhibition *in vivo* using a murine infection model. To do this, 20 mg/kg of ZA was administered to a cohort of BALB/c mice (n=5) via intraperitoneal injection followed by a challenge with sub-lethal doses of *S. aureus*. This procedure was repeated twice (day 14 and day 28) and after 40 days animals were sacrificed. The serum was collected to determine the immunoglobulin titers against EsxA, EsxB, EsxC and EsxD substrates by performing an ELISA. Lower IgM antibody titers against all Esx-substrates of the T7SS were detected (Fig. IV.16). In this assay the lower titers of IgM antibodies against EsxB, EsxC and EsxD were statistically significant in comparison to the antibody titers of infected, non-treated mice. All together, these results indicate that ZA inhibits secretion of T7SS-related substrates *in vivo*, probably by reducing the T7SS secretion efficiency and thus making it an attractive molecule to further explore alternative antimicrobial therapies against *S. aureus* infections.

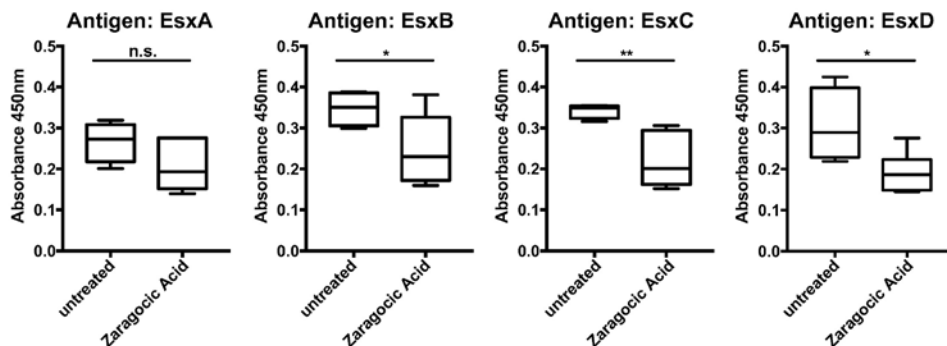


**Fig. IV.16: Anti-FMM molecules can inhibit secretion of T7SS substrates *in vivo*.**

Indirect ELISA to study effect of zaragozic acid on antibody response against EsxA-D. Zaragozic acid was administered to BALB/c mice via intraperitoneal injection followed by challenge with sublethal dose of staphylococci. Procedure was repeated on day 14 and day 28 to prime antibody response. Graphs show IgM antibody titers against EsxA-D in untreated versus treated animals. Statistical analysis was performed using unpaired t-test (\*P<0.05; \*\*P<0.01).



## V DISCUSSION

### V.1 The lipid raft controversy

The initial formulation of the lipid raft hypothesis was an attempt to explain the biochemical and microscopical findings that GPI-anchored and other membrane-bound signaling proteins are resistant to an extraction with cold non-ionic detergents. Simons and Ikonen postulated that these rafts are not susceptible to detergent treatment due to the tight packaging of sphingolipids, GPI-anchored proteins and cholesterol [20]. Yet, the situation *in vivo* is seemingly more complex due to the presence of a variety of lipid species, a constant lipid and protein turnover, involvement of cellular structures such as the cytoskeleton and the size of only a few nanometers. Limited knowledge about this paired with limitations of available methods and a poor definition what a 'lipid raft' actually is, led to criticism that rafts are only an artefact resulting from the extraction procedure [66,69,283]. Initially, lipid rafts and accompanying proteins were experimentally isolated in a membrane fraction that is insoluble in non-ionic detergents and floats on low-density fractions of sucrose gradient [19,20,74]. While this method was considered the gold-standard in the early years of lipid raft research, it raised a lot of skepticism and ambiguous observations questioning the existence of such lipid domains or even lipid rafts in general. This is due to reports showing that the non-ionic detergents such as Triton X-100 leads to formation of holes in the membrane and thus may lead to unspecific raft clustering [34]. Yet, the use of several different detergents [23-28], as well as the use of detergent-free procedures [22,29,30] led to comparable results, that were manifested by proteomic analysis of the entire eukaryotic raft proteome [36]. Albeit subtle changes in the DRM content were detected, the hole-punching effect of detergents and the consecutive clustering does not seem to bias the isolation procedure compared to other isolation procedures. Nonetheless, it must be emphasized that the DRM membrane fraction does not equal lipid rafts and any protein candidate co-purified with the DRM should be explored in further experiments, for instance whether it co-localizes with known raft markers.

Moreover, initial studies that substantiated the existence of lipid rafts were seen with skepticism, since many of them rely on the abovementioned DRM isolation protocols and on fluorescence microscopy coupled to crosslinking methods [284,285]. This

includes crosslinking and consecutive immunohistochemistry staining with antibodies of DRM proteins that revealed co-localization [284] or fluorescence resonance energy transfer of fluorescent folate and its cognate receptors in a cholesterol-dependent fashion [285]. Yet, sometimes fusing proteins to a fluorescent tag can influence the behavior of the protein, so any experiment was kept in a background that the clustering into rafts may be an artefact of the labeling method: This could be due to the fluorescent tag itself or due to the crosslinking procedure and consecutive labeling with antibodies [286-288]. Likewise, attempts to use fluorescently labelled lipids always must be treated with caution, because similar to proteins, an endogenous modification of lipid structures might interfere with their physicochemical properties. Thus, the formation of lipid domains was thus often critically evaluated as being a potential artefacts of clustering due to the labeling methods and direct evidence that lipid rafts exist in living cells were lacking [289,290].

Also, it must be taken into consideration that *ex vivo* experiments lack important cellular structures and organelles, for instance the cytoskeleton. This includes giant-plasma membrane vesicles (GPMVs) that originate from host cell membranes [291,292] or synthetically generated membranes and vesicles (e.g. giant unilamellar vesicles, GUVs)[293]. They are often used for labeling studies and show formation of lipid domains. However, the absence of lipid/protein dynamics and turnover can strongly influence behavior of biological membranes [2].

A recent study thus addressed the abovementioned issues (namely fluorescent labeling or studying lipid domain formation *ex vivo*) by using a non-molecule based labeling technique with nanometer resolution in a living organism to demonstrate the existence of lipid domains *in vivo* [294]. To this end *B. subtilis* cells were used for metabolic deuterium labeling, since labeling of atoms with deuterium was shown not influence the behavior of the molecule itself [295,296]. The authors of this study then used small angle neutron scattering to analyze membrane organization of lipids on the nanometer scale and they indeed showed that lipids cluster into ~40 nm sized domains *in vivo*, consistent with the size range proposed by fluorescent labeling of raft marker proteins. This was the first report showing that a living system indeed harbors lipid domains in the membrane, whose detection was not biased by biochemical labeling of proteins or lipids with tags or antibodies [294].

Another elegant example that supports the existence of lipid rafts *in vivo* in an unbiased fashion, is the lipid composition of the human immunodeficiency virus (HIV) that displays a similar lipid arrangement as lipid rafts [70,297,298]. Several viruses were described to use lipid rafts (mostly the presence of cholesterol) for their assembly and budding. Particularly enveloped viruses, such as HIV are good examples that point towards the existence of rafts. It was already suggested that HIV transmembrane proteins localized within rafts after palmitoylation and virus budding is hindered in the absence of cholesterol [299]. Strikingly, the analysis of the HIV lipidome revealed similarities to lipid rafts including cholesterol and sphingolipid enrichment [298]. Moreover, HIVs are decorated with several GPI-anchored proteins [300]. These examples demonstrate not only that rafts serve as platform for viral membrane protein multimerization and budding, but the similarities of the lipidome of HIV and lipid rafts also suggest that rafts indeed exist *in vivo*.

Advances in biophysical, biochemical and analytical methods to investigate lipid rafts contributed to an evolution of the lipid raft definition from being referred as 'a simple cluster of sphingolipids, cholesterol and GPI-anchored proteins' to 'highly dynamic, heterogeneous, nanometer-sized membrane domains that transiently form micrometer sized platforms that involve a plethora of lipid species and proteins' [50]. Nonetheless, one should always take into consideration novel aspects to reshape the definition of rafts. This may include latest insights of research in membrane organization, not taking the initial theory as a dogma or neglect recent findings, due to their incompatibility with the initial raft hypothesis due to lack of technical possibilities [283].

Despite a multitude of evidences that accumulated along with elaborated and more sophisticated techniques demonstrating the existence of rafts, it remains to be elucidated on which time-scale rafts exist in a cell: It is suggested that the nanometer-rafts are only stable for several milliseconds, which often might not be enough time for biochemical reactions of two interacting proteins brought together in the rafts. Thus, it opens the question whether nano-rafts serve only as an 'assemble-and-release' platform, meaning that lipid rafts and their harbored chaperons only serve as a transient assembling platform by providing a distinct environment to favor assembly of two (or more) interaction partners, which are then more stable upon assembly and will be release from the raft-lipid enrichment as an oligo- or multimer. Alternatively, only the so-called superrafts or macrodomains serve as actual assembling platforms and

nanodomains only contain single, unpaired interaction partners in a steady-state. Especially the role of nanodomains will be an interesting subject of future research to get insights into raft mechanisms in the nanometer range within the time frame of a millisecond.

## **V.2 Bacterial models to study molecular traits of lipid rafts**

The example illustrated in the previous paragraph, where *B. subtilis* was used as a model to prove the existence of lipid domains *in vivo*, strengthens the idea of using bacterial models to elucidate fundamental questions in membrane organization mediated by lipid rafts or the related prokaryotic FMMs. The advantage of using bacteria is the reduced complexity in the lipidome and the overall cellular structure, while at the same time maintaining a similar sophistication in terms of membrane organization. Bacteria also produce lipid species with physicochemical properties similar to cholesterol or sphingolipids and the scaffold protein flotillin is conserved in the bacterial genome. Understanding bacterial FMMs can lead to new findings in prokaryotic membrane biology that might contribute to answer long-standing questions in the field of eukaryotic lipid raft research.

In chapter II of this work, it was investigated if information about the scaffold protein flotillin can be obtained using a bacterial model system. The motivation for this approach came from observations of eukaryotic neurological disorders, such as Alzheimer's or Parkinson's disease. Those diseases are characterized by an upregulation of flotillins in affected tissues, yet it is not known whether an upregulation of flotillin is the cause or the consequence of these diseases. Thus, a synthetic *B. subtilis* strain was generated overexpressing one or both of its endogenous flotillin proteins. In the tested conditions, no effects were observed when only a single flotillin (FloA or FloT) was overexpressed. However, simultaneous overexpression of both FloA and FloT led to defects in cell physiology: Firstly, an increased subpopulation of matrix producers led to formation of a robust biofilm in an undomesticated strain mostly consisting of the biofilm matrix protein TasA. Secondly, flotillin overexpression led to reduced cell length and gave rise to abnormal (spherical and ellipsoid) cell types indicating a defect during division. Mechanistically, this double overexpression of flotillins in *B. subtilis* leads to an unusual stabilization of the FMM-harbored protease FtsH, which has been shown earlier to interact with both FloT and FloA [122,126,137]. Moreover, both flotillins are required

for its functionality [126]. The finding that only simultaneous overexpression of both flotillins causes FtsH-mediated defects in cell morphology, is in line with the functional redundancy described earlier [126]. It also might explain the lack of an obvious phenotype for strains overexpressing single flotillins. Since in the scope of this chapter only effects on cell division and cell differentiation were examined, it remains to be tested whether a single overexpression might also show defects in cellular processes that were assigned to either FloA or FloT and not to both, e.g. PhoR signaling for FloA or ResE signaling for FloT as described recently [132].

The defects in cell differentiation were detected using the domesticated *B. subtilis* strain PY79 that lost the capability to form a robust and wrinkled biofilm – a morphology that it is typically observed in natural isolates such as NCIB3610 [301,302]. The molecular basis of this disability is both determined by the absence of surfactin, a paracrine signal that is critical for triggering biofilm formation via KinC [303], a point mutation in one gene of the *eps* operon and a few others [302]. Therefore, macrocolonies of PY79 typically appear flat and fragile, due to this lack of structural integrity. Therefore, the effects of flotillin overexpression might not be mediated by KinC-associated surfactin detection and this might also explain the weaker phenotype observed in the NCIB3610 isolate, where this pathway is still active.

Cell shape defects, as described in this work, are often a result of uncoordinated division. Particularly cell size is a result of coordinated cell elongation and cell septation [165]. This connection becomes already obvious in rich medium, where cell elongation is accelerated and is thus faster relative to septation, which eventually leads to elongated cells [304]. The same phenotype is observed if septation efficiency is reduced. On the other hand, increased septation efficiency or reduced elongation cause the opposite effect, namely reduced cell length. For the observation that flotillin overexpression reduces cell length, the relationship between elongation and septation efficiency was taken into consideration: Since FloA and FloT overexpression did not affect growth rate, it was proposed that septation efficiency and not cell elongation is affected.

On the question, as to how flotillin overexpression affects septation efficiency, existing *B. subtilis* data of FMM proteins during exponential growth phase were consulted and checked for regulators of Z-ring formation [126]. Indeed, the protein EzrA, a negative regulator of Z-ring formation, whose detailed role during division is still under

investigation, was shown to be part of the FMM protein cargo in *B. subtilis* [126,305-307]. The results of this work suggest that EzrA is a potential target of FtsH proteolysis and the hyperstabilization of FtsH by flotillin overexpression leads to degradation of EzrA. In turn, this leads to increased septation efficiency and thus gives rise to short and aberrant cells. It remains to be elucidated whether EzrA is a directly or indirectly affected by the action of FtsH. Since FtsH is a known AAA+ metalloprotease, it is tempting to speculate that EzrA might be proteolytically cleaved by FtsH to regulate septum formation, yet a direct proof for this hypothesis is still elusive. Supporting this notion is the finding that the opposing effect (elongated, filamentous cells) was already described in literature for an FtsH mutant, yet no molecular mechanisms were known that mediate this phenotype [124].

In summary, chapter II provides evidences that a synthetically driven imbalance of flotillin levels indeed causes a malfunction of associated FMM-processes. This finding might provide helpful insights in the development of eukaryotic diseases, where flotillin overexpression might also affect proteins residing in rafts. If hyperstabilization of raft-harbored enzymes or proteins occurs in eukaryotic cells in a similar fashion as in *B. subtilis*, elevated levels of flotillin might be the causative of aberrances in cell physiology and thus contribute to disease development. Using simple bacterial models for understanding important principles in lipid rafts might be applicable to elucidate other important facets in membrane organization.

### **V.3 The *S. aureus* DRM proteome and T7SS assembly as a case study**

A central part of this work was to elucidate the DRM proteome of *S. aureus* and to reveal dynamic changes in its composition in different condition. Due to its clinical relevance, FMMs of *S. aureus* might be a very important cellular structure for this pathogen to organize virulence-related cellular processes. In depth understanding of the FMM protein content and its adaption to a changing environment provide helpful insights, which virulence-related signaling mechanisms are depending on FMMs and could thus be attacked by targeted dispersal of FMMs with small molecules.

When using proteomic approaches to determine the DRM/DSM proteome, it is not only important to assign a protein to one membrane phase or another. It is also important to determine if one distinct protein can be detected in both DRM and DSM and to what

extent. This is important when considering the following statement of Levental and Veatch:

*“In reality, raft and non-raft domains in biological membranes are relatively similar, so most components do not partition exclusively into either of the domains; however, this does not preclude compartments of distinct composition. An important aspect of raft functionalization is dynamic regulation of their composition.” [2]*

To this end, mass spectrometry based label-free quantification was used for the DRM proteome analysis, a technique that required no labeling prior to identification. LFQ analysis did not only shed light if one protein is residing only in the DRM, but also if proteins are enriched in one phase or the other. This DRM proteome analysis thus provides a roadmap for potential FMM-associated proteins, which can further be explored for a functional FMM dependence.

The hierarchical cluster analysis presented in chapter III revealed that a core set of proteins is residing in the FMMs at any tested conditions (Cluster A and B, Fig. III.4), and additionally the FMM cargo adapts to the given conditions (Clusters C – F, Fig. III.4). Certainly, this observation is in large parts the result of changes in the overall transcriptome that allow the cells to adapt to a changing environment. For instance, proteins regulated by the FUR-repressor appear in iron-limiting condition and were not present in other tested conditions (e.g. IsdE, the membrane bound component of the Isd-heme uptake system or siderophore-synthesis proteins SbnE or SbnC) [260]. But interestingly, there is also a specific group of proteins within each cluster, which enriches in the DRM in one tested condition, whereas in other conditions these proteins are excluded from or to a lesser extent found in the DRM fraction (and thus possibly within the FMMs). Addressing how this is mechanistically possible may be subject of future studies and this dataset might provide the basis to reveal underlying mechanisms on how proteins are targeted to FMMs. Several interesting examples were found in this dataset: For instance, the mechanosensing channel MscS, which is a homo-multimeric transporter possibly involved in coping with osmotic stress [308]. MscS is DRM enriched in iron-limiting condition and DSM enriched in all other tested conditions. Another example is the transmembrane efflux transporter SA2056, which interacts with FemX, PBP1 and PBP2 and thus has probably an accessory role in peptidoglycan synthesis [309]. Likewise, SA2056 is only partly enriched in the DRM in stationary phase, whereas

in all other tested conditions it was enriched in the DSM. One might speculate that MscS and SA2056 are sequestered to the FMMs to become assembled as a complex that is required during this particular condition. The underlying stimuli could be (I.) the presence of other functionally or structurally connected proteins (e.g. part of the same complex), (II.) targeted sequestration to FMMs (e.g. by the scaffolding activity of flotillin) or (III.) a post-translational modification to target it to FMMs. Exploring this DRM-targeting mechanism which would be an interesting subject of future studies.

As aforementioned, proteins identified in the DRM proteome analysis are not FMM-dependent *per se* and should be empirically tested if they functionally require the distinct environment of the FMMs or the scaffold activity of flotillin. As a proof of principle, the assembly of the type VII secretion system (T7SS) was used as a case study to demonstrate the functional dependence of an exemplified protein complex that relies on the integrity of FMMs and the action of its scaffold protein FloA.

This is an intriguing example to study, because one component was exclusively associated with the DRM (EssA), whereas other components were detected in both membrane phases, either enriched in the DRM (EssB, EsaA) or enriched in the DSM (EssC). Analyzing the T7SS complex formation in the context of FMM-mediated membrane organization, will thus contribute to the understanding why only selected proteins of a protein complex are enriched in the DRM, while others preferably enrich in the DSM and how flotillin contributes to this process.

The work presented in chapter IV shows that FloA transiently interacts with EssB as the only membrane-bound protein of the T7SS apparatus. Non-integer FMMs, where FloA is absent, show reduced secretion efficiency and differences in the oligomeric behavior of the T7SS complex. The molecular basis for this might be the stimulatory effect of FloA for the interaction of EssB to EssA. Taking together these experimental findings, following working model can be proposed (see chapter III).

The direct physical interaction of FloA with EssB makes EssB accessible for its interaction with EssA. This interaction step might take place in the protected and distinct environment of FMM membrane regions, which is consistent with the finding that EssA and EssB, are highly enriched in the DRM. Presumably, the interaction of EssB to other T7SS except EssA (namely EsaA and EssC) is not affected, since they can still be detected in pulldown experiments in a  $\Delta floA$  mutant background. Probably, a non-



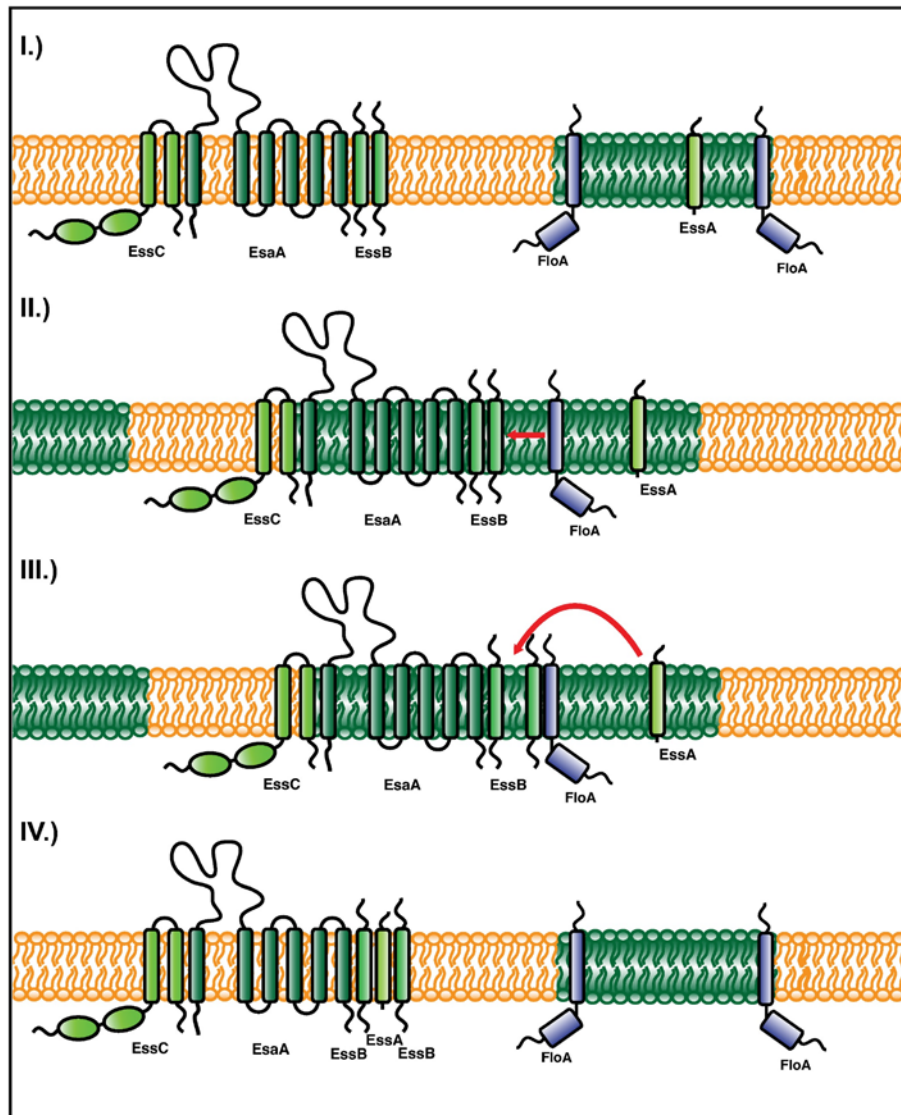


**Fig. V.1 Working model how the assembly of the T7SS is mediated by FloA/FMMs.**

I.) A pre-existing, probably non-functional T7SS complex consisting of EssC, EsaA and an EssB oligomer (here represented by two EssB molecules) resides in the non-FMM membrane (yellow). FMMs (green) contain EssA and FloA. II.) The EssC-EsaA-EssB precomplex is transiently recruited to the FMMs. This allows FloA to interact with EssB. III.) The scaffold activity of FloA promotes the interaction of EssB to EssA. This could help to incorporate EssA into the EssC-EsaA-EssB subcomplex. IV.) The fully assembled T7SS complex is released from rafts and is now functional.

functional EssC-EsaA-EssB pre-complex is self-assembled (I.), which transiently relocates into or at the borders of the FMMs by an unknown stimulus (II.). This is consistent with the DRM/DSM distribution of the T7SS proteins (See Fig. IV.2). Then, FloA promotes the interaction of EssB to EssA and the incorporation of EssA into the preexisting complex (III.) and a fully functional T7SS assembles (IV.). One can speculate that the EssA-EssB interaction needs to be overcome a kinetic hindrance by the help of flotillin, which is a typical feature of scaffold proteins. Following this theory might also explain why in the absence of flotillin, a residual activity of the system (see secretion Fig. IV.5) is still detectable. The effect FloA exerts on EssB and detailed underlying molecular

mechanisms are still speculative. One may anticipate subtle steric changes of EssB after binding to FloA, which in turn allows the interaction to EssA. Yet, further experiments will be needed to validate this hypothesis, e.g. by super resolution microscopy in combination with lipid raft stain such as C-laurdan or re-constitution of this tripartite interaction of FloA, EssB and EssA using recombinantly purified proteins.

The assembly step promoted by the FloA scaffolding activity might be a regulatory step during T7SS activation and may only take place upon certain stimuli that are for instance triggered during an infection. Also, the postulated model above suggests only a transient association of the T7SS within the FMMs. Such a FMM-mediated assembly of a protein complex might also be applicable for other protein complexes of the FMMs. If FMM-association is indeed transient, it might help understand the current debate of the field of FMM research, why FloA-interacting proteins only co-localized for a few milliseconds [132,133,163]: Transient co-localization of proteins and protein complexes with FloA/FMMs might be sufficient to form protein oligomers and complexes, which are then again released from the FMMs.

Selecting the T7SS as a case study to verify FMM dependence, is an interesting example due to its important contribution to progression of staphylococcal infections. Perturbation of FMM-associated processes by small molecules has been described previously [117,244,245] and targeting T7SS activity might ameliorate the infective potential of this pathogen. During an infection, the *S. aureus* T7SS is critical for the development of abscesses in a murine model [218,220]. *S. aureus* is able to evade immune mechanisms by using a plethora of virulence factors to eventually disseminate into peripheral organs to establish formation a purulent abscess [310]. The secretion of the T7SS substrates EsxA and EsxB have been shown to be important to form kidney, liver and other peripheral abscesses [218,221]. Furthermore, the T7SS substrate EsxC is crucial for maturation of kidney abscesses over a prolonged period of time leading to establishment of a persistent infection [220]. EsxC was shown to be produced throughout the course of a persistent infection, since infected animals generate antibody responses against EsxC within a 30 days infection [220]. Although the actual host cell targets are unknown, it is suggested that Esx substrates interfere with several immune regulatory mechanisms (e.g. apoptosis, cytokine responses), similar to T7SS substrates of mycobacterial species in order to generate a severe persistent infection [222,223,311]. A recent study indeed demonstrated that in a *S. aureus* strain deficient in

effectively delivering T7SS substrates to the extracellular space displays substantial changes in the cytokine levels during an infection (e.g. IL-1b or IL-12) [222].

Nonetheless, the biology of the T7SS in *S. aureus* is just beginning to be understood and the T7SS seems not only to be an important virulence determinant, but also contributes to competition with other staphylococci [222,224,240]. Several other aspects of the staphylococcal T7SS are currently investigated: For instance, studies that are under development claim a connection of the T7SS to iron metabolism similar to mycobacteria [205-207,312] and attribute an essential role of the EsaB regulator for T7SS that is contradictory to data published earlier [220,313].

Also, the oligomeric behavior of the T7SS is currently under debate. There are reports arguing in favor of the assembly of a heterogeneous T7SS protein complex in *S. aureus* as it occurs in mycobacteria [234,235,314]. Experimental data however, show no heteromeric interaction between T7SS protein components in *S. aureus* cells [233] and therefore, the assembly of T7SS in *S. aureus* has been revised. The results presented in chapter IV of this work suggest that T7SS indeed forms a complex consisting of (at least) EssA, EssB, EssC and EsaA. It is possible that both hypotheses are correct and not necessarily mutually exclusive. T7SS assembly is influenced by the activity of proteins that catalyzes T7SS oligomerization, such as flotillin. Thus, it is possible that T7SS assembly is transient during the lifespan of the bacterium and likely regulated by the activity of scaffold proteins that are expressed at a particular time point during bacterial growth or in response to a specific signal. Probably these signals are produced during an infection, in which T7SS activity is required and it is therefore challenging to reproduce these conditions in laboratory growth. This is consistent with experimental finding that T7SS hetero-oligomers are only detected after *in vivo* treatment with a short-spaced (12 Å) chemical cross-linker. Additionally, there are other technical aspects that could be considered to reconcile the different takes on T7SS assembly. As an example, the choice and concentration of detergent to solubilize membrane proteins is critical to obtain a good balance between membrane disaggregation and extraction of membrane proteins in their natural oligomeric states. Subtle variations in the use of the detergent were shown to affect oligomeric behavior of membrane proteins results notably [315].

After demonstrating that there is a link between T7SS functionality and FMM integrity, the dispersal of FMMs by small molecules was used an innovative antimicrobial strategy

that could reduce the virulence potential of *S. aureus* during a persistent infection. The experiments of chapter IV showed the potential antimicrobial effect of Simvastatin, 5-doxyol stearic acid (5-DSA) and zaragozic acid (ZA) for their ability to perturb FMM organization and reduce T7SS functionality. Thus, these anti-FMM molecules can inhibit secretion of T7SS-substrates. Treated cells reduce extracellular amounts of EsxA, EsxB and EsxC *in vitro* and also *in vivo* using a murine infection model. Anti-FMM compounds can be a promising anti-microbial strategy to simultaneously interfere with molecular pathways that contribute to the virulence potential of *S. aureus* toward eliminating hard-to-treat *S. aureus* infections. *S. aureus* infections are considered endemic in hospitals, which has an approximately 20 % mortality rate and is currently a leading cause of death by a single infectious agent [247].

## VI MATERIAL & METHODS

### VI.1 Chemicals and materials

#### VI.1.1 Common chemicals and consumables

Chemicals were purchased from following suppliers: Merck (Darmstadt), AppliChem (Darmstadt), Roth (Karlsruhe) and Sigma-Aldrich (Steinheim). Material for molecular biology studies were purchased from Macherey & Nagel (Düren), Qiagen (Hilden) and New England Biolabs (Frankfurt am Main). Consumables were purchased by local distributors and autoclaved before use.

#### VI.1.2 Proteins, enzymes and specialized chemicals.

The following Table VI.1 lists all proteins, enzymes and chemicals used in this work.

**Table VI.1 All proteins, enzymes and other specialized chemicals used in this work.**

<b>Compound</b>	<b>Manufacturer</b>
1 kb DNA Ladder	New England Biolabs
2-Nitrophenyl $\beta$ -D-galactopyranoside (ONPG)	Applichem
3,3',5,5'-tetramethylbenzidine (TMB)	Life Technologies
Ambicin L (recombinant Lysostaphin)	Ambiproducs
Anti-FLAG® M2 Magnetic Beads	Sigma-Aldrich
BN-PAGE equipment	Life Technologies
Cellytic™ MEM Protein Extraction Kit	Sigma-Aldrich
Color Prestained Protein Standard, Broad Range	New England Biolabs
Dithiobis(succinimidyl propionate) (DSP)	Thermo Scientific
DNase I	New England Biolabs
n-Dodecyl $\beta$ -D-maltoside (DDM)	Anatrace
Dexyl maltose neopentyl glycol (DM-NPG)	Anatrace
Expand™ Long Template PCR System	Roche
FM4-64	Invitrogen
Glass beads, acid washed, < 106 microns	Sigma-Aldrich
Hoechst 3342	Invitrogen
Lysozyme	Roth
Ni-NTA Superflow	Qiagen
PD-10 Desalting Columns	GE Healthcare

<b>Compound</b>	<b>Manufacturer</b>
Phusion Polymerase	New England Biolabs
Proteinase K	Merck
PVDF Membrane	Biorad
Restriction Endonucleases	New England Biolabs
RNase A	Sigma-Aldrich
Roti®-Phenol/Chloroform/Isoamylalkohol	Roth
Rotiphorese® NF-Acrylamid/Bis-Lösung 40 % (29:1)	Roth
Simvastatin	Sigma-Aldrich
T4 DNA Ligase	New England Biolabs
Zaragozic Acid A trisodium salt	Santa Cruz Biotechnology

### VI.1.3 Laboratory equipment

The following Table VI.2 lists all laboratory equipment used in this work.

Table VI.2 Laboratory equipment used in this work

<b>Laboratory equipment</b>	<b>Manufacturer</b>
Casting module Mini-Protean Tetra Cell	Bio-Rad
Cell homogenizer Fastprep24	MP Biomedicals
Cooling centrifuge 5427 R	Eppendorf
Electrophoresis system Mini-Protean Tetra Cell	Bio-Rad
Electrophoresis system XCell SureLock	Life Technologies
Gel iX imager	Intas Science Imaging
Horizontal electrophoresis systems PerfectBlue Mini S, M	Peqlab
ImageQuant LAS4000 biomolecular imager	GE Healthcare
Microcentrifuge Biofuge 13	Heraeus
Micropulser Electroporator	Bio-Rad
Multifuge X3R	Thermo Fisher
Nanodrop 2000	Peqlab
Power supplies peqPOWER E250, E300	Peqlab
PowerPac HC High current power supply	Bio-Rad
Semi-dry electroblotter PerfectBlue SEDEC M	Peqlab
Spectrometer Ultrospec 3100 pro	Amersham Biosciences
Thermocycler T3	Biometra
Ultracentrifuge fixed angle rotors type 45Ti, 70Ti, 70.1Ti	Beckman & Coulter
Ultracentrifuge Optima™ L-100 XP	Beckman & Coulter
Wetblotter Mini Trans-Blot Cell	Bio-Rad

### VI.1.4 Software

The following Table VI.3 lists all software used in this work.

Table VI.3 software used in this work

Software	Manufacturer
ImageJ/Fiji	OpenSource
Photoshop CS5	Adobe
Illustrator CS4	Adobe
FlowJo	FlowJo
Las AF	Leica
Papers3	Mekentosji
ZEN Black Edition	Zeiss
CLC Main Workbench	Qiagen
Prism 7	Graphpad
MarvinSketch	Chemaxon
Office 365	Microsoft

### VI.1.5 Buffers formulations

Lysis Buffer	20 mM Tris 10 mM EDTA pH 7.5
3x DNA-Loading Buffer	0.1 mM Orange G 30 % (v/v) glycerol
50x TAE-Buffer	2 M Tris 1 M Acetic acid 0.05 M EDTA pH 8.0
1x TAE	20 ml 50x TAE-Buffer ad 1 l ddH <sub>2</sub> O
10x transfer buffer	860 mM Glycine 250 mM Tris-HCl

1x Transfer Buffer	200 ml Methanol 100 ml 10x Transfer Buffer 700 ml dH <sub>2</sub> O
10x TBS	200 mM Tris 1.5 M NaCl pH 7.4
1x TBS-T	100 ml 10x TBS 500 µl Tween-20 ad 1 l dH <sub>2</sub> O
Running buffer (TGS)	25 mM Tris 192 mM glycine 0.1 % (w/v) SDS pH 8.3
4x Laemmli-Buffer	250 mM Tris-HCl 40 % (v/v) glycerol 4 % SDS 0.02 % (w/v) bromophenol blue 10 % (v/v) β-mercaptoethanol pH 6.8
Coomassie staining solution	5 g Coomassie Brilliant Blue R-250 100 ml Acetic Acid 400 ml Methanol
Destaining solution	700 ml dH <sub>2</sub> O 200 ml Methanol 100 ml Acetic acid
BN-PAGE running buffer	50 mM BisTris 50 mM Tricine pH 6.8



Dark-blue running buffer	0.02 % (w/v) Coomassie Brilliant Blue G250 50 mM BisTris 50 mM Tricine pH 6.8
Light-blue running buffer	0.002 % (w/v) Coomassie Brilliant Blue G250 50 mM BisTris 50 mM Tricine pH 6.8
Native-PAGE sample buffer	50 mM BisTris 6 M HCl 50 mM NaCl 10 % w/v Glycerol 0.001 % Ponceau S pH 7.2
PBS	137 mM NaCl 2.7 mM KCl 10 mM Na <sub>2</sub> HPO <sub>4</sub> 1.8 mM KH <sub>2</sub> PO <sub>4</sub> pH 7.4
Z-Buffer	60 mM Na <sub>2</sub> HPO <sub>4</sub> · 7 H <sub>2</sub> O 40 mM NaH <sub>2</sub> PO <sub>4</sub> · H <sub>2</sub> O 10 mM KCl 1 mM MgSO <sub>4</sub> 50 mM β-mercaptoethanol pH 7.0
0.1 M Phosphate buffer	60 mM Na <sub>2</sub> HPO <sub>4</sub> · 7 H <sub>2</sub> O 40 mM NaH <sub>2</sub> PO <sub>4</sub> · H <sub>2</sub> O pH 7.0

Stacking Gel (6.7 %)	2.5 ml H <sub>2</sub> O 1.5 ml 0.5 M Tris-HCl pH 6.8 0.6 ml acrylamide/bis 37.5:1, 40 % 50 µl 10 % (w/v) SDS 20 µl 10 % (w/v) APS 20 µl TEMED
Resolving Gel	2.5 ml 1.5 M Tris-HCl pH 8.8 10 % 12 % 15 % 18 % 4.8 4.2 3.6 2.8 ml ddH <sub>2</sub> O 2.5 3.1 3.8 4.5 ml acrylamid/bis 37.5:1 100 µl 10 % (w/v) SDS 50 µl 10 % (w/v) APS 15 µl TEMED
Tris-Tricine cathode buffer	100 mM Tris-HCl 100 mM tricine 0.1 % (w/v) SDS pH 8.25
Tris-Tricine Anode buffer	0.2 M Tris base pH 8.9
Chemiluminescent solution	900 µl chemiluminescence solution A 100 µl chemiluminescence solution B 0.9 µl 30 % (v/v) H <sub>2</sub> O <sub>2</sub>
Chemiluminescent solution A	100 mM Tris-HCl pH 8.6 0.025 % (w/v) luminol
Chemiluminescent solution B	0.11 % (w/v) <i>p</i> -coumaric acid in DMSO
SMM-buffer	1 M sucrose 40 mM MgCl <sub>2</sub> 40 mM maleic acid pH 6.5



chemically defined medium established by Branda et al. [142]. The ingredients for MSgg were sterilized and added separately to desalted, autoclaved water. To prepare solid media in petri dishes, 1.5 % (w/v) agar was additionally added prior to autoclaving. Soft agar was prepared by adding 0.5 % (w/v) agar to the respective medium.

### VI.2.6 Media formulations

LB (Lennox)	10 g / l Tryptone 5 g / l Yeast extract 5 g / l NaCl
TSB medium	30 g / l commercial mixture of BD Biosciences
MSgg medium	5 mM potassium phosphate (pH 7.0) 100 mM MOPS (pH 7.0) 2 mM MgCl <sub>2</sub> 700 mM CaCl <sub>2</sub> 50mM MnCl <sub>2</sub> 50 mM FeCl <sub>3</sub> 1 mM ZnCl <sub>2</sub> 2 mM thiamine 0.5 % (v/v) glycerol 0.5 % (w/v) glutamate 0.005 % (w/v) tryptophan 0.005 % (w/v) phenylalanine 0.005 % (w/v) tyrosine
10x MC	100 mM potassium phosphate pH 7.0 30 mM sodium citrate 2 % (w/v) glucose 22 mg / ml ferric ammonium citrate 0.1 % casein hydrolysate 0.2 % potassium glutamate

Competence medium	100 µl 10x MC 3 µl 1 M MgSO <sub>4</sub> 5 µl 1 % (w/v) tryptophan 5 µl 1 % (w/v) phenylalanine 5 µl 1 % (w/v) tyrosine Ad 1 ml dH <sub>2</sub> O
TY-medium	10 g / l Tryptone 5 g / l Yeast extract 5 g / l NaCl 10 mM MgSO <sub>4</sub> (prior to use) 100 µM MnSO <sub>4</sub> (prior to use)

### VI.2.7 Antibiotics and media supplements

The antibiotics used in this study, as well as the suppliers and applied concentrations are listed in Table VI.4. Other supplements that were added to liquid or solid media, e.g. inducers or anti-FMM molecules are listed in Table VI.5.

Table VI.4 Antibiotics used in this work

Compound	Supplier	Final concentration [µg/ml]		
		in <i>B. subtilis</i>	in <i>S. aureus</i>	in <i>E. coli</i>
Ampicillin	Roth	-	-	100
Chloramphenicol	Sigma	5	-	25
Erythromycin	Applichem	1	5 (RN4220), 100 (USA300)	-
Kanamycin	Roth	10	-	50
Lincomycin	Sigma	25	-	-
Spectinomycin	Sigma	100	600	-
Tetracyclin	Applichem	5	-	-

Table VI.5 Media supplements used in this study

Compound	Supplier	Final concentration	Purpose
X-Gal	Roth	40 – 100 µg/ml	Blue-/White-Screening
Sodium citrate	Sigma	5 mM (SPP1) 20 mM (ϕ11)	Phage removal

IPTG	Applichem	0.1 – 10 mM	Inducer of P <sub>hp</sub> promoter
Xylose	Roth	0.001 – 1 % (v/v)	Inducer of P <sub>xyI</sub> promoter
5-doxyl stearic acid	Sigma	150 $\mu$ M	Anti-FMM compound
Simvastatin	Sigma	20 $\mu$ M	Anti-FMM compound
Zaragozic acid	Applichem	50 $\mu$ M	Anti-FMM compound

### VI.3 Microbiology techniques

#### VI.3.1 Bacterial two-/three-hybrid

To screen for interaction of proteins, the bacterial two hybrid system of Euromedex was used. The system is based on fusing two proteins of interest to fragments (T18 and T25) of an adenylate cyclase. Upon interaction, the enzyme is reconstituted and produces cAMP, which can be monitored by activity measurements of a CAP (cAMP binding protein)-controlled  $\beta$ -galactosidase.  $\beta$ -galactosidase activity can be correlated to the interaction of the two proteins of interest [268].

The proteins of interest were cloned in frame into the provided plasmids (pUT18, pUT18C, pKT25, pKNT25), 5 ng of purified plasmids were co-transformed into *E. coli* BTH101 and selected on agar plates containing streptomycin, ampicillin, and kanamycin. For X-Gal screening on agar-plates, a single colony was picked and inoculated in liquid LB medium supplemented with streptomycin, ampicillin, and kanamycin. After growth over night at 30°C, 2  $\mu$ l were spotted on LB agar plates containing antibiotics, 0.5 mM IPTG and 40  $\mu$ g/ml X-Gal.

To assess activity of  $\beta$ -galactosidase, colorimetric conversion of  $\sigma$ -nitrophenyl- $\beta$ -D-galactoside (ONPG) was assayed. To this end, cells were grown in liquid LB with streptomycin, ampicillin, kanamycin, and 0.5 mM IPTG. Before lysis, cells were chilled on ice for 20 minutes. Subsequently, cells were sedimented with 11,000 g for 10 minutes in a pre-cooled centrifuge and washed once in chilled Z-buffer. Optical density of cells was recorded at 600 nm. Subsequently, cells were diluted 1:10 in Z-buffer, lysed by mixing with 0.05 % (w/v) SDS and 10 % (v/v) chloroform and incubated at 28°C for 5 minutes. ONPG was dissolved in 0.1 M phosphate buffer with a final concentration of 4 mg / ml and 200  $\mu$ l were added to the lysate followed by incubation at 28°C. The reaction time (T) was recorded and when sufficient yellow color was observable reaction was stopped by addition of 500  $\mu$ l 1 M NaCO<sub>3</sub>. Afterwards, debris was removed by centrifugation for

5 minutes at 13,000 g. The absorbance of the cleared lysate was recorded at 420 nm (for metabolized ONPG) and 550 nm (for debris contamination). Miller units (MU) were calculated as follows:

$$\beta\text{-galactosidase activity [MU]} = 1000 \cdot \frac{OD_{420} - 1.75 \cdot OD_{550}}{T \cdot V \cdot OD_{600}}$$

OD<sub>420</sub> and OD<sub>550</sub> are the measurements from the reaction mixture, OD<sub>600</sub> reflects the optical density, T represents the reaction time and V is the volume of the culture used for the assay. According to manufacturer's instructions, interactions in a bacterial two hybrid assay are considered positive above a threshold of 700 MU.

Bacterial three-hybrids were performed as recently published by Schneider et al. [132,160]. Briefly, to assess the influence of a third protein on the interaction of two others, the third protein was cloned into pSEVA-Vector 641, which is part of the SEVA modular vector system and contains a gentamycin resistance cassette, a standardized MCS and a pBBR1 backbone [274]. For bacterial-three hybrid assays, X-Gal and ONPG experiments were performed as described above, but supplemented with gentamycin with a final concentration of 10 µg/ml for plasmid maintenance.

### **VI.3.2 Crosslinking**

#### **VI.3.2.1 *In vivo* crosslinking with DSP**

*In vivo* chemical crosslinking (e.g. for BN-PAGE analysis) was performed using the amine-reactive crosslinker DSP (dithiobis(succinimidyl propionate)). DSP is a membrane-permeable reagent that specifically links NHS-esters within a distance of 12 Ångström. For crosslinking, cells of a 50 ml culture were collected by centrifugation (10 minutes, 4000 g, 4°C) and washed twice in cold PBS to remove excess growth medium. Next, cells were resuspended in 9 ml cold PBS, supplemented with 1 ml 10 mM DSP in DMSO and incubated on ice for 2 hours. The reaction was stopped by adding Tris-HCl pH 7.5 to a final concentration of 20 mM and incubated for 15 minutes. Cells were then collected by centrifugation and lysed as described in chapter VI.6.1.2.

#### **VI.3.2.2 Paraformaldehyde crosslinking**

For chemical fixation prior to microscopical analysis, cells were treated with paraformaldehyde that creates covalent bonds between proteins [320]. Cells were harvested from growth medium by centrifugation (3 minutes with 9,000 g) and washed

two times with PBS. Then, cells were resuspended in 4 % (w/v) paraformaldehyde and incubated for 4 minutes. Thereafter, cells were washed three more times with PBS, concentrated and spotted on agar pads for microscopical analysis (see chapter VI.7.1).

### **VI.3.3 Biofilms and Pellicles**

*B. subtilis* biofilms and pellicles were grown in MSgg medium (See chapter VI.2.5). For the formation of surface-attached biofilms an inoculum LB plate was grown over night at 37°C. 2 µl of a dense cell suspension were spotted on the surface of an MSgg agar plate and grown for 5 days at 30°C. For the formation of pellicles, cells were grown in liquid LB medium overnight and diluted 1:100 in 1 ml MSgg, transferred to 24-well plates and incubated overnight at 30°C.

## **VI.4 Molecular biology techniques**

### **VI.4.1 Polymerase chain reaction**

#### **VI.4.1.1 Polymerase chain reaction PCR (Phu/Taq)**

For amplification of DNA fragments, the PCR (polymerase chain reaction) was performed with Taq or Phusion polymerase [321]. The primers used in this work are listed in chapter IX.2, plasmid DNA or genomic DNA was used as a template. For Taq polymerase PCR reaction was performed as follows:

5 µl	10x Reaction Buffer
1 µl	10 mM dNTPs (dATP, dTTP, dGTP, dCTP)
1 µl	DMSO
1 µl	5 µM forward primer
1 µl	5 µM reverse primer
1 µl	Template DNA
1 µl	Taq Polymerase
ad 50 µl	dH <sub>2</sub> O

For PCRs carried out with Taq polymerase, following cycling program was used:



Initial denaturation	95°C	5:00 min	
Denaturation	95°C	1:00 min	
Annealing	54°C	1:00 min	
Extension	72°C	1:00 min (per 1 kb amplicon)	
Final Elongation	72°C	10:00 min	

For PCRs with the Phusion polymerase, the reaction was pipetted according to the following scheme:

10 µl	5x GC Buffer
1 µl	10 mM dNTPs (dATP, dTTP, dGTP, dCTP)
1 µl	DMSO
1 µl	5 µM forward primer
1 µl	5 µM reverse primer
1 µl	Template DNA
0.75 µl	Phusion Polymerase
ad 50 µl	dH <sub>2</sub> O

Following cycling program was used for PCRs with Phusion polymerase:

Initial denaturation	98°C	2:00 min	
Denaturation	98°C	0:10	
Annealing	54°C	0:10	
Extension	72°C	0:15 (per 1 kb amplicon)	
Final Elongation	72°C	10:00	

#### VI.4.1.2 Colony PCR

After plating transformants on selective media, colonies were verified by colony PCR. To this end, single colonies of *E. coli*, *B. subtilis* or *S. aureus* were picked with a sterile pipette tip and transferred into 10 µl dH<sub>2</sub>O. Cell were lysed by boiling in a microwave for 90 seconds at 800 watts. 1 µl lysate were used as a template for conventional PCR as described in chapter VI.4.1.1.

#### VI.4.1.3 Joining PCR

Gene deletions with antibiotic markers, translational and transcriptional fusions were generated by fusing PCR products by long-flanking homology PCR [322]. This PCR

reaction requires a 5'-primer extension homologous to the fragment to join with. Individual fragments were amplified using conventional PCR (see chapter VI.4.1.1) and subsequently purified (see chapter VI.4.3.3). The concentration of the fragments was determined using a Nanodrop 2000 spectrophotometer VI.4.2. The reaction was pipetted as follows:

250 µg	upstream fragment
250 µg	downstream fragment
[500 µg	resistance cassette if applicable]
5 µl	10x Expand Long Template Buffer 2
1 µl	10 mM dNTPs (dATP, dTTP, dGTP, dCTP)
2 µl	5 µM forward primer
2 µl	5 µM reverse primer
0.75 µl	Expand Long Template Enzyme Mix
ad 50 µl	dH <sub>2</sub> O

For the long-flanking homology PCR, a two-step cycling program was used. The time for the extension step is depending on the length of the final product.

Initial denaturation	94°C	2:00	
Denaturation	94°C	0:10	← 10x
Annealing	54°C	0:30	
Extension	68°C	2 min per kb	
Denaturation	94°C	0:10	← 25x
Annealing	54°C	0:30	
Extension	68°C	2 min per kb + 20 sec	
Final Extension	68°C	7:00	

#### VI.4.2 DNA quantification with Nanodrop

DNA quantity of purified plasmids, PCR products or gel-excised DNA fragments were quantified spectroscopically using the Nanodrop 2000 spectrometer.

### **VI.4.3 DNA Isolation**

#### **VI.4.3.1 Plasmid DNA isolation**

Plasmids were isolated using the NucleoSpin plasmid isolation kit from Macherey-Nagel. Typically, plasmids were isolated from a 1 ml overnight culture. For low copy plasmids like pKT25, pKNT25 or pMAD plasmids, manufacturer's instruction for 'isolation of low-copy plasmids' were followed and 10 ml of an overnight culture were used for plasmid isolation. Plasmids were eluted with 50  $\mu$ l Elution buffer and concentration was determined using the Nanodrop spectrometer (see chapter VI.4.2).

#### **VI.4.3.2 Isolation of genomic DNA**

For isolation of genomic DNA of *B. subtilis*, a 1 ml overnight culture was collected by centrifugation (2 minutes at 13,000 rpm) and resuspended in 700  $\mu$ l lysis buffer. Lysozyme was added to a final concentration of 350  $\mu$ g/ml, 10  $\mu$ l RNase A of a 1 mg/ml stock were added and cells were incubated for 15 minutes at 37°C. After that, 10  $\mu$ l proteinase K of a 10 mg/ml stock solution was added and incubated for 15 minutes at 55°C.

The cell lysate was then mixed with equal amount of phenol and inverted several times until emulsified. The emulsion was then centrifuged for 10 minutes at 13,000 rpm. The upper, aqueous phase containing genomic DNA was transferred to a new tube. After adding 70  $\mu$ l of 3 M sodium acetate, the DNA was precipitated with 700  $\mu$ l isopropanol and pelleted by centrifugation for 15 minutes at 13,000 rpm. Finally, the DNA pellet was washed with 70 % (w/w) ethanol. After drying, the DNA pellets were resuspended in 50  $\mu$ l of 50 mM Tris pH 7.0.

To isolate genomic DNA of *S. aureus*, 200  $\mu$ l of an overnight culture were collected by centrifugation for 2 minutes at 13,000 rpm and resuspended in 700  $\mu$ l lysis buffer, 17.5  $\mu$ l lysostaphin was added from a 1 mg/ml stock solution instead of lysozyme. The remaining procedure was identical to *B. subtilis* gDNA isolation as described above.

#### **VI.4.3.3 DNA purification from gel / PCR**

Purification of PCR-products or gel-excised DNA bands was carried out with NucleoSpin® Gel and PCR Clean-up Kit (Macherey-Nagel) according to the provided instruction manual. The volume of elution buffer was individually adjusted for subsequent procession steps.

#### VI.4.4 Restriction

For vector cloning, DNA was digested with following restriction enzymes of New England Biolabs: BamHI-HF, EcoRI-HF, EcoRV-HF, HindIII, KpnI-HF, NarI, NcoI, NcoI-HF, NheI-HF, PstI, Sall-HF, SacII, SapI, SpeI, SphI-HF and XhoI. Restriction reaction was prepared as follows:

1 µg	DNA
10 µl	10x supplied restriction Buffer
1 µl	restriction enzyme
[1 µl	second restriction enzyme; only for double digest]
ad 50 µl	dH <sub>2</sub> O

Digestions were performed for 1 hour at 37°C in a pre-warmed water bath. For double restriction, a second restriction enzyme was added to the reaction simultaneously. If not applicable due to buffer incompatibilities, the second restriction was performed after purification of the first reaction with DNA-cleanup kit in chapter VI.4.3.3.

#### VI.4.5 Gel electrophoresis and gel documentation

DNA was separated in a TAE-based electrophoresis system with TAE gels containing 0.8 % (w/v) agarose. DNA samples were mixed with 3x DNA Loading Buffer and 5 µl of a 1 kb DNA Ladder (New England Biolabs) was used as a size standard. The gel was run at a constant voltage of 90 Volts for 45-60 minutes. Gel documentation was carried out on a Gel iX20 imaging system of Intas Science Imaging.

#### VI.4.6 Ligation

For ligation of digested plasmid DNA and PCR products, the amount of DNA was determined by Nanodrop measurements (See chapter VI.4.2). The reaction was performed in a total volume 20 µl containing the 2 µl of the 10x reaction buffer, vector and insert molecules in a molar ration of 3:1, 5:1 or 9:1 and 0.8 µl T4 DNA Ligase of New England Biolabs. Ligation was performed for 1 hour at room temperature and plasmids were dialyzed afterwards before electroporation.

### **VI.4.7 *E. coli* transformation**

#### **VI.4.7.1 Preparation of frozen aliquots of electro-competent cells**

To prepare frozen stocks of electrocompetent *E. coli* cells, strains were freshly streaked on LB agar plates and a single colony was picked to set overnight culture. The overnight was used to inoculate 1:100 in 1 liter liquid LB medium. Cells were grown at 37°C until they reach mid-log phase ( $OD_{600} = 0.5 - 1$ ). After that, the culture was chilled on ice for 15 – 30 minutes to stop growth and keep cells in exponential growth phase. Afterwards the cells were pelleted in a precooled centrifuge at 4000 g for 15 minutes. Pelleting was repeated with sterile, cold water to remove excess medium. Finally, the cells were resuspended in 10 ml of 10 % (v/v) glycerol and stored as 40  $\mu$ l aliquots at -80°C.

#### **VI.4.7.2 Transformation by electroporation**

Purified or ligated plasmids were transformed into *E. coli* by electroporation. For electroporation 3 – 5  $\mu$ l of a dialyzed ligation mix or 1  $\mu$ l of a 1:200 dilution of purified plasmid was used. An aliquot of electrocompetent cells was thawed on ice, mixed with plasmid DNA and transferred to a 0.1 cm pre-chilled electroporation cuvette. Electroporation was carried out by applying a pulse with a voltage of  $V=1.8$  kV and cells were immediately resuspended in 1 ml LB. Then, cells were shaken one hour at 37°C and plated on LB with appropriate antibiotics.

### **VI.4.8 Sanger Sequencing**

To verify presence of target constructs and exclude mutations, all strains were confirmed by Sanger sequencing (GATC Biotech) [323]. To sequence plasmids, 5  $\mu$ l of purified plasmid DNA with a concentration of 80 - 100 ng/ $\mu$ l, together with 5  $\mu$ l of 5  $\mu$ M of the corresponding primer were sent for sequencing. Genomic integrations were confirmed after gDNA isolation (Chapter VI.4.3.2), followed by PCR amplification of the integrated construct (Chapter VI.4.1.1). 5  $\mu$ l of the purified PCR (20 – 80 ng/ $\mu$ l) product and 5  $\mu$ l of 5  $\mu$ M of the corresponding primer were sent for sequencing. The maximum of sequencing reads is 1000 nt; to check sequences longer than 1000 nt, several primers were used to ensure complete coverage of the desired sequence.

## **VI.5 Generation of genetically modified strains**

### ***VI.5.1 Bacillus subtilis***

#### **VI.5.1.1 Competent cells**

To transform *B. subtilis* PY79, one freshly streaked colony was grown in 1 ml 1x MC (see chapter VI.2.6) at 37°C in a sterile glass tube with a non-air-tight lid to ensure access of atmospheric oxygen. Cells were grown for 4 – 5 h until reaching late-exponential growth phase. 2 – 3 µg linear DNA (linearized plasmid or purified PCR product) or 1:20 – 1:200 dilution of genomic DNA were used to mix with 200 µl cells in a fresh tube. Cells were grown for 2 more hours at 37°C and plated on LB supplemented with appropriate selection marker. Raising colonies were verified by colony PCR and sequencing (see chapters VI.4.1.2 and VI.4.8).

#### **VI.5.1.2 Deletions with resistance gene marker cassettes**

Construction of gene deletions in *B. subtilis* with an antibiotic resistance marker cassette were performed by transforming a DNA-fragment that contains a resistance marker gene flanked with 500 bp homology sites located upstream and downstream of the region to be deleted. First, upstream and downstream flanking regions of the sequence to be deleted, as well as respective antibiotic resistance cassette were amplified with regular PCR (see chapter VI.4.1.1). For this PCR primers were used that carry a 5'-extension complementary to the respective fragment to join with. Then fragments were joined by LFH-PCR (see chapter VI.4.1.3) and the final LFH-PCR product was transformed into *B. subtilis*, selected with respective antibiotic and clones were verified by colony PCR and sequencing (see chapters VI.4.1.2 and VI.4.8).

#### **VI.5.1.3 Marker-less gene deletion with pMAD**

Marker-less gene deletions were generated using the temperature-sensitive pMAD vector [266]. To delete genes, 500 of its upstream and downstream flanking regions were joined via LFH-PCR (see chapter VI.4.1.3) and cloned into the pMAD plasmid (chapter VI.4). The pMAD plasmid has a  $\beta$ -galactosidase and a temperature sensitive origin of replication and is only maintained in the cells growing at low temperatures ( $\leq 30^\circ\text{C}$ ). The plasmid was transformed into *B. subtilis* (see chapter VI.5.1.1) and cells were plated on LB mls plates (25 µg/ml erythromycin and 1 µg/ml lincomycin) for selection and incubated at 30°C. Raising clones were validated by blue/white-screening

on LB X-Gal plates for the presence of the plasmid. Positive clones carrying the plasmid were then grown in 1 ml liquid LB for 6 h at 42°C and plated on LB mls X-Gal plates to force recombinant integration of the entire plasmid into the genome (1<sup>st</sup> recombination). Plates were incubated for 48 h at 42°C. Blue colony appearance indicates the presence of the plasmid-backbone in the genome. This stable integration of the entire plasmid into the genome was stored as a glycerol stock.

In a second recombination step, the plasmid backbone including and the target sequence will be removed by a homologues recombination event. Therefore, blue colonies of the 1<sup>st</sup> recombination step were grown in 1 ml LB for 6 h at 30°C and subsequently shifted to 42°C and grown for 3 more hours. Serial dilutions were plated on LB X-Gal plates and incubated for 48 hours at 42°C. Raising blue colonies still carry the entire plasmid, whereas white colonies lost the plasmid backbone by homologues recombination and were reverted to wild type or to desired mutant. Thus, white colonies were screened for the loss of the sequence of interest by colony PCR and confirmed by sequencing (see chapters VI.4.1.2 and VI.4.8).

#### **VI.5.1.4 Phage transduction**

Shuttling of constructs from PY79 to the undomesticated isolate NCIB3610 was achieved by phage transduction using the SPP1 bacteriophage [324]. Phage lysates were generated by growing the *B. subtilis* donor strain for 2 – 3 h in TY medium. 200 µl cells were mixed with 100 µl SPP1 wild type phage lysates in different dilutions ( $10^{-3}$  –  $10^{-6}$ ) and incubated for 15 minutes at 37°C without agitation. Subsequently, cells were mixed with 3 ml hot (~65°C) TY soft agar and spread on TY plates. After 8 – 16 h incubation at 37°C, phage hallows were harvested by scraping off soft agar and resuspended in 5 ml TY medium. Intact cells and soft agar were spun down for 10 minutes with 1500 rpm. The supernatant containing phages was treated with 1 µl DNase I, sterile-filtered and stored at 4°C.

For re-infection, the recipient strain was grown for 2 – 3 hours in 10 ml TY medium until reaching an optical density of  $OD_{600} = 1.0 - 1.5$ . 10 ml of 1:10 diluted recipient cells were mixed with 30 µl phage lysate and incubated for 30 minutes at 37°C without agitation. Cells were collected by centrifugation at 4000 rpm for 15 minutes. The cells in the pellet were resuspended and spread on LB plates containing corresponding antibiotic and

1 mM sodium citrate to lyse excess phages. Positive clones were verified by colony PCR and sequencing (see chapters VI.4.1.2 and VI.4.8).

### VI.5.1.5 Cloning vectors

All *B. subtilis* vectors used in this work were cloned and maintained in *E. coli* (see chapter VI.4). pMAD was used to generate markerless deletions in PY79 (see chapter VI.5.1.3) and ectopic integration vectors were used to integrate translational or transcriptional fusions into neutral, non-essential sites of the genome (*amyE*, *lacA* or *thrC*). Before transformation, plasmids were linearized to ensure that only target construct and not entire plasmid will be integrated into the genome. If constructs were integrated into the *thrC* locus, cells growing in MSgg were supplemented with 1 % (w/v) threonine. All integration sites and features of the plasmids are listed in Table VI.6.

Table VI.6 All *B. subtilis* cloning vectors used in this study

Plasmid	Integration locus	Resistance genes	Function	Ref.
pBM001	<i>lacA</i>	<i>bla</i> , <i>mls</i>	Chimera of pDR111 and pDR183 for ectopic integration of IPTG inducible gene of interest into <i>lacA</i>	This work
pDG1731cm	<i>thrC</i>	<i>bla</i> , <i>mls</i> , <i>cat</i>	Ectopic integration into <i>thrC</i>	[325]
pDR111	<i>amyE</i>	<i>bla</i> , <i>spc</i>	Integration of IPTG-inducible gene into <i>amyE</i>	[326]
pDR183	<i>lacA</i>	<i>bla</i> , <i>mls</i>	Ectopic integration into <i>lacA</i>	[327]
pMAD	-	<i>bla</i> , <i>ermC</i>	Temperature sensitive plasmid to create marker-less deletions	[266]
pSG1154	<i>amyE</i>	<i>bla</i> , <i>spc</i>	Plasmid to fuse GFP to the C-terminal end of a gene of interest under control of a xylose-inducible promoter	[328]
pX	<i>amyE</i>	<i>bla</i> , <i>cat</i>	Integration of xylose-inducible gene into <i>amyE</i>	[329]



## **VI.5.2 *Staphylococcus aureus***

### **VI.5.2.1 Competent Cells + Transformation**

For preparation of frozen aliquots of competent cells of *S. aureus* RN4220, cells were grown in 500 ml TSB at 37°C until reaching  $OD_{540} = 0.2 - 0.25$ . Cells were spun down for 10 minutes with 6000 rpm for 10 minutes at 4°C. Pellet was washed four times with ice cold 0.5 M sucrose while constantly decreasing volume to 1/20<sup>th</sup> of starting volume. Finally, cells were resuspended in 5 ml ice cold 0.5 M sucrose. 200 µl aliquots were flash frozen in liquid nitrogen and stored at -80°C.

For transformation of plasmid DNA in *S. aureus* RN4220, an aliquot of competent cells was thawed on ice, mixed with ~1 µg plasmid DNA and incubated for 15 minutes on ice. Cells were then transferred to chilled electroporation cuvette (0.1 cm, Bio-Rad) and after pulsing, cells were recovered with 500 µl TSB. Cells were shaken for 1 h before plating on TSB plate containing respective selection marker.

### **VI.5.2.2 Deletions pMAD and labeling with pMAD derivatives**

The generation of markerless deletions with pMAD or ectopically integrated, markerless translational fusions with the pMAD variants pLac or pAmy in *S. aureus* was performed as described in chapter VI.5.1.3 [266,267]. In contrast to the *B. subtilis* protocol, *S. aureus* was grown in TSB and selected on TSB Ery (X-Gal) plates with a concentration of 2 µg/ml and 100 µg/ml erythromycin for RN4220 and USA300\_TCH1516, respectively. RN4220 was only used for electroporation and to maintain free or genome-integrated plasmids (1<sup>st</sup> recombination), which were then shuttled to USA300\_TCH1516 via Φ11-phage transduction (see chapter VI.5.2.3). Thus, the second recombination was performed only performed in USA300\_TCH1516 and raising white colonies were screened with colony PCR (chapter VI.4.8). The construct was checked by sequencing and by fluorescence microscopy or western blotting.

The pMAD plasmids used to generate *S. aureus* mutants were all cloned and maintained in *E. coli* (see chapter VI.4). All plasmids and their features used in this work are listed in Table VI.7.

Table VI.7 All *S. aureus* cloning vectors used in this study.

Plasmid	Integration locus	Resistance genes	Function
pMAD	-	<i>bla, mls</i>	Temperature sensitive plasmid to create marker-less deletions
pAmy	<i>cel</i>	<i>bla, mls</i>	pMAD variant to integrate gene of interest into the non-essential amylase locus <i>cel</i>
pAmy <sub>xyI</sub>	<i>cel</i>	<i>bla, mls</i>	pMAD variant to integrate gene of interest into the non-essential amylase locus <i>cel</i> , controlled by a xylose promoter
pIac	<i>lac</i>	<i>bla, mls</i>	pMAD variant to integrate gene of interest into the non-essential $\beta$ -galactosidase locus <i>lac</i>
pLac <sub>xyI</sub>	<i>lac</i>	<i>bla, mls</i>	pMAD variant to integrate gene of interest into the non-essential $\beta$ -galactosidase locus <i>lac</i> , controlled by a xylose promoter

### VI.5.2.3 Phage transduction

To transfer genomic material from the laboratory strain RN4220 to the clinical isolate USA300\_TCH1516, the bacteriophage  $\Phi$ 11 was used [330]. Phage lysates were generated by growing donor strain for 6 hours in 10 ml TSB. Cells were then supplemented 5 mM CaCl<sub>2</sub> and heated up for 2 minutes to 56°C. Then 300  $\mu$ l cells were mixed with 100  $\mu$ l  $\Phi$ 11 wild type phage lysates in different dilutions ( $10^{-1}$  –  $10^{-6}$ ) and incubated for 15 minutes at room temperature without agitation. Thereafter, cells were mixed with 5 ml hot (~65°C) LB soft agar containing 5 mM CaCl<sub>2</sub> and spread on LB plates. After 10 – 16 hours incubation at 37°C, the soft agar layer of plates with confluent lysis was scraped off and resuspended in 5 ml LB supplemented with 5 mM CaCl<sub>2</sub>. The suspension was vortexed thoroughly to break the soft agar and then intact cells and soft agar was removed by centrifugation for 10 minutes with 4,000 g. The supernatant containing the phages was sterile-filtered and stored at 4°C.

For transduction of target alleles, the recipient strain was grown for 6 hours in 10 ml TSB, supplemented with 5 mM CaCl<sub>2</sub>, mixed with 100  $\mu$ l of  $\Phi$ 11 phage lysate and incubated for 15 minutes at room temperature without agitation. Cells were then plated on TSB plates containing 20 mM sodium citrate and respective selection marker. Raising colonies were verified with colony PCR and sequencing (see chapters VI.4.1.2 and VI.4.8).

## **VI.6 Biochemistry**

### **VI.6.1 Sample preparation**

#### **VI.6.1.1 Preparation of cell extracts**

Whole cell extracts of *B. subtilis* and *S. aureus* were prepared by pelleting cells equivalent 1 ml with OD<sub>600</sub>=1.5. Cells were resuspended in 50 µl lysis buffer supplemented with 1 mM PMSF and 1 µg / ml lysozyme for *B. subtilis* and 50 µg / ml lysostaphin for *S. aureus*, respectively. Samples were incubated for 20 – 30 minutes at 37°C until sample becomes translucent. 50 µl of 2x Laemmli buffer was added and samples were boiled for 5 minutes at 95°C. 10-20 µl were used for SDS-PAGE or western blot analysis (chapter VI.6.5.1 and VI.6.6).

#### **VI.6.1.2 Isolation of cytosolic fraction and crude membrane fraction**

To separate cytosolic proteins from membrane proteins, cells were grown in a 50 ml culture to stated optical density. *B. subtilis* cells were lysed in 10 ml SMM buffer supplemented with 1 mg/ml lysozyme and 1 mM PMSF. For lysis of *S. aureus*, cells were resuspended in 10 ml PBS-lysis buffer supplemented with 10 µg/ml lysostaphin and 1 mM PMSF. Cells were then incubated at 37°C for 10 minutes before mechanical lysis with a Fast-Prep Shaker. For that cells were mixed with glass beads and shaken for 40 sec with a speed of 6.5 m/sec. Two rounds of lysis were performed and sample was chilled on ice in between for 2 minutes. After lysis, unbroken cells and debris were removed by centrifugation for 10 minutes with 11,000 g at 4°C. Cleared lysate was subjected to ultracentrifugation for 1 h at 100,000 g at 4°C. The supernatant contains cytosolic proteins and the pellet containing the membrane proteins was resuspended in 20 mM Tris pH 8.0 or PBS. For long-term storage membrane pellets were supplemented with 20 % (v/v) glycerol, flash-frozen in liquid nitrogen and stored at -80°C.

#### **VI.6.1.3 Isolation of DRM/DSM**

Detergent-resistant and detergent-sensitive membrane fractions (DRM/DSM) were isolated using the CellLytic MEM protein extraction kit (Sigma-Aldrich). For that, cell membrane fractions were isolated as described in chapter VI.6.1.2. A total of 4 mg proteins was used to mix with provided lysis and separation buffer and incubated on ice for 10 minutes, followed by a centrifugation step in a pre-cooled centrifuge for 10 minutes with 11,000 g at 4°C. The sample was then incubated for 5 minutes at 30°C and

centrifuged with 3,000 g for 3 minutes at room temperature. The upper phase containing the DSM was removed and the lower phase containing DRM was washed by adding wash buffer and incubating on ice for 10 minutes, followed by incubation at 30°C for 5 minutes and phase separation by centrifugation with 3,000 g for 3 minutes. The washing procedure was repeated three times. Eventually, equal volumes of DRM and DSM were precipitated with acetone (see chapter VI.6.2.2). Precipitated DRM/DSM protein pellets were taken up in 200 µl 1x Laemmli buffer and 10 – 20 µl of the sample were used for SDS-PAGE and western blot analysis.

#### **VI.6.1.4 Culture supernatants**

For the preparation of culture supernatants, cells were grown in 10 ml TSB medium to the stated growth phase. Cells were collected by centrifugation for 10 minutes with 4000 g at 4°C. Supernatants were sterile-filtered through a syringe filter with a pore size of 0.2 µm. 2 ml of the culture supernatants were precipitated with TCA (see chapter VI.6.2.1). Proteins equivalent to 0.4 – 1.6 ml culture supernatant were used for immunoblot analysis (chapter VI.6.6).

#### **VI.6.1.5 Biofilm Matrix**

To isolate proteins of the *B. subtilis* biofilm matrix, cells were grown as pellicles as described in chapter VI.3.3. The floating biofilm matrix was mildly sonicated with 12 pulses (power output 0.7 and cycle 50 %) to separate the cells from the biofilm matrix. After that, cells were removed by centrifugation for 10 minutes at 4,000 g and the supernatant containing the biofilm matrix was filter-sterilized using 0.2 µm pore-filters. The samples were then precipitated with TCA (see chapter VI.6.2.1) and used for SDS-PAGE and immunoblot analysis.

#### **VI.6.1.6 BN-PAGE samples**

To prepare samples for BN-PAGE, the membrane fraction was isolated as described in chapter VI.6.1.2. Samples were then supplemented with 4x Native-PAGE sample buffer and supplemented with stated concentration of detergent. For solubilization, samples were incubated over night at 4°C while rotating. Then, insoluble material was removed by centrifugation for 30 minutes with 20,000 g at 4°C. The supernatants containing solubilized proteins were recovered and stored at -80°C. Before performing gel electrophoresis, samples were supplemented with 1/10<sup>th</sup> of NativePAGE sample additive, which contains 5 % Coomassie Brilliant Blue G-250.

## **VI.6.2 Precipitation of proteins**

### **VI.6.2.1 TCA precipitation**

Proteins were precipitated from aqueous solution with trichloroacetic acid (TCA). The protein solution was supplemented with 100 % (w/v) TCA to final concentration of 5 % and incubated on ice overnight. Precipitated proteins were then collected by centrifugation for 15 minutes with 15,000 g at 4°C. Consecutively, protein pellets were washed carefully with ice-cold acetone and then with ice-cold ethanol. Protein pellets were taken up in 1x Laemmli buffer and if required, the pH was re-adjusted with 1 µl 1.5 M Tris-HCl pH 8.8.

### **VI.6.2.2 Aceton precipitation**

Aceton precipitation of proteins was performed by adding 4 volumes of ice-cold acetone to the sample followed by an incubation for 1 h at -20°C. Precipitated proteins were collected by centrifugation for 15 minutes with 15,000 g at 4°C and washed two more times with ice-cold acetone. Protein pellets were dried at 95°C for 5 minutes and taken up in 1x Laemmli buffer.

## **VI.6.3 Quantifying Proteins with Nanodrop**

The concentration of proteins in aqueous solutions was determined by measuring light absorbance at a wavelength of 280 nm with the Nanodrop 2000 spectrometer. The measurement is based on measuring absorbance of visible light at 280 nm by tyrosine and tryptophan residues.

## **VI.6.4 Pulldowns**

Co-immunoprecipitation of FLAG-tagged or His-tagged proteins was achieved using M2 FLAG-capture beads (Sigma-Aldrich) and Ni-NTA resin (Qiagen), respectively. For capturing of FLAG-tagged proteins, the crude membrane fraction was isolated (chapter VI.6.1.2) and solubilized in 50 mM Tris-HCl pH7.5, 50 mM NaCl supplemented with 0.25 % DDM. Insoluble material was removed for 1 h with 100,000 g at 4°C and 4 mg solubilized membrane proteins were mixed with 20 µl pre-equilibrated beads. After rotation for 2 h at 4°C, beads were washed four times in 50 mM Tris-HCl pH 7.5, 50 mM NaCl while constantly decreasing detergent concentration (two washes with 0.125 % DDM, two washes with 0.02 % DDM). Captured proteins were eluted by boiling

beads in 50  $\mu$ l 1x Laemmli buffer. The sample was then subjected to SDS-PAGE and consecutive immunoblotting.

For immunoprecipitation of His-tagged FloA and interacting proteins, the crude membrane fractions were isolated as described in chapter VI.6.1.2 and solubilized in His-binding buffer (50 mM Tris-HCl pH 7.5, 500 mM NaCl, 20 mM imidazole, 10 % (v/v) glycerol, 1 % (v/v) Tween-20) containing 0.25 % DDM. Insoluble material was removed by centrifugation for 1 hour with 100,000 g at 4°C. A total of 1 mg solubilized proteins was incubated with 150  $\mu$ l Ni-NTA resin and rotated for 2 hours at 4°C. The resin was then washed twice in buffer W1 (50 mM Tris-HCl pH 7.5, 500 mM NaCl, 20 mM imidazole, 10 % (v/v) glycerol), twice in buffer W2 (50 mM Tris-HCl pH 7.5, 500 mM NaCl, 50 mM imidazole, 10 % (v/v) glycerol) and eluted with 200  $\mu$ l elution buffer (50 mM Tris-HCl pH 7.5, 500 mM NaCl, 1 M imidazole, 10 % (v/v) glycerol). The elution fraction was concentrated by TCA precipitation (see chapter VI.6.2.1) before proceeding with on SDS-PAGE and immunoblotting (chapters VI.6.5.1 and VI.6.6).

## **VI.6.5 Gel-electrophoresis**

### **VI.6.5.1 SDS-PAGE**

Separation of proteins was carried out in an electric field using discontinuous SDS polyacrylamide gel electrophoresis (SDS-PAGE) [331]. Proteins were focused in a wide-meshed stacking gel (6.7 % acrylamide) before separation in the resolving gel. For SDS-PAGE analysis, equipment of Bio-Rad was used. In this work, proteins were separated in gels containing 10, 12.5, 15 or 18 % acrylamide (see chapter VI.1.5). For the analysis of proteins up to 20 kDa, 15 – 18 % acrylamide gels were used along with a Tris-Tricine buffer system (chapter VI.1.5). Proteins > 20 kDa were resolved using Tris-Glycine-SDS (TGS) running buffer and gels with 12.5 % (for the range of 20 – 100 kDa) or 10 % (> 100 kDa) acrylamide. Protein samples were prepared as described in chapters VI.6.1.1 – VI.6.1.5. 5 – 40  $\mu$ l sample were loaded on gel. To estimate size of the proteins, 5  $\mu$ l of the ColorPlus prestained protein marker (New England Biolabs) was used. Proteins were separated at a constant voltage of 150 V.

### **VI.6.5.2 BN-PAGE**

The separation of protein complexes or proteins in their native state was performed using blue native polyacrylamide gel electrophoresis (BN-PAGE) [332]. Electrophoresis equipment, gels (3-12 % gradient) and buffers were purchased from Life Technologies.

Protein samples were prepared as described in chapter VI.6.1.6. 5 – 15  $\mu$ l sample was loaded on the gel corresponding to a total amount of 200 – 400  $\mu$ g protein per lane. For size estimation, 5  $\mu$ l of Native Mark Protein Standard (Life Technologies) was used. For gel electrophoresis, two types of cathode buffers are used: Dark-blue running buffer was used for consecutive Coomassie staining of the gel. For immunoblotting a combination of dark-blue running buffer was used until the running front migrated  $\sim 1/3$  through the gel. Then cathode buffer was exchanged to light-blue running buffer. Electrophoresis was performed at 4°C with 150 V for 1 hour, followed by increased voltage at 250 V until running front left the gel.

## **VI.6.6 Western blotting**

### **VI.6.6.1 Semi-dry/wet blotting**

Proteins were transferred onto a PVDF membrane via semi-dry transfer or wet transfer. Prior to assembly, PVDF membranes were equilibrated by successively washing in methanol (90 seconds), water (5 minutes) and transfer buffer (5 minutes). Likewise, SDS gel and Whatman papers were equilibrated in transfer buffer. The stack was assembled and transferred to a semi-dry blotting apparatus or into a wet transfer cassette and submerged in a blotting tank filled with chilled transfer buffer. The semi-dry transfer was set at room temperature for 30 minutes at 15 V. Wet transfer of the proteins to the PVDF membrane, was performed in a chamber with an ice pack and constantly stirred to mitigate the heat production during the transfer. The transfer was performed for 1 h at 100 V.

### **VI.6.6.2 Fixing proteins and blocking PVDF membrane**

After transferring proteins to membrane, the membrane was blocked for 1 h in TBS-T containing 5 – 10 % non-fat dried milk powder or 3 % bovine serum albumin (Table VI.8) to reduce unspecific binding of the antibodies.

Before blocking of BN-PAGE transfers, proteins were fixed on the membrane by incubation in 8 % acetic acid for 15 minutes followed by air-drying of the membrane and re-wetting in methanol for 30 seconds. PVDF membrane was then rinsed shortly in TBS-T before continuing with blocking.

### VI.6.6.3 Antibody incubation

After blocking, the primary antibody was diluted in blocking reagent and added for 1 h at room temperature or at 4°C over night while rocking gently. After incubation with the primary antibody, the membrane was washed three times for 5 minutes in TBS-T and the secondary antibody was added for 1 h at room temperature while rocking gently. Then, membrane was washed three more times for 5 minutes. Dilutions, source, and respective blocking reagents of the antibodies used in this work are listed in Table VI.8.

**Table VI.8 Antibodies used in this work**

<b>Antibody</b>	<b>Source</b>	<b>Supplier</b>	<b>Dilution</b>	<b>Blocking reagent</b>
anti-chicken IgY-HRP	rabbit	Life Technologies	1:5000	5 % milk
anti-EsaA	rabbit	[219]	1:10000	5 % milk
anti-EssB	rabbit	Geibel Lab	1:4000	5 % milk
anti-EssC	rabbit	[219]	1:10000	5 % milk
anti-EsxC	rabbit	[219]	1:1000	5 % milk
anti-FLAG	mouse	Sigma-Aldrich	1:1000	5 % milk
anti-FloA	chicken	[245]	1:10000	5 % milk
anti-GFP	rabbit	Living Colors	1:5000	5 % milk
anti-GroEL	rabbit	Sigma-Aldrich	1:5000	3 % BSA
anti-mCherry	rabbit	Biovision	1:5000	5 % milk
anti-mouse IgG-HRP	donkey	Thermo Fisher	1:10000	5 % milk
anti-mouse IgM-HRP	goat	Elabscience	1:5000	3 % BSA
anti-rabbit IgG-HRP	donkey	Life Technologies	1:20000	5 % milk
anti-YtnP	chicken	[270]	1:500	5 % milk

### VI.6.6.4 Development

Immunoblots were developed by detection of chemiluminescence using the ImageQuant LAS4000 biomolecular imager. Chemiluminescence was generated by adding freshly mixed chemiluminescence solution (see chapter VI.1.5). Signal was detected with automatic exposure time in high resolution mode. Raw images were processed using ImageJ and Photoshop.

### VI.6.7 Coomassie staining

After separation with gel electrophoresis, the proteins were visualized by Coomassie staining. The SDS-PAGE gel was incubated in Coomassie staining solution for one hour at mild agitation. Hereafter, the gel was washed with water and incubated in destaining solution until the background vanished and bands were clearly visible.



## **VI.6.8 Recombinant protein expression**

### **VI.6.8.1 EsxA-D, YtnP**

Recombinant expression of YtnP or Esx-proteins (EsxA – EsxD) was performed using the pET20b(+) vector that fuses a C-terminal Hexahistidine tag to the respective protein. The construct was transformed into *E. coli* BL-21 DE3 Gold (Stratagene) and single colonies were used to start an overnight culture. Cells were diluted 1:100 in 50 ml LB and grown at 37°C until reaching an optical density of  $OD_{600} \sim 0.6$ . Expression of recombinant proteins was induced by adding 1 mM IPTG for 4-5 h at 37°C. Cells were collected by centrifugation (10 minutes, 4,000 g, 4°C) and pellets were resuspended in 50 mM Tris-HCl pH 7.5, 500 mM NaCl, 20 mM imidazole, 10 % (v/v) glycerol, 1 % (v/v) Tween-20 and 0.2 µg / ml Lysozyme (Sigma-Aldrich). After 10 minutes incubation at 37°C, cells were lysed by mechanically in a fast-prep shaker (three times 45 sec with 6.5 m/sec). Then, the lysate was cleared by centrifugation for 10 minutes with 10,000 g at 4°C, mixed with pre-equilibrated Ni-NTA resin (Qiagen) and incubated for 30 minutes at 4°C while rotating. The resin was washed twice in 50 mM Tris-HCl pH 7.5, 500 mM NaCl, 10 % (v/v) glycerol and 1 mM PMSF while increasing imidazole concentration from 20 to 50 mM. His-tagged proteins were then eluted from the resin with 50 mM Tris-HCl pH 7.5, 500 mM NaCl, 1 M imidazole, 10 % (v/v) glycerol and 1 mM PMSF. Imidazole was removed by using PD-10 Desalting columns (GE Healthcare). Proteins were supplemented with 20 % (v/v) glycerol and stored at -80°C.

### **VI.6.8.2 EsaAEssABC + FloA and size exclusion chromatography**

The pBAD-*esaAessABC* plasmid was transformed into commercial *E. coli* One Shot TOP10 expression cells (Life Technologies) and if necessary pASK-IBA3C-floA was co-transformed. Cells were grown at 37°C in liquid LB medium until reaching an optical density of  $OD_{600} \sim 0.8$  and expression was induced by adding 0.2 % L-arabinose (for pBAD plasmid) and 0.2 µg/ml anhydrotetracycline (for pASK-IBA3C) for 24 h at 18°C. Cell pellets were resuspended in 50 mM Tris-HCl pH 8.0, 300 mM NaCl, 20 mM MgCl<sub>2</sub> and 1 mM DTT and lysed by French-press mediated lyses (3 cycles with 10,000 psi). The cell lysate was clarified by centrifugation for 20 minutes at 10,000 g and membrane fractions were collected by ultracentrifugation for 60 min at 185,000 g. The membranes were homogenized and solubilized in 50 mM Tris-HCl pH 8.0, 50 mM NaCl, 10 mM MgCl<sub>2</sub>, 1 mM EDTA and 1 mM DTT, 0.5 % (w/v) DDM (Anatrace) and

0.75 % (w/v) dexyl maltose neopentyl glycol (DM-NPG) (Anatrace). The membrane proteins were then clarified by ultracentrifugation for 60 minutes at 100,000 g.

The supernatant was directly loaded onto a Superose 6 10/300 column (GE Healthcare) that was equilibrated with 50 mM Tris-HCl pH8.0, 50 mM NaCl, 10 mM MgCl<sub>2</sub> and 0.025 % (w/v) DM-NPG. The eluted fractions were collected and analyzed by western blotting.

## VI.7 Microscopy

### VI.7.1 Sample preparation for microscopy

For microscopical analysis cells were harvested at stated optical density by centrifugation with 9000 g for 3 minutes. Cells were washed two times with PBS to remove excess growth medium. Paraformaldehyde crosslinking was carried out if necessary (see chapter VI.3.2.2). For membrane and DNA staining, cells were incubated for ten minutes with 1  $\mu$ M FM4-64 and 1  $\mu$ g/ml Hoechst 33342, respectively. After that cells were washed twice with PBS and spotted on a cover slide with an agarose pad made of PBS + 0.8 % (w/v) agarose.

### VI.7.2 Fluorescence microscopy

Fluorescence microscopy was carried out on a Leica DMI6000 microscope equipped with a Leica CRT6000 illumination system and a Leica DFC630FX color camera. Fluorescent proteins and dyes were detected using filters and excitation times specified in Table VI.9. Raw images of Z-stack series were recorded and deconvoluted using the deconvolution algorithm of the LasAF software. Further image processing was performed with ImageJ and Photoshop.

**Table VI.9** Fluorescent proteins and dyes used in this work and their corresponding emission/excitation filters and excitation time.

<b>Fluorescent compound</b>	<b>Excitation filter</b>	<b>Emission filter</b>	<b>Excitation time [ms]</b>
eGFP	BP480/40	BP527/30	100 – 200
GFPmut1	BP480/40	BP527/30	100 – 200
eYFP	BP500/20	BP535/30	100 – 200
mCherry	BP546/40	BP600/40	200 – 400
Hoechst	BP360/40	BP470/70	50
FM4-64	BP546/40	BP600/40	100

### **VI.7.3 Structured illumination microscopy**

For super-resolution imaging, cells were imaged on a Zeiss ELYRA S.1 structured illumination microscopy (SIM) system, equipped with a Plan-Apochromat oil-immersion objective (63x) with a numerical aperture of 1.4. Raw images were generated with three grid rotations and five phases. The SIM images were reconstructed using the software ZEN 2012. Further image processing was performed using ImageJ.

### **VI.7.4 Stereoscope**

*B. subtilis* biofilms and pellicles were imaged using a Nikon SMZ 1500 stereoscope connected to a Leica DFC295 color camera. Pictures were acquired with Zeiss Axio Vision Software and processed with ImageJ.

### **VI.8 Flow cytometry**

To analyze subpopulations in *B. subtilis* biofilms, flow cytometric analysis was carried out. *B. subtilis* biofilms were suspended in PBS and cells were dispersed from biofilm matrix by sonication (12 pulses, power output 0.7, cycle 50 %). After dispersion, cells were fixed with paraformaldehyde (see chapter VI.3.2.2) and resuspended in PBS buffer. If necessary, cells were diluted several times in PBS prior to flow cytometry. Flow cytometry was carried out in a MACSquant Analyzer. For YFP fluorescence detection, a 488 nm laser was used and fluorescence was detected using a 525/50 nm filter. The photomultiplier voltage was 462 V. For each sample 50,000 ungated events were measured with a flow rate of 1,500 – 3,000 events per second. Flow cytometry data was analyzed using FlowJo 9.5.1.

### **VI.9 Animal experiments & ELISA**

Cohorts of 3-week old BALB/c mice (n=6) were intravenously infected with 100 µl suspension containing 1 x 10<sup>6</sup> CFU staphylococci in PBS. For anti-FMM molecule treatment, 20 mg/kg zaragozic acid (in PBS) was administered intraperitoneally 30 minutes prior to challenge with staphylococci. Procedure was repeated twice (on day 14 and day 28). Animals were sacrificed after 40 days and blood samples were collected by cardiac puncture. Blood sera were collected and examined by an Enzyme-linked immunosorbent assay (ELISA) for antibody titers of EsxA-D. Briefly, recombinant His-tagged Esx proteins were purified as stated above, diluted in PBS to a final concentration of 10 µg/ml and coated on 96-well plates (Nunc, MaxiSorp). The plates were then

incubated overnight at 4°C and subsequently blocked with 5 % BSA (bovine serum albumin) in PBS. The serum samples were then diluted 1:50 in PBS and incubated on the plates for 1 h at 37°C. Then, plates were washed with PBS-T (PBS + 0.05 % Tween) and incubated with anti-mouse IgM antibodies (1:5000 dilution) for 1 h at 37°C. After a final washing step with PBS-T, 100 µl TMB (3,3',5,5'-tetramethylbenzidine; Life Technologies) were added to each well until sufficient color development was observed. Then reaction was stopped by adding 100 µl 1 N NaOH and consecutively absorbance was measured at 450 nm.

---

## VII REFERENCES

1. Gorter E, Grendel F: **On bimolecular layers of lipoids on the chromocytes of the blood.** *J Exp Med* 1925, **41**:439–443.
2. Levental I, Veatch S: **The Continuing Mystery of Lipid Rafts.** *J Mol Biol* 2016, **428**:4749–4764.
3. Krogh A, Larsson B, Heijne von G, Sonnhammer EL: **Predicting transmembrane protein topology with a hidden Markov model: application to complete genomes.** *J Mol Biol* 2001, **305**:567–580.
4. Dupuy AD, Engelman DM: **Protein area occupancy at the center of the red blood cell membrane.** *Proc Natl Acad Sci USA* 2008, **105**:2848–2852.
5. Singer S, Nicolson G: **Fluid Mosaic Model of Structure of Cell-Membranes.** *Science* 1972, **175**:720–&.
6. Lee AG, Birdsall NJ, Metcalfe JC, Toon PA, Warren GB: **Clusters in lipid bilayers and the interpretation of thermal effects in biological membranes.** *Biochemistry* 1974, **13**:3699–3705.
7. Wunderlich F, Ronai A, Speth V, Seelig J, Blume A: **Thermotropic lipid clustering in tetrahymena membranes.** *Biochemistry* 1975, **14**:3730–3735.
8. Wunderlich F, Kreutz W, Mahler P, Ronai A, Heppeler G: **Thermotropic fluid goes to ordered “discontinuous” phase separation in microsomal lipids of Tetrahymena. An X-ray diffraction study.** *Biochemistry* 1978, **17**:2005–2010.
9. Karnovsky MJ: **The concept of lipid domains in membranes.** *J Cell Biol* 1982, **94**:1–6.
10. Veatch SL, Keller SL: **Organization in lipid membranes containing cholesterol.** *Phys Rev Lett* 2002, **89**:268101.
11. Veatch SL, Keller SL: **Separation of liquid phases in giant vesicles of ternary mixtures of phospholipids and cholesterol.** *Biophys J* 2003, **85**:3074–3083.
12. Feigenson GW, Buboltz JT: **Ternary phase diagram of dipalmitoyl-PC/dilauroyl-PC/cholesterol: nanoscopic domain formation driven by cholesterol.** *Biophys J* 2001, **80**:2775–2788.
13. Goh SL, Amazon J, Feigenson GW: **Towards a Better Raft Model: Modulated Phases in the 4-Component Bilayer Mixture, DSPC/DOPC/POPC/CHOL.** *Biophys J* 2013, **104**:82a.
14. Heberle FA, Buboltz JT, Stringer D, Feigenson GW: **Fluorescence methods to detect phase boundaries in lipid bilayer mixtures.** *Biochim Biophys Acta* 2005, **1746**:186–192.
15. Rodriguez-Boulán E, Nelson W: **Morphogenesis of the polarized epithelial cell phenotype.** *Science* 1989, **245**:718–725.
16. van Meer G, Stelzer EH, Wijnaendts-van-Resandt RW, Simons K: **Sorting of sphingolipids in epithelial (Madin-Darby canine kidney) cells.** *J Cell Biol* 1987, **105**:1623–1635.
17. Simons K, van Meer G: **Lipid sorting in epithelial cells.** *Biochemistry* 1988, **27**:6197–6202.

18. van Meer G: **Lipid traffic in animal cells.** *Annu Rev Cell Biol* 1989, **5**:247–275.
19. Brown DA, Rose JK: **Sorting of Gpi-Anchored Proteins to Glycolipid-Enriched Membrane Subdomains During Transport to the Apical Cell-Surface.** *Cell* 1992, **68**:533–544.
20. Simons K, Ikonen E: **Functional rafts in cell membranes.** *Nature* 1997, **387**:569–572.
21. Brown DA, London E: **Functions of lipid rafts in biological membranes.** *Annu Rev Cell Dev Biol* 1998, **14**:111–136.
22. Smart EJ, Ying YS, Mineo C, Anderson RG: **A detergent-free method for purifying caveolae membrane from tissue culture cells.** *Proc Natl Acad Sci USA* 1995, **92**:10104–10108.
23. Schuck S, Honsho M, Ekroos K, Shevchenko A, Simons K: **Resistance of cell membranes to different detergents.** *Proc Natl Acad Sci USA* 2003, **100**:5795–5800.
24. Madore N, Smith KL, Graham CH, Jen A, Brady K, Hall S, Morris R: **Functionally different GPI proteins are organized in different domains on the neuronal surface.** *EMBO J* 1999, **18**:6917–6926.
25. Drevot P, Langlet C, Guo XJ, Bernard AM, Colard O, Chauvin JP, Lasserre R, He H-T: **TCR signal initiation machinery is pre-assembled and activated in a subset of membrane rafts.** *EMBO J* 2002, **21**:1899–1908.
26. Ilangumaran S, Arni S, van Echten-Deckert G, Borisch B, Hoessli DC: **Microdomain-dependent Regulation of Lck and Fyn Protein-Tyrosine Kinases in T Lymphocyte Plasma Membranes.** *Mol Biol Cell* 1999, **10**:891–905.
27. Röper K, Corbeil D, Huttner WB: **Retention of prominin in microvilli reveals distinct cholesterol-based lipid micro-domains in the apical plasma membrane.** *Nat Cell Biol* 2000, **2**:582–592.
28. Slimane TA, Trugnan G, van Ijzendoorn SC, Hoekstra D: **Raft-mediated Trafficking of Apical Resident Proteins Occurs in Both Direct and Transcytotic Pathways in Polarized Hepatic Cells: Role of Distinct Lipid Microdomains.** *Mol Biol Cell* 2002, **14**:611–624.
29. Song KS, Li Shengwen, Okamoto T, Quilliam LA, Sargiacomo M, Lisanti MP: **Copurification and direct interaction of Ras with caveolin, an integral membrane protein of caveolae microdomains. Detergent-free purification of caveolae microdomains.** *J Biol Chem* 1996, **271**:9690–9697.
30. Macdonald JL, Pike LJ: **A simplified method for the preparation of detergent-free lipid rafts.** *J Lipid Res* 2005, **46**:1061–1067.
31. Jacobson K, Mouritsen OG, Anderson RGW: **Lipid rafts: at a crossroad between cell biology and physics.** *Nat Cell Biol* 2007, **9**:7–14.
32. Pike LJ: **The challenge of lipid rafts.** *J Lipid Res* 2009, **50 Suppl**:S323–8.
33. Lebedzinska M, Szabadkai GR, Jones AWE, Duszynski J, Wieckowski MR: **Interactions between the endoplasmic reticulum, mitochondria, plasma membrane and other subcellular organelles.** *Int J Biochem Cell B* 2009, **41**:1805–1816.

34. Mayor S, Maxfield FR: **Insolubility and redistribution of GPI-anchored proteins at the cell surface after detergent treatment.** *Mol Biol Cell* 1995, **6**:929–944.
35. Minogue S, Waugh MG: **Lipid rafts, microdomain heterogeneity and inter-organelle contacts: impacts on membrane preparation for proteomic studies.** *Biol Cell* 2012, **104**:618–627.
36. Foster LJ, De Hoog CL, Mann M: **Unbiased quantitative proteomics of lipid rafts reveals high specificity for signaling factors.** *Proc Natl Acad Sci USA* 2003, **100**:5813–5818.
37. Owen DM, Magenau A, Williamson D, Gaus K: **The lipid raft hypothesis revisited--new insights on raft composition and function from super-resolution fluorescence microscopy.** *Bioessays* 2012, **34**:739–747.
38. Head BP, Patel HH, Insel PA: **Interaction of membrane/lipid rafts with the cytoskeleton: Impact on signaling and function Membrane/lipid rafts, mediators of cytoskeletal arrangement and cell signaling.** *Biochim Biophys Acta* 2014, **1838**:532–545.
39. Allen JA, Halverson-Tamboli RA, Rasenick MM: **Lipid raft microdomains and neurotransmitter signalling.** *Nat Rev Neurosci* 2007, **8**:128–140.
40. Cheng JPX, Nichols BJ: **Caveolae: One Function or Many?** *Trends Cell Biol* 2016, **26**:177–189.
41. Palade GE: **Fine Structure of Blood Capillaries.** *J Appl Phys* 1953, **24**:1424–1424.
42. Yamada E: **The fine structure of the gall bladder epithelium of the mouse.** *J Biophys Biochem Cytol* 1955, **1**:445–458.
43. Langhorst MF, Reuter A, Stuermer CAO: **Scaffolding microdomains and beyond: the function of reggie/flotillin proteins.** *Cell Mol Life Sci* 2005, **62**:2228–2240.
44. Staubach S, Hanisch F-G: **Lipid rafts: signaling and sorting platforms of cells and their roles in cancer.** *Expert Rev Proteomic* 2011, **8**:263–277.
45. Stuermer CAO: **The reggie/flotillin connection to growth.** *Trends Cell Biol* 2010, **20**:6–13.
46. Otto GP, Nichols BJ: **The roles of flotillin microdomains - endocytosis and beyond.** *J Cell Sci* 2011, **124**:3933–3940.
47. Simons K, Toomre D: **Lipid rafts and signal transduction.** *Nat Rev Mol Cell Biol* 2000, **1**:31–39.
48. Kurrle N, John B, Meister M, Tikkanen R: **Function of Flotillins in Receptor Tyrosine Kinase Signaling and Endocytosis: Role of Tyrosine Phosphorylation and Oligomerization.** In *Protein Phosphorylation in Human Health*. InTech; 2012.
49. Mukherjee S, Maxfield FR: **Role of membrane organization and membrane domains in endocytic lipid trafficking.** *Traffic* 2000, **1**:203–211.
50. Pike LJ: **Rafts defined: a report on the Keystone Symposium on Lipid Rafts and Cell Function.** 2006:1597–1598.

51. Skibbens JE, Roth MG, Matlin KS: **Differential Extractability of Influenza-Virus Hemagglutinin During Intracellular-Transport in Polarized Epithelial-Cells and Nonpolar Fibroblasts.** *J Cell Biol* 1989, **108**:821–832.
52. Sargiacomo M, Sudol M, Tang Z, Lisanti MP: **Signal transducing molecules and glycosyl-phosphatidylinositol-linked proteins form a caveolin-rich insoluble complex in MDCK cells.** *J Cell Biol* 1993, **122**:789–807.
53. Danielsen EM, van Deurs B: **A transferrin-like GPI-linked iron-binding protein in detergent- insoluble noncaveolar microdomains at the apical surface of fetal intestinal epithelial cells.** *J Cell Biol* 1995, **131**:939–950.
54. Hashimoto-Tane A, Saito T: **Dynamic Regulation of TCR-Microclusters and the Microsynapse for T Cell Activation.** *Front Immunol* 2016, **7**:255.
55. Xavier R, Brennan T, Li Q, McCormack C, Seed B: **Membrane compartmentation is required for efficient T cell activation.** *Immunity* 1998, **8**:723–732.
56. Zhang W, Tribble RP, Samelson LE: **LAT palmitoylation: its essential role in membrane microdomain targeting and tyrosine phosphorylation during T cell activation.** *Immunity* 1998, **9**:239–246.
57. Filipp D, Leung BL, Zhang J, Veillette A, Julius M: **Enrichment of lck in lipid rafts regulates colocalized fyn activation and the initiation of proximal signals through TCR alpha beta.** *J Immunol* 2004, **172**:4266–4274.
58. Fragoso R, Ren D, Zhang X, Su MW-C, Burakoff SJ, Jin Y-J: **Lipid raft distribution of CD4 depends on its palmitoylation and association with Lck, and evidence for CD4-induced lipid raft aggregation as an additional mechanism to enhance CD3 signaling.** *J Immunol* 2003, **170**:913–921.
59. Chichili GR, Westmuckett AD, Rodgers W: **T Cell Signal Regulation by the Actin Cytoskeleton.** *J Biol Chem* 2010, **285**:14737–14746.
60. Langhorst MF, Reuter A, Luxenhofer G, Boneberg E-M, Legler DF, Plattner H, Stuermer CAO: **Preformed reggie/flotillin caps: stable priming platforms for macrodomain assembly in T cells.** *FASEB J* 2006, **20**:711–713.
61. Cheng PC, Dykstra ML, Mitchell RN, Pierce SK: **A role for lipid rafts in B cell antigen receptor signaling and antigen targeting.** *J Exp Med* 1999, **190**:1549–1560.
62. Sheets ED, Holowka D, Baird B: **Membrane organization in immunoglobulin E receptor signaling.** *Curr Opin Chem Biol* 1999, **3**:95–99.
63. Simons K, Ehehalt R: **Cholesterol, lipid rafts, and disease.** *J Clin Invest* 2002, **110**:597–603.
64. Del Real G, Jiménez-Baranda S, Lacalle RA, Mira E, Lucas P, Gómez-Moutón C, Carrera AC, Martínez-A C, Mañes S: **Blocking of HIV-1 infection by targeting CD4 to nonraft membrane domains.** *J Exp Med* 2002, **196**:293–301.
65. Samuel BU, Mohandas N, Harrison T, McManus H, Rosse W, Reid M, Haldar K: **The role of cholesterol and glycosylphosphatidylinositol-anchored proteins of erythrocyte rafts in regulating raft protein content and malarial infection.** *J Biol Chem* 2001, **276**:29319–29329.
66. Munro S: **Lipid rafts: Elusive or illusive?** *Cell* 2003, **115**:377–388.



67. Kusumi A, Koyama-Honda I, Suzuki K: **Molecular dynamics and interactions for creation of stimulation-induced stabilized rafts from small unstable steady-state rafts.** *Traffic* 2004, **5**:213–230.
68. Sharma P, Varma R, Sarasij RC, Ira, Gousset K, Krishnamoorthy G, Rao M, Mayor S: **Nanoscale organization of multiple GPI-anchored proteins in living cell membranes.** *Cell* 2004, **116**:577–589.
69. Shaw AS: **Lipid rafts: now you see them, now you don't.** *Nat Immunol* 2006, **7**:1139–1142.
70. Simons K, Gerl MJ: **Revitalizing membrane rafts: new tools and insights.** *Nat Rev Mol Cell Biol* 2010, **11**:688–699.
71. Bauer M, Pelkmans L: **A new paradigm for membrane-organizing and -shaping scaffolds.** *FEBS Lett* 2006, **580**:5559–5564.
72. Chapman SA, Asthagiri AR: **Quantitative effect of scaffold abundance on signal propagation.** *Mol Syst Biol* 2009, **5**:313.
73. Good MC, Zalatan JG, Lim WA: **Scaffold proteins: hubs for controlling the flow of cellular information.** *Science* 2011, **332**:680–686.
74. Bickel PE, Scherer PE, Schnitzer JE, Oh P, Lisanti MP, Lodish HF: **Flotillin and epidermal surface antigen define a new family of caveolae-associated integral membrane proteins.** *J Biol Chem* 1997, **272**:13793–13802.
75. Schulte T, Paschke KA, Laessing U, Lottspeich F, Stuermer CA: **Reggie-1 and reggie-2, two cell surface proteins expressed by retinal ganglion cells during axon regeneration.** *Development* 1997, **124**:577–587.
76. Lang DM, Lommel S, Jung M, Ankerhold R, Petrusch B, Laessing U, Wiechers MF, Plattner H, Stuermer CA: **Identification of reggie-1 and reggie-2 as plasmamembrane-associated proteins which cocluster with activated GPI-anchored cell adhesion molecules in non-caveolar micropatches in neurons.** *J Neurobiol* 1998, **37**:502–523.
77. Galbiati F, Volonte D, Goltz JS, Steele Z, Sen J, Jurcsak J, Stein D, Stevens L, Lisanti MP: **Identification, sequence and developmental expression of invertebrate flotillins from *Drosophila melanogaster*.** *Gene* 1998, **210**:229–237.
78. Málaga-Trillo E, Laessing U, Lang DM, Meyer A, Stuermer CAO: **Evolution of duplicated reggie genes in zebrafish and goldfish.** *J Mol Evol* 2002, **54**:235–245.
79. Morrow IC, Rea S, Martin S, Prior IA, Prohaska R, Hancock JF, James DE, Parton RG: **Flotillin-1/reggie-2 traffics to surface raft domains via a novel golgi-independent pathway. Identification of a novel membrane targeting domain and a role for palmitoylation.** *J Biol Chem* 2002, **277**:48834–48841.
80. Neumann-Giesen C, Falkenbach B, Beicht P, Claasen S, Lüers G, Stuermer CAO, Herzog V, Tikkanen R: **Membrane and raft association of reggie-1/flotillin-2: role of myristoylation, palmitoylation and oligomerization and induction of filopodia by overexpression.** *Biochem J* 2004, **378**:509–518.
81. Tavernarakis N, Driscoll M, Kyrpidis NC: **The SPFH domain: implicated in regulating targeted protein turnover in stomatins and other membrane-associated proteins.** *Trends Biochem Sci* 1999, **24**:425–427.

82. Browman DT, Hoegg MB, Robbins SM: **The SPFH domain-containing proteins: more than lipid raft markers.** *Trends Cell Biol* 2007, **17**:394–402.
83. Morrow IC, Parton RG: **Flotillins and the PHB domain protein family: rafts, worms and anaesthetics.** *Traffic* 2005, **6**:725–740.
84. Rivera-Milla E, Stuermer C, Malaga-Trillo E: **Ancient origin of reggie (flotillin), reggie-like, and other lipid-raft proteins: convergent evolution of the SPFH domain.** *Cell Mol Life Sci* 2006, **63**:343–357.
85. Zhao F, Zhang J, Liu Y-S, Li L, He Y-L: **Research advances on flotillins.** *Virology* 2011, **8**:479.
86. Kalka D, Reitzenstein von C, Kopitz J, Cantz M: **The plasma membrane ganglioside sialidase cofractionates with markers of lipid rafts.** *Biochem Biophys Res Commun* 2001, **283**:989–993.
87. Stuermer CA, Lang DM, Kirsch F, Wiechers M, Deininger SO, Plattner H: **Glycosylphosphatidyl inositol-anchored proteins and fyn kinase assemble in noncaveolar plasma membrane microdomains defined by reggie-1 and -2.** *Mol Biol Cell* 2001, **12**:3031–3045.
88. Stuermer CAO, Langhorst MF, Wiechers MF, Legler DF, Hanwehr Von SH, Guse AH, Plattner H: **PrPc capping in T cells promotes its association with the lipid raft proteins reggie-1 and reggie-2 and leads to signal transduction.** *FASEB J* 2004, **18**:1731–1733.
89. Liu J, Deyoung SM, Zhang M, Dold LH, Saltiel AR: **The stomatin/prohibitin/flotillin/HflK/C domain of flotillin-1 contains distinct sequences that direct plasma membrane localization and protein interactions in 3T3-L1 adipocytes.** *J Biol Chem* 2005, **280**:16125–16134.
90. Slaughter N, Laux I, Tu X, Whitelegge J, Zhu X, Effros R, Bickel P, Nel A: **The flotillins are integral membrane proteins in lipid rafts that contain TCR-associated signaling components: implications for T-cell activation.** *Clin Immunol* 2003, **108**:138–151.
91. Brawek B, Schwendele B, Riestler K, Kohsaka S, Lerdkrai C, Liang Y, Garaschuk O: **Impairment of in vivo calcium signaling in amyloid plaque-associated microglia.** *Acta Neuropathol.* 2014, **127**:495–505.
92. Vetrivel KS, Meckler X, Chen Y, Nguyen PD, Seidah NG, Vassar R, Wong PC, Fukata M, Kounnas MZ, Thinakaran G: **Alzheimer disease A $\beta$  production in the absence of S-palmitoylation-dependent targeting of BACE1 to lipid rafts.** *J Biol Chem* 2009, **284**:3793–3803.
93. Kokubo H, Lemere CA, Yamaguchi H: **Localization of flotillins in human brain and their accumulation with the progression of Alzheimer's disease pathology.** *Neurosci Lett* 2000, **290**:93–96.
94. Jacobowitz DM, Kallarakal AT: **Flotillin-1 in the substantia nigra of the Parkinson brain and a predominant localization in catecholaminergic nerves in the rat brain.** *Neurotox Res* 2004, **6**:245–257.
95. Hazarika P, McCarty MF, Prieto VG, George S, Babu D, Koul D, Bar-Eli M, Duvic M: **Up-regulation of Flotillin-2 is associated with melanoma progression and modulates expression of the thrombin receptor protease activated receptor 1.** *Cancer Res* 2004, **64**:7361–7369.

96. Rudner DZ, Losick R: **Protein subcellular localization in bacteria.** *CSH Perspect Biol* 2010, **2**:a000307–a000307.
97. Mitra SD, Afonina I, Kline KA: **Right Place, Right Time: Focalization of Membrane Proteins in Gram-Positive Bacteria.** *Trends Microbiol* 2016, **24**:611–621.
98. Mileykovskaya E, Dowhan W: **Visualization of Phospholipid Domains in *Escherichia coli* by Using the Cardiolipin-Specific Fluorescent Dye 10-N-Nonyl Acridine Orange.** *J Bacteriol* 2000, **182**:1172–1175.
99. Mileykovskaya E, Dowhan W: **Cardiolipin membrane domains in prokaryotes and eukaryotes.** *Biochim Biophys Acta* 2009, **1788**:2084–2091.
100. Mileykovskaya E, Ryan AC, Mo X, Lin C-C, Khalaf KI, Dowhan W, Garrett TA: **Phosphatidic acid and N-acylphosphatidylethanolamine form membrane domains in *Escherichia coli* mutant lacking cardiolipin and phosphatidylglycerol.** *J Biol Chem* 2009, **284**:2990–3000.
101. Strahl H, Bürmann F, Hamoen LW: **The actin homologue MreB organizes the bacterial cell membrane.** *Nat Commun* 2014, **5**:3442.
102. Müller A, Wenzel M, Strahl H, Grein F, Saaki TNV, Kohl B, Siersma T, Bandow JE, Sahl H-G, Schneider T, et al.: **Daptomycin inhibits cell envelope synthesis by interfering with fluid membrane microdomains.** *Proc Natl Acad Sci USA* 2016, **113**:E7077–E7086.
103. Mileykovskaya E, Dowhan W: **Role of membrane lipids in bacterial division-site selection.** *Curr Opin Microbiol* 2005, **8**:135–142.
104. Barák I, Muchová K: **The role of lipid domains in bacterial cell processes.** *Int J Mol Sci* 2013, **14**:4050–4065.
105. Crowley JT, Toledo AM, LaRocca TJ, Coleman JL, London E, Benach JL: **Lipid exchange between *Borrelia burgdorferi* and host cells.** *PLOS Pathog* 2013, **9**:e1003109.
106. Lin M, Rikihisa Y: ***Ehrlichia chaffeensis* and *Anaplasma phagocytophilum* lack genes for lipid A biosynthesis and incorporate cholesterol for their survival.** *Infect Immun* 2003, **71**:5324–5331.
107. Dahl J: **The role of cholesterol in mycoplasma membranes.** *Subcell Biochem* 1993, **20**:167–188.
108. López D: **Molecular composition of functional microdomains in bacterial membranes.** *Chem Phys Lipids* 2015, **192**:3–11.
109. Kannenberg E, Poralla K: **The influence of hopanoids on growth of *Mycoplasma mycoides*.** *Arch Microbiol* 1982, **133**:100–102.
110. Sáenz JP, Sezgin E, Schwille P, Simons K: **Functional convergence of hopanoids and sterols in membrane ordering.** *Proc Natl Acad Sci USA* 2012, **109**:14236–14240.
111. Sáenz JP, Grosser D, Bradley AS, Lagny TJ, Lavrynenko O, Broda M, Simons K: **Hopanoids as functional analogues of cholesterol in bacterial membranes.** *Proc Natl Acad Sci USA* 2015, **112**:11971–11976.
112. Kontnik R, Bosak T, Butcher RA, Brocks JJ, Losick R, Clardy J, Pearson A: **Sporulenes, heptaprenyl metabolites from *Bacillus subtilis* spores.** *Org. Lett.* 2008, **10**:3551–3554.

113. Bosak T, Losick RM, Pearson A: **A polycyclic terpenoid that alleviates oxidative stress.** *Proc Natl Acad Sci USA* 2008, **105**:6725–6729.
114. Liu GY, Nizet V: **Color me bad: microbial pigments as virulence factors.** *Trends Microbiol* 2009, **17**:406–413.
115. Vershinin A: **Biological functions of carotenoids - diversity and evolution.** *Biofactors* 1999, **10**:99–104.
116. Taylor RF: **Bacterial triterpenoids.** *Microbiol Rev* 1984, **48**:181–198.
117. López D, Kolter R: **Functional microdomains in bacterial membranes.** *Gene Dev* 2010, **24**:1893–1902.
118. Feng X, Hu Y, Zheng Y, Zhu W, Li K, Huang C-H, Ko T-P, Ren F, Chan H-C, Nega M, et al.: **Structural and functional analysis of *Bacillus subtilis* YisP reveals a role of its product in biofilm production.** *Chem Biol* 2014, **21**:1557–1563.
119. Hinderhofer M, Walker CA, Friemel A, Sturmer CA, Möller HM, Reuter A: **Evolution of prokaryotic SPFH proteins.** *BMC Evol Biol* 2009, **9**:10.
120. Bramkamp M, López D: **Exploring the Existence of Lipid Rafts in Bacteria.** *Microbiol Mol Biol Rev* 2015, **79**:81–100.
121. Zhang H-M, Li Z, Tsudome M, Ito S, Takami H, Horikoshi K: **An alkali-inducible flotillin-like protein from *Bacillus halodurans* C-125.** *Protein J* 2005, **24**:125–131.
122. Donovan C, Bramkamp M: **Characterization and subcellular localization of a bacterial flotillin homologue.** *Microbiology* 2009, **155**:1786–1799.
123. Lysenko E, Ogura T, Cutting SM: **Characterization of the *ftsH* gene of *Bacillus subtilis*.** *Microbiology* 1997, **143** :971–978.
124. Zellmeier S, Zuber U, Schumann W, Wiegert T: **The Absence of FtsH Metalloprotease Activity Causes Overexpression of the W-Controlled *pbpE* Gene, Resulting in Filamentous Growth of *Bacillus subtilis*.** *J Bacteriol* 2003, **185**:973–982.
125. Le ATT, Schumann W: **The Spo0E phosphatase of *Bacillus subtilis* is a substrate of the FtsH metalloprotease.** *Microbiology* 2009, **155**:1122–1132.
126. Yepes A, Schneider J, Mielich-Süss B, Koch G, García-Betancur J-C, Ramamurthi KS, Vlamakis H, López D: **The biofilm formation defect of a *Bacillus subtilis* flotillin-defective mutant involves the protease FtsH.** *Mol Microbiol* 2012, **86**:457–471.
127. Kihara A, Akiyama Y, Ito K: **A protease complex in the Escherichia coli plasma membrane: HflKC (HflA) forms a complex with FtsH (HflB), regulating its proteolytic activity against SecY.** *EMBO J* 1996, **15**:6122–6131.
128. Kihara A, Akiyama Y, Ito K: **Different pathways for protein degradation by the FtsH/HflKC membrane-embedded protease complex: an implication from the interference by a mutant form of a new substrate protein, YccA.** *J Mol Biol* 1998, **279**:175–188.
129. Kihara A, Akiyama Y, Ito K: **Host regulation of lysogenic decision in bacteriophage lambda: transmembrane modulation of FtsH (HflB), the cII degrading protease, by HflKC (HflA).** *Proc Natl Acad Sci USA* 1997, **94**:5544–5549.

130. Kihara A, Ito K: **Translocation, Folding, and Stability of the HflKC Complex with Signal Anchor Topogenic Sequences.** *J Biol Chem* 1998, **273**:29770–29775.
131. Bach JN, Bramkamp M: **Dissecting the molecular properties of prokaryotic flotillins.** *PLOS One* 2015, **10**:e0116750.
132. Schneider J, Klein T, Mielich-Süss B, Koch G, Franke C, Kuipers OP, Kovács ÁT, Sauer M, López D: **Spatio-temporal remodeling of functional membrane microdomains organizes the signaling networks of a bacterium.** *PLOS Genet* 2015, **11**:e1005140.
133. Dempwolff F, Schmidt FK, Hervás AB, Stroh A, Rösch TC, Riese CN, Dersch S, Heimerl T, Lucena D, Hülsbusch N, et al.: **Super Resolution Fluorescence Microscopy and Tracking of Bacterial Flotillin (Reggie) Paralogs Provide Evidence for Defined-Sized Protein Microdomains within the Bacterial Membrane but Absence of Clusters Containing Detergent-Resistant Proteins.** *PLOS Genet* 2016, **12**:e1006116.
134. Solis GP, Hoegg M, Munderloh C, Schrock Y, Málaga-Trillo E, Rivera-Milla E, Stuermer CAO: **Reggie/flotillin proteins are organized into stable tetramers in membrane microdomains.** *Biochem J* 2007, **403**:313–322.
135. Green JB, Lower RPJ, Young JPW: **The NfeD protein family and its conserved gene neighbours throughout prokaryotes: functional implications for stomatin-like proteins.** *J Mol Evol* 2009, **69**:657–667.
136. Dempwolff F, Möller HM, Graumann PL: **Synthetic motility and cell shape defects associated with deletions of flotillin/reggie paralogs in *Bacillus subtilis* and interplay of these proteins with NfeD proteins.** *J Bacteriol* 2012, **194**:4652–4661.
137. Bach JN, Bramkamp M: **Flotillins functionally organize the bacterial membrane.** *Mol Microbiol* 2013, **88**:1205–1217.
138. Toledo A, Pérez A, Coleman JL, Benach JL: **The lipid raft proteome of *Borrelia burgdorferi*.** *Proteomics* 2015, **15**:3662–3675.
139. Vlamakis H, Chai Y, Beaugerard P, Losick R, Kolter R: **Sticking together: building a biofilm the *Bacillus subtilis* way.** *Nat Rev Microbiol* 2013, **11**:157–168.
140. Hobley L, Harkins C, MacPhee CE, Stanley-Wall NR: **Giving structure to the biofilm matrix: an overview of individual strategies and emerging common themes.** *FEMS Microbiol Rev* 2015, **39**:649–669.
141. Mielich-Süss B, López D: **Molecular mechanisms involved in *Bacillus subtilis* biofilm formation.** *Environ Microbiol* 2014, **17**:555–565.
142. Branda SS, González-Pastor JE, Ben-Yehuda S, Losick R, Kolter R: **Fruiting body formation by *Bacillus subtilis*.** *Proc Natl Acad Sci USA* 2001, **98**:11621–11626.
143. Romero D, Aguilar C, Losick R, Kolter R: **Amyloid fibers provide structural integrity to *Bacillus subtilis* biofilms.** *Proc Natl Acad Sci USA* 2010, **107**:2230–2234.

144. Hogley L, Ostrowski A, Rao FV, Bromley KM, Porter M, Prescott AR, MacPhee CE, van Aalten DMF, Stanley-Wall NR: **BslA is a self-assembling bacterial hydrophobin that coats the *Bacillus subtilis* biofilm.** *Proc Natl Acad Sci USA* 2013, **110**:13600–13605.
145. Kobayashi K, Iwano M: **BslA(YuaB) forms a hydrophobic layer on the surface of *Bacillus subtilis* biofilms.** *Mol Microbiol* 2012, **85**:51–66.
146. Branda SS, Chu F, Kearns DB, Losick R, Kolter R: **A major protein component of the *Bacillus subtilis* biofilm matrix.** *Mol Microbiol* 2006, **59**:1229–1238.
147. Kearns DB, Chu F, Branda SS, Kolter R, Losick R: **A master regulator for biofilm formation by *Bacillus subtilis*.** *Mol Microbiol* 2005, **55**:739–749.
148. Errington J: **Regulation of endospore formation in *Bacillus subtilis*.** *Nat Rev Microbiol* 2003, **1**:117–126.
149. Fujita M, González-Pastor JE, Losick R: **High- and Low-Threshold Genes in the Spo0A Regulon of *Bacillus subtilis*.** *J Bacteriol* 2005, **187**:1357–1368.
150. López D, Kolter R: **Extracellular signals that define distinct and coexisting cell fates in *Bacillus subtilis*.** *FEMS Microbiol Rev* 2010, **34**:134–149.
151. Shemesh M, Chai Y: **A combination of glycerol and manganese promotes biofilm formation in *Bacillus subtilis* via histidine kinase KinD signaling.** *J Bacteriol* 2013, **195**:2747–2754.
152. Kolodkin-Gal I, Elsholz AKW, Muth C, Girguis PR, Kolter R, Losick R: **Respiration control of multicellularity in *Bacillus subtilis* by a complex of the cytochrome chain with a membrane-embedded histidine kinase.** *Gene Dev* 2013, **27**:887–899.
153. López D, Fischbach MA, Chu F, Losick R, Kolter R: **Structurally diverse natural products that cause potassium leakage trigger multicellularity in *Bacillus subtilis*.** *Proc Natl Acad Sci USA* 2009, **106**:280–285.
154. Burbulys D, Trach KA, Hoch JA: **Initiation of sporulation in *B. subtilis* is controlled by a multicomponent phosphorelay.** *Cell* 1991, **64**:545–552.
155. Perego M, Hoch JA: **Protein aspartate phosphatases control the output of two-component signal transduction systems.** *Trends Genet* 1996, **12**:97–101.
156. Perego M: **A new family of aspartyl phosphate phosphatases targeting the sporulation transcription factor Spo0A of *Bacillus subtilis*.** *Mol Microbiol* 2001, **42**:133–143.
157. Deuerling E, Mogk A, Richter C, Purucker M, Schumann W: **The *ftsH* gene of *Bacillus subtilis* is involved in major cellular processes such as sporulation, stress adaptation and secretion.** *Mol Microbiol* 1997, **23**:921–933.
158. Albright LM, Huala E, Ausubel FM: **Prokaryotic signal transduction mediated by sensor and regulator protein pairs.** *Annu Rev Genet* 1989, **23**:311–336.
159. Wagner RM, Kricks L, López D: **Functional Membrane Microdomains Organize Signaling Networks in Bacteria.** *J Membr Biol* 2016, doi:10.1007/s00232-016-9923-0.
160. Schneider J, Mielich-Süss B, Böhme R, López D: ***In vivo* characterization of the scaffold activity of flotillin on the membrane kinase KinC of *Bacillus subtilis*.** *Microbiology* 2015, **161**:1871–1887.

161. López D: **Connection of KinC to flotillins and potassium leakage in *Bacillus subtilis*.** *Microbiology* 2015, **161**:1180–1181.
162. Devi SN, Vishnoi M, Kiehler B, Haggett L, Fujita M: ***In vivo* functional characterization of the transmembrane histidine kinase KinC in *Bacillus subtilis*.** *Microbiology* 2015, doi:10.1099/mic.0.000054.
163. López D, Koch G: **Exploring functional membrane microdomains in bacteria: an overview.** *Curr Opin Microbiol* 2017, **36**:76–84.
164. Nakano MM, Zuber P, Glaser P, Danchin A, Hulett FM: **Two-component regulatory proteins ResD-ResE are required for transcriptional activation of *fnr* upon oxygen limitation in *Bacillus subtilis*.** *J Bacteriol* 1996, **178**:3796–3802.
165. Young KD: **Bacterial Shape: Two-Dimensional Questions and Possibilities.** *Annu Rev Microbiol* 2010, **64**:223–240.
166. Margolin W: **FtsZ and the division of prokaryotic cells and organelles.** *Nat Rev Mol Cell Biol* 2005, **6**:862–871.
167. Carballido-López R, Formstone A: **Shape determination in *Bacillus subtilis*.** *Curr Opin Microbiol* 2007, **10**:611–616.
168. Dempwolff F, Wischhusen HM, Specht M, Graumann PL: **The deletion of bacterial dynamin and flotillin genes results in pleiotrophic effects on cell division, cell growth and in cell shape maintenance.** *BMC Microbiol* 2012, **12**:298.
169. Bi EF, Lutkenhaus J: **FtsZ ring structure associated with division in *Escherichia coli*.** *Nature* 1991, **354**:161–164.
170. Löwe J, Amos LA: **Crystal structure of the bacterial cell-division protein FtsZ.** *Nature* 1998, **391**:203–206.
171. Peters PC, Migocki MD, Thoni C, Harry EJ: **A new assembly pathway for the cytokinetic Z ring from a dynamic helical structure in vegetatively growing cells of *Bacillus subtilis*.** *Mol Microbiol* 2007, **64**:487–499.
172. Nanninga N: **Cell division and peptidoglycan assembly in *Escherichia coli*.** *Mol Microbiol* 1991, **5**:791–795.
173. Gamba P, Veening JW, Saunders NJ, Hamoen LW, Daniel RA: **Two-Step Assembly Dynamics of the *Bacillus subtilis* Divisome.** *J Bacteriol* 2009, **191**:4186–4194.
174. Yang X, Lyu Z, Miguel A, McQuillen R, Huang KC, Xiao J: **GTPase activity-coupled treadmilling of the bacterial tubulin FtsZ organizes septal cell wall synthesis.** *Science* 2017, **355**:744–747.
175. Bisson-Filho AW, Hsu Y-P, Squyres GR, Kuru E, Wu F, Jukes C, Sun Y, Dekker C, Holden S, VanNieuwenhze MS, et al.: **Treadmilling by FtsZ filaments drives peptidoglycan synthesis and bacterial cell division.** *Science* 2017, **355**:739–743.
176. Wagstaff JM, Tsim M, Oliva MA, García-Sánchez A, Kureisaite-Ciziene D, Andreu JM, Löwe J: **A Polymerization-Associated Structural Switch in FtsZ That Enables Treadmilling of Model Filaments.** *mBio* 2017, **8**:e00254–17.

177. Wu LJ, Errington J: **Coordination of cell division and chromosome segregation by a nucleoid occlusion protein in *Bacillus subtilis*.** *Cell* 2004, **117**:915–925.
178. Bernhardt TG, de Boer PAJ: **SlmA, a nucleoid-associated, FtsZ binding protein required for blocking septal ring assembly over Chromosomes in *E. coli*.** *Mol. Cell* 2005, **18**:555–564.
179. Rothfield L, Taghbalout A, Shih Y-L: **Spatial control of bacterial division-site placement.** *Nat Rev Microbiol* 2005, **3**:959–968.
180. Bramkamp M, van Baarle S: **Division site selection in rod-shaped bacteria.** *Curr Opin Microbiol* 2009, **12**:683–688.
181. Errington J, Daniel RA, Scheffers D-J: **Cytokinesis in bacteria.** *Microbiol Mol Biol Rev* 2003, **67**:52–65– table of contents.
182. Levin P, Kurtser I, Grossman A: **Identification and characterization of a negative regulator of FtsZ ring formation in *Bacillus subtilis*.** *Proc Natl Acad Sci USA* 1999, **96**:9642–9647.
183. Chung K-M, Hsu H-H, Yeh H-Y, Chang B-Y: **Mechanism of regulation of prokaryotic tubulin-like GTPase FtsZ by membrane protein EzrA.** *J Biol Chem* 2007, **282**:14891–14897.
184. Chung KM, Hsu HH, Govindan S, Chang BY: **Transcription Regulation of *ezrA* and Its Effect on Cell Division of *Bacillus subtilis*.** *J Bacteriol* 2004, **186**:5926–5932.
185. Costa TRD, Felisberto-Rodrigues C, Meir A, Prevost MS, Redzej A, Trokter M, Waksman G: **Secretion systems in Gram-negative bacteria: structural and mechanistic insights.** *Nat Rev Microbiol* 2015, **13**:343–359.
186. Veenendaal AKJ, van der Does C, Driessen AJM: **The protein-conducting channel SecYEG.** *Biochim Biophys Acta* 2004, **1694**:81–95.
187. Rapoport TA: **Protein translocation across the eukaryotic endoplasmic reticulum and bacterial plasma membranes.** *Nature* 2007, **450**:663–669.
188. Driessen AJM, Nouwen N: **Protein translocation across the bacterial cytoplasmic membrane.** *Annu Rev Biochem* 2008, **77**:643–667.
189. Tsirigotaki A, De Geyter J, Sostaric N, Economou A, Karamanou S: **Protein export through the bacterial Sec pathway.** *Nat Rev Microbiol* 2017, **15**:21–36.
190. Hendrick JP, Wickner W: **SecA protein needs both acidic phospholipids and SecY/E protein for functional high-affinity binding to the *Escherichia coli* plasma membrane.** *J Biol Chem* 1991, **266**:24596–24600.
191. Abdallah AM, Gey van Pittius NC, Champion PAD, Cox J, Luirink J, Vandenbroucke-Grauls CMJE, Appelmelk BJ, Bitter W: **Type VII secretion - mycobacteria show the way.** *Nat Rev Microbiol* 2007, **5**:883–891.
192. Gerlach RG, Hensel M: **Protein secretion systems and adhesins: the molecular armory of Gram-negative pathogens.** *Int J Med Microbiol* 2007, **297**:401–415.
193. Desvaux M, Hébraud M, Talon R, Henderson IR: **Secretion and subcellular localizations of bacterial proteins: a semantic awareness issue.** *Trends Microbiol* 2009, **17**:139–145.



194. Goyal P, Krasteva PV, Van Genven N, Gubellini F, Van den Broeck I, Troupiotis-Tsailaki A, Jonckheere W, Péhau-Arnaudet G, Pinkner JS, Chapman MR, et al.: **Structural and mechanistic insights into the bacterial amyloid secretion channel CsgG.** *Nature* 2014, **516**:250–.
195. Abby SS, Cury J, Guglielmini J, Néron B, Touchon M, Rocha EPC: **Identification of protein secretion systems in bacterial genomes.** *Sci Rep* 2016, **6**:23080.
196. Green ER, Meccas J: **Bacterial Secretion Systems: An Overview.** *Microbiol Spectr* 2016, **4**.
197. Lasica AM, Ksiazek M, Madej M, Potempa J: **The Type IX Secretion System (T9SS): Highlights and Recent Insights into Its Structure and Function.** *Front Cell Infect Mi* 2017, **7**.
198. Tareen AM, Lüder CGK, Zautner AE, Groß U, Heimesaat MM, Bereswill S, Lugert R: **The *Campylobacter jejuni* Cj0268c Protein Is Required for Adhesion and Invasion In Vitro.** *PLOS One* 2013, **8**:e81069.
199. Heimesaat MM, Lugert R, Fischer A, Alutis M, Kühl AA, Zautner AE, Tareen AM, Göbel UB, Bereswill S: **Impact of *Campylobacter jejuni* cj0268c Knockout Mutation on Intestinal Colonization, Translocation, and Induction of Immunopathology in Gnotobiotic IL-10 Deficient Mice.** *PLOS One* 2014, **9**:e90148.
200. Hutton ML, D'Costa K, Rossiter AE, Wang L, Turner L, Steer DL, Masters SL, Croker BA, Kaparakis-Liaskos M, Ferrero RL: **A *Helicobacter pylori* Homolog of Eukaryotic Flotillin Is Involved in Cholesterol Accumulation, Epithelial Cell Responses and Host Colonization.** *Front Cell Infect Mi* 2017, **7**:323.
201. Ates LS, Houben ENG, Bitter W: **Type VII Secretion: A Highly Versatile Secretion System.** *Microbiol Spectr* 2016, **4**.
202. Sorensen AL, Nagai S, Houen G, Andersen P, Andersen AB: **Purification and characterization of a low-molecular-mass T-cell antigen secreted by *Mycobacterium tuberculosis*.** *Infect Immun* 1995, **63**:1710–1717.
203. Stanley SA, Cox JS: **Host-pathogen interactions during *Mycobacterium tuberculosis* infections.** *Curr Top Microbiol Immunol* 2013, **374**:211–241.
204. Pym AS, Brodin P, Brosch R, Huerre M, Cole ST: **Loss of RD1 contributed to the attenuation of the live tuberculosis vaccines *Mycobacterium bovis* BCG and *Mycobacterium microti*.** *Mol Microbiol* 2002, **46**:709–717.
205. Siegrist MS, Unnikrishnan M, McConnell MJ, Borowsky M, Cheng T-Y, Siddiqi N, Fortune SM, Moody DB, Rubin EJ: **Mycobacterial Esx-3 is required for mycobactin-mediated iron acquisition.** *Proc Natl Acad Sci USA* 2009, **106**:18792–18797.
206. Siegrist MS, Steigedal M, Ahmad R, Mehra A, Dragset MS, Schuster BM, Philips JA, Carr SA, Rubin EJ: **Mycobacterial Esx-3 Requires Multiple Components for Iron Acquisition.** *mBio* 2014, **5**:–14.
207. Tufariello JM, Chapman JR, Kerantzas CA, Wong K-W, Vilchèze C, Jones CM, Cole LE, Tinaztepe E, Thompson V, Fenyö D, et al.: **Separable roles for *Mycobacterium tuberculosis* ESX-3 effectors in iron acquisition and virulence.** *Proc Natl Acad Sci USA* 2016, doi:10.1073/pnas.1523321113.

208. Flint JL, Kowalski JC, Karnati PK, Derbyshire KM: **The RD1 virulence locus of *Mycobacterium tuberculosis* regulates DNA transfer in *Mycobacterium smegmatis*.** *Proc Natl Acad Sci USA* 2004, **101**:12598–12603.
209. Coros A, Callahan B, Battaglioli E, Derbyshire KM: **The specialized secretory apparatus ESX-1 is essential for DNA transfer in *Mycobacterium smegmatis*.** *Mol Microbiol* 2008, **69**:794–808.
210. Rosenberg OS, Dovala D, Li X, Connolly L, Bendebury A, Finer-Moore J, Holton J, Cheng Y, Stroud RM, Cox JS: **Substrates Control Multimerization and Activation of the Multi-Domain ATPase Motor of Type VII Secretion.** *Cell* 2015, **161**:501–512.
211. Warne B, Harkins CP, Harris SR, Vatsiou A, Stanley-Wall N, Parkhill J, Peacock SJ, Palmer T, Holden MTG: **The Ess/Type VII secretion system of *Staphylococcus aureus* shows unexpected genetic diversity.** *BMC Genomics* 2016, **17**:222.
212. Zoltner M, Ng WMAV, Money JJ, Fyfe PK, Kneuper H, Palmer T, Hunter WN: **EssC: domain structures inform on the elusive translocation channel in the Type VII secretion system.** *Biochem J* 2016, **473**:1941–1952.
213. Baptista C, Barreto HC, São-José C: **High levels of DegU-P activate an Esat-6-like secretion system in *Bacillus subtilis*.** *PLoS One* 2013, **8**:e67840.
214. Huppert LA, Ramsdell TL, Chase MR, Sarracino DA, Fortune SM, Burton BM: **The ESX System in *Bacillus subtilis* Mediates Protein Secretion.** *PLoS One* 2014, **9**:e96267.
215. Fyans JK, Bignell D, Loria R, Toth I, Palmer T: **The ESX/type VII secretion system modulates development, but not virulence, of the plant pathogen *Streptomyces scabies*.** *Molecular Plant Pathology* 2012, **14**:119–130.
216. Garufi G, Butler E, Missiakas D: **ESAT-6-Like Protein Secretion in *Bacillus anthracis*.** *J Bacteriol* 2008, **190**:7004–7011.
217. Pinheiro J, Reis O, Vieira A, Moura IM, Zanolli Moreno L, Carvalho F, Pucciarelli MG, García-Del Portillo F, Sousa S, Cabanes D: ***Listeria monocytogenes* encodes a functional ESX-1 secretion system whose expression is detrimental to in vivo infection.** *Virulence* 2016, doi:10.1080/21505594.2016.1244589.
218. Burts ML, Williams WA, DeBord K, Missiakas DM: **EsxA and EsxB are secreted by an ESAT-6-like system that is required for the pathogenesis of *Staphylococcus aureus* infections.** *Proc Natl Acad Sci USA* 2005, **102**:1169–1174.
219. Kneuper H, Cao ZP, Twomey KB, Zoltner M, Jäger F, Cargill JS, Chalmers J, van der Kooi-Pol MM, van Dijl JM, Ryan RP, et al.: **Heterogeneity in ess transcriptional organization and variable contribution of the Ess/Type VII protein secretion system to virulence across closely related *Staphylococcus aureus* strains.** *Mol Microbiol* 2014, **93**:928–943.
220. Burts ML, DeDent AC, Missiakas DM: **EsaC substrate for the ESAT-6 secretion pathway and its role in persistent infections of *Staphylococcus aureus*.** *Mol Microbiol* 2008, **69**:736–746.
221. Wang Y, Hu M, Liu Q, Qin J, Dai Y, He L, Li T, Zheng B, Zhou F, Yu K, et al.: **Role of the ESAT-6 secretion system in virulence of the emerging community-associated *Staphylococcus aureus* lineage ST398.** *Sci Rep* 2016, **6**:25163.

222. Anderson M, Ohr RJ, Aly KA, Nocadello S, Kim HK, Schneewind CE, Schneewind O, Missiakas D: **EssE promotes *Staphylococcus aureus* ESS-dependent protein secretion to modify host immune responses during infection.** *J Bacteriol* 2016, **199**:e00527–16.
223. Korea CG, Balsamo G, Pezzicoli A, Merakou C, Tavarini S, Bagnoli F, Serruto D, Unnikrishnan M: **Staphylococcal Exs Proteins Modulate Apoptosis and Release of Intracellular *Staphylococcus aureus* during Infection in Epithelial Cells.** *Infect Immun* 2014, **82**:4144–4153.
224. Cao Z, Casabona MG, Kneuper H, Chalmers JD, Palmer T: **The type VII secretion system of *Staphylococcus aureus* secretes a nuclease toxin that targets competitor bacteria.** *Nat Microbiol* 2016, **2**:16183.
225. Tanaka Y, Kuroda M, Yasutake Y, Yao M, Tsumoto K, Watanabe N, Ohta T, Tanaka I: **Crystal structure analysis reveals a novel forkhead-associated domain of ESAT-6 secretion system C protein in *Staphylococcus aureus*.** *Proteins* 2007, **69**:659–664.
226. Zoltner M, Ng WMAV, Money JJ, Fyfe PK, Kneuper H, Palmer T, Hunter WN: **N-terminal FHA domain from EssC a component of the bacterial Type VII secretion apparatus.** 2016, doi:10.2210/pdb5fwh/pdb.
227. São-José C, Baptista C, Santos MA: ***Bacillus subtilis* operon encoding a membrane receptor for bacteriophage SPP1.** *J Bacteriol* 2004, **186**:8337–8346.
228. São-José C, Lhuillier S, Lurz R, Melki R, Lepault J, Santos MA, Tavares P: **The ectodomain of the viral receptor YueB forms a fiber that triggers ejection of bacteriophage SPP1 DNA.** *J Biol Chem* 2006, **281**:11464–11470.
229. Jakutyte L, Baptista C, São-José C, Daugelavičius R, Carballido-López R, Tavares P: **Bacteriophage infection in rod-shaped Gram-positive bacteria: evidence for a preferential polar route for phage SPP1 entry in *Bacillus subtilis*.** *J Bacteriol* 2011, **193**:4893–4903.
230. Zoltner M, Fyfe PK, Palmer T, Hunter WN: **Characterization of *Staphylococcus aureus* EssB, an integral membrane component of the Type VII secretion system: atomic resolution crystal structure of the cytoplasmic segment.** *Biochem J* 2013, **449**:469–477.
231. Zoltner M, Norman DG, Fyfe PK, Mkami El H, Palmer T, Hunter WN: **The architecture of EssB, an integral membrane component of the type VII secretion system.** *Structure* 2013, **21**:595–603.
232. Chen Y-H, Anderson M, Hendrickx AP, Missiakas D: **Characterization of EssB, a protein required for secretion of ESAT-6 like proteins in *Staphylococcus aureus*.** *BMC Microbiol* 2012, **12**:219.
233. Jäger F, Zoltner M, Kneuper H, Hunter WN, Palmer T: **Membrane interactions and self-association of components of the Ess/Type VII secretion system of *Staphylococcus aureus*.** *FEBS Lett* 2016, **590**:349–357.
234. Houben ENG, Bestebroer J, Ummels R, Wilson L, Piersma SR, Jiménez CR, Ottenhoff THM, Luirink J, Bitter W: **Composition of the type VII secretion system membrane complex.** *Mol Microbiol* 2012, **86**:472–484.

235. Beckham KSH, Ciccarelli L, Bunduc CM, Mertens HDT, Ummels R, Lugmayr W, Mayr J, Rettel M, Savitski MM, Svergun DI, et al.: **Structure of the mycobacterial ESX-5 type VII secretion system membrane complex by single-particle analysis.** *Nat Microbiol* 2017, **2**:17047.
236. Sundaramoorthy R, Fyfe PK, Hunter WN: **Structure of *Staphylococcus aureus* EsxA suggests a contribution to virulence by action as a transport chaperone and/or adaptor protein.** *J Mol Biol* 2008, **383**:603–614.
237. Champion PAD, Stanley SA, Champion MM, Brown EJ, Cox JS: **C-terminal signal sequence promotes virulence factor secretion in *Mycobacterium tuberculosis*.** *Science* 2006, **313**:1632–1636.
238. Fortune SM, Jaeger A, Sarracino DA, Chase MR, Sasseti CM, Sherman DR, Bloom BR, Rubin EJ: **Mutually dependent secretion of proteins required for mycobacterial virulence.** *Proc Natl Acad Sci USA* 2005, **102**:10676–10681.
239. Anderson M, Aly KA, Chen Y-H, Missiakas D: **Secretion of atypical protein substrates by the ESAT-6 secretion system of *Staphylococcus aureus*.** *Mol Microbiol* 2013, **90**:734–743.
240. Ohr RJ, Anderson M, Shi M, Schneewind O, Missiakas D: **EssD, a nuclease effector of the *Staphylococcus aureus* ESS pathway.** *J Bacteriol* 2016, **199**:e00528–16.
241. Anderson M, Chen Y-H, Butler EK, Missiakas DM: **EsaD, a secretion factor for the Ess pathway in *Staphylococcus aureus*.** *J Bacteriol* 2011, **193**:1583–1589.
242. LaRocca TJ, Crowley JT, Cusack BJ, Pathak P, Benach J, London E, Garcia-Monco JC, Benach JL: **Cholesterol lipids of *Borrelia burgdorferi* form lipid rafts and are required for the bactericidal activity of a complement-independent antibody.** *Cell Host Microbe* 2010, **8**:331–342.
243. LaRocca TJ, Pathak P, Chiantia S, Toledo A, Silviu JR, Benach JL, London E: **Proving lipid rafts exist: membrane domains in the prokaryote *Borrelia burgdorferi* have the same properties as eukaryotic lipid rafts.** *PLoS Pathog* 2013, **9**:e1003353.
244. Somani VK, Aggarwal S, Singh D, Prasad T, Bhatnagar R: **Identification of Novel Raft Marker Protein, FlotP in *Bacillus anthracis*.** *Front Microbiol* 2016, **7**:169.
245. Koch G, Wermser C, Acosta IC, Kricks L, Stengel ST, Yepes A, López D: **Attenuating *Staphylococcus aureus* Virulence by Targeting Flotillin Protein Scaffold Activity.** *Cell Chem Biol* 2017, doi:10.1016/j.chembiol.2017.05.027.
246. Kreiswirth B, Kornblum J, Arbeit RD, Eisner W, Maslow JN, McGeer A, Low DE, Novick RP: **Evidence for a clonal origin of methicillin resistance in *Staphylococcus aureus*.** *Science* 1993, **259**:227–230.
247. Klevens RM, Morrison MA, Nadle J, Petit S, Gershman K, Ray S, Harrison LH, Lynfield R, Dumyati G, Townes JM, et al.: **Invasive Methicillin-Resistant *Staphylococcus aureus* Infections in the United States.** *JAMA* 2007, **298**:1763–1771.
248. Clauditz A, Resch A, Wieland K-P, Peschel A, Götz F: **Staphyloxanthin plays a role in the fitness of *Staphylococcus aureus* and its ability to cope with oxidative stress.** *Infect Immun* 2006, **74**:4950–4953.

249. Liu C-I, Liu GY, Song Y, Yin F, Hensler ME, Jeng W-Y, Nizet V, Wang AH-J, Oldfield E: **A cholesterol biosynthesis inhibitor blocks *Staphylococcus aureus* virulence.** *Science* 2008, **319**:1391–1394.
250. Bondarenko PV, Chelius D, Shaler TA: **Identification and relative quantitation of protein mixtures by enzymatic digestion followed by capillary reversed-phase liquid chromatography-tandem mass spectrometry.** *Anal Chem* 2002, **74**:4741–4749.
251. Liu T, Qian W-J, Strittmatter EF, Camp DG, Anderson GA, Thrall BD, Smith RD: **High-throughput comparative proteome analysis using a quantitative cysteinyl-peptide enrichment technology.** *Anal Chem* 2004, **76**:5345–5353.
252. Ono M, Shitashige M, Honda K, Isobe T, Kuwabara H, Matsuzuki H, Hirohashi S, Yamada T: **Label-free quantitative proteomics using large peptide data sets generated by nanoflow liquid chromatography and mass spectrometry.** *Mol Cell Proteomics* 2006, **5**:1338–1347.
253. Ong S-E, Blagoev B, Kratchmarova I, Kristensen DB, Steen H, Pandey A, Mann M: **Stable isotope labeling by amino acids in cell culture, SILAC, as a simple and accurate approach to expression proteomics.** *Mol Cell Proteomics* 2002, **1**:376–386.
254. Gygi SP, Rist B, Gerber SA, Turecek F, Gelb MH, Aebersold R: **Quantitative analysis of complex protein mixtures using isotope-coded affinity tags.** *Nat Biotechnol* 1999, **17**:994–999.
255. Yao X, Freas A, Ramirez J, Demirev PA, Fenselau C: **Proteolytic 18O labeling for comparative proteomics: model studies with two serotypes of adenovirus.** *Anal Chem* 2001, **73**:2836–2842.
256. Thompson A, Schäfer J, Kuhn K, Kienle S, Schwarz J, Schmidt G, Neumann T, Johnstone R, Mohammed AKA, Hamon C: **Tandem mass tags: a novel quantification strategy for comparative analysis of complex protein mixtures by MS/MS.** *Anal Chem* 2003, **75**:1895–1904.
257. Liu NQ, Dekker LJM, Stingl C, Güzel C, De Marchi T, Martens JWM, Foekens JA, Luidert TM, Umar A: **Quantitative proteomic analysis of microdissected breast cancer tissues: comparison of label-free and SILAC-based quantification with shotgun, directed, and targeted MS approaches.** *J Proteome Res* 2013, **12**:4627–4641.
258. Koch G, Yepes A, Förstner KU, Wermser C, Stengel ST, Modamio J, Ohlsen K, Foster KR, López D: **Evolution of Resistance to a Last-Resort Antibiotic in *Staphylococcus aureus* via Bacterial Competition.** *Cell* 2014, **158**:1060–1071.
259. Cox J, Hein MY, Lubner CA, Paron I, Nagaraj N, Mann M: **Accurate proteome-wide label-free quantification by delayed normalization and maximal peptide ratio extraction, termed MaxLFQ.** *Mol Cell Proteomics* 2014, **13**:2513–2526.
260. Hammer ND, Skaar EP: **Molecular mechanisms of *Staphylococcus aureus* iron acquisition.** *Annu Rev Microbiol* 2011, **65**:129–147.
261. Jorge AM, Hoiczuk E, Gomes JP, Pinho MG: **EzrA Contributes to the Regulation of Cell Size in *Staphylococcus aureus*.** *PLOS One* 2011, **6**:e27542.
262. Blaauwen den T, Andreu JM, Monasterio O: **Bacterial cell division proteins as antibiotic targets.** *Bioorg Chem* 2014, **55**:27–38.

263. Kusaka J, Shuto S, Imai Y, Ishikawa K, Saito T, Natori K, Matsuoka S, Hara H, Matsumoto K: **Septal localization by membrane targeting sequences and a conserved sequence essential for activity at the COOH-terminus of *Bacillus subtilis* cardiolipin synthase.** *Res Microbiol* 2016, **167**:202–214.
264. Batte JL, Samanta D, Elasri MO: **MsaB activates capsule production at the transcription level in *Staphylococcus aureus*.** *Microbiology* 2016, **162**:575–589.
265. Paprotka K, Giese B, Fraunholz MJ: **Codon-improved fluorescent proteins in investigation of *Staphylococcus aureus* host pathogen interactions.** *J Microbiol Methods* 2010, **83**:82–86.
266. Arnaud M, Chastanet A, Débarbouillé M: **New vector for efficient allelic replacement in naturally nontransformable, low-GC-content, Gram-positive bacteria.** *Appl Environ Microbiol* 2004, **70**:6887–6891.
267. Yepes A, Koch G, Waldvogel A, García-Betancur J-C, López D: **Reconstruction of mreB expression in *Staphylococcus aureus* via a collection of new integrative plasmids.** *Appl Environ Microbiol* 2014, **80**:3868–3878.
268. Karimova G, Pidoux J, Ullmann A, Ladant D: **A bacterial two-hybrid system based on a reconstituted signal transduction pathway.** *Proc Natl Acad Sci USA* 1998, **95**:5752–5756.
269. Gustafsson MG: **Surpassing the lateral resolution limit by a factor of two using structured illumination microscopy.** *J Microsc* 2000, **198**:82–87.
270. Schneider J, Yepes A, Garcia-Betancur JC, Westedt I, Mielich B, López D: **Streptomycin-induced expression in *Bacillus subtilis* of YtnP, a lactonase-homologous protein that inhibits development and streptomycin production in *Streptomyces griseus*.** *Appl Environ Microbiol* 2012, **78**:599–603.
271. Reisinger V, Eichacker LA: **Analysis of membrane protein complexes by blue native PAGE.** *Proteomics* 2006, **6 Suppl 2**:6–15.
272. Wittig I, Braun H-P, Schägger H: **Blue native PAGE.** *Nat Protoc* 2006, **1**:418–428.
273. Eubel H, Braun H-P, Millar AH: **Blue-native PAGE in plants: a tool in analysis of protein-protein interactions.** *Plant Methods* 2005, **1**:11.
274. Silva-Rocha R, Martínez-García E, Calles B, Chavarría M, Arce-Rodríguez A, las Heras de A, Páez-Espino AD, Durante-Rodríguez G, Kim J, Nikel PI, et al.: **The Standard European Vector Architecture (SEVA): a coherent platform for the analysis and deployment of complex prokaryotic phenotypes.** *Nucleic Acids Res* 2013, **41**:D666–D675.
275. Unnikrishnan M, Constantinidou C, Palmer T, Pallen MJ: **The Enigmatic Esx Proteins: Looking Beyond Mycobacteria.** *Trends Microbiol* 2017, **25**:192–204.
276. Selle M, Hertlein T, Oesterreich B, Klemm T, Kloppot P, Müller E, Ehricht R, Stentzel S, Bröker BM, Engelmann S, et al.: **Global antibody response to *Staphylococcus aureus* live-cell vaccination.** *Sci Rep* 2016, **6**:24754.
277. Bergstrom JD, Kurtz MM, Rew DJ, Amend AM, Karkas JD, Bostedor RG, Bansal VS, Dufresne C, VanMiddlesworth FL, Hensens OD: **Zaragozic acids: a family of fungal metabolites that are picomolar competitive inhibitors of squalene synthase.** *Proc Natl Acad Sci USA* 1993, **90**:80–84.

278. Endo A, Kuroda M, Tanzawa K: **Competitive inhibition of 3-hydroxy-3-methylglutaryl coenzyme a reductase by ML-236A and ML-236B fungal metabolites, having hypocholesterolemic activity.** *FEBS Lett* 1976, **72**:323–326.
279. Grammenos A, Mouithys-Mickalad A, Guelluy PH, Lismont M, Piel G, Hoebeker M: **ESR technique for noninvasive way to quantify cyclodextrins effect on cell membranes.** *Biochem Biophys Res Commun* 2010, **398**:350–354.
280. Kardash ME, Dzuba SA: **Communication: Orientational self-ordering of spin-labeled cholesterol analogs in lipid bilayers in diluted conditions.** *J Chem Phys* 2014, **141**:211101.
281. Ježek P, Freisleben H-J: **Fatty acid binding site of the mitochondrial uncoupling protein.** *FEBS Lett* 1994, **343**:22–26.
282. Wu F, Gaffney BJ: **Dynamic behavior of fatty acid spin labels within a binding site of soybean lipoxygenase-1.** *Biochemistry* 2006, **45**:12510–12518.
283. Sevcsik E, Schütz GJ: **With or without rafts? Alternative views on cell membranes.** *Bioessays* 2016, **38**:129–139.
284. Harder T, Scheiffele P, Verkade P, Simons K: **Lipid domain structure of the plasma membrane revealed by patching of membrane components.** *J Cell Biol* 1998, **141**:929–942.
285. Varma R, Mayor S: **GPI-anchored proteins are organized in submicron domains at the cell surface.** *Nature* 1998, **394**:798–801.
286. Swulius MT, Chen S, Jane Ding H, Li Z, Briegel A, Pilhofer M, Tocheva EI, Lybarger SR, Johnson TL, Sandkvist M, et al.: **Long helical filaments are not seen encircling cells in electron cryotomograms of rod-shaped bacteria.** *Biochem Biophys Res Commun* 2011, **407**:650–655.
287. Swulius MT, Jensen GJ: **The helical MreB cytoskeleton in Escherichia coli MC1000/pLE7 is an artifact of the N-Terminal yellow fluorescent protein tag.** *J Bacteriol* 2012, **194**:6382–6386.
288. Errington J: **Bacterial morphogenesis and the enigmatic MreB helix.** *Nat Rev Microbiol* 2015, **13**:241–248.
289. Harder T, Simons K: **Caveolae, DIGs, and the dynamics of sphingolipid-cholesterol microdomains.** *Curr Opin Cell Biol* 1997, **9**:534–542.
290. Weimbs T, Low SH, Chapin SJ, Mostov KE: **Apical targeting in polarized epithelial cells: There's more afloat than rafts.** *Trends Cell Biol* 1997, **7**:393–399.
291. Baumgart T, Hammond AT, Sengupta P, Hess ST, Holowka DA, Baird BA, Webb WW: **Large-scale fluid/fluid phase separation of proteins and lipids in giant plasma membrane vesicles.** *Proc Natl Acad Sci USA* 2007, **104**:3165–3170.
292. Sezgin E, Kaiser H-J, Baumgart T, Schwille P, Simons K, Levental I: **Elucidating membrane structure and protein behavior using giant plasma membrane vesicles.** *Nat Protoc* 2012, **7**:1042–1051.
293. Kahya N: **Protein-protein and protein-lipid interactions in domain-assembly: lessons from giant unilamellar vesicles.** *Biochim Biophys Acta* 2010, **1798**:1392–1398.

294. Nickels JD, Chatterjee S, Stanley CB, Qian S, Cheng X, Myles DAA, Standaert RF, Elkins JG, Katsaras J: **The *in vivo* structure of biological membranes and evidence for lipid domains.** *PLoS Biol* 2017, **15**:e2002214.
295. Jacrot B: **The study of biological structures by neutron scattering from solution.** *Rep Prog Phys* 2001, **39**:911–953.
296. Marty V, Jasnin M, Fabiani E, Vauclare P, Gabel F, Trapp M, Peters J, Zaccai G, Franzetti B: **Neutron scattering: a tool to detect *in vivo* thermal stress effects at the molecular dynamics level in micro-organisms.** *J R Soc Interface* 2013, **10**:20130003–20130003.
297. Aloia RC, Tian H, Jensen FC: **Lipid composition and fluidity of the human immunodeficiency virus envelope and host cell plasma membranes.** *Proc Natl Acad Sci USA* 1993, **90**:5181–5185.
298. Brügger B, Glass B, Haberkant P, Leibrecht I, Wieland FT, Krausslich HG: **The HIV lipidome: A raft with an unusual composition.** *Proc Natl Acad Sci USA* 2006, **103**:2641–2646.
299. Waheed AA, Freed EO: **Lipids and membrane microdomains in HIV-1 replication.** *Virus Res* 2009, **143**:162–176.
300. Nguyen DH, Hildreth JEK: **Evidence for Budding of Human Immunodeficiency Virus Type 1 Selectively from Glycolipid-Enriched Membrane Lipid Rafts.** *J Virol* 2000, **74**:3264–3272.
301. McLoon AL, Kolodkin-Gal I, Rubinstein SM, Kolter R, Losick R: **Spatial Regulation of Histidine Kinases Governing Biofilm Formation in *Bacillus subtilis*.** *J Bacteriol* 2011, **193**:679–685.
302. McLoon AL, Guttenplan SB, Kearns DB, Kolter R, Losick R: **Tracing the Domestication of a Biofilm-Forming Bacterium.** *J Bacteriol* 2011, **193**:2027–2034.
303. López D, Vlamakis H, Losick R, Kolter R: **Paracrine signaling in a bacterium.** *Gene Dev* 2009, **23**:1631–1638.
304. Weart RB, Lee AH, Chien A-C, Haeusser DP, Hill NS, Levin PA: **A metabolic sensor governing cell size in bacteria.** *Cell* 2007, **130**:335–347.
305. Haeusser DP, Schwartz RL, Smith AM, Oates ME, Levin PA: **EzrA prevents aberrant cell division by modulating assembly of the cytoskeletal protein FtsZ.** *Mol Microbiol* 2004, **52**:801–814.
306. Haeusser DP, Garza AC, Buscher AZ, Levin PA: **The division inhibitor EzrA contains a seven-residue patch required for maintaining the dynamic nature of the medial FtsZ ring.** *J Bacteriol* 2007, **189**:9001–9010.
307. Singh JK, Makde RD, Kumar V, Panda D: **A Membrane Protein, EzrA, Regulates Assembly Dynamics of FtsZ by Interacting with the C-Terminal Tail of FtsZ.** *Biochemistry* 2007, **46**:11013–11022.
308. Booth IR, Blount P: **The MscS and MscL Families of Mechanosensitive Channels Act as Microbial Emergency Release Valves.** *J Bacteriol* 2012, **194**:4802–4809.



309. Quiblier C, Luczak-Kadlubowska A, Holdener E, Alborn D, Schneider T, Wiedemann I, Pinho MG, Sahl H-G, Rohrer S, Berger-Bächi B, et al.: **The *Staphylococcus aureus* Membrane Protein SA2056 Interacts with Peptidoglycan Synthesis Enzymes.** *Antibiotics (Basel)* 2013, **2**:11–27.
310. Cheng AG, DeDent AC, Schneewind O, Missiakas D: **A play in four acts: *Staphylococcus aureus* abscess formation.** *Trends Microbiol* 2011, **19**:225–232.
311. Simeone R, Bottai D, Brosch R: **ESX/type VII secretion systems and their role in host–pathogen interaction.** *Curr Opin Microbiol* 2009, **12**:4–10.
312. Casabona MG, Kneuper H, de Lima DA, Harkins CP: **Heme-Iron Plays A Key Role In The Regulation Of The Ess/Type VII Secretion System Of *Staphylococcus aureus* RN6390.** *bioRxiv* 2017, doi:10.1101/145433.
313. Casabona MG, Buchanan G, Zoltner M, Harkins CP, Holden MTG, Palmer T: **EsaB is a core component of the *Staphylococcus aureus* Type VII secretion system.** *bioRxiv* 2017, doi:10.1101/151316.
314. van Winden VJC, Ummels R, Piersma SR, Jiménez CR, Korotkov KV, Bitter W, Houben ENG: **Mycosins Are Required for the Stabilization of the ESX-1 and ESX-5 Type VII Secretion Membrane Complexes.** *mBio* 2016, **7**:e01471–16.
315. Huynh KW, Cohen MR, Moiseenkova-Bell VY: **Application of Amphipols for Structure-Functional Analysis of TRP Channels.** *J Membr Biol* 2014, **247**:843–851.
316. Youngman P, Perkins JB, Losick R: **Construction of a cloning site near one end of Tn917 into which foreign DNA may be inserted without affecting transposition in *Bacillus subtilis* or expression of the transposon-borne erm gene.** *Plasmid* 1984, **12**:1–9.
317. Reusch RN, Hiske TW, Sadoff HL: **Poly-beta-hydroxybutyrate membrane structure and its relationship to genetic transformability in *Escherichia coli*.** *J Bacteriol* 1986, **168**:553–562.
318. Kreiswirth BN, Löfdahl S, Betley MJ, O'Reilly M, Schlievert PM, Bergdoll MS, Novick RP: **The toxic shock syndrome exotoxin structural gene is not detectably transmitted by a prophage.** *Nature* 1983, **305**:709–712.
319. Gonzalez BE, Martinez-Aguilar G, Hultén KG, Hammerman WA, Coss-Bu J, Avalos-Mishaan A, Mason EO, Kaplan SL: **Severe Staphylococcal Sepsis in Adolescents in the Era of Community-Acquired Methicillin-Resistant *Staphylococcus aureus*.** *Pediatrics* 2005, **115**:642–648.
320. Dapson RW: **Macromolecular changes caused by formalin fixation and antigen retrieval.** *Biotech Histochem* 2007, **82**:133–140.
321. Mullis KB, Faloona FA: **Specific synthesis of DNA in vitro via a polymerase-catalyzed chain reaction.** *Meth Enzymol* 1987, **155**:335–350.
322. Wach A: **PCR-synthesis of marker cassettes with long flanking homology regions for gene disruptions in *S. cerevisiae*.** *Yeast* 1996, **12**:259–265.
323. Sanger F, Nicklen S, Coulson AR: **DNA sequencing with chain-terminating inhibitors.** *Proc Natl Acad Sci USA* 1977, **74**:5463–5467.
324. Yasbin RE, Young FE: **Transduction in *Bacillus subtilis* by bacteriophage SPP1.** *J Virol* 1974, **14**:1343–1348.

325. Guérout-Fleury AM, Frandsen N, Stragier P: **Plasmids for ectopic integration in *Bacillus subtilis***. *Gene* 1996, **180**:57–61.
326. Britton RA, Eichenberger P, Gonzalez-Pastor JE, Fawcett P, Monson R, Losick R, Grossman AD: **Genome-wide analysis of the stationary-phase sigma factor (sigma-H) regulon of *Bacillus subtilis***. *J Bacteriol* 2002, **184**:4881–4890.
327. Doan T, Marquis KA, Rudner DZ: **Subcellular localization of a sporulation membrane protein is achieved through a network of interactions along and across the septum**. *Mol Microbiol* 2005, **55**:1767–1781.
328. Lewis P, Marston A: **GFP vectors for controlled expression and dual labelling of protein fusions in *Bacillus subtilis***. *Gene* 1999, **227**:101–109.
329. Kim L, Mogk A, Schumann W: **A xylose-inducible *Bacillus subtilis* integration vector and its application**. *Gene* 1996, **181**:71–76.
330. Rudin L, Sjöström JE, Lindberg M, Philipson L: **Factors affecting competence for transformation in *Staphylococcus aureus***. *J Bacteriol* 1974, **118**:155–164.
331. Laemmli UK: **Cleavage of structural proteins during the assembly of the head of bacteriophage T4**. *Nature* 1970, **227**:680–685.
332. Schagger H, Jagow von G: **Blue native electrophoresis for isolation of membrane protein complexes in enzymatically active form**. *Anal Biochem* 1991, **199**:223–231.

## VIII ABBREVIATIONS

% (v/v)	% (volume/volume)
% (w/v)	% (weight/volume)
°C	degree Celsius
amp	ampicillin
APS	ammonium persulfate
BN-PAGE	blue-native polyacrylamide gel electrophoresis
bp	base pair
CL	cardiolipin
cm	chloramphenicol
dATP	deoxyadenosine triphosphate
dCTP	deoxycytidine triphosphate
dGTP	deoxyguanosine triphosphate
dH <sub>2</sub> O	distilled water
DDM	n-Dodecyl β-D-maltoside
DMSO	dimethylsulfoxide
DNA	deoxyribonucleic acid
DNase	deoxyribonuclease
dNTP	deoxyribonucleoside triphosphate
DRM	detergent resistant membrane
DSM	detergent sensitive membrane
DSP	dithiobis(succinimidyl propionate)
DTT	dithiothreitol
dTTP	deoxythymidine triphosphate
EDTA	ethylenediaminetetraacetic acid
erm	erythromycin
FMM	functional membrane microdomain
g	relative centrifugal force
gDNA	genomic DNA
GFP	green fluorescent protein
GOI	gene of interest
IPTG	isopropyl β-D-thiogalactopyranoside
IQR	interquartile range
kDa	kilodalton
km	kanamycin
LB	Lysogeny Broth
LFH PCR	long flanking homology polymerase chain reaction
LFQ	label-free quantification
M	molar
MDa	megadalton
MU	Miller Units
mls	macrolide lincosamide streptogramin
MOPS	3-(N-morpholino)propanesulfonic acid
MS	mass spectrometry
Ni-NTA	Ni <sup>2+</sup> -charged nitriloacetic acid

nt	nucleotides
o.n.	over night
OD	optical density
ONPG	o-Nitrophenyl- $\beta$ -D-galactopyranosid
PBS	phosphate buffered saline
PCR	polymerase chain reaction
PE	phosphatidylethanolamine
PG	phosphatidylglycerol
P <sub>hp</sub>	(IPTG-inducible) Hyperspank Promoter
PMSF	phenylmethylsulfonylfluorid
PVDF	polyvinylidene difluoride
rcf	relative centrifugal force
RFP	red fluorescent protein
RNase	ribonuclease
rpm	revolutions per minute
SDS	sodium dodecyl sulfate
SDS-PAGE	sodium dodecyl sulfate polyacrylamide gel electrophoresis
SIM	simvastatin
spc	spectinomycin
T7SS	type VII secretion system
TCA	trichloroacetic acid
TEMED	N,N,N',N'-Tetramethylethane-1,2-diamine
tet	tetracyclin
TRIS	tris(hydroxymethyl)aminomethane
TSB	tryptic soy broth
vol	volume
wt	wild type
X-Gal	5-Brom-4-chlor-3-indoxyl- $\beta$ -D-galactopyranosid
YFP	yellow fluorescent protein
ZA	zaragozic acid
5-DSA	5-doxyyl stearic acid

#### Dimensions

n	Nano ( $10^{-9}$ )
$\mu$	Micro ( $10^{-6}$ )
m	Milli ( $10^{-3}$ )
k	Kilo ( $10^3$ )
M	Mega ( $10^6$ )

Amino acid single letter and three letter codes were used according the IUPAC system.

## IX APPENDIX 1

### IX.1 List of strains

Strain	Organism	Genotype / plasmid	Reference
<b>Wild types</b>			
BM-18	<i>B. subtilis</i> PY79	wild type	[316]
DL-1	<i>B. subtilis</i> NCIB3610	wild type	[142]
BM-176	<i>S. aureus</i> RN4220	wild type	[318]
BM-178	<i>S. aureus</i> USA300_TCH1516	wild type	[319]
DL-95	<i>E. coli</i> DH5 $\alpha$	wild type	[317]
DL-1124	<i>E. coli</i> BL21 DE3 Gold	wild type	Stratagene
BM-263	<i>E. coli</i> BTH101	wild type	Euromedex
<b>Plasmids</b>			
BM-261	<i>E. coli</i> DH5 $\alpha$	pKT25- <i>zip</i>	Euromedex
BM-262	<i>E. coli</i> DH5 $\alpha$	pUT18C- <i>zip</i>	Euromedex
BM-579	<i>E. coli</i> DH5 $\alpha$	pKT25- <i>floA</i>	This study
BM-271	<i>E. coli</i> DH5 $\alpha$	pKNT25- <i>floA</i>	This study
BM-310	<i>E. coli</i> DH5 $\alpha$	pUT18- <i>floA</i>	This study
BM-577	<i>E. coli</i> DH5 $\alpha$	pUT18C- <i>floA</i>	[245]
BM-543	<i>E. coli</i> DH5 $\alpha$	pKT25- <i>esaA</i>	This study
BM-503	<i>E. coli</i> DH5 $\alpha$	pKNT25- <i>esaA</i>	This study
BM-281	<i>E. coli</i> DH5 $\alpha$	pUT18- <i>esaA</i>	This study
BM-546	<i>E. coli</i> DH5 $\alpha$	pUT18C- <i>esaA</i>	This study
BM-458	<i>E. coli</i> DH5 $\alpha$	pKT25- <i>essA</i>	This study
BM-311	<i>E. coli</i> DH5 $\alpha$	pKNT25- <i>essA</i>	This study
BM-268	<i>E. coli</i> DH5 $\alpha$	pUT18- <i>essA</i>	This study
BM-299	<i>E. coli</i> DH5 $\alpha$	pUT18C- <i>essA</i>	This study
BM-327	<i>E. coli</i> DH5 $\alpha$	pKT25- <i>essB</i>	This study
BM-312	<i>E. coli</i> DH5 $\alpha$	pKNT25- <i>essB</i>	This study
BM-269	<i>E. coli</i> DH5 $\alpha$	pUT18- <i>essB</i>	This study
BM-280	<i>E. coli</i> DH5 $\alpha$	pUT18C- <i>essB</i>	This study
BM-499	<i>E. coli</i> DH5 $\alpha$	pKT25- <i>essC</i>	This study
BM-500	<i>E. coli</i> DH5 $\alpha$	pKNT25- <i>essC</i>	This study
BM-270	<i>E. coli</i> DH5 $\alpha$	pUT18- <i>essC</i>	This study
BM-305	<i>E. coli</i> DH5 $\alpha$	pUT18C- <i>essC</i>	This study
BM-514	<i>E. coli</i> DH5 $\alpha$	pSEVA641- <i>P<sub>lac</sub>-floA</i>	[245]
BM-424	<i>E. coli</i> DH5 $\alpha$	pET20b- <i>esxA</i>	This study
BM-425	<i>E. coli</i> DH5 $\alpha$	pET20b- <i>esxB</i>	This study
BM-456	<i>E. coli</i> DH5 $\alpha$	pET20b- <i>esxC</i>	This study
BM-461	<i>E. coli</i> DH5 $\alpha$	pET20b- <i>esxD</i>	This study
DL-1321	<i>E. coli</i> DH5 $\alpha$	pET15- <i>ytnP</i>	[270]
BM-614	<i>E. coli</i> DH5 $\alpha$	pASK-IBA3C- <i>floA</i>	This study
BM-615	<i>E. coli</i> DH5 $\alpha$	pBAD- <i>esaAessABC</i>	This study

Strain	Organism	Genotype / plasmid	Reference
<b><i>B. subtilis</i> strains</b>			
BM-224	<i>B. subtilis</i> PY79	<i>amyE::P<sub>yqeZ</sub>-floA-gfp</i> (spc)	[126]
BM-20	<i>B. subtilis</i> PY79	<i>amyE::P<sub>hp</sub>-floA-gfp</i> (spc)	This study
BM-223	<i>B. subtilis</i> PY79	<i>amyE::P<sub>yuaF</sub>-floT-gfp</i> (spc)	[126]
BM-21	<i>B. subtilis</i> PY79	<i>amyE::P<sub>hp</sub>-floT-gfp</i> (spc)	This study
BM-246	<i>B. subtilis</i> PY79	$\Delta$ <i>tasA::spc</i>	This study
BM-225	<i>B. subtilis</i> PY79	$\Delta$ <i>sinR::spc</i>	This study
BM-248	<i>B. subtilis</i> PY79	$\Delta$ <i>tasA::km</i> $\Delta$ <i>sinR::spc</i>	This study
BM-19	<i>B. subtilis</i> PY79	<i>amyE::P<sub>hp</sub>-floA</i> (spc)	This study
BM-28	<i>B. subtilis</i> PY79	<i>amyE::P<sub>hp</sub>-floT</i> (spc)	This study
BM-29	<i>B. subtilis</i> PY79	<i>amyE::P<sub>hp</sub>-floT</i> (spc)	This study
BM-247	<i>B. subtilis</i> PY79	<i>lacA::P<sub>hp</sub>-floA</i> (mls) <i>amyE::P<sub>hp</sub>-floT</i> (spc) <i>lacA::P<sub>hp</sub>-floA</i> (mls) $\Delta$ <i>tasA::km</i>	This study
BM-126	<i>B. subtilis</i> PY79	<i>thrC::P<sub>tapA</sub>-yfp</i> (km)	This study
BM-243	<i>B. subtilis</i> PY79	<i>amyE::P<sub>hp</sub>-floA</i> (spc) <i>thrC::P<sub>tapA</sub>-yfp</i> (km)	This study
BM-244	<i>B. subtilis</i> PY79	<i>amyE::P<sub>hp</sub>-floT</i> (spc) <i>thrC::P<sub>tapA</sub>-yfp</i> (km)	This study
BM-242	<i>B. subtilis</i> PY79	<i>amyE::P<sub>hp</sub>-floT</i> (spc) <i>lacA::P<sub>hp</sub>-floA</i> (mls) <i>thrC::P<sub>tapA</sub>-yfp</i> (km)	This study
BM-168	<i>B. subtilis</i> PY79	<i>amyE::P<sub>hp</sub>-floT</i> (spc) <i>lacA::P<sub>hp</sub>-floA</i> (mls) $\Delta$ <i>ftsH::km</i>	This study
BM-249	<i>B. subtilis</i> PY79	$\Delta$ <i>ftsH::tet</i>	This study
BM-250	<i>B. subtilis</i> PY79	$\Delta$ <i>ftsH::tet</i> <i>thrC::P<sub>tapA</sub>-yfp</i> (km)	This study
BM-245	<i>B. subtilis</i> PY79	<i>amyE::P<sub>hp</sub>-floT</i> (spc) <i>lacA::P<sub>hp</sub>-floA</i> (mls) <i>thrC::P<sub>tapA</sub>-yfp</i> (km) $\Delta$ <i>ftsH::tet</i>	This study
BM-222	<i>B. subtilis</i> PY79	<i>amyE::P<sub>xyI</sub>-ftsZ-gfp</i> (cm)	This study
BM-226	<i>B. subtilis</i> PY79	<i>amyE::P<sub>xyI</sub>-ftsZ-gfp</i> (cm) <i>lacA::P<sub>hp</sub>-floT/floA</i> (mls)	This study
BM-144	<i>B. subtilis</i> PY79	<i>amyE::P<sub>xyI</sub>-ezrA-gfp</i> (spc)	This study
BM-151	<i>B. subtilis</i> PY79	<i>amyE::P<sub>xyI</sub>-ezrA-gfp</i> (cm) <i>lacA::P<sub>hp</sub>-floT/floA</i> (mls)	This study
BM-198	<i>B. subtilis</i> PY79	<i>amyE::P<sub>xyI</sub>-ezrA-gfp</i> (cm) <i>lacA::P<sub>hp</sub>-floT/floA</i> (mls) $\Delta$ <i>ftsH::km</i>	This study
BM-197	<i>B. subtilis</i> PY79	<i>amyE::P<sub>xyI</sub>-ezrA-gfp</i> (cm) $\Delta$ <i>ftsH::km</i>	This study
BM-207	<i>B. subtilis</i> PY79	<i>amyE::P<sub>xyI</sub>-ezrA-gfp</i> (cm) <i>lacA::P<sub>hp</sub>-ftsH</i> (mls)	This study

Strain	Organism	Genotype / plasmid	Reference
DL-7	<i>B. subtilis</i> NCIB3610	$\Delta$ tasA::spc $\Delta$ eps::tet	[303]
DL-5	<i>B. subtilis</i> NCIB3610	$\Delta$ sinR::spc	[147]
BM-40	<i>B. subtilis</i> NCIB3610	amyE::P <sub>hp</sub> -floA (spc)	This study
BM-37	<i>B. subtilis</i> NCIB3610	amyE::P <sub>hp</sub> -floT (spc)	This study
BM-59	<i>B. subtilis</i> NCIB3610	amyE::P <sub>hp</sub> -floT (spc) lacA::P <sub>hp</sub> -floA (mls)	This study
<b><i>S. aureus</i> strains</b>			
BM-199	<i>S. aureus</i> USA300_TCH1516	$\Delta$ floA::spc	This study
BM-493	<i>S. aureus</i> USA300_TCH1516	$\Delta$ T7SS (markerless)	This study
BM-554	<i>S. aureus</i> USA300_TCH1516	$\Delta$ essA (markerless)	This study
BM-516	<i>S. aureus</i> USA300_TCH1516	$\Delta$ essB (markerless)	This study
BM-585	<i>S. aureus</i> USA300_TCH1516	$\Delta$ essA (markerless) amy::P <sub>xyI</sub> -essA-mars	This study
BM-590	<i>S. aureus</i> USA300_TCH1516	$\Delta$ essA (markerless) amy::P <sub>xyI</sub> -essA-mars $\Delta$ floA::spc	This study
BM-426	<i>S. aureus</i> USA300_TCH1516	pLac <sub>xyI</sub> -flag-essB	This study
BM-460	<i>S. aureus</i> USA300_TCH1516	amy::P <sub>xyI</sub> -floA-his	This study
BM-465	<i>S. aureus</i> USA300_TCH1516	amy::P <sub>xyI</sub> -floA-his pLac <sub>xyI</sub> -flag-essB	This study
BM-459	<i>S. aureus</i> USA300_TCH1516	amy::P <sub>SA1403</sub> -floA-mars lac::P <sub>esxA</sub> -gfp-essB	This study
BM-605	<i>S. aureus</i> USA300_TCH1516	pLac <sub>xyI</sub> -esxA-flag	This study
BM-606	<i>S. aureus</i> USA300_TCH1516	$\Delta$ floA::spc pLac <sub>xyI</sub> -esxA-flag	This study
BM-607	<i>S. aureus</i> USA300_TCH1516	$\Delta$ T7SS (markerless) pLac <sub>xyI</sub> -esxA-flag	This study
BM-481	<i>S. aureus</i> USA300_TCH1516	pLac <sub>xyI</sub> -esxB-flag	This study
BM-482	<i>S. aureus</i> USA300_TCH1516	pLac <sub>xyI</sub> -esxB-flag $\Delta$ floA::spc	This study
BM-604	<i>S. aureus</i> USA300_TCH1516	pLac <sub>xyI</sub> -esxB-flag $\Delta$ T7SS (markerless)	This study
BM-589	<i>S. aureus</i> USA300_TCH1516	$\Delta$ essB (markerless) lac::P <sub>esxA</sub> -gfp-essB	This study
BM-593	<i>S. aureus</i> USA300_TCH1516	$\Delta$ essB (markerless) lac::P <sub>esxA</sub> -gfp-essB $\Delta$ floA::spc	This study
BM-566	<i>S. aureus</i> USA300_TCH1516	$\Delta$ essB (markerless) lac::P <sub>xyI</sub> -flag-essB	This study
BM-571	<i>S. aureus</i> USA300_TCH1516	$\Delta$ essB (markerless) lac::P <sub>xyI</sub> -flag-essB $\Delta$ floA::spc	This study

Strain	Organism	Genotype / plasmid	Reference
BM-586	<i>S. aureus</i> USA300_TCH1516	$\Delta$ essB (markerless) <i>amy::P<sub>xyl</sub>-essA-mars</i> <i>lac::P<sub>xyl</sub>-flag-essB</i>	This study
BM-591	<i>S. aureus</i> USA300_TCH1516	$\Delta$ essB (markerless) <i>amy::P<sub>xyl</sub>-essA-mars</i> <i>lac::P<sub>xyl</sub>-flag-essB</i> $\Delta$ floA::spc	This study
BM-400	<i>S. aureus</i> USA300_TCH1516	<i>amy::P<sub>SA1403</sub>-floA-mars</i>	This study

## IX.2 List of primers

Purpose	Name	Sequence (5'-3')
<b><i>B. subtilis</i> strains and mutants</b>		
Cloning of <i>floT</i> into pDR111	YuaGSallfw	AAAAGTCGACTAAGGAGGAAGTACTATGACAATGCCG ATTATAAT
	YuaGSphIrv	AAAAGCATGCTTACTCTGATTTTGGATCG
Cloning of <i>floA</i> into pBM001	YqfASallfw	AAAAGTCGACTAAGGAGGAAGTACTATGGATCCGTCA ACACTTA
	YqfASphIrv	AAAAGCATGCTTATGATTTGCGGTCTTCAT
Cloning of <i>floT-gfp</i> into pDR111	GFPsphIrv	AAAAGCATGCTTATTTGTATAGTTCATCCATGC
Cloning of <i>floA-floT</i> into pBM001	YuaGYqfAOp2	CAGTTACCATACGGTTCTG
	YuaGYqfAOp3	CAGAACCGTATGGTAACTGATGGATCCGTCAACACTT A
Cloning of <i>ftsH</i> into pDR111	FtsHSallfw	AAAAGTCGACTAAGGAGGAAGTACTATGAATCGGGTC TTCCGT
	FtsHSphI	AAAAGCATGCAGAAAGCGAATTACTCTTTTC
Cloning of <i>ftsZ-gfp</i> into pX	FtsZSphI	AAAAACTAGTTAAGGAGGAAGTACTGCATGTTGGAGT TCGAAAC
	FtsZ-GFP 2	AGTTCTTCTCCTTTACTCATGCCGCGTTTATTACGGT T
	FtsZ-GFP 3	AACCGTAATAAACGCGGATGAGTAAAGGAGAAGAACT
	GFPBamHIrv	AAAAGGATCCATCTGAAGTCTGGACATTTA
Cloning of <i>ezrA</i> into pSG1554	EzrAKpnI	AAAAGGTACCATGGAGTTTGTTCATTGGATT
	EzrAXhoIrv	AAAACCTCGAGAGCGGATATGTCAGCTTTG
<i>ftsH::tet</i> deletion	Ftshtet1	CAGCGACCGCATTGTATT
	Ftshtet2	GAGAACAACCTGCACCATTGCAAGATGCCGATCAGCT TTCATAA
	Ftshtet3	GGGATCAACTTTGGGAGAGAGTTCTATGCTGCCAAGA GAAGACCGTT
	Ftshtet4	AGCTTTGCTGCACGCGA



Purpose	Name	Sequence (5'-3')
	tetfw	TCTTGCAATGGTGCAGGTTGTTCTC
	tetrv	GAACTCTCTCCCAAAGTTGATCCC
<b><i>S. aureus</i> strains and mutants</b>		
Cloning of <i>essA-mars</i> into pAmy <sub>xy1</sub>	EssANhelfw	TTTTGCTAGCGGAAGGAGTTTTTGCTTATGTTGATGA ATAGCGTGAT
	EssArv + MARS tail	CATCTTCTGATGATGCCATAATGTTACTTTTACGTGC TG
	MARSfw + EssA tail	CAGCACGTAAAAGTAACATTATGGCATCATCAGAAGA TG
	MARSEcoIrv	AAAAGAATTCTTATCCTGCACCTGTTGAA
Cloning of <i>flag-essB</i> into pLac <sub>xy1</sub>	FLAGNhelfw	TTTTGCTAGCGGAAGGAGTTTTTGCTTATGGACTACA AAGACCATGAC
	FLAGrv + EssB tail	AGGGTTATGATTTTTAACCATTTTATCGTCGTCATCT TTGTAG
	EssBfw + FLAG tail	CTACAAAGATGACGACGATAAAATGGTTAAAAATCAT AACCT
	EssBXhoIrv	AAAACCTCGAGGCTCAGTCCTATACTATT
Cloning of <i>P<sub>esxA-gfp-essB</sub></i> into pLac	PesxABamHIfw	AAAAGGATCCTACTGATTGTTGTTAAGATCA
	PesxArv + GFP tail	AGTTCTTCTCCTTTACTCATAACTAGAAACCTCCTGA ATA
	GFPfw + PesxA tail	TATTTCAGGAGGTTTCTAGTTATGAGTAAAGGAGAAGA ACT
	GFPrv + EssB tail	AGGGTTATGATTTTTAACCATTTTGTATAGTTCATCC ATGC
	EssBfw + GFP tail	GCATGGATGAACTATACAAATGGTTAAAAATCATAA CCCT
	EssBSpeIrv	AAAAACTAGTTTGCCTCAGTCCTATACTA
Cloning of <i>esxA-flag</i> into pLac <sub>xy1</sub>	EsxANhelfw	TTTTGCTAGCGGAAGGAGTTTTTGCTTATGGCAATGA TTAAGATGAG
	EsxArv + FLAG tail	GTCATGGTCTTTGTAGTCTTGCAAACCGAAATTATTA GA
	FLAGfw + EsxA tail	TCTAATAATTTTCGGTTTGCAAGACTACAAAGACCATG AC
	FLAGXhoIrv	AAAACCTCGAGTTACTATTTATCGTCGTCATC
Cloning of <i>esxB-flag</i> into pLac <sub>xy1</sub>	EsxBNhelfw	TTTTGCTAGCGGAAGGAGTTTTTGCTTATGGTGGAT ATAAAGGTAT
	EsxBrv + FLAG tail	GTCATGGTCTTTGTAGTCTGGGTTCCACCTATCAAG
	FLAGfw + EsxB tail	CTTGATAGGGTGAACCCAGACTACAAAGACCATGAC
Cloning of <i>floA-mars</i> into pAmy- <i>P<sub>floA-floA-yfp</sub></i>	FloAHindIIIfw	AAAAAAAAGCTTATGTTTAGTTTAAG
	FloArv + MARS tail	CATCTTCTGATGATGCCATATGTTTCAGGTGACTCATC ATCA
	MARSfw + FloA tail	TGATGATGAGTCACCTGAACATATGGCATCATCAGAA GATG
	MARSBamHIrv	AAAAGGATCCTTATCCTGCACCTGTTGAA

<b>Purpose</b>	<b>Name</b>	<b>Sequence (5'-3')</b>
Cloning of <i>essA</i> -flankings into pMAD	$\Delta$ essA_LFH1_Sall	AAAAGTCGACTATAGTTATGAACGTGCCAA
	$\Delta$ essA_LFH2	ACTTTTACGTGCTGATTCATTTAGATTAATCTCTCTT TCTTA
	$\Delta$ essA_LFH3	TAAGAAAGAGAGATTAATCTAAATGAATCAGCACGTA AAAGT
	$\Delta$ essA_LFH4_BamHI	AAAAGGATCCGTATGATTGTCAATTAATGTCA
Cloning of <i>essB</i> -flankings into pMAD	$\Delta$ essB_LFH1_Sall	AAAAGTCGACAAGACAGCAAAGCGGTTAA
	$\Delta$ essB_LFH2	TCTTTGCCTCAGTCCTATACTATTTTTCCCTCTATAG TAA
	$\Delta$ essB_LFH3	TTACTATAGGAGGAAAAATAGTATAGGACTGAGGCAA AGA
	$\Delta$ essB_LFH4_BamHI	AAAAGGATCCTATGATCACCAATGTAAGCT
Cloning of T7SS-flankings into pMAD	$\Delta$ T7SS_LFH1_Sall	AAAAGTCGACTACTGATTGTTGTTAAGATCA
	$\Delta$ T7SS_LFH2	TTTAGTCTTACATTAAGATAGTAACTAGAAACCTCCT GAATA
	$\Delta$ T7SS_LFH3	TATTCAGGAGGTTTCTAGTTACTATCTTAATGTAAGA CTAAA
	$\Delta$ T7SS_LFH4_BamHI	AAAAGGATCCAAAGATTACACAGTGCAAATA
<b>Bacterial two hybrid plasmids</b>		
Cloning of <i>esaA</i> into pUT18 and pKNT25	EsaAHindIII <sub>fw</sub>	AAAAAAGCTTATGAAAAAGAAAAATTGGATTTA
	EsaAKpnI <sub>rv</sub>	AAAAGGTACCCGATTAATCTCTCTTTCTTAAA
Cloning of <i>esaA</i> into pUT18C	EsaAKpnI <sub>fw</sub>	AAAAGGTACCGATGAAAAAGAAAAATTGGATTTA
	EsaASacI <sub>rv</sub>	AAAAGAGCTCTTAGATTAATCTCTCTTTCTTA
Cloning of <i>esaA</i> into pKT25	EsaAXbaI <sub>fw</sub>	AAAATCTAGACATGAAAAAGAAAAATTGGATTTA
	EsaAKpnI <sub>rv</sub>	AAAAGGTACCTTAGATTAATCTCTCTTTCTTA
Cloning of <i>essA</i> into all vectors	EssABamHI <sub>fw</sub>	AAAAGGATCCCATGTTGATGAATAGCGTGAT
	EssAKpnI <sub>rv</sub>	AAAAGGTACCCGTCAATGTTACTTTTACGTGCTG
Cloning of <i>essB</i> into pUT18 and pKNT25	EssBHindIII <sub>fw</sub>	AAAAAAGCTTATGGTTAAAAATCATAACCCT
	EssBBamHI <sub>rv</sub>	AAAAGGATCCTCTTTTTTTCTTTTCAGCTTCTTG
Cloning of <i>essB</i> into pUT18C and pKT25	EssB(pUT18)Sall <sub>fw</sub>	AAAAGTCGACTATGGTTAAAAATCATAACCCT
	EssB(pKT25)PstI <sub>fw</sub>	AAAAGTGCAGGGATGGTTAAAAATCATAACCCT
	EssBBamHI <sub>rv</sub>	AAAAGGATCCTCTTTTTTTCTTTTCAGCTTCTTG
Cloning of <i>essC</i> into pUT18	EssCSal <sub>fw</sub>	AAAAGTCGACATGCATAAATTGATTATAAAAATAT
	EssCBamHI <sub>rv</sub>	AAAAGGATCCTCTTTAAACCATCTAATCTTTTGA
Cloning of <i>essC</i> into pUT18C	EssCSal <sub>fw</sub>	AAAAGTCGACTATGCATAAATTGATTATAAAAATAT
	EssCBamHI <sub>rv</sub>	AAAAGGATCCCTATTTAAACCATCTAATCTTTT
Cloning of <i>essC</i> into pKT25	EssCPstI <sub>fw</sub>	AAAAGTGCAGGGATGCATAAATTGATTATAAAAATAT
	EssCBamHI <sub>rv</sub>	AAAAGGATCCTCTTTAAACCATCTAATCTTTTGA

Purpose	Name	Sequence (5'-3')
Cloning of <i>floA</i> into all vectors	FloABamHI <sub>fw</sub>	AAAAGGATCCCATGTTTAGTTTAAGTTTTATCG
	FloAKpnI <sub>rv</sub>	AAAAGGTACCCGATGTTTCAGGTGACTCATCA
<b>Overexpression vectors</b>		
Cloning of <i>esxA</i> into pET20b(+)	EsxANdeI <sub>fw</sub>	AAAACATATGGCAATGATTAAGATGAG
	EsxAXhoI <sub>rv</sub>	AAAACCTCGAGTTGCAAACCGAAATTATTAGA
Cloning of <i>esxB</i> into pET20b(+)	EsxBNdeI <sub>fw</sub>	AAAACATATGGGTGGATATAAAGGTAT
	EsxBXhoI <sub>rv</sub>	AAAACCTCGAGTGGGTTCCACCTATCAAG
Cloning of <i>esxC</i> into pET20b(+)	EsxCNdeI <sub>fw</sub>	AAAACATATGATGAATTTTAATGATATTGAAAC
	EsxCXhoI <sub>rv</sub>	AAAACCTCGAGATTCATTGCTTTATTAAAATATTC
Cloning of <i>esxD</i> into pET20b(+)	EsxDNdeI <sub>fw</sub>	AAAACATATGATGACGTTGAGTGGAATAAT
	EsxDXhoI <sub>rv</sub>	AAAACCTCGAGTCCCTCAATATTATAGTAAAG

### IX.3 List of figures

Fig. I.1: Biosynthetic pathway to produce terpenoids .....	10
Fig. I.2: Signaling cascade that regulates subpopulations of matrix producers and spores .....	15
Fig. I.3 Organization of the type VII secretion system (T7SS) of <i>S. aureus</i> .....	21
Fig. III.1: Schematic overview of the LFQ workflow. ....	51
Fig. III.2: SDS-PAGE analysis of proteins samples used for LFQ analysis. ....	51
Fig. III.3: Scatterplots of all identified proteins in LFQ analysis. ....	52
Fig. III.4: Hierarchical clustering of DRM-membrane proteome during four different conditions: .....	54
Fig. IV.1. Synthetic strains render functional T7SS. ....	57
Fig. IV.2: Proteins of the T7SS are confined to the FMM in <i>S. aureus</i> . ....	58
Fig. IV.3: Bacterial two hybrid analyses to test interaction of T7SS membrane proteins with FloA. ....	59
Fig. IV.4: FloA interacts with the T7SS protein EssB. ....	60
Fig. IV.5: FloA deletion reduces secretion efficiency of T7SS substrates.....	62
Fig. IV.6: Absence of FloA affects subcellular localization of EssB .....	63
Fig. IV.7: Absence of FloA affects oligomeric behavior of T7SS membrane proteins.....	64
Fig. IV.8: FloA is important for the interaction of EssB with EssA, but not EsaA or EssC	65
Fig. IV.9: Bacterial three-hybrid analysis to probe interaction of EssB with other T7SS membrane proteins.....	66
Fig. IV.10: Impact of FloA on reconstituted T7SS in <i>E. coli</i> .....	67
Fig. IV.11: Absence of flotillin decreases antibody production in infected mice. ....	68
Fig. IV.12 Growth of <i>S. aureus</i> in presence of different combinations of anti-FMM molecules .....	69
Fig. IV.13: Anti-FMM affects focal membrane organization of FloA. ....	70
Fig. IV.14: Anti-FMM molecules can inhibit secretion of T7SS substrates <i>in vitro</i> .....	71
Fig. IV.15: Anti-FMM molecules do not affect T7SS membrane protein abundance.....	72
Fig. IV.16: Anti-FMM molecules can inhibit secretion of T7SS substrates <i>in vivo</i> . ....	72
Fig. V.1 Working model how the assembly of the T7SS is mediated by FloA/FMMs.....	81

## IX.4 List of tables

Table VI.1 All proteins, enzymes and other specialized chemicals used in this work.....	85
Table VI.2 Laboratory equipment used in this work.....	86
Table VI.3 software used in this work.....	87
Table VI.4 Antibiotics used in this work.....	93
Table VI.5 Media supplements used in this study .....	93
Table VI.6 All <i>B. subtilis</i> cloning vectors used in this study.....	104
Table VI.7 All <i>S. aureus</i> cloning vectors used in this study.....	106
Table VI.8 Antibodies used in this work.....	112
Table VI.9 Fluorescent proteins and dyes used in this work and their corresponding emission/excitation filters and excitation time.....	114

## X APPENDIX 2

### X.1 Statement of individual author contribution

Declaration of author contribution to the publication presented in chapter II.

<b>Publication</b>			
'Overproduction of flotillin influences cell differentiation and shape in <i>Bacillus subtilis</i> .' (2013) mBio 4(6): e00719-13			
<b>Participated in</b>	<b>Author initials,</b> Responsibility decreasing form left to right		
Study design	DL	BMS	JS
Methods development			
Data collection	BMS	JS	DL
Data analysis and interpretation	BMS	JS	DL
Manuscript writing			
<i>Writing of introduction</i>	DL	BMS	JS
<i>Writing of materials &amp; methods</i>	BMS	DL	JS
<i>Writing of results &amp; discussion</i>	DL	BMS	JS
<i>Writing of first draft</i>	BMS	DL	JS

Following people contributed to this work:

- Several plasmids used in this work were generated by the technical assistant Isa Westedt.
- The plasmids for the reconstitution of the T7SS in *E. coli* were designed and constructed by Nicole Mietrach, as well as the workflow for purification. Experiments on the Äkta purifier were performed with the great help of Nicole Mietrach and Nikolaos Famelis.
- Experimental design and data analysis for the LFQ-mass spectrometry were performed together with Dr. Jens Vanselow (AG Schlosser, Rudolf-Virchow Zentrum, Würzburg).
- Mouse experiments were designed in collaboration with Dr. Tobias Hertlein and Dr. Knut Ohlsen (IMIB Würzburg). Dr. Tobias Hertlein performed staphylococcal infections of mice and serum was collected and isolated by Liane Dreher (AG Ohlsen).

## X.2 Affidavit

I hereby confirm that my thesis entitled '*Elucidating structural and functional aspects of prokaryotic membrane microdomains*' is the result of my own work. I did not receive any help or support from commercial consultants. All sources and/or materials applied are listed and specified in the thesis.

Furthermore, I confirm that this thesis has not yet been submitted as part of another examination process neither in identical nor in similar form.

Würzburg, July 24<sup>th</sup>, 2017

---

*Benjamin Mielich-Süß*

Hiermit erkläre ich an Eides statt, die Dissertation „*Aufklärung struktureller und funktioneller Aspekte von prokaryotischen Membranmikrodomänen*“ eigenständig, d.h. insbesondere selbstständig und ohne Hilfe eines kommerziellen Promotionsberaters, angefertigt und keine anderen als die von mir angegebenen Quellen und Hilfsmittel verwendet zu haben.

Ich erkläre außerdem, dass die Dissertation weder in gleicher noch in ähnlicher Form bereits in einem anderen Prüfungsverfahren vorgelegen hat.

Würzburg, den 24. Juli 2017

---

*Benjamin Mielich-Süß*

### X.3 Publications

#### Publications directly related to this work

Garcia-Fernandez E, Koch G, Fekete A, Stengel S, Schneider J, **Mielich-Süss B**, Geibel S, Markert S, Stigloher C, Lopez D. Disassembly of functional membrane microdomains relapses antibiotic resistance in *Staphylococcus aureus* – *under review*

**Mielich-Süss B**, Wagner R, Mietrach N, Hertlein T, Marincola G, Ohlsen K, Geibel S, Lopez D. The scaffold activity of flotillin contributes to the assembly of type-VII secretion system in *Staphylococcus aureus* – *under review*

**Mielich-Süss B**, Schneider J, Lopez D. 2013. Overproduction of flotillin influences cell differentiation and shape in *Bacillus subtilis*. *mBio* 4(6): e00719-13.

#### Publications unrelated to this work

Schneider J, **Mielich-Süss B**, Böhme R, Lopez D. 2015. *In vivo* characterization of the scaffold activity of flotillin on the membrane kinase KinC of *Bacillus subtilis*. *Microbiology*. 2015 Sep;161(9):1871-87.

Schneider J, Klein T, **Mielich-Süss B**, Koch G, Franke C, Kuipers OP, Kovács AT, Sauer M, Lopez D. 2015. Spatio-temporal remodeling of functional membrane microdomains organizes the signaling networks of a bacterium. *PLoS Genet*. 2015 Apr 24;11(4):e1005140.

**Mielich-Süss B**, Lopez D. 2015. Molecular Mechanisms involved in *Bacillus subtilis* biofilm formation. *Environmental Microbiology* 17(3):555-65.

Yepes A, Schneider J, **Mielich B**, Koch G, Garcia-Betancur JC, Ramamurthi KS, Vlamakis H, Lopez D. 2012. The biofilm formation defect of a *Bacillus subtilis* flotillin-defective mutant involves the protease FtsH. *Molecular Microbiology* 86:457-471.

Schneider J, Yepes A, Garcia-Betancur JC, Westedt I, **Mielich B**, Lopez D. 2012. Streptomycin-induced expression in *Bacillus subtilis* of YtnP, a lactonase-homologous protein that inhibits development and streptomycin production in *Streptomyces griseus*. *Applied and Environmental Microbiology* 78, 599-603.

#### Active participation in international meetings/congresses

**Mielich-Süss B**, Lopez D. Bacterial Lipid Rafts are important for the functionality of the Type VII Secretion System in *Staphylococcus aureus*. EUREKA! Symposium 2016, Würzburg – *Invited student speaker*

**Mielich-Süss B**, Schneider J, Lopez D. Flotillin controls the assembly of protein complexes related to staphylococcal virulence. VAAM 2016, Jena/Germany – *Oral presentation*

**Mielich-Süss B**, Schneider J, Lopez D. Flotillin controls the assembly of protein complexes related to staphylococcal virulence. EMBO/ESF Bacterial Networks 2015, Sant-Feliu De Guixols/Spainien – *Poster presentation*

**Mielich-Süss B**, Schneider J, Lopez D. Overexpression of flotillins affects cell differentiation and shape in *Bacillus subtilis*. VAAM 2015, Marburg/Germany – *Oral presentation*

**Mielich-Süss B**, Schneider J, Lopez D. Overexpression of flotillins affects cell differentiation and shape in *Bacillus subtilis*. MolMicroMeeting 2014, Würzburg/Germany – *Poster presentation*



## X.4 Acknowledgments

At this point I want to say thank you and express my gratitude to all the people that contributed to this work, may it be intellectually, financially, or emotionally:

First, I want to thank Daniel Lopez for accepting me as a PhD student in his lab and letting me work on this exiting project. I highly appreciate his support and motivation throughout the years. Especially his excitement for science was always an amazing driving force.

Also, I want to thank Prof. Thomas Rudel and Prof. Marc Bramkamp for being part of my committee and Prof. Thomas Dandekar to be the chair of my committee.

A special thank I want to say to the people that were in there when I started in the Lopez lab, especially Dr. Ana Yepes and Dr. Gudrun Koch, that taught me a lot in science and how to deal with *S. aureus*. You were always very supporting and it was a lot of fun.

I want to thank all the lab mates that I shared a fantastic time with both in the lab and outside: Dr.(!) Johannes Schneider, Charlotte Wemser (:'-D), Rabea Wagner, Lara Kricks, Nicole Mietrach and Nikolaos Famelis, who not only have been great PhD fellows, but also great friends. In particular, I want to thank Rabea for her great help during the revision of the T7SS-FloA story and proof-reading this thesis. Thank you Charly, for all the fun and scientific discussions, for the spontaneous vis-à-vis lab meetings, for being my conference-buddy and last survivor of the Lopez-Lab in Würzburg. I think we kept the spirit alive after the lab moved to Spain.

Dr. Sebastian Geibel for giving me shelter during my remaining time in Würzburg. The incorporation into that room led to a both fun (Trash-music Friday, Lab Olympics, ...), as well as great scientific exchange and collaboration on the T7SS project.

I am thankful to all the people from the Ohlsen Lab, for including us into their weekly seminar after the lab moved and for the collaboration. I thank Tobias Hertlein for helping with the infections.

I am very grateful to the GSLS for both the financial support throughout all the years and being part of this great program.

Thanks to my family for the financial and mental support during the last years.

Finally, I want to say special thank to my wife Anni and my daughter Lilly for keeping me going, encouraging me, and always making me smile after a tough day in the lab.

## **X.5 Curriculum Vitae**